19941228 045

A QUANTITATIVE FEEDBACK THEORY FCS DESIGN

FOR THE SUBSONIC ENVELOPE OF THE VISTA F-16

INCLUDING CONFIGURATION VARIATION

THESIS
Scott N. Phillips
Major, USAF

AFIT/GE/ENG/94D-24.

DEPARTMENT OF THE AIR FORCE

AIR UNIVERSITY

AIR FORCE INSTITUTE OF TECHNOLOGY

Wright-Patterson Air Force Base, Ohio

AFIT/GE/ENG/94D-24.

A QUANTITATIVE FEEDBACK THEORY FCS DESIGN

FOR THE SUBSONIC ENVELOPE OF THE VISTA F-16

INCLUDING CONFIGURATION VARIATION

THESIS
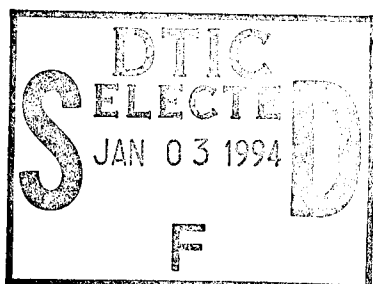Scott N. Phillips
Major, USAF

AFIT/GE/ENG/94D-24.

Approved for public release; Distribution unlimited

AFIT/GE/ENG/94D-24.

A QUANTITATIVE FEEDBACK THEORY FCS DESIGN FOR THE SUBSONIC ENVELOPE OF THE VISTA F-16 INCLUDING CONFIGURATION VARIATION

THESIS

Presented to the Faculty of the Graduate School of Engineering

of the Air Force Institute of Technology

Air University

In Partial Fulfillment of the

Requirements for the Degree of

Master of Science in Electrical Engineering

Scott N. Phillips, B.S. Electrical Engineering

Major, USAF

December, 1994

Acknowledgements

I would like to express my thanks to my thesis advisors, Constantine H. Houpis and Mier Pachter, and my sponsor, Captain Steve Rasmussen, without whose patience and guidance this research effort would not have been possible. Next, I would like to express my heartfelt gratitude to my wife, Jacqueline, and three children, Chad, Megan, and Kristin, for their understanding and support during this time-consuming project. They are the ones who truly made the greatest sacrifice by allowing me the time I needed. Finally, I thank God (who no doubt chuckles at our feeble efforts to describe and understand what he has created) for the blessings he has bestowed upon me.

Scott N. Phillips

Table of Contents

List of Figures

List of Tables

AFIT/GE/ENG/94D-24.

Abstract

An aircraft's response to control inputs varies widely throughout its flight envelope. The aircraft configuration also impacts control response through variations in center of gravity and moments of inertia. Designing a flight control system (FCS) to accomodate the full flight envelope and configuration set of an aircraft is clearly a complex undertaking. Quantitative feedback theory (QFT) is a design tool which enables the engineer to attack this task in an efficient way. Although QFT is a robust control design technique, it is an interactive algorithm allowing the engineer full control over compensator order and gain. In this research effort, a full subsonic flight envelope FCS is designed for the VISTA F-16 aircraft using QFT. Four aircraft configurations are considered. The strict control of the compensator order and gain allowed by QFT facilitates the attainment of desired performance while avoiding physical saturations. In addition, flying qualities are imbedded in the longitudinal design through the use of a control parameter which varies with the aircraft's energy state. This parameter is synthesized to closely reflect the actual control desires of the pilot throughout the aircraft flight envelope. Linear simulations with realistically large control inputs are used to validate the design.

A QUANTITATIVE FEEDBACK THEORY FCS DESIGN FOR THE SUBSONIC ENVELOPE OF THE VISTA F-16 INCLUDING CONFIGURATION VARIATION

I. Introduction

1.1 Research Justification

Traditionally, flight control engineers have taken a conservative, brute force approach to designing a full envelope flight control system (FCS) for an aircraft. First, many design points within and along the border of the flight envelope of an aircraft are selected. These design points are usually airspeed-altitude combinations as shown by the X's in Figure 1.1. Second, individual compensator designs are accomplished for each of these airspeed-altitude points. Third, smooth transitions between these compensators must be engineered. Making the transitions imperceptible to the pilot is very difficult and time-consuming because each airspeed-altitude design point can be approached from an infinite number of initial conditions. Obviously, if the number of the airspeed-altitude design points can be reduced, thus reducing the number of transitions required, the design process can be made more efficient, and the resulting FCS less complex.

One possible way to reduce the number of necessary design points is to apply a robust control design technique to the problem. A compensator synthesized using robust control principles should certainly be able to handle large parts of, if not the whole, flight envelope. Unfortunately, most attempts at applying robust control design algorithms to practical, "real world" problems have been dismal failures [7]. This is because although the problem is well posed, the resulting compensator is impractical to implement. Either the compensator is of too high an order, or the compensator gain is too large to accommodate "real world" nonlinearities. Also, any sensor noise present is accentuated by this high gain. The typical reason for these poor results is that the robust design
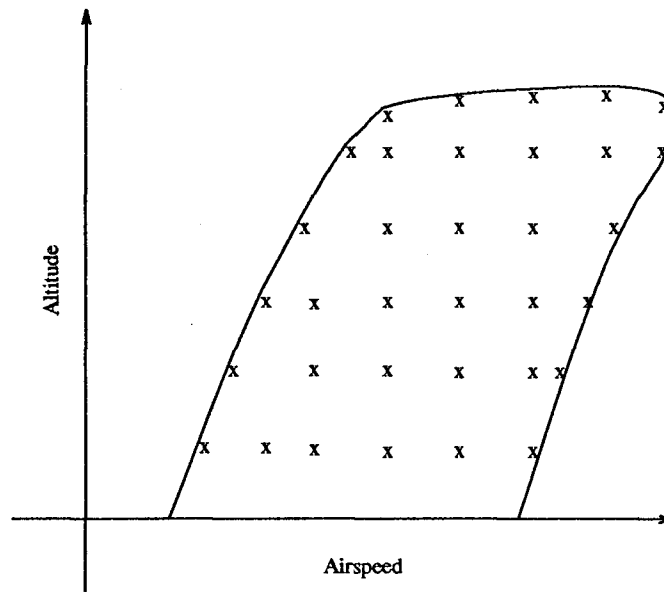
Figure 1.1   Airspeed-Altitude Design Points used in Traditional FCS Design

is synthesized in the essentially noiseless world of the digital computer, and then validated on the digital computer through the use of small signal, linear simulation. Is it any wonder that these designs exhibit unstable or unsatisfactory behavior when removed from this sterilized environment?

One robust control design technique that has the potential to avoid the aforementioned pitfalls is quantitative feedback theory (QFT). QFT is a mathematically rigorous, frequency domain, robust control design technique. Although a QFT design effort could very easily result in a compensator of high order and of high gain, it does give the designer complete control over the gain and order of the compensator; hence, QFT is not constrained to produce an impractical compensator. In addition, if a decision is made to decrease or limit the order or gain of a compensator, the performance tradeoffs due to this action can be clearly seen by the designer.

Due to the complex mathematics involved, the QFT design process can be very tedious and time-consuming if applied without the help of a capable computer-aided design (CAD) tool. As a result, most QFT design efforts prior to the development of a QFTCAD package by Sating in 1992 were constrained to be of very limited scope [9].

The only full subsonic flight envelope design effort using QFT has been that of Reynolds in 1993 [8]. Reynolds used QFT to design an FCS for the subsonic flight envelope of the VISTA F-16. Although Reynolds included all variations in the aircraft's response to control surface deflections due to airspeed and altitude changes, he did not include any variations caused by changes in the aircraft center of gravity (CG). Center of gravity changes are a result of either fuel consumption or the addition or expenditure of external stores. Reynold's recommendations were to extend his research to include CG variations along with those caused by airspeed and altitude changes [8].

In summary, although excellent FCS's have been designed for aircraft using traditional design methods, the synthesis of those FCS's has been a costly, time-consuming endeavor. Thus, limiting robustness in FCS design results in a convoluted, complex, full envelope design. QFT offers the hope of incorporating enough robustness to simplify the design process and the resulting FCS, but not so much robustness that the resulting FCS is impractical to implement due to violation of physical limitations imposed by the "real world" (i.e., actuator saturation or sensor noise amplification).

1.2 Research Objectives

The objectives of this research effort are:

1. Design a practical FCS for the subsonic flight envelope of the VISTA F-16 using QFT.

   (a) Include parameter uncertainty due to variations in the aircraft CG.

   (b) Keep compensator gain scheduling to an absolute minimum.

   (c) Achieve performance comparable to the current F-16 FCS.

   (d) Achieve Level 1 flying qualities.

   (e) Critically validate the resulting design with full consideration of "real world" factors such as control surface deflection limits and actuator rate limits.

2. Further QFT's standing as a viable robust control design method that can be applied to

practical problems and produce implementable results.

II. Research Methodology

The primary tool used to accomplish this flight control system design is QFT. However, due to the necessity to keep in touch with the "real world", an integrated design process which includes time domain simulation is utilized. Although such a process involves some iteration, the flexibility and insight provided by QFT keep it to a minimum. In other words, once a violation of a physical limitation is identified, the designer merely makes an insightfull adjustment to the present design rather than repeating another complete design iteration. Although unacceptable in mathematics, such trial and error is an accepted engineering practice. The parameter uncertainty for the QFT design is quantified by linear time-invariant perturbation aircraft models collected for many airspeed-altitude data points throughout and along the edges of the VISTA F-16 subsonic flight envelope. These aircraft models are generated for several different aircraft configurations. Generation of the aircraft models is discussed in Chapter III. Frequency domain validation is performed by the QFTCAD, and time domain validation is accomplished by examining the results of *Matlab* linear time simulations of the system's response to realistically large input signals.

2.1 QFT Description

A thorough discussion of the QFT design process is presented in the references and is not reproduced here [5]. However, the fundamentals of the technique as they apply to this research are addressed.

QFT is a two degree of freedom design technique utilizing the fundamental multiple-input single-output (MISO) structure illustrated in Figure 2.1 [5,6]. The two degrees of freedom available to the designer are the compensator G and the prefilter F. The characteristics of the uncompensated system are contained in the plant P.

2.1.1 Quantifying Parameter Uncertainty.   Before beginning a QFT design, the uncertainty to be handled by the design must be quantified. In the case of an FCS design, this
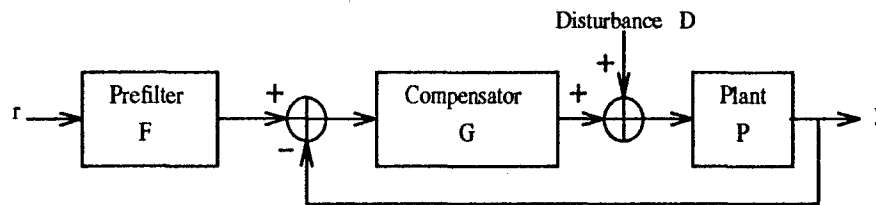
Figure 2.1   QFT MISO Design Structure

uncertainty is the variation in aircraft response to control surface deflections caused primarily by changes in airspeed, altitude, and CG position. This uncertainty is embodied in the aircraft's stability derivatives. Therefore, to quantify the uncertainty, aircraft stability derivatives for many airspeed-altitude-CG combinations spanning the flight envelope and aircraft configurations of interest are collected. These stability derivatives are assembled into transfer functions representing the aircraft response to the deflection of its control surfaces. These input-output transfer functions are referred to as the aircraft plants.

2.1.2   Frequency Templates.   Frequency templates are used in QFT to display parameter uncertainty. A frequency template is generated by plotting the open-loop frequency response of each aircraft plant at a particular frequency. The result is a collection of points (one for each plant) on a two-dimensional graph of relative angle versus relative magnitude as illustrated by the X's in Figure 2.2. Then, as shown in the figure, a polygon is drawn by connecting the outermost frequency response points so that all other points are contained within the polygon. This polygon is the template which corresponds to a given frequency and displays the uncertainty, in the frequency domain, embodied by all of the aircraft plants at that particular frequency. A family of templates is generated for a representative set of frequencies in the range of interest for a particular design. The resulting family of templates quantifies the parameter uncertainty of the system across the full design frequency spectrum.

The overall size of the templates indicates to the designer how much uncertainty the compensator will have to handle and whether or not a single compensator will be able to do the job. In
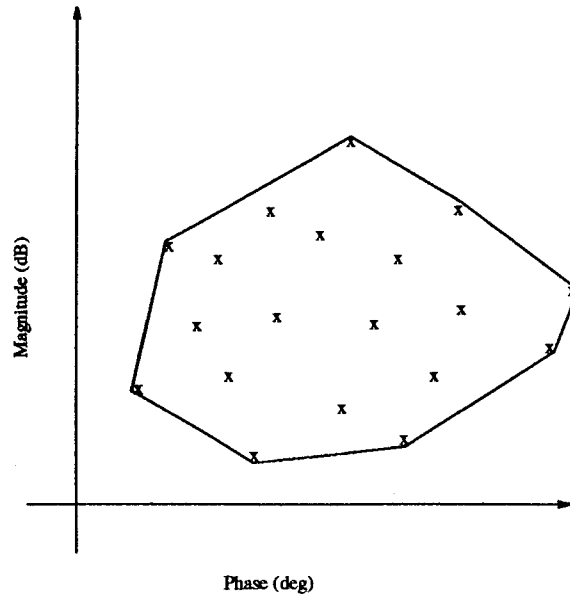
Figure 2.2   QFT Frequency Template

addition, if it is determined that the compensator design must be split into more than one part (i.e., full envelope robustness cannot be achieved), the templates provide valuable insight as to where in the parameter space the design should be divided.

2.1.3   Definition of Specifications.   In a QFT design, it is necessary to define frequency domain specifications for tracking response, stability, and external disturbance rejection.

Design tracking specifications are typically defined in the time domain and must be transformed into the frequency domain in order to be used in QFT. This transformation is accomplished by modelling the acceptable range of desired time domain responses of the system by two transfer functions (e.g., one representing the most underdamped response allowed, and the other representing the most overdamped response allowed). The frequency response of these models is plotted to form upper and lower tracking bounds, T_{RU} and T_{RL}, as depicted in Figure 2.3. The difference between T_{RU} and T_{RL} at a particular frequency is referred to as δ_R and represents the acceptable variation between the frequency responses of all of the plants at that frequency. In other words, δ_R defines the frequency domain robustness required of the design at each frequency. To facilitate the
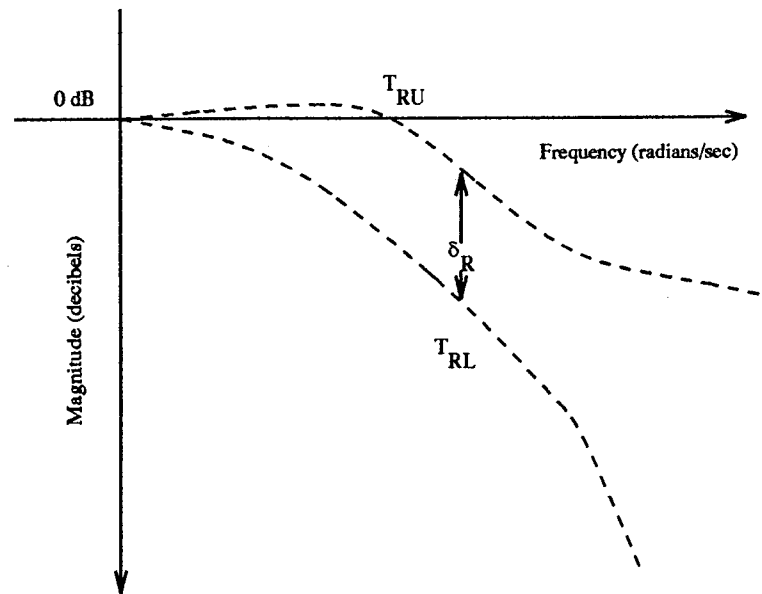
Figure 2.3   QFT Tracking Specification Bounds

design of the compensator, T_{RU} and T_{RL} should be synthesized so that δ_R monotonically increases above the 0 decibel (dB) crossing frequency of T_{RU} [5].

Stability specifications are typically expressed in frequency domain terms of open-loop phase and/or gain margins and can be used directly in QFT.

External disturbance rejection specifications for a disturbance input to the plant, as shown by D in Figure 2.1, are typically modelled by a constant value (e.g., -20 dB) for all frequencies as shown by T_{DU} in Figure 2.4. Since disturbances to the plant input are the only disturbance of interest in this FCS design, disturbances to the plant output are not discussed; however, disturbances to the output can be accounted for in a QFT design if required [5].

2.1.4   QFT Design Nichols Chart Boundaries.   The uncertainty embodied by the frequency templates is used along with the desired performance dictated by the tracking, stability, and disturbance rejection models to generate QFT design boundaries on a Nichols chart. These design boundaries are used to guide the synthesis of a compensator to achieve the desired results.
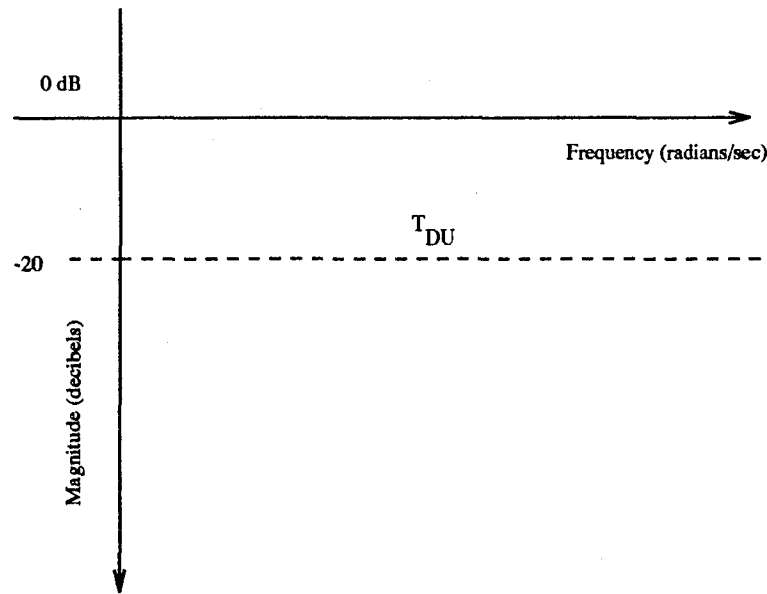
Figure 2.4   QFT External Disturbance Rejection Specification Bound

Prior to generating these design boundaries, the designer selects a nominal plant. The system open-loop transfer function (OLTF) generated using this nominal plant is the only one used in the design of the compensator. The nominal plant is typically a plant located at a particular position along the border of the frequency templates. This selection is heavily dependent on the specific design requirements, but some general guidelines are presented in the reference [5].

Once a nominal plant is selected, Nichols chart tracking, external disturbance rejection, and stability design boundaries are generated for each one of the template frequencies. Referencing Figure 2.1, the nominal OLTF from the output of the prefilter F to the system output y is

$$L_o = GP_o \qquad (2.1)$$

where P_o is the nominal plant. The design boundaries are generated to direct the shaping of this nominal loop, L_o.

The previously computed frequency templates are used to synthesize the Nichols chart boundaries, which, if satisfied by the nominal loop, guarantee that all of the open-loop functions $L_i = GP_i$

2-5
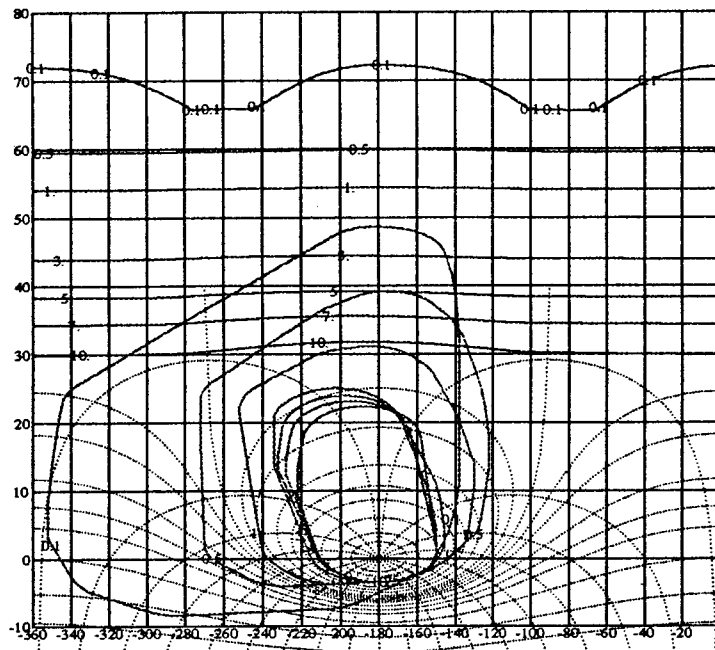
Figure 2.5   QFT Nichols Chart Design Boundaries

meet the tracking, stability, and external disturbance rejection specifications. The procedure used

to generate these boundaries is thoroughly discussed in the reference [5]. An example of these

Nichols chart boundaries is shown in Figure 2.5, where the stability boundaries are the closed

boundaries encircling the {0 dB, -180 degree} point, and the horizontal boundaries are a composite

boundary formed by displaying the most restrictive (i.e., the highest on the Nichols chart) of the

tracking and disturbance rejection boundaries at each phase angle [1]. Note that there is a stability

and composite boundary for each one of the template frequencies.

2.1.5   QFT Compensator Design.   The compensator G of Figure 2.1 is now synthesized

by plotting $L_o = GP_o$ on the Nichols chart containing the design boundaries. Poles and zeros are

added to G and its gain adjusted until the boundaries are satisfied by the nominal loop. If the

uncompensated OLTF P_o is not type 1 (i.e., it lacks pure integral action), the first step taken is

to give G a pole at the origin to guarantee zero steady-state tracking error of a step input and to

provide disturbance rejection [5].

To satisfy a tracking or disturbance boundary, the magnitude-phase point of L_o corresponding to the boundary frequency must lie on or above the boundary. Also, to satisfy a stability boundary the magnitude-phase point of L_o corresponding to the boundary frequency must lie outside the boundary. A typical loop shaping Nichols chart is depicted in Figure 2.6 [1]. The nominal loop is the line which starts at the top of the figure at -180 degrees of phase and then curves right to avoid the stability boundaries and finally curves left once below the stability boundaries.

Satisfying the tracking boundary at a particular frequency ensures that the required robustness is achieved by all of the closed-loop frequency responses at that frequency. In other words, the difference between the smallest magnitude and largest magnitude frequency response of all the closed-loop functions

$$\frac{GP_i}{1 + GP_i} \tag{2.2}$$

is less than or equal to the δ_R (defined in Figure 2.3) that corresponds to that tracking boundary frequency.

The synthesis of a compensator that ensures the nominal loop satisfies all of the tracking boundaries results in closed-loop frequency responses like those shown in Figure 2.7. As is seen in the figure, all of the closed-loop frequency responses are within δ_R of one another at all frequencies, but they do not yet fall between T_{RU} and T_{RL}; hence, although the required robustness has been achieved, the performance of the system does not yet meet specifications.

Satisfying the disturbance boundary at a particular frequency ensures that the magnitude of all of the closed-loop frequency responses at that frequency from the disturbance input D of Figure 2.1 are less than T_{DU} of Figure 2.4. It follows that if a compensator is synthesized which ensures L_o satisfies all of the disturbance rejection boundaries, then the frequency responses of all the disturbance input closed-loop functions

$$T_{D_i} = \frac{P_i}{1 + GP_i} \tag{2.3}$$

2-7
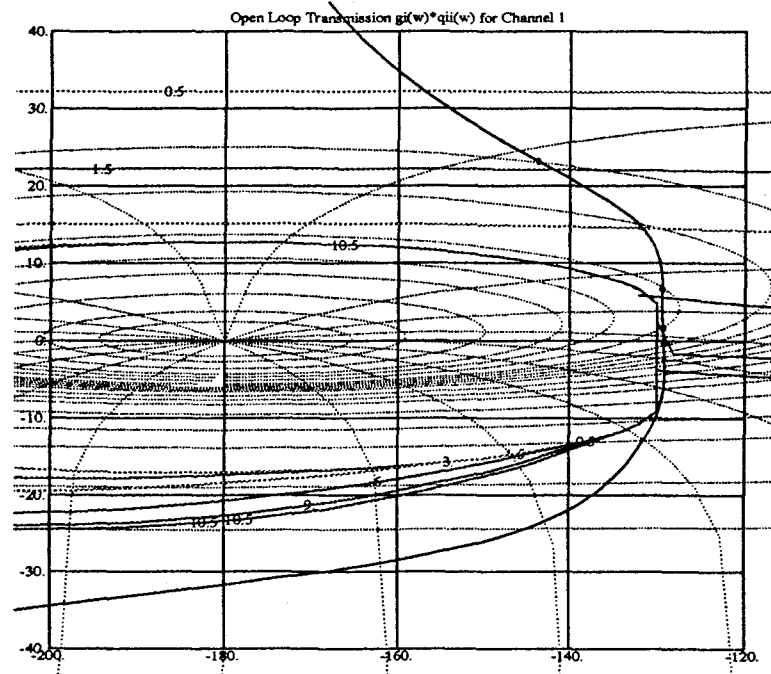
Figure 2.6   QFT Nominal Loop Shaping Nichols Chart
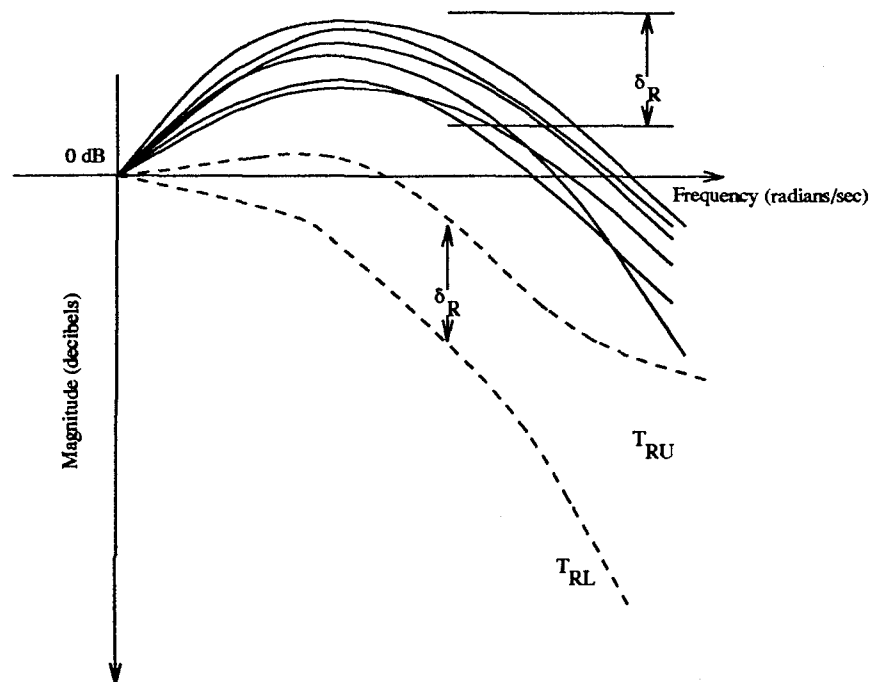
Figure 2.7   Tracking Input Closed-Loop Frequency Responses after Compensator Design
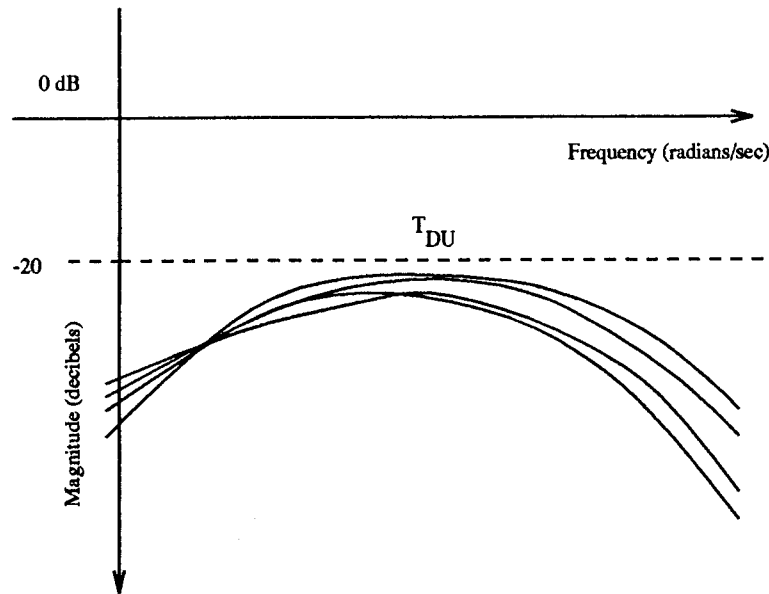
Figure 2.8   Disturbance Input Closed-Loop Frequency Responses after Compensator Design

lie below T_{D_U} for all frequencies as shown in Figure 2.8.

If the composite boundaries are satisfied, then the results displayed in Figures 2.7 and 2.8 are achieved simultaneously.

The necessary stability of the system can only be achieved by shaping L_o to remain outside the closed stability boundaries at all frequencies.

This is the point in the QFT design process at which the designer can evaluate the gain and order of G. If G needs to be reduced in order or gain, the designer can graphically see the design tradeoffs involved. The tradeoffs that can be readily evaluated on the Nichols chart include degredation of tracking response or disturbance rejection, decrease of stability (phase margin angle or gain margin dB), and the increase in phase or gain margin frequencies. Therefore, the designer can not only intelligently reduce the order or gain of G, but is immediately aware of the consequences of doing so.

2.1.6   QFT Prefilter Design.   The purpose of the prefilter F of Figure 2.1 is to shift the robust frequency responses of Figure 2.7 so that they fall between T_{RU} and T_{RL}. Therefore, this
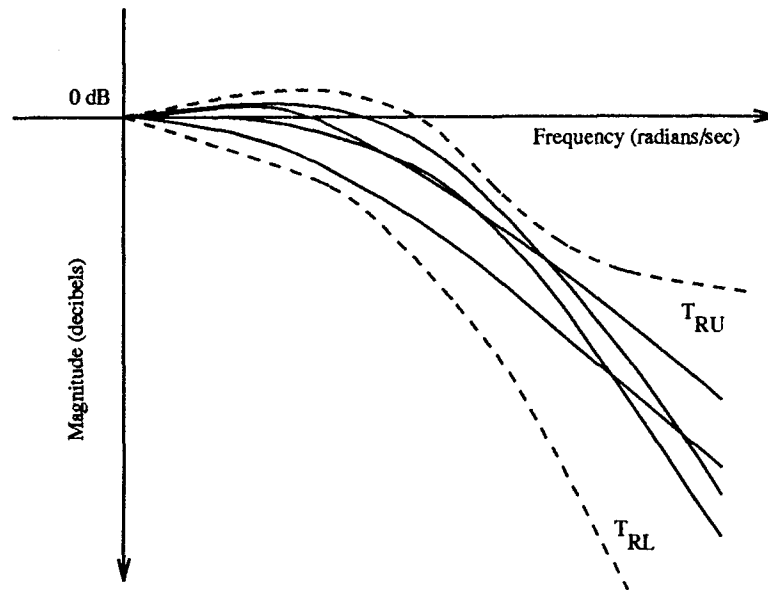
Figure 2.9 Successful QFT Design Closed-Loop Frequency Responses

final step in the QFT design process results in a design that produces the desired performance. Figure 2.9 illustrates the frequency responses of all the closed-loop functions

$$T_{R_i} = \frac{FGP_i}{1 + GP_i} \tag{2.4}$$

resulting from a successful QFT design.

2.1.7 Multiple-Input Multiple-Output QFT. All of the preceding discussion of the QFT design process has been directed towards MISO systems, but QFT can also be applied to multiple-input multiple-output (MIMO) control systems like the one in Figure 2.10. This is possible because any MIMO system can be represented equivalently as m^2 MISO unity feedback loops, where m is the dimension of a square MIMO system. The full proof of this equivalence can be found elsewhere and only the definition of the equivalent MISO loops will be presented here [5,6].

The structure of the equivalent MISO loops of a 2 X 2 MIMO control system is shown in Figure 2.11. The first subscript used in the figure refers to the output and the second subscript refers to the input. As an example, y_{12} refers to the part of the first output of the MIMO system
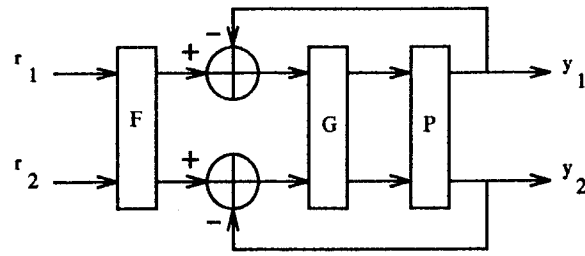
Figure 2.10   2 X 2 MIMO Control System
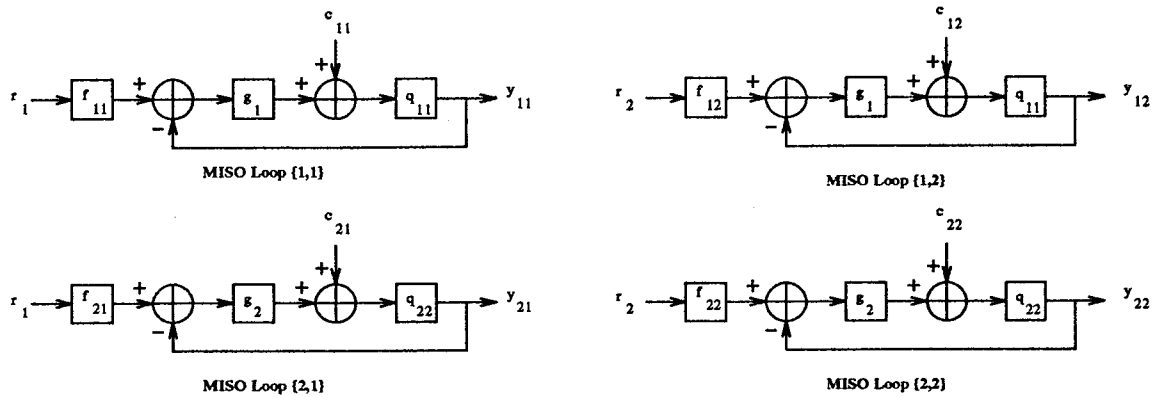
Figure 2.11   Equivalent QFT MISO Loops of a 2 X 2 MIMO Control System

that is a result of an input to the second MIMO input port. The prefilter and compensator are typically designed as diagonal and hence have the following structure.

$$
F = \begin{bmatrix} f_1 & 0 \\ 0 & f_2 \end{bmatrix} \tag{2.5}
$$

$$
G = \begin{bmatrix} g_1 & 0 \\ 0 & g_2 \end{bmatrix} \tag{2.6}
$$

The c_{ij}'s in Figure 2.11 represent the internal cross-coupling interaction of all the other loops with the loop of interest. The presence of the c_{ij}'s in the design structure makes this MISO structure fully representative of the original MIMO system.

The q_{ij}'s of Figure 2.11 are the elements of the equivalent MISO structure that embody the characteristics of the plant and are defined as follows. Let the inverse of the original plant be defined as

$$P^{-1} = \begin{bmatrix} p_{11}^{*} & p_{12}^{*} \\ p_{21}^{*} & p_{22}^{*} \end{bmatrix}. \tag{2.7}$$

The q_{ij}'s are then defined as the elements of the matrix

$$Q = \begin{bmatrix} \frac{1}{p_{11}^{*}} & \frac{1}{p_{12}^{*}} \\ \frac{1}{p_{21}^{*}} & \frac{1}{p_{22}}^{*} \end{bmatrix}. \tag{2.8}$$

Once the Q matrix has been calculated, each of the four loops can be designed using the MISO procedures outlined in the previous sections.

2.1.8   QFTCAD.   Fortunately, the QFTCAD package developed by Sating automates the design tasks described in the preceding sections and is utilized heavily during this design effort [1]. Without this package, a QFT design of this magnitude would be prohibitively tedious and time-consuming.

2.2   Time Simulation Description

All time simulations in this research are performed using *Matlab*'s 'rk45' algorithm [11]. This algorithm performs Runge-Kutta fifth order integration using fourth order step-size control. The tolerance of the integration is set at 10^{-5} and the minimum step size is set to 10^{-8}.

Also, the time simulations are conducted for a period of only five seconds for two reasons. First, when controlling an aircraft, pilots make control inputs more frequently than once every five seconds. To consider simulation for longer than a five second period would not make sense since the pilot will most likely have made several control inputs during that period. In other words, the low end of a pilot's control bandwidth is greater than 0.2 radians per second (rps). Second, the

linear perturbation aircraft models used in this design do not remain valid for simulations extended beyond five seconds.

2.3 Specific Design Guidelines

During the QFT longitudinal and lateral channel compensator synthesis, several guidelines are followed. First, the primary frequency range of interest for meeting tracking response specifications is 0.5 to 3.5 rps, which corresponds to a typical pilot's control bandwidth [7].

Second, the set of template frequencies used during the QFT portion of the design is

$$\omega_i = \{0.05,\ 0.075,\ 0.1,\ 0.25,\ 0.5,\ 0.75,\ 1,\ 3,\ 5,\ 7,\ 10,\ 15,\ 20,\ 25,\ 30,\ 50\}\ rps. \qquad (2.9)$$

Third, the compensators are designed so that the bending modes of the aircraft are not excited. These bending modes are isolated to frequencies above 30 rps; hence, to prevent their excitation, the phase margin frequency ω_ϕ of all the compensated OLTF's must be kept at or below 30 rps [7]. To satisfy this ω_ϕ requirement, the nominal plant for this design is chosen as the plant located at the top of the 30 rps frequency template. In this case, if the nominal OLTF has an ω_ϕ of 30 rps, it is guaranteed that all other plant OLTF's have an ω_ϕ of less than 30 rps; therefore, none of the plant responses interact with the bending modes of the aircraft. This choice of nominal plant is the only one that allows the designer to easily limit the ω_ϕ of all plant OLTF's.

Fourth, restrictions are placed on the compensators themselves. The resulting compensators must be of third-order or less, and no poles of the compensators are to be faster than 60 rps. The first of these restrictions is to keep the compensator dimension to an implementable level. The second restriction is imposed in anticipation of future digitization of the design. The detrimental aliasing effects present when digitizing at the typical sampling rates used in flight control (e.g., 50 Hz) are avoided if the compensator poles are selected to comply with the 60 rps restriction.

2-13

Control Surface	Deflection Limit
horizontal tail	±20 degrees
flaperons	±20 degrees
rudder	±30 degrees

Table 2.1   Control Surface Deflection Limits

Fifth, the physical limitations of actual aircraft hardware that restrict the FCS design are defined. One piece of hardware considered is the control surface hydro-mechanical actuator. The actuator has a 60 degree per second rate limit. If a rate higher than this is demanded, the actuator is saturated. The aircraft control surfaces also impose restrictions on the FCS design. The deflection limit used in this design for each of the aircraft control surfaces is listed in Table 2.3. If the FCS demands more deflection than is physically available, control surface saturation occurs. Both actuator rate and control surface deflection saturation may significantly degrade performance and reduce FCS stability, and are therefore avoided in this design.

Finally, the prefilters chosen must not restrict the control bandwidth of the pilot. The typical bandwidth of a pilot is 0.5 to 3.5 rps [7]; Consequently, the prefilters of this design must have bandwidths of no less than 3.5 rps.

III. FCS Design Aircraft Model

To quantify the parameter uncertainty involved in a subsonic flight envelope FCS design including changes in the aircraft CG, linear time-invariant (LTI) aircraft models are generated that span the airspeed-altitude-CG parameter space. These aircraft models are used as the plants in the ensuing QFT design.

3.1 LTI Aircraft Model Generation

The tool chosen to generate the required LTI aircraft models is the Simulation/Rapid-Prototyping Facility (SRF) which is available at the Wright-Patterson Air Force Base Flight Dynamics Laboratory [4]. Once an altitude, airspeed, and configuration are input to the SRF, nonlinear equations of motion are linearized about this operating point and stability derivatives in the form of state space **A** and **B** matrices are generated. The arrangement of the stability derivatives in the

state space equation $\dot{x} = \mathbf{A}x + \mathbf{B}u$ is shown in Equation (3.1).

$$
\begin{bmatrix} \dot{\theta} \\ \dot{u} \\ \dot{\alpha} \\ \dot{q} \\ \dot{\phi} \\ \dot{\beta} \\ \dot{p} \\ \dot{r} \end{bmatrix}
=
\begin{bmatrix}
0 & 0 & 0 & 1 & 0 & 0 & 0 & 0 \\
X_\theta & X_u & X_\alpha & X_q & 0 & 0 & 0 & 0 \\
Z_\theta & Z_u & Z_\alpha & Z_q & 0 & 0 & 0 & 0 \\
M_\theta & M_u & M_\alpha & M_q & 0 & 0 & 0 & 0 \\
0 & 0 & 0 & 0 & 0 & 0 & 1 & \phi_r \\
0 & 0 & 0 & 0 & Y_\phi & Y_\beta & Y_p & Y_r \\
0 & 0 & 0 & 0 & 0 & L_\beta & L_p & L_r \\
0 & 0 & 0 & 0 & 0 & N_\beta & N_p & N_r
\end{bmatrix}
\begin{bmatrix} \theta \\ u \\ \alpha \\ q \\ \phi \\ \beta \\ p \\ r \end{bmatrix}
$$

$$(3.1)$$

$$
+
\begin{bmatrix}
0 & 0 & 0 & 0 & 0 \\
X_{\delta_{elev}} & 0 & X_{\delta_{flap}} & 0 & 0 \\
Z_{\delta_{elev}} & 0 & Z_{\delta_{flap}} & 0 & 0 \\
M_{\delta_{elev}} & 0 & M_{\delta_{flap}} & 0 & 0 \\
0 & 0 & 0 & 0 & 0 \\
0 & Y_{\delta_{dftail}} & 0 & Y_{\delta_{ail}} & Y_{\delta_{rud}} \\
0 & L_{\delta_{dftail}} & 0 & L_{\delta_{ail}} & L_{\delta_{rud}} \\
0 & N_{\delta_{dftail}} & 0 & N_{\delta_{ail}} & N_{\delta_{rud}}
\end{bmatrix}
\begin{bmatrix} \delta_{elev} \\ \delta_{dftail} \\ \delta_{flap} \\ \delta_{ail} \\ \delta_{rud} \end{bmatrix}
$$

The units of each of the states listed in Equation (3.1) are listed in Table 3.1. It is evident from this state space representation that the longitudinal and lateral channels are considered completely decoupled or independent of one another. This is consistent with the steady level trim conditions at which the plants are generated.

3-2

State	Units
θ	deg
u	ft/sec
α	deg
q	deg/sec
ϕ	deg
β	deg
p	deg/sec
r	deg/sec

Table 3.1   Units of Aircraft Model States

3.2   Longitudinal Aircraft Model

The state space longitudinal aircraft model extracted from Equation (3.1) is

$$
\begin{bmatrix} \dot{\theta} \\ \dot{u} \\ \dot{\alpha} \\ \dot{q} \end{bmatrix} = \begin{bmatrix} 0 & 0 & 0 & 1 \\ X_\theta & X_u & X_\alpha & X_q \\ Z_\theta & Z_u & Z_\alpha & Z_q \\ M_\theta & M_u & M_\alpha & M_q \end{bmatrix} \begin{bmatrix} \theta \\ u \\ \alpha \\ q \end{bmatrix} + \begin{bmatrix} 0 \\ X_{\delta_{elev}} \\ Z_{\delta_{elev}} \\ M_{\delta_{elev}} \end{bmatrix} \begin{bmatrix} \delta_{elev} \end{bmatrix}.
\tag{3.2}
$$

The flap function of the F-16 flaperons is selected only during the takeoff and landing phases of flight; hence, since the takeoff and landing phases of flight are not considered in this FCS design, the δ_{flap} control input has been eliminated.

Pilot control inputs are typically spaced no further apart than five seconds; therefore, five seconds is accepted as an appropriate time period of interest in flight control system design. Due to the dominance of the short period mode in the five seconds following a control input, the short period approximation is used in the longitudinal channel design process. The resulting short period approximation state space model is shown in Equation (3.3).

$$
\begin{bmatrix} \dot{\alpha} \\ \dot{q} \end{bmatrix} = \begin{bmatrix} Z_\alpha & Z_q \\ M_\alpha & M_q \end{bmatrix} \begin{bmatrix} \alpha \\ q \end{bmatrix} + \begin{bmatrix} Z_{\delta_{elev}} \\ M_{\delta_{elev}} \end{bmatrix} \begin{bmatrix} \delta_{elev} \end{bmatrix}
\tag{3.3}
$$

In Equation (3.3), the control input δ_{elev} refers to the symmetric component of aircraft horizontal tail deflections.

The corresponding state space output equation $y = \mathbf{C}x + \mathbf{D}u$ for this short period longitudinal system is,

$$y = \begin{bmatrix} 1 & 0 \\ 0 & 1 \end{bmatrix} \begin{bmatrix} \alpha \\ q \end{bmatrix} + \begin{bmatrix} 0 \\ 0 \end{bmatrix} \begin{bmatrix} \delta_{elev} \end{bmatrix}. \tag{3.4}$$

One final action taken is to change the sign of the SRF generated $\mathbf{B}$ matrix of Equation (3.3). This action establishes the convention of positive elevator deflection resulting in positive changes in q and α.

In summary, since the longitudinal channel is fully decoupled from the lateral channel (see Equation (3.1)) and the flaps are eliminated as a control input, the resulting longitudinal model represents a single-input single-output (SISO) system void of any cross-coupling effects from the lateral channel.

3.3 Lateral Aircraft Model

Unlike the longitudinal channel where an approximation (short period) is made, the full lateral state space model including the spiral, dutch roll, and roll modes is used in the lateral channel

design. The lateral state space model extracted from Equation (3.1) is listed in Equation (3.5).

$$
\begin{bmatrix} \dot{\phi} \\ \dot{\beta} \\ \dot{p} \\ \dot{r} \end{bmatrix} = \begin{bmatrix} 0 & 0 & 1 & \phi_r \\ Y_\phi & Y_\beta & Y_p & Y_r \\ 0 & L_\beta & L_p & L_r \\ 0 & N_\beta & N_p & L_r \end{bmatrix} \begin{bmatrix} \phi \\ \beta \\ p \\ r \end{bmatrix}
$$

$$
+ \begin{bmatrix} 0 & 0 & 0 \\ Y_{\delta_{dftail}} & Y_{\delta_{ail}} & Y_{\delta_{rud}} \\ L_{\delta_{dftail}} & L_{\delta_{ail}} & L_{\delta_{rud}} \\ N_{\delta_{dftail}} & N_{\delta_{ail}} & N_{\delta_{rud}} \end{bmatrix} \begin{bmatrix} \delta_{dftail} \\ \delta_{ail} \\ \delta_{rud} \end{bmatrix}
$$

$$(3.5)$$

In Equation (3.5) the three control inputs δ_{dftail}, δ_{ail}, and δ_{rud} correspond to differential deflection of the horizontal tails, aileron deflection of the flaperons, and rudder deflection, respectively.

The corresponding state space output equation $y = \mathbf{C}x + \mathbf{D}u$ for the lateral system is,

$$
y = \begin{bmatrix} 1 & 0 & 0 & 0 \\ 0 & 1 & 0 & 0 \\ 0 & 0 & 1 & 0 \\ 0 & 0 & 0 & 1 \end{bmatrix} \begin{bmatrix} \phi \\ \beta \\ p \\ r \end{bmatrix} + \begin{bmatrix} 0 & 0 & 0 \\ 0 & 0 & 0 \\ 0 & 0 & 0 \\ 0 & 0 & 0 \end{bmatrix} \begin{bmatrix} \delta_{dftail} \\ \delta_{ail} \\ \delta_{rud} \end{bmatrix} \tag{3.6}
$$

A final action taken is to change the sign of the SRF generated $\mathbf{B}$ matrix of Equation (3.5). This action establishes the convention of positive aileron and differential tail deflections resulting in positive changes in p and the convention of positive rudder deflection resulting in positive changes in r and negative changes in β.

The resulting lateral model represents a 3 X 2 MIMO system void of any cross-coupling effects from the longitudinal channel.

3.4 Parameter Space Boundaries

The subsonic flight conditions spanned by this design include all flying airspeeds between and including the altitudes of 1,000 and 50,000 feet. Variation in aircraft CG position is accomplished by generating models for the preceding flight conditions for each of four different aircraft configurations available in the SRF [4]. These configurations are:

1. Clean (no external fuel tanks)

2. Centerline fuel tank

3. Two wing tanks

4. Three external fuel tanks (centerline and wings)

In Reynold's thesis, the first of these configurations was the only one considered.

Reynold's procedure for determining the low airspeed (left) side of the flight envelope by examining the behavior of the short period and phugoid roots of the aircraft longitudinal model of Equation (3.2) is repeated in this thesis [8]. The addition of external fuel tanks does have an effect on the airspeed below which the SRF will initialize and on the airspeed at which the short period and phugoid mode poles become well behaved. Hence, the left edge of the flight envelope is slightly different for each configuration.

Another consequence of the external fuel tanks is the introduction of transonic effects at a lower airspeed than for a clean configuration. Therefore, the behavior of the short period and phugoid mode poles between 0.8 and 0.9 Mach for the configurations with fuel tanks is observed. The highest Mach at which the modes become well behaved is used as the high airspeed (right) side of the subsonic flight envelope.

3.5   Validation of Parameter Space Data Points

One important issue to be settled is whether or not any flight condition/configuration data points exist in the parameter space that contain plant variation not already accounted for by the data points already selected. In other words, it needs to be validated that every bit of the aircraft plant variation for the design parameter space is contained in the generated LTI models. This can be determined by examining QFT frequency templates.

First, all of the short period longitudinal transfer functions from δ_{elev} to pitch rate q are loaded into the QFTCAD. The details of the procedure for generating transfer functions using *Matlab* and then formatting them for input into the QFTCAD are included in Appendix A. This generation procedure is used throughout this research in order to handle a large number of plants efficiently.

Second, the plants that form the perimeter of each frequency template are noted from an expanded template view like that shown in Figure 3.1 [1]. In all, 66 plants are labelled as perimeter plants. Next, the flight conditions corresponding to these perimeter plants are referenced. If all of the perimeter plants correspond to flight condition/configuration data points on the edge of the flight envelope, then the templates can only be expanded by gathering data for invalid flight conditions outside the actual VISTA F-16 flight envelope.

After referencing the flight conditions used by the SRF to generate the perimeter plants, it is determined that all of these plants are "edge of the envelope" plants except for a handful between the altitudes of 10,000 and 30,000 feet and between the airspeeds of 0.5 and 0.7 Mach. Consequently, additional plants are generated by the SRF using altitudes of 10,000, 20,000, and 30,000 feet and airspeeds at 0.05 Mach increments between 0.4 and 0.8 Mach. The short period approximation of the resulting plants is added to the 66 perimeter plants and input into the QFTCAD to see if any increase in template size is achieved. Figures 3.2 and 3.3 depict the templates for the original perimeter plants and those for the original plus the added plants, respectively. The difference
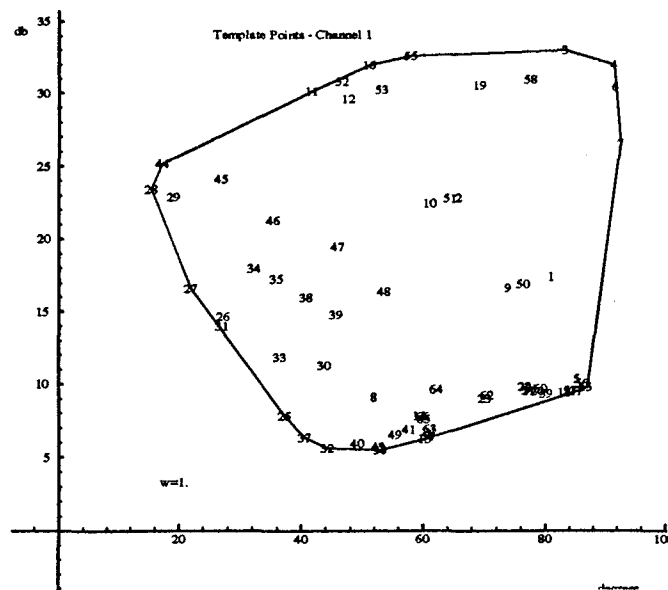
Figure 3.1   Expanded View of Frequency Template

between the two sets of templates is imperceptible in these figures. An expanded template view

reveals that a slight increase in template size (lower left region) is achieved by adding the extra

plants. This expanded view is illustrated for a frequency of 1 rps in Figure 3.4. The numbers above

66 in the figure represent the added plants. Also, the example expanded template in Figure 3.1 is

the template for only the original 66 perimeter plants The increase in template size can be seen

when it is compared to the template of Figure 3.4. Since the additional plants do increase the size

of the frequency templates, they are retained as parameter space data points.

At the completion of this QFT frequency template parameter space validation, it is stated with

some certainty that the frequency templates do encompass all of the plant uncertainty introduced

by variations in flight condition and configuration throughout the full subsonic flight envelope of

the VISTA F-16.

A complete list of the flight condition/configuration data points used in the design is contained

in Appendix B. In addition, a tabulation of SRF-generated stability derivatives and other pertinent

model data is found in the supplement to this thesis.

3-8
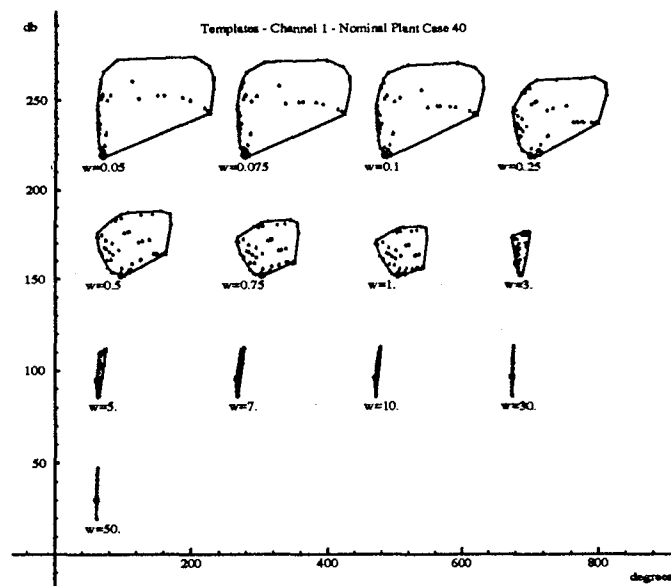
Figure 3.2   QFT Frequency Templates of Original Perimeter Plants
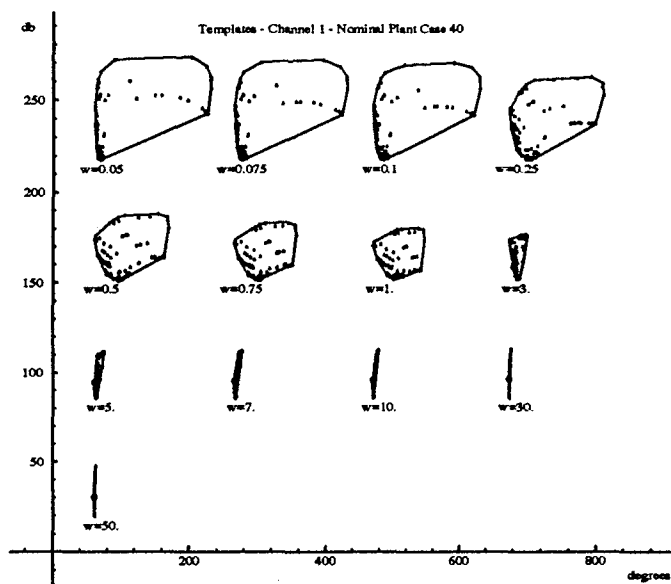
Figure 3.3   QFT Frequency Templates of Original and Added Validation Plants
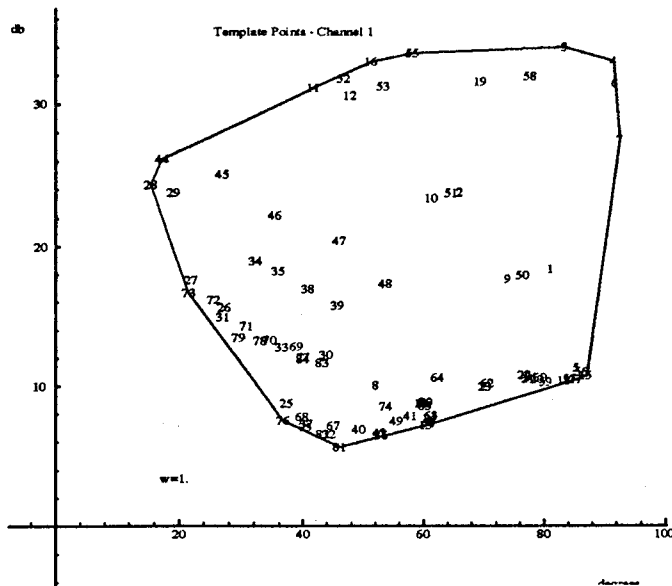
Figure 3.4   Expanded View of Frequency Template for $\omega = 1$ rps

3.6   Control Surface Actuator Model

The fourth-order actuator model used in Reynold's thesis is also chosen for this design and has the transfer function given in Equation (3.7).

$$\frac{\delta_{control}(s)}{\delta_{control_{(cmd)}}(s)} = \frac{(20.2)(71.4)^2(144.8)}{(s+20.2)(s+144.8)[s^2 + 2(0.736)(71.4)s + (71.4)^2]} \tag{3.7}$$

The "control" subscript in Equation (3.7) refers to any of the control surfaces of the aircraft. As discussed in Reynold's thesis, a fourth-order model is chosen instead of a first-order model due to its superior modelling of the actual actuator frequency response phase at higher frequencies [8].

IV. Longitudinal Channel Design

An integrated approach is used to accomplish the longitudinal channel FCS design. Quantitative feedback theory is used to design a compensator that meets frequency domain specifications and then time domain simulation is used to determine if any control surface deflection or actuator rate limits are exceeded. If either of these physical limitations is violated, the QFT compensator is adjusted and the time simulation is repeated.

4.1 Longitudinal Channel Inner Loop Design

Because the F-16 is statically unstable, the first step in the longitudinal channel design is to synthesize an inner feedback loop to stabilize any plants that have an unstable short period mode. The feedback parameter used is pitch rate q. This step is typical in classical flight contol system design and was also used in Reynold's design [3,8].

The overriding priority of the inner loop is to stabilize all of the plants so that an outer loop can be accomplished around stable effective plants. Also, since the short period approximation of the longitudinal dynamics is used, only the short period mode instabilities, and not those of the phugoid mode, are reflected.

The QFTCAD is used to design this loop using a 10 degree phase margin angle stability specification. This stability specification is input into the QFTCAD along with the structure shown in Figure 4.1. The previously generated transfer functions of $\frac{q}{\delta_{elev}}$ used to validate the parameter space are utilized (see Section 3.5). The resulting second-order compensator needed to stabilize all of the plants is given by Equation (4.1).

$$G_q(s) = \frac{0.75(s+10)(s+30)}{s(s+60)} \qquad (4.1)$$
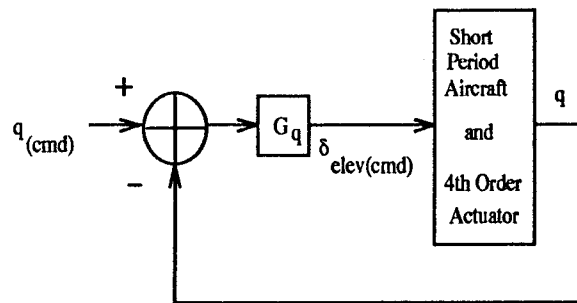
Figure 4.1   Inner Loop Design Structure
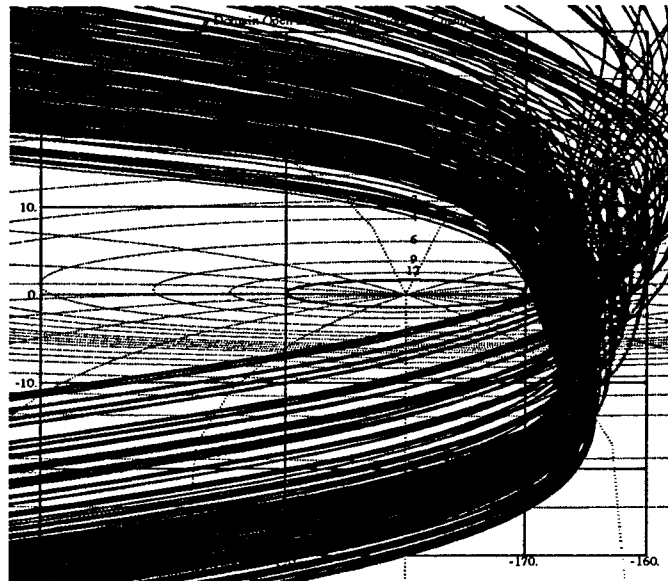
Figure 4.2   QFTCAD   Stability   Validation   for q Feedback   Inner   Loop   with
$G_q(s) = \frac{0.75(s+10)(s+30)}{s(s+60)}$

The corresponding QFTCAD stability validation Nichols plot is depicted in Figure 4.2. It is clear

from this figure that all of the plants cross the 0 dB line at a phase angle greater than -170 degrees,

thus satisfying the 10 degree phase margin angle requirement.

4.2   Longitudinal Channel Outer Loop Design

Before proceeding with an outer loop design, two issues must be addressed. The first is

selecting an outer loop feedback parameter and the second is validating the anticipated benefits of

an inner loop in the design.

4.2.1 Longitudinal Outer Loop Control Parameter. Although in Reynold's thesis the longitudinal outer loop parameter utilized was α for $\bar{q} \leq 130$ psf and C^* or N_z for $\bar{q} > 130$ psf, a different approach is attempted in this thesis [8]. This new approach involves a concerted effort to imbed flying qualities into the design by selecting an outer loop parameter which corresponds closely to what the pilot actually desires to control when he actuates the control stick.

Two assumptions are central in the development of the outer loop parameter. First, that the pilot possesses a general awareness of the energy state of the aircraft, and second, that the parameter the pilot wishes to control varies with the aircraft energy state. The author's expertise as an experienced F-16 pilot is relied upon to generate this dynamic parameter.

At lower energy states, where little aircraft g is available, the pilot commands primarily pitch rate q to accomplish his flight tasks. As the aircraft energy state increases and more g is available, the pilot turns more of his attention towards managing the g load, and less to managing q. The outer loop parameter is labelled C^* and is referred to as such in the remainder of this thesis. A physical explanation for the proportion of q and g_{pil} used to form C^* is that very few inflight tasks demanding precise pitch rate control by the pilot are performed at high dynamic pressures; however, precise tracking tasks are common at low and medium dynamic pressures. In addition, at high energy states where maximum aircraft g is available and sustainable, it is important that the pilot be able to accurately control g load so that his physical limitations are not exceeded. Figure 4.3 displays the proportion of q and g_{pil} that blend to create C^* at all subsonic $\bar{q}$, where g_{pil} is defined as the positive g force felt by the pilot. The crossover of q and g_{pil} on the figure corresponds approximately to the dynamic pressure at which the maximum allowable g is available to the pilot.

The C^* parameter is generated from the short period longitudinal state space plant of Equation (3.3) as follows. First, the longitudinal state space output relation $y = \mathbf{C}x + \mathbf{D}u$ of Equation (3.4) is augmented as shown in Equation (4.2), where the *shper* subscript refers to the state

4-3
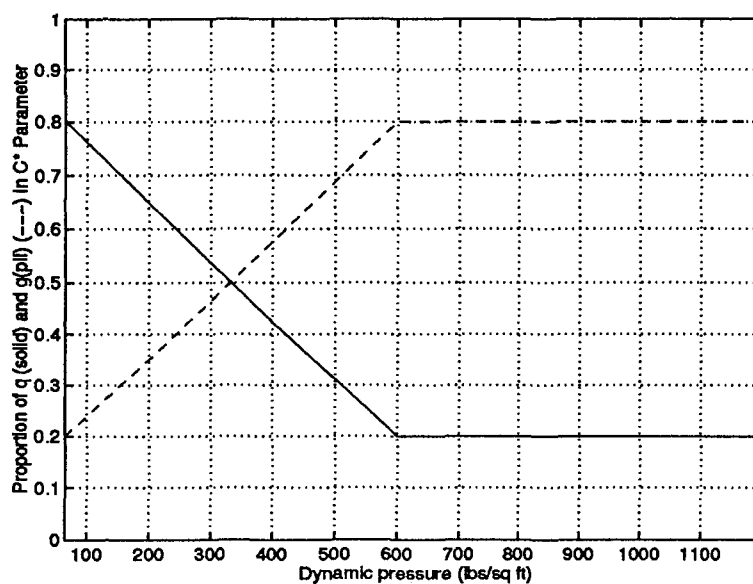
Figure 4.3   Allocation of q and g_{pil} in C^* Outer Loop Parameter versus $\bar{q}$

space matrices of Equation (3.3).

$$
y = \begin{bmatrix} C_{shper} \\ A_{shper} \end{bmatrix} \begin{bmatrix} \alpha \\ q \end{bmatrix} + \begin{bmatrix} D_{shper} \\ B_{shper} \end{bmatrix} \begin{bmatrix} \delta_{elev} \end{bmatrix} \tag{4.2}
$$

The resulting output vector of the augmented longitudinal system is,

$$
y = \begin{bmatrix} \alpha \\ q \\ \dot{\alpha} \\ \dot{q} \end{bmatrix}. \tag{4.3}
$$

The parameter g_{pil} is now generated using the relation

$$
g_{pil} = -N_z = -(\frac{\pi}{5796})[U(\dot{\alpha} - q) - l_x \dot{q}] \tag{4.4}
$$

(a) No Inner Loop

(b) Inner Loop Incorporated
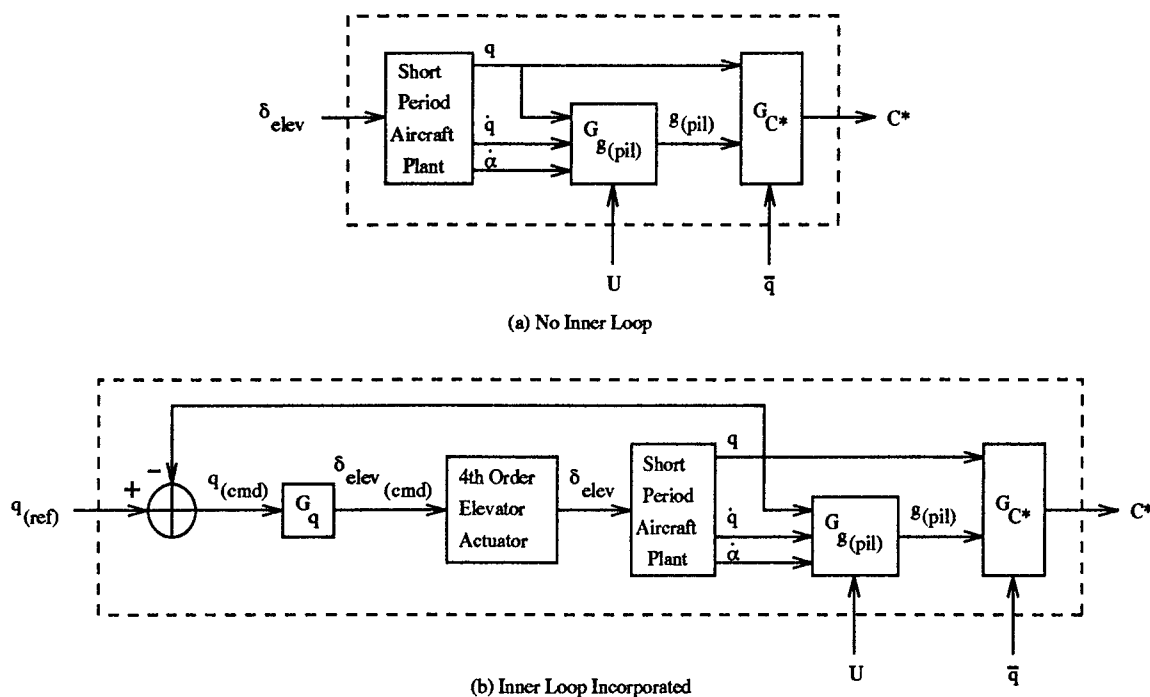
Figure 4.4   The C^* Plant Structures with and without an Inner Loop

where U is trim velocity in the x body axis direction and l_x is the distance from the aircraft center of gravity to the pilot station. Although the position of the aircraft center of gravity is slightly different for each aircraft configuration, a nominal value of 13.95 feet is used to generate g_{pil}. A detailed derivation of Equation (4.4) can be found in Reynold's thesis [8]. Finally, q and g_{pil} are blended to produce the dynamic pressure dependent C^* parameter profile depicted in Figure 4.3.

4.2.2   Inner Loop Benefits.   To evaluate the benefit of an inner loop in this design, frequency templates are generated for C^* with and without an inner loop. If the QFT frequency templates for the system with an inner loop are smaller in the desired frequency range, the inner loop is deemed to be of benefit; otherwise, the incorporation of an inner loop not only complicates the design but results in an outer loop compensator of higher order.

The necessary plant transfer functions for C^* are generated by *Matlab* using the structures illustrated in Figure 4.4 and then loaded into the QFTCAD.
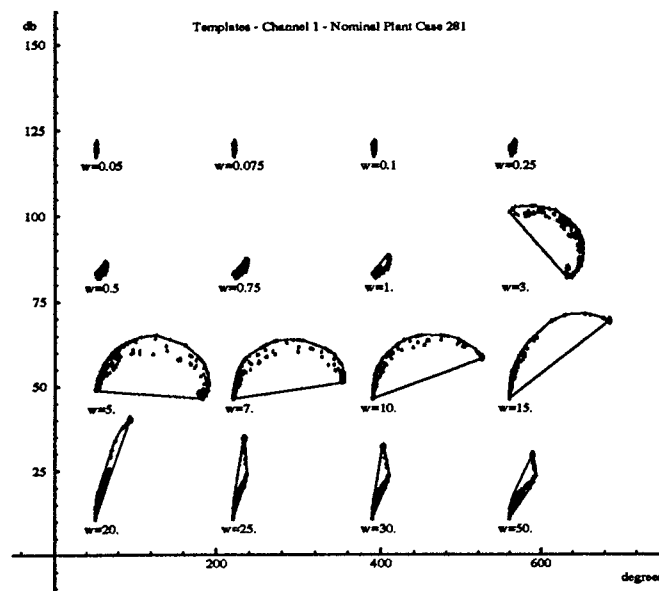
Figure 4.5   QFTCAD Frequency Templates for System with Inner Loop

The QFTCAD frequency templates for the longitudinal system with an inner loop are shown in Figure 4.5. These templates are compared to those in Figure 4.6, which are for the system without an inner loop. By examining these two figures, it is noted that the inner loop feedback does dramatically decrease the template size at low frequencies, but it increases the template size in the middle and high frequencies of interest in the design. Uncertainty at low frequencies is much easier to compensate for than uncertainty in the middle to high design frequencies. In addition, uncertainty below the typical control bandwidth of a pilot can be essentially dismissed. Consequently, the inner loop does not ease, but hinders the design effort and is therefore not incorporated.

4.2.3   Longitudinal QFT Specifications.   With the outer loop parameter and inner loop benefit issues settled, the next and necessary step in the design of the outer loop is the definition of the specification models required as input to the QFTCAD. The document used as the primary source for flying quality specifications is Military Standard 1797A (Mil Std) [2]. The specifications
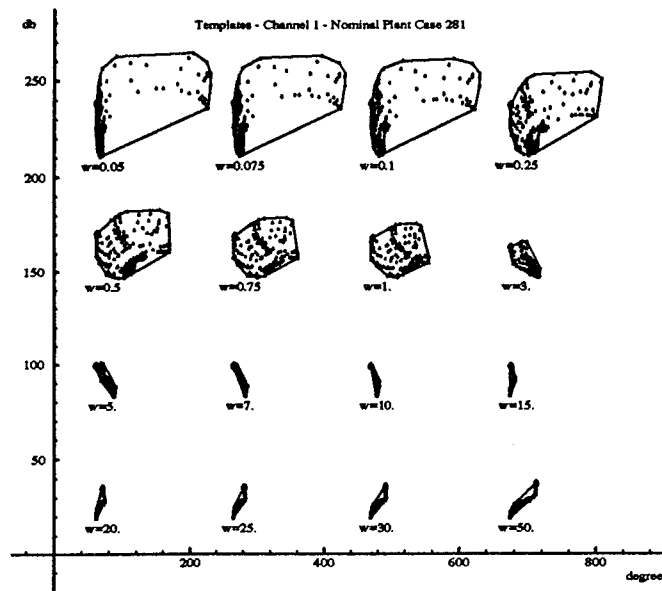
Figure 4.6   QFTCAD Frequency Templates for System **without** Inner Loop

Parameter	Specification
t_1	$t_{1_{max}} \leq 0.12$ second
Δt	$\frac{9}{V} \leq \Delta t \leq \frac{500}{V}$
$\frac{\Delta q_2}{\Delta q_1}$	$\frac{\Delta q_2}{\Delta q_1} \leq 0.3$

Table 4.1   Mil Std Longitudinal Time Domain Tracking Specifications

from the Mil Std used in this design are those necessary for the achievement of Level 1 flying qualities.

4.2.3.1   Tracking Specifications.   In the Mil Std the time domain tracking specifications are defined by analyzing a typical pitch rate response to a stick force step input. Figure 4.7 depicts a typical underdamped response to a step input with the necessary parameters used to define time domain tracking specifications labelled. Table 4.1 sets forth the specifications needed to achieve Level 1 flying qualities, where V is the aircraft velocity in feet per second. The t_1 parameter defines a maximum onset delay requirement, the Δt parameter dictates an onset rate requirement, and the $\frac{\Delta q_2}{\Delta q_1}$ ratio imposes a minimum damping requirement.

4-7
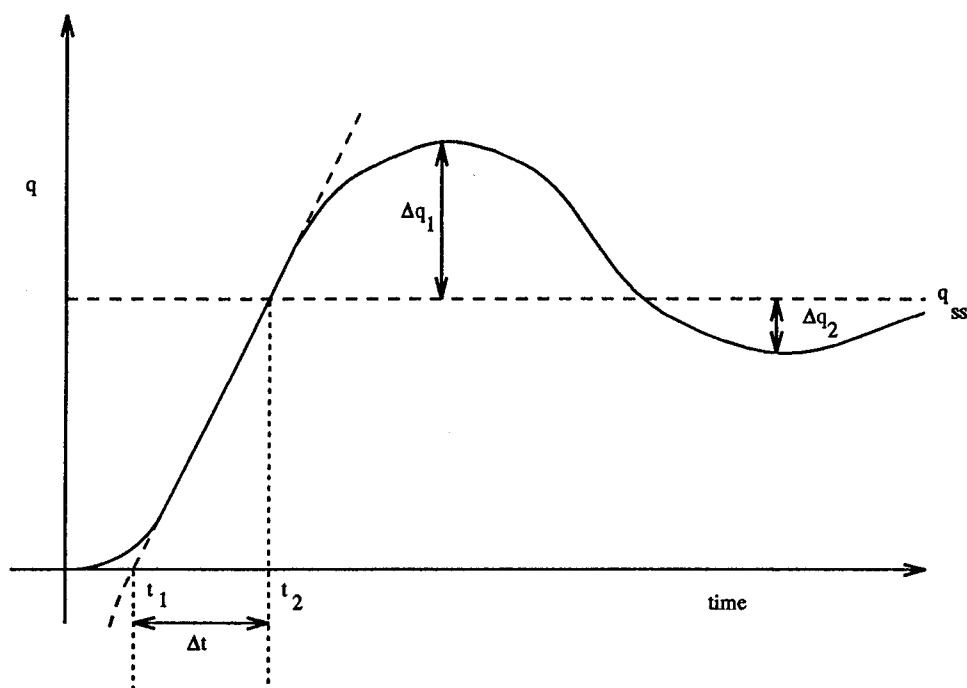
Figure 4.7 Step Response used to Define Longitudinal Response Specifications

A couple of difficulties exist when attempting to map these time domain specifications into the frequency domain. First, the specifications in Table 4.1 are based only on pitch rate response, but the outer loop parameter of this design is not solely pitch rate. Second, the allowable range of Δt varies with flight condition (aircraft velocity) and is therefore a floating specification.

The first of these difficulties is addressed in the following way. At the lower aircraft energy levels (i.e., at low airspeeds), C^* is primarily composed of pitch rate. The onset delay (t_1) and onset rate (Δt) requirements are most difficult to satisfy at low dynamic pressures due to reduced control surface effectiveness. Also, the Mil Std does not set forth any explicit time domain specifications for g_{pil} response to pilot pitch stick commands. Hence, the pitch rate step response specifications are used as the starting point for synthesizing QFT upper and lower tracking bound models.

Next, the issue of the floating Δt specifications is settled by selecting reasonable upper and lower limits on Δt based on the fact the lower velocity plants respond more slowly to pitch stick commands than the higher velocity plants.

The initial form of the upper tracking bound transfer function model is

$$T_{RU} = \frac{\omega_n{}^2}{s^2 + 2\zeta\omega_n + \omega_n{}^2}.$$ (4.5)

It is found that ζ must be greater than or equal to 0.35 in order to satisfy the $\frac{\Delta q_2}{\Delta q_1}$ damping specification from Table 4.1. A ζ of 0.4 is selected for the upper tracking bound model.

Next, an ω_n of 0.7 radians per second is selected for two reasons. First, most of the plant uncertainty occurs at frequencies less than or equal to 1 radian per second (see templates in Figure 4.6). Second, placing the responses with the greatest overshoot and slowest settling in the lower frequencies allows the pilot the most time to compensate for these undesired response characteristics, or possibly places these characteristics in frequencies below the bandwidth of the pilot.

The upper limit of a typical pilot's bandwidth is approximately 3.5 rps [7]. Consequently, the upper tracking bound model must have a bandwidth of at least 3.5 radians per second. A target bandwidth of 5 radians per second is chosen for the upper bound and is defined as the frequency at which the magnitude of the frequency response of the upper bound model descends through -3 dB. It is necessary to add a zero to the model in order to achieve the required bandwidth.

The time response overshoot $M_o = \Delta q_1$ is not given a maximum value by the Mil Std. A value of $M_o = 0.75$ is arbitrarily chosen as this maximum value to allow for a small Δt. A pole-zero pair is added to the model to achieve these characteristics while complying with the target bandwidth previously set forth. The resulting upper tracking bound model is

$$T_{RU} = \frac{5(s + 0.7)^2}{(s^2 + 0.56s + 0.49)(s + 5)}.$$ (4.6)

Model	t_1	Δt	$\frac{\Delta q_2}{\Delta q_1}$
T_{RU}	0	0.215	0.255
T_{RL}	0.113	1.132	overdamped

Table 4.2 QFT Upper and Lower Tracking Bound Model Step Response Characteristics

The primary concern in the synthesis of the lower tracking bound model is that the onset rate t_1 does not exceed 0.12 seconds. The initial model is

$$T_{RL} = \frac{2}{s+2} \tag{4.7}$$

chosen to ensure a bandwidth of 2 radians per second. The model is then augmented with another pole to fulfill the QFT requirement that the upper and lower bounds diverge above the frequency the upper bound crosses through 0 dB. This additional pole is placed at the lowest frequency possible without increasing the onset rate beyond 0.12 seconds. The resulting lower tracking bound model is

$$T_{RL} = \frac{6}{(s+2)(s+3)}. \tag{4.8}$$

These upper and lower QFT tracking bound models require all plants to have an onset rate less than 0.12 seconds, $M_o \le 0.75$, a $\frac{\Delta q_2}{\Delta q_1}$ ratio less than 0.3, and a bandwidth between 2 and 5 radians per second. Table 4.2 lists the exact characteristics of the step input time responses of the tracking models. In addition, Figure 4.8 depicts both the frequency response magnitude and step input time response plots of the QFT tracking bound models.

4.2.3.2 QFT Stability Specifications.   The required stability specifications are clearly set forth in the Mil Std. The open-loop frequency response of all plants must have a phase margin angle of at least 30 degrees and a gain margin of at least 6 dB. The 30 degree phase margin angle requirement is entered directly into the QFTCAD to generate the stability bounds, and the 6 dB gain margin is verified visually on the QFTCAD Nichols chart displays.
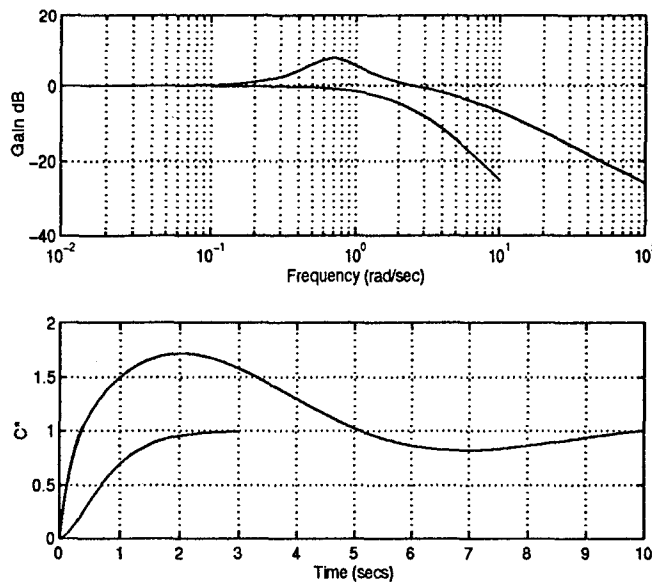
Figure 4.8   Frequency Response Magnitude (top) and Step Input Time Response (bottom) of QFT Upper and Lower Longitudinal Tracking Bound Models

4.2.3.3   QFT Disturbance Specifications.   A thorough discussion of modelling eleva-tor trim changes as an external disturbance is presented in Reynold's thesis [8]. It is uncertain, however, as to what level of disturbance rejection is desired or required in order to prevent the elevator trim changes from posing a problem to the pilot during longitudinal tracking tasks. In light of this uncertainty and considering the difficulty of satisfying even the tracking specifications required in this design, disturbance rejection is not prioritized above tracking. Instead, disturbance rejection is treated as a by product of meeting tracking specifications as opposed to being pursued as an end in itself. This is not unreasonable considering the fact that the longitudinal compensator of this design is required to have pure integral action which gives the system inherent disturbance rejection properties.

4.2.4   F-16 Longitudinal Performance Requirements.   To achieve performance compara-ble to the current F-16 FCS, performance benchmarks must be established. The performance benchmarks used in this design are

1. α - attain 25°, but do not exceed 30°

2. g_{pil} - attain 9 g's, but do not exceed 9.45 g's

Only the benchmark which is achieved first at each dynamic pressure is demanded of the FCS. For instance, at low dynamic pressures only benchmark 1 applies and at high dynamic pressures only benchmark 2 applies.

4.2.5   QFT Longitudinal Channel Design.   The plan of attack for the outer loop design is to synthesize the simplest compensator possible (maximum of third-order and with poles $\leq$ 60 rps) to meet the tracking specifications for the frequency range of 0.5 to 3.5 radians per second. The design is also required to meet stability specifications for all frequencies. If a single compensator cannot achieve the tracking or stability requirements, then either the gain of the compensator will be scheduled on $\bar{q}$, or a completely different compensator will be generated to be switched to at a particular $\bar{q}$.

4.2.5.1   QFTCAD Plant Input.   The C^* plants previously generated by *Matlab* from the structure of Figure 4.4(a) are used in the outer loop design. Once the plants are loaded, the effective plants P_e (which include the actuator dynamics) and the Q matrices are generated. In this generation process, the QFTCAD cancels poles and zeros within 0.001 of one another and eliminates all poles and zeros outside of the dynamic frequency range of 10^{-5} to 10^4 rps. The resulting plant, effective plant, and q transfer functions for all plants are listed in the supplement to this thesis.

4.2.5.2   QFTCAD Structure.   The structure entered into the QFTCAD for the longitudinal design is portrayed in Figure 4.9. Recall that the proportion of pitch rate and g_{pil} which make up C^* is dependent on the current dynamic pressure of the aircraft (see Figure 4.3).
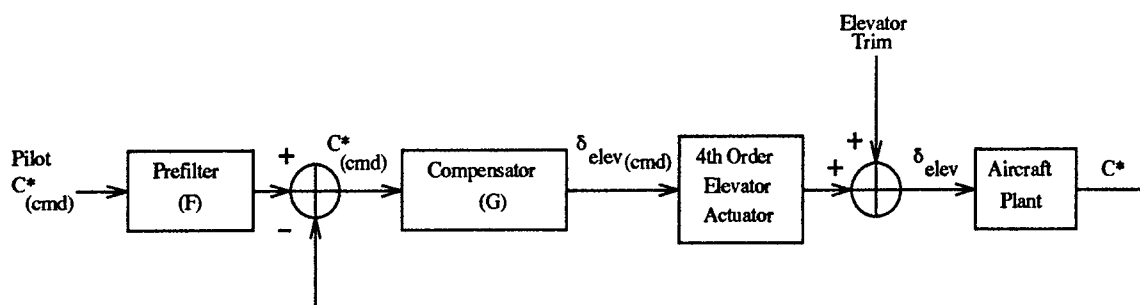
Figure 4.9   QFTCAD Longitudinal Channel Structure

4.2.5.3   QFT Design Boundaries.   The specifications discussed in Section 4.2.3 are entered into the QFTCAD to be used to generate design boundaries on the Nichols chart. However, before the boundaries can be generated, two items must be accomplished.

First, frequency templates must be formed. Recall that in this design templates are formed for the frequency spectrum

$$\omega = \{0.05, 0.075, 0.1, 0.25, 0.5, 0.75, 1, 3, 5, 7, 10, 15, 20, 25, 30, 50\}\ rps. \tag{4.9}$$

Second, a nominal plant is selected. Plant 281 is selected as the nominal plant due to its position at the top of the 30 rps template. The frequency templates for the outer loop are shown in Figure 4.6 with plant 281 shown as the nominal.

The QFTCAD now generates the tracking and stability boundaries to be used in the design. External disturbance boundaries are not generated because of the reasons discussed in Sections 3.2 and 4.2.3.3.

4.2.5.4   Outer Loop Compensator Design.   The QFTCAD 'Design Compensator' feature is selected, and the nominal open-loop function is shaped through the synthesis of the outer loop compensator G_{C^*}. To ensure zero steady-state step input tracking error and to enhance disturbance rejection, G_{C^*} is given a pole at the origin to make the forward transfer function Type 1 [5]. Next, poles and zeros are added to the compensator so that the nominal loop satisfies
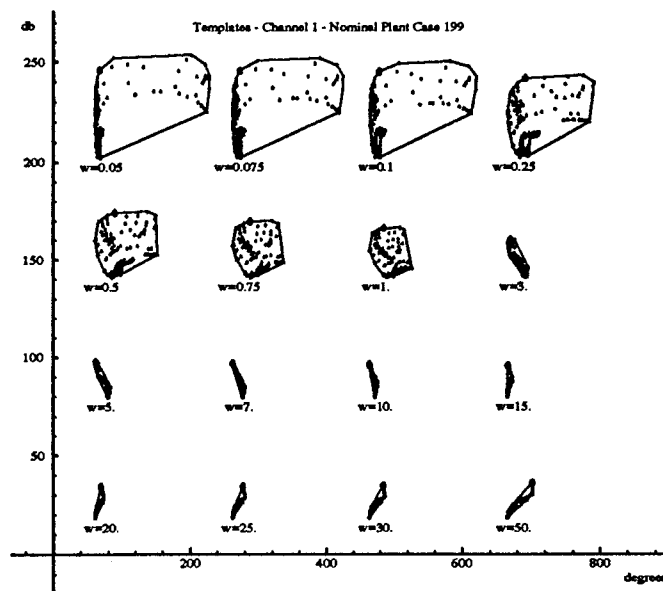
Figure 4.10   QFTCAD Longitudinal Frequency Templates for Clean, One Fuel Tank, and Two Fuel Tank Configurations

the necessary tracking and stability specifications set forth in Section 4.2.3. The compensator is then simulated using *Matlab* to observe the time domain performance of all of the plants and to identify any actuator rate or control surface deflection saturations. During this process, the first-order prefilter

$$F_{C^*} = \frac{3.5}{s + 3.5} \tag{4.10}$$

is used due to its bandwidth of 3.5 rps.

In the first design attempt, a single compensator of third-order could not shape the nominal loop to satisfy all of the tracking and stability boundaries. Rather than designing two separate compensators or applying gain scheduling, it is decided to eliminate all of the three fuel tank configured plants and then reaccomplish the design. The three tank F-16 configuration is normally used only in long range deployment missions, and not in weapon employment missions. Therefore, Level 1 flying qualities are required of only the clean, one fuel tank, and two fuel tank configurations. The QFTCAD frequency templates for the remaining 199 plants are displayed in Figure 4.10.

4-14
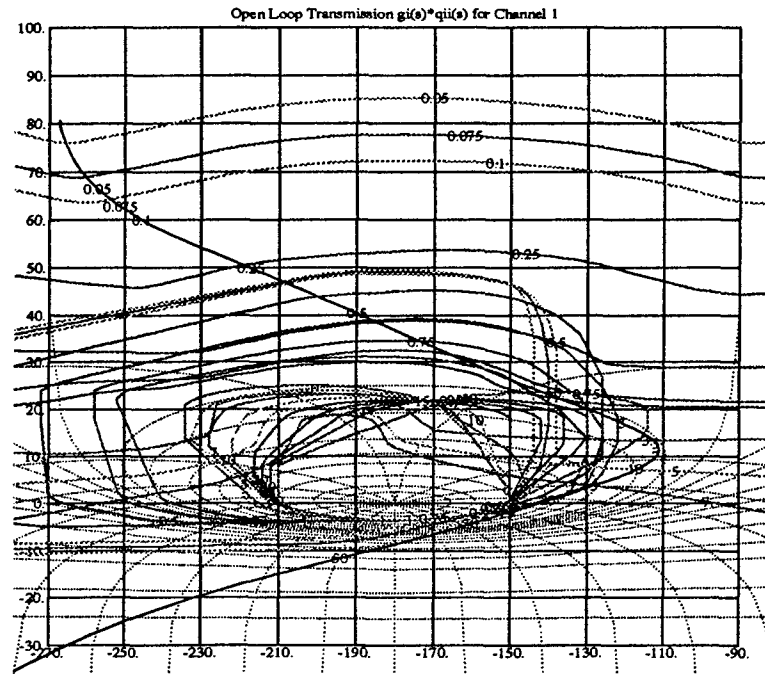
Figure 4.11 QFTCAD Nominal Loop Shaping Nichols Chart for $G_{C*} = \frac{3.3(s+1.7)(s+3.5)}{s(s+12)}$

After removing the three tank configurations, the QFTCAD/time simulation process described in the previous paragraphs results in the compensator

$$G_{C*} = \frac{3.3(s+1.7)(s+3.5)}{s(s+12)}. \tag{4.11}$$

The QFTCAD nominal loop shape along with tracking and stability bounds is depicted on the Nichols chart in Figure 4.11. This figure clearly shows that the nominal loop has an ω_ϕ of approximately 20 rps and a gain margin of greater than 6 dB. Since the nominal plant is located at the top of the frequency templates from 20 to 50 rps, all of the other plant loops have an ω_ϕ less than and a gain margin greater than the nominal loop. This figure also shows that the very low frequency tracking bounds are violated, but the bounds in the desired range of 0.5 to 3.5 rps are satisfied.

The 'Design Prefilter' QFTCAD display for $F_{C*} = \frac{3.5}{s+3.5}$ is shown in Figure 4.12. Since the very low frequency tracking bounds are not satisfied during the loop shaping, the upper and lower
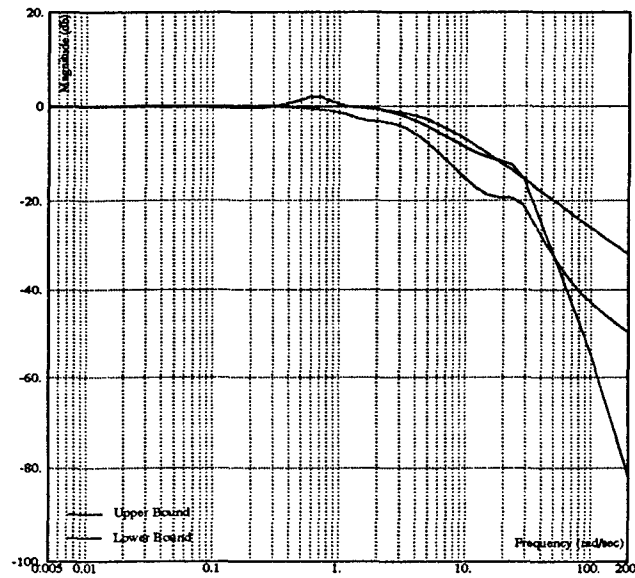
Figure 4.12   QFTCAD Prefilter Nichols Chart for $F_{C^*} = \frac{3.5}{s+3.5}$

prefilter bounds cannot be satisfied at these frequencies, but in the frequency range of 0.5 to 10 rps, the prefilter bounds are satisfied.

4.2.6   Longitudinal Design Time Domain Analysis.   The first step in the time domain analysis is to subject the compensated system to a unit C^*_{cmd} step input. The results of this simulation for a representative sample of plants spanning the full range of $\bar{q}$ are illustrated in Figures 4.13 and 4.14. The plots of δ_{elev} and α depict perturbations from the initial condition trim values, and not the total values including trim. The ballooning above 1.25 observed in the C^* step responses is for aircraft plants corresponding to dynamic pressures below 200 pounds per square foot (psf). The q response of every plant is evaluated against the requirements of Table 4.1. A tabulation of the results of this evaluation is contained in Appendix C.1. An inspection of the data in the appendix confirms that the onset delay, onset rate, and damping requirements of Table 4.1 are met by all plant models.

The method applied in this design to avoid physical saturations while meeting performance requirements is to scale the stick force input of the pilot rather than to directly schedule the

4-16
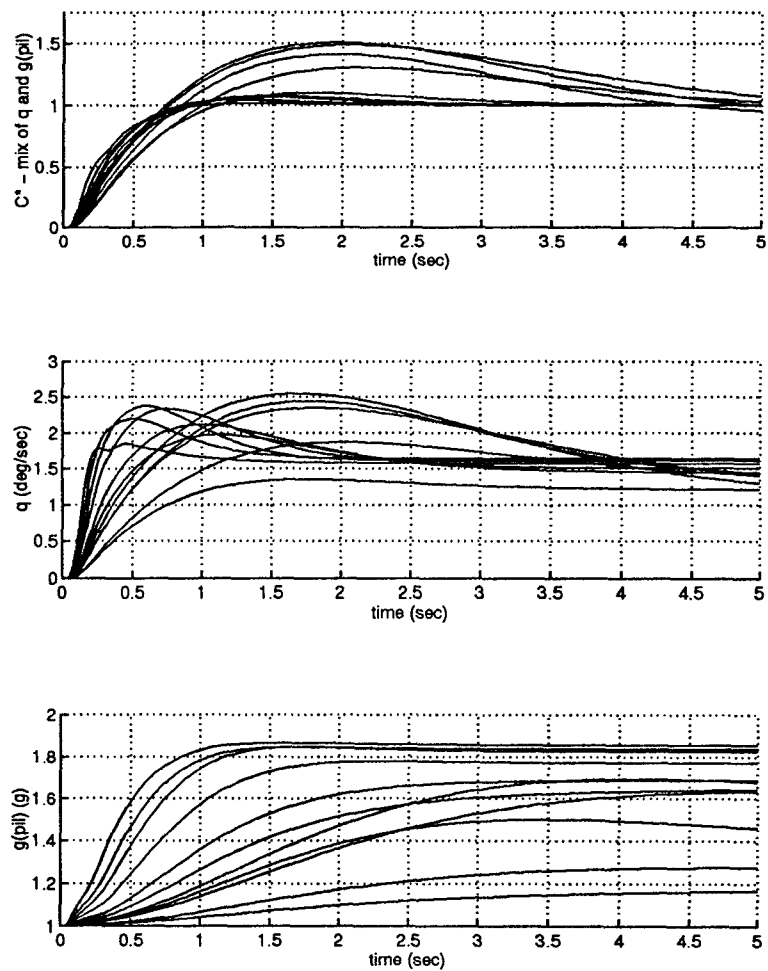
Figure 4.13   Compensated System Time Response to Unit C^*_{cmd} Step Input (1 of 2)
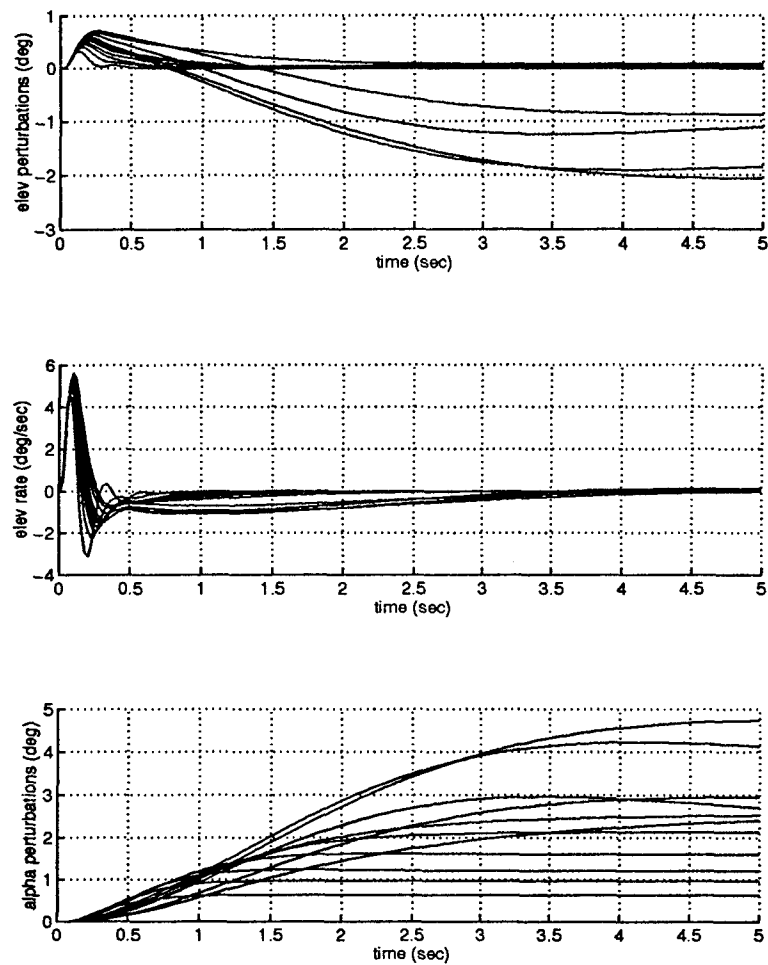
Figure 4.14   Compensated System Time Response to Unit C^*_{cmd} Step Input (2 of 2)

compensator gain. To accomplish the stick force scaling, a maximum C^*_{cmd} profile scheduled on $\bar{q}$ is synthesized using the results of the unit C^*_{cmd} step input time simulation. The data generated for each plant by Equations (4.12) through (4.15) is plotted versus $\bar{q}$ to form upper and lower bounds for this $C^*_{cmd(max)}$ profile.

$$min \begin{bmatrix} \frac{20-trim_{elev}}{max\{\delta_{elev(pert)}\}}, \ for \ \delta_{elev(pert)} > 0, \\ \\ and \\ \\ -\frac{20+trim_{elev}}{min\{\delta_{elev(pert)}\}}, \ for \ \delta_{elev(pert)} < 0 \end{bmatrix} \qquad (4.12)$$

$$\frac{60}{\delta_{elev(max)}} \qquad (4.13)$$

$$\frac{25 - \alpha_{trim}}{\alpha_{pert_{(ss)}}} \qquad (4.14)$$

$$\frac{8}{g_{pil_{(ss)}} - 1} \qquad (4.15)$$

The maximum C^*_{cmd} at a particular $\bar{q}$ must lie below the plot of Equations (4.12) and (4.13) in order to avoid elevator deflection and actuator rate limitations, respectively. Also, to achieve performance comparable to the current F-16 FCS, the $C^*_{cmd(max)}$ must, for all $\bar{q}$, allow the aircraft to reach either 25 degrees of α or 9 g's at the pilot station, whichever occurs first. This condition is met when the $C^*_{cmd(max)}$ profile is above the lowest of the two plots of Equations (4.14) and (4.15). The resulting maximum C^*_{cmd} profile is displayed in Figure 4.15 along with the upper and lower bounds. In order to help declutter the presentation, the lower bound reflecting desired α and g_{pil} performance is combined into a single bound by plotting only the minimum of the two individual bounds.

Next, the longitudinal FCS is subjected to step inputs equal to the maximum C^*_{cmd} from Figure 4.15 to validate the expected performance. The results of this simulation are recorded in Figures 4.16 and 4.17. It is evident in these figures that all of the aircraft plants not only meet, but some exceed the desired α and g_{pil} performance. A listing of the results of this simulation for
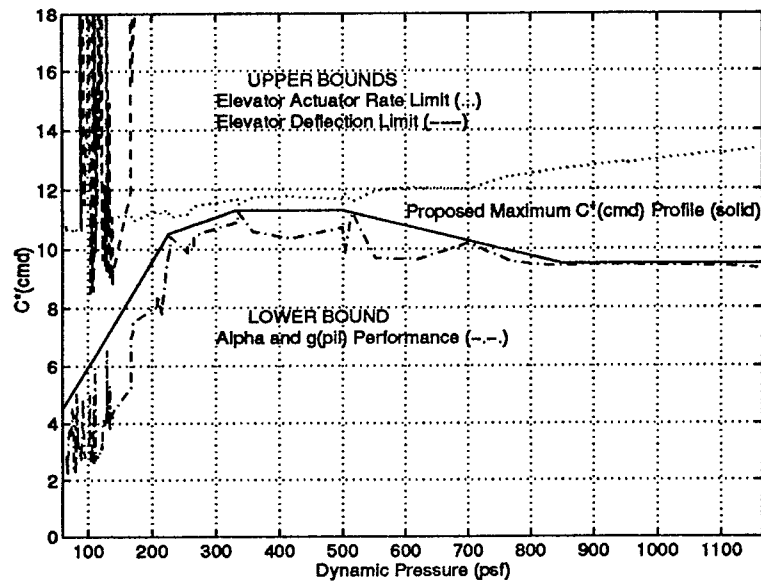
Figure 4.15   Maximum C^*_{cmd} Profile vs. $\bar{q}$ Along with Upper and Lower Bounds

all plants is contained in Appendix C.2. The fact that the desired maximum values of α and g_{pil} are exceeded warrants the discussion of limiters in the next section.

4.2.6.1   Longitudinal Channel Limiters.   Due to concern about loss of aircraft control, loss of pilot consciousness, or overstress of the aircraft itself, the need for longitudinal channel limiters is now assessed. In order to ensure aircraft stability, a maximum transient α of 30 degrees is desired. Also, a maximum overshoot of five percent (0.45 g for a 9 g aircraft) in g_{pil} is pursued. Finally, an upper limit of 6 g's per second is placed on g onset rate in order to reduce the likelihood of pilot loss-of-consciousness during the initiation of high g maneuvers. The time responses of Figures 4.16 and 4.17 indicate that limiters are required to satisfy these requirements.

An ad hoc limiter scheme involving rate and magnitude limiting of α and g_{pil} is concocted to satisfy the requirements set forth in the previous paragraph. Since α and g_{pil} are not each independently controlled by C^*_{cmd}, the limiting scheme is not as straight forward as simple regulation through feedback. Instead, the C^*_{cmd} input by the pilot is reduced through feedback as rates or magnitudes exceed certain values. Figure 4.18 graphically illustrates the ad hoc limiters used in

4-20
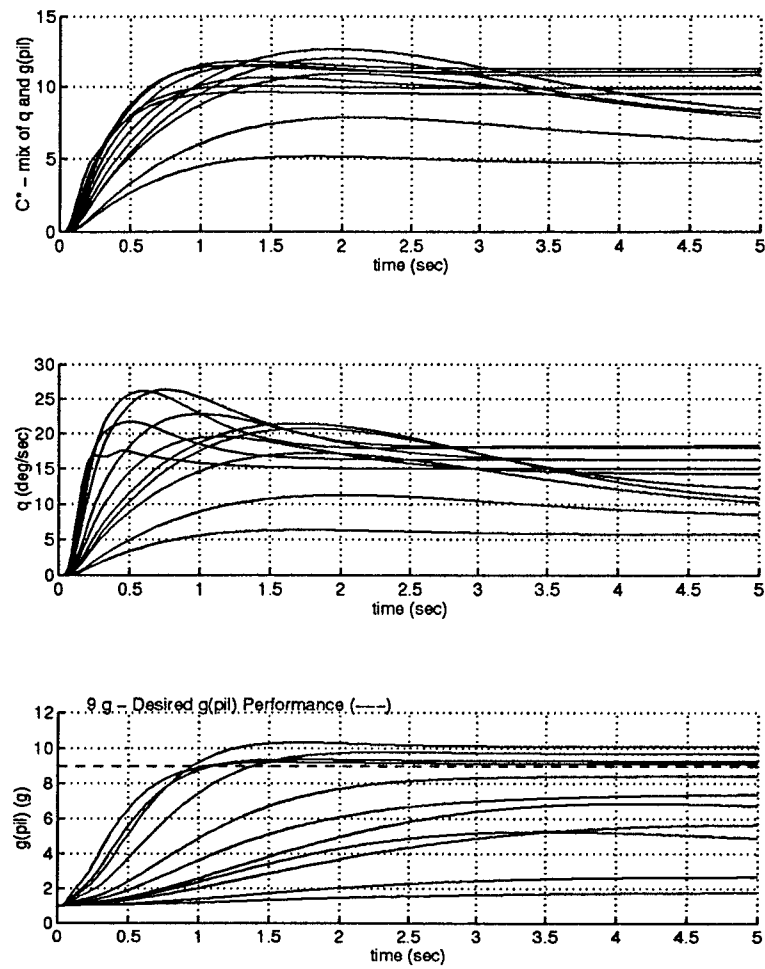
Figure 4.16   Compensated System Time Response to Maximum C^*_{cmd} Step Input (1 of 2)
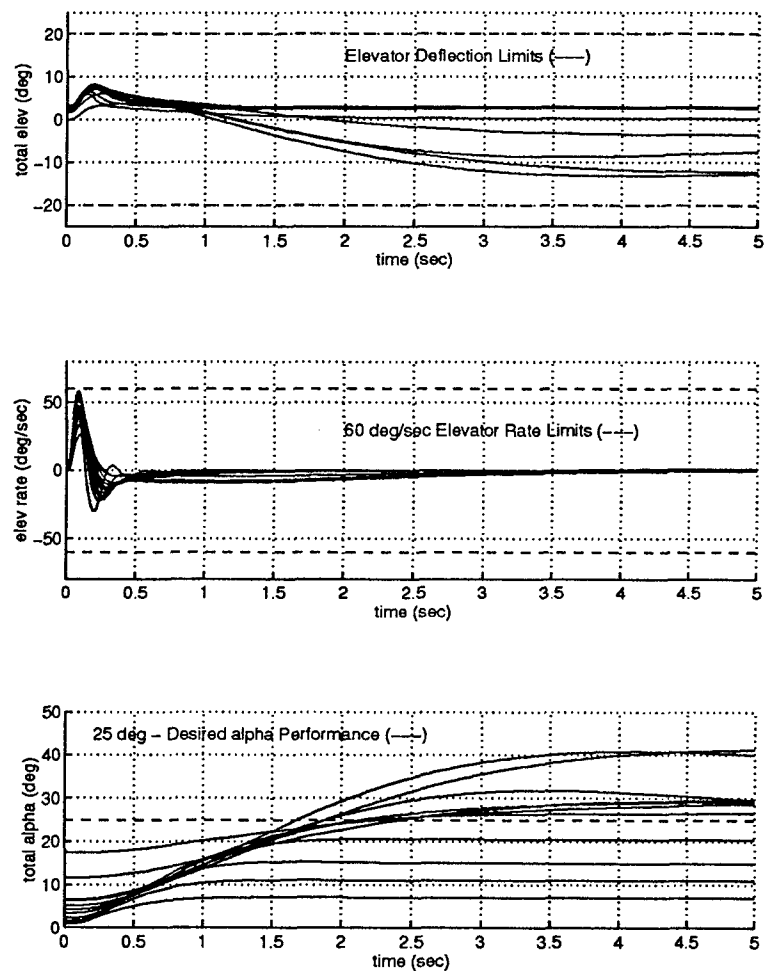
Figure 4.17   Compensated System Time Response to Maximum C^*_{cmd} Step Input (2 of 2)

this design. The graphs indicate how C^*_{cmd} is scaled according to the rates and magnitudes of α and g_{pil}. Plots (a) and (c) indicate that no magnitude limiting is initiated until above the desired g_{pil} and α performance requirements of 9 g's and 25 degrees, respectively. Any limiting below these values is the result of rate limiting. The action of the g rate limiter in Figure 4.18(b) during the initiation of a high g maneuver is to keep the g onset rate from exceeding the 6 g per second limit early in the maneuver, to stabilize this onset rate, and then to slow the onset rate again when approaching the maximum g of 9.45 to prevent overshoot. The α rate limiter of plot (d) slows the α rate so as to prevent an overshoot of the 30 degree maximum. The two dimensional look-up tables used in *Matlab* to simulate the rate limiters of plots (b) and (d) are found in Appendix D. Figure 4.22 indicates how the limiters fit into the design structure.

4.2.7 Longitudinal Design Validation. The QFTCAD is used to perform frequency domain validation and *Matlab* is used to perform time domain validation of the design.

4.2.7.1 QFTCAD Frequency Domain Validation. To confirm that all of the remaining 198 open-loop transfer functions meet the 30 degree phase margin angle and 6 dB gain margin stability requirements, the QFTCAD 'Stability Validation' feature is selected. Figure 4.19 depicts the resulting Nichols chart. Examination of this figure reveals that all 199 open-loop functions do in fact meet the desired stability specifications.

Next, by selecting the QFTCAD 'Tracking Validation' feature, the closed-loop frequency responses for all 199 plants are plotted along with the upper and lower frequency domain tracking bounds, T_{RU} and T_{RL}. These Bode plots are displayed in Figure 4.20. Both the anticipated violation of the tracking bounds at the very low frequencies and the satisfaction of the tracking bounds between 0.5 and 3.5 rps are evident; hence, the design achieves the desired frequency domain tracking specifications.
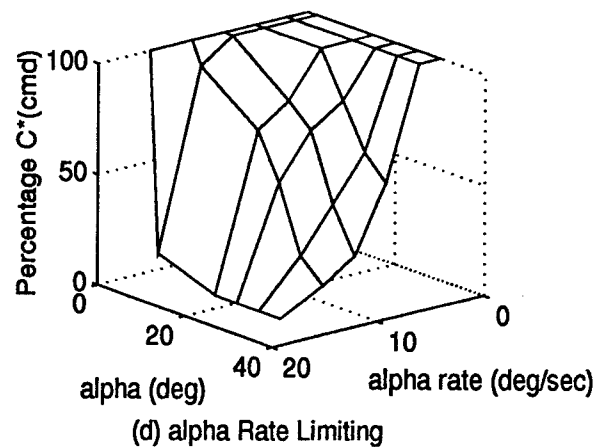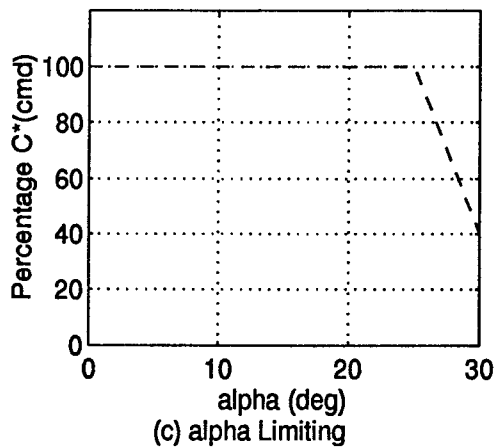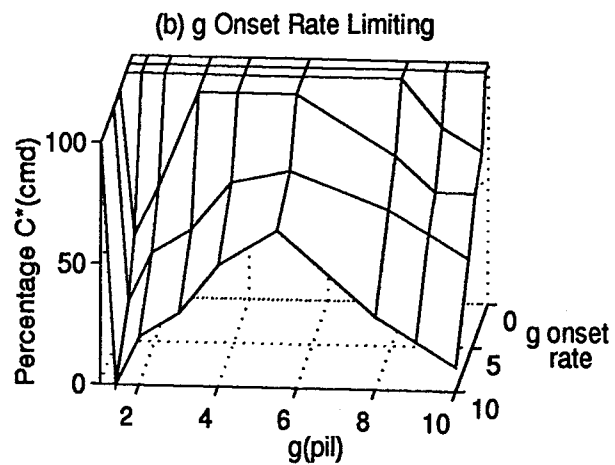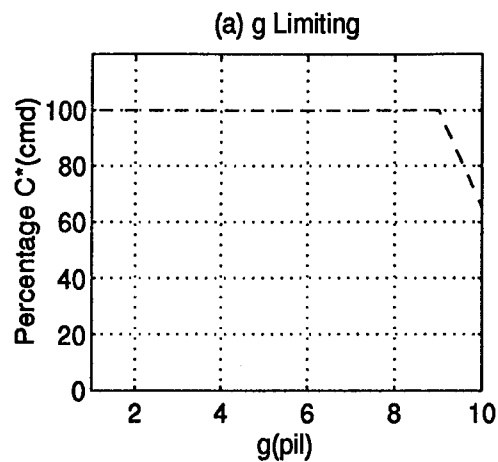
Figure 4.18   Graphical Display of α and g_{pil} Limiters
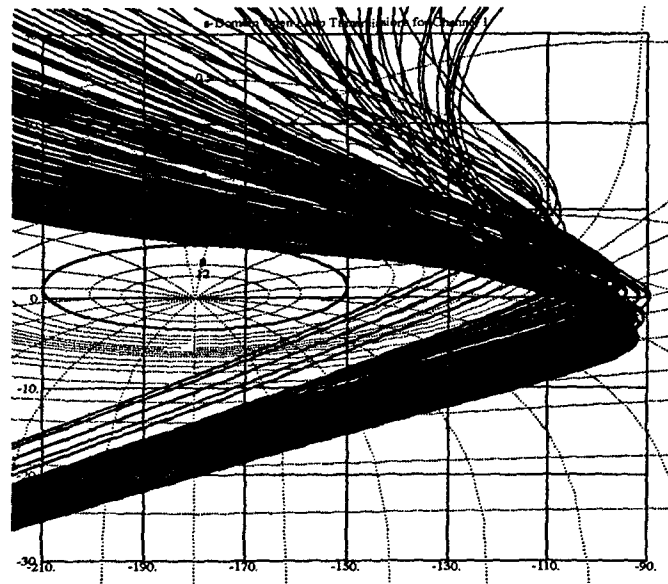
Figure 4.19   QFTCAD Stability Validation Nichols Chart
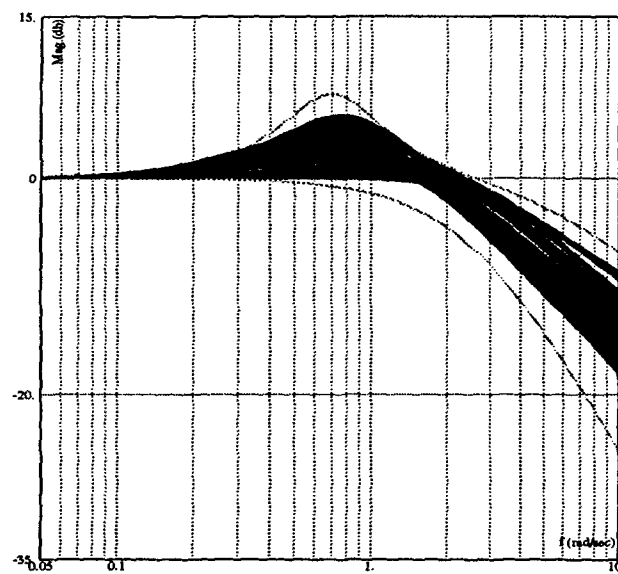
Figure 4.20   QFTCAD Tracking Validation Bode Plots
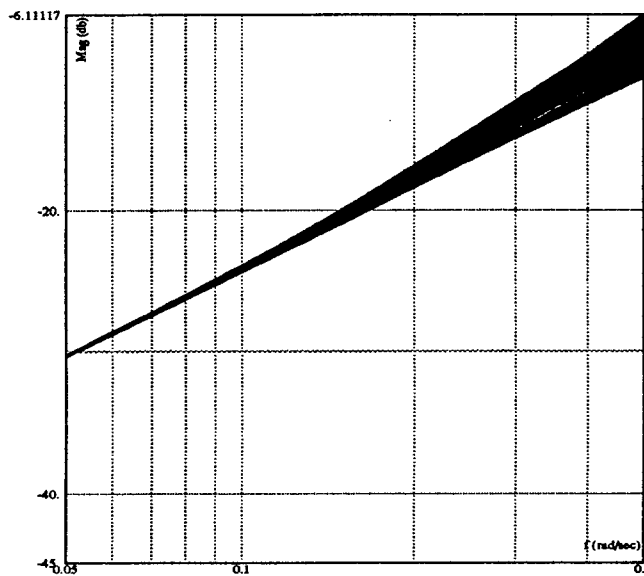
Figure 4.21   QFTCAD Tracking Validation Bode Plots

The QFTCAD 'External Disturbance Rejection Validation' feature generates Bode magnitude plots for each plant indicating the level of external disturbance rejection achieved. The resulting Bode plots for the longitudinal system are shown in Figure 4.21 where the external disturbance considered is the change in elevator trim as a result of changes in flight condition. Reynolds estimated that for $\omega < 0.157$ rps the effects of elevator trim disturbances should be considered [8]. Applying this frequency range estimate to the plots of Figure 4.21, it is concluded that a respectable disturbance rejection of -20 dB is achieved by the longitudinal design.

4.2.7.2   Longitudinal Design Time Domain Validation.   A representative set of system time responses to maximum C^*_{cmd} step inputs with the longitudinal limiter scheme in place is displayed in Figures 4.23 and 4.24. A comparison of these figures to Figures 4.16 and 4.17 shows that the limiter scheme accomplishes its intended purpose. A tabular listing of the results of this simulation for all plants with the limiters in place is found in Appendix C.3. These figures and the appendix data demonstrate that the design meets the performance benchmarks while avoiding actuator rate and control surface deflection saturations.

4-26
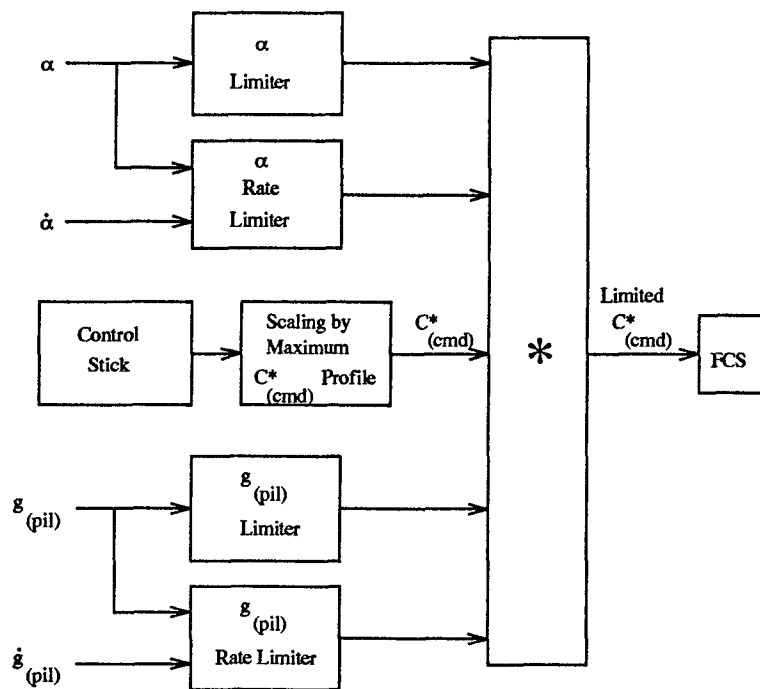
Figure 4.22   Longitudinal Limiter Structure

4.3   Final Longitudinal Channel Design

The final design in the longitudinal channel is best described by the block diagram illustrated in Figure 4.25. To summarize, the pitch stick force from the pilot is first scaled by the maximum C^*_{cmd} profile and then scaled by the limiters. This scaled pitch stick force is then filtered and enters the C^* compensator feedback loop, where it is transformed into an appropriate input to the elevator. Both the prefilter and compensator of the longitudinal design satisfy the requirements set forth in Section 2.3.
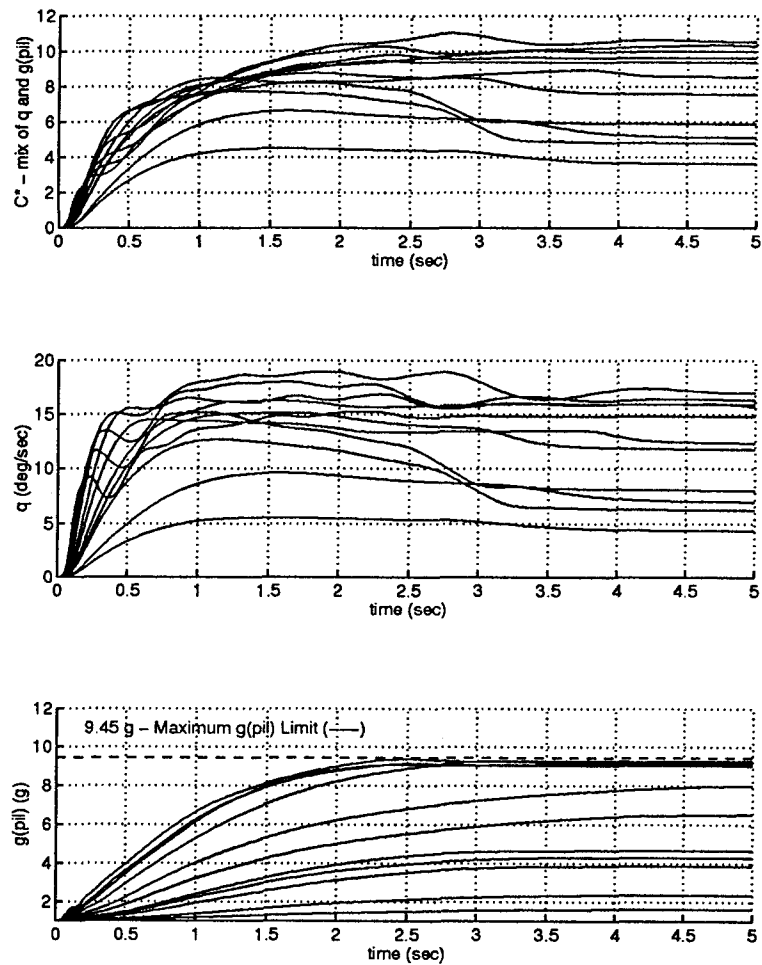
Figure 4.23   Compensated System Time Response to Maximum C^*_{cmd} Step Input with Limiters in Place (1 of 2)
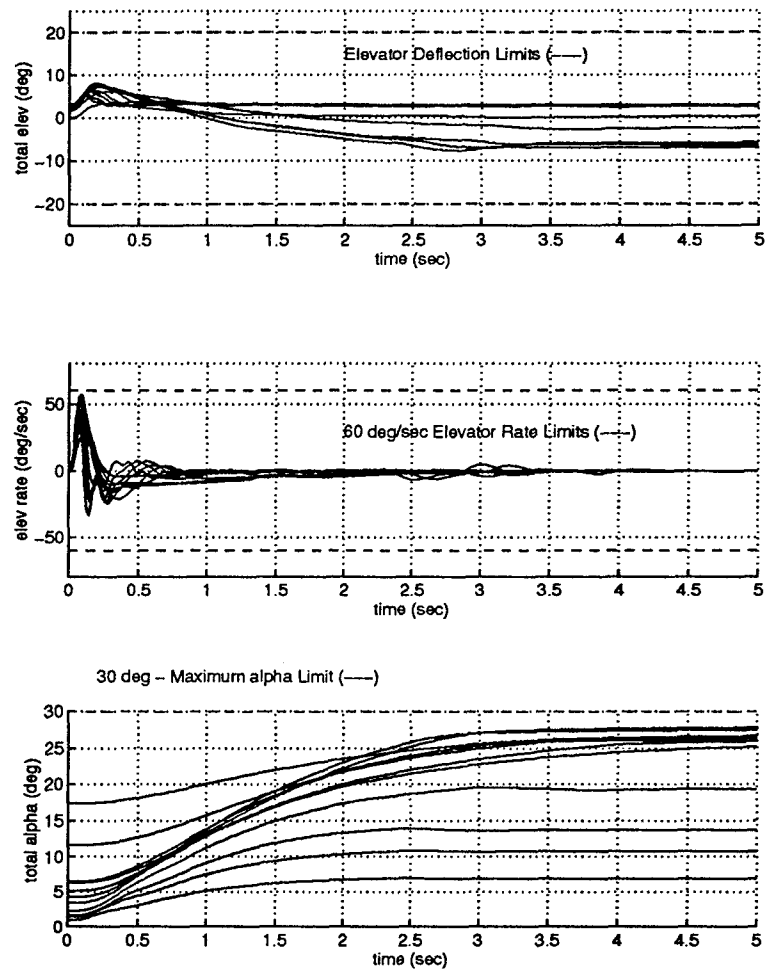
Figure 4.24   Compensated System Time Response to Maximum C^*_{cmd} Step Input with Limiters in Place (2 of 2)
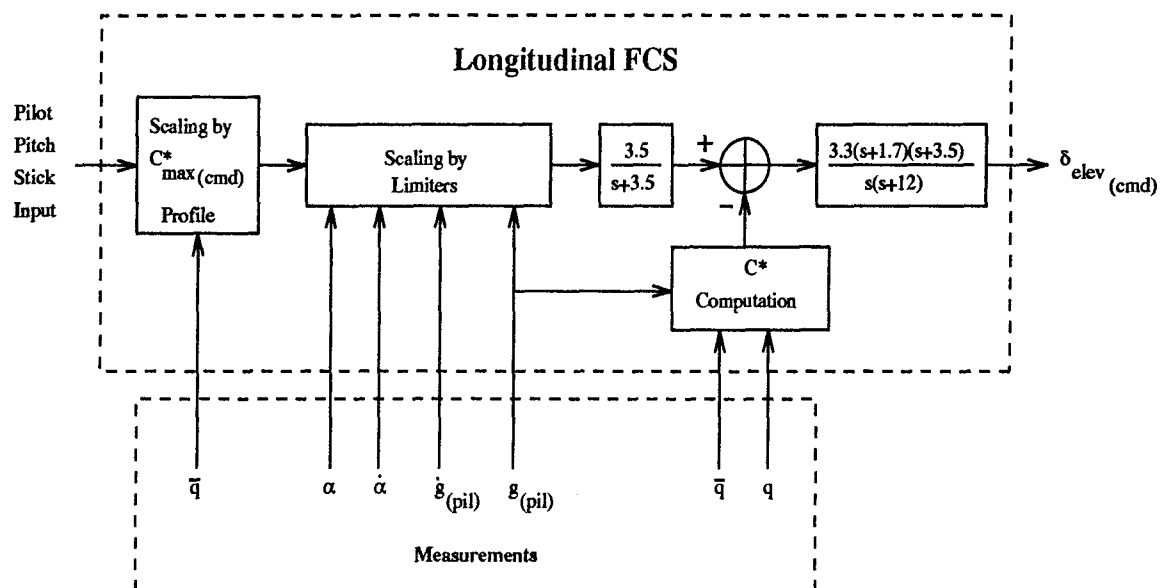
Figure 4.25   Final Longitudinal FCS Design Block Diagram

V. Lateral Channel Design

The lateral design follows the same integrated approach that is used in the longitudinal channel design (see introduction to Chapter IV).

5.1 Dutch Roll Damping Loop Design

In line with traditional lateral FCS design and Reynold's research, the first step taken is to improve the dutch roll mode damping of the basic lateral aircraft plants [3, 8]. This is done by feeding yaw rate r back through a washout filter of the form

$$H_{wo} = \frac{K\tau s}{1 + \tau s} \tag{5.1}$$

to the rudder. This loop acts to limit undesired yaw rates caused by flaperon and horizontal tail deflection during the initiation of rolling maneuvers for a transient period equal to τ seconds, while not interfering with the steady state yaw rates of a sustained turning maneuver [3]. A block diagram of this dutch roll damping loop is illustrated in Figure 5.1.

A root locus analysis of the open-loop transfer functions (OLTF's) from rudder input to yaw rate output is performed. The transfer functions of the lateral aircraft plants corresponding to the maximum and minimum dynamic pressure are chosen for this analysis. The objective of the analysis is to determine values of K and τ of the washout filter described by Equation (5.1) that achieve the
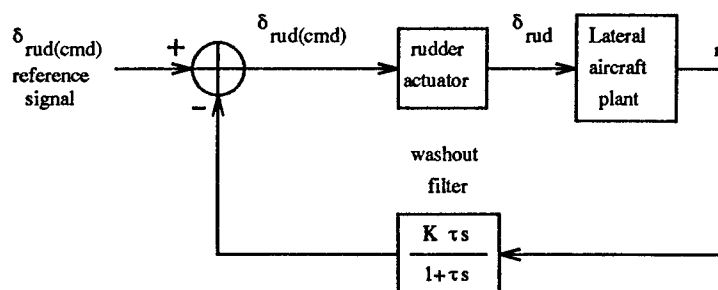
Figure 5.1   Dutch Roll Damping Washout Circuit Block Diagram
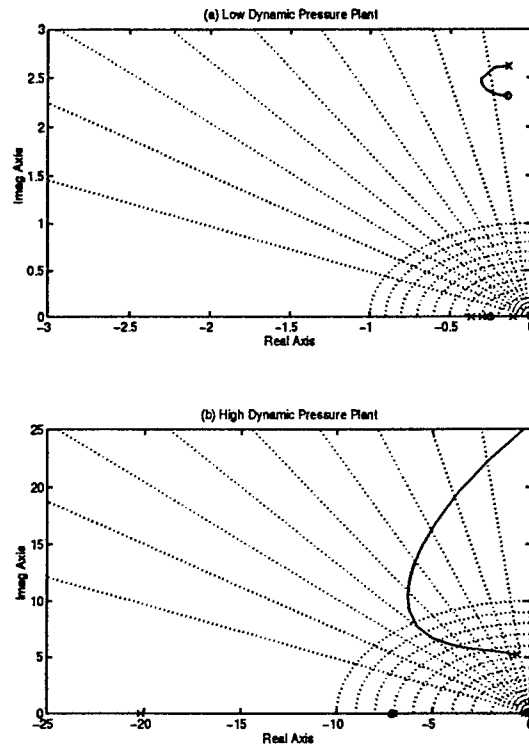
Figure 5.2   Dutch Roll Damping Loop Root Locus Plots for $\tau = 3.33$ seconds

best damping ratio (ζ) of the dutch roll mode poles of both the high and low $\bar{q}$ closed-loop transfer functions (CLTF's).

Although the ζ of the high $\bar{q}$ plant is improved dramatically by the introduction of the washout filter, the damping ratio of the low $\bar{q}$ plant is not. Consequently, the τ selected is the value which results in the greatest possible damping ratio for the low $\bar{q}$ plant root locus. The τ that accomplishes this is 3.33 seconds, and is the same as that used by Reynolds [8]. The resulting root locus plots for the high and low $\bar{q}$ plant OLTF's are depicted in Figure 5.2.

Next, a value of K is selected to maximize the damping of the closed-loop dutch roll mode poles of both of the loci of Figure 5.2. Although a K of 4 maximizes the ζ of the low $\bar{q}$ plant dutch roll mode poles, it pushes the high $\bar{q}$ plant dutch roll mode towards instability. Hence, a smaller gain must be chosen as a compromise. A gain of 2.6 achieves essentially equal closed-loop dutch roll mode damping for both plants. The +'s in Figure 5.3 show the position of the closed-loop

(a) Low Dynamic Pressure Plant

(b) High Dynamic Pressure Plant
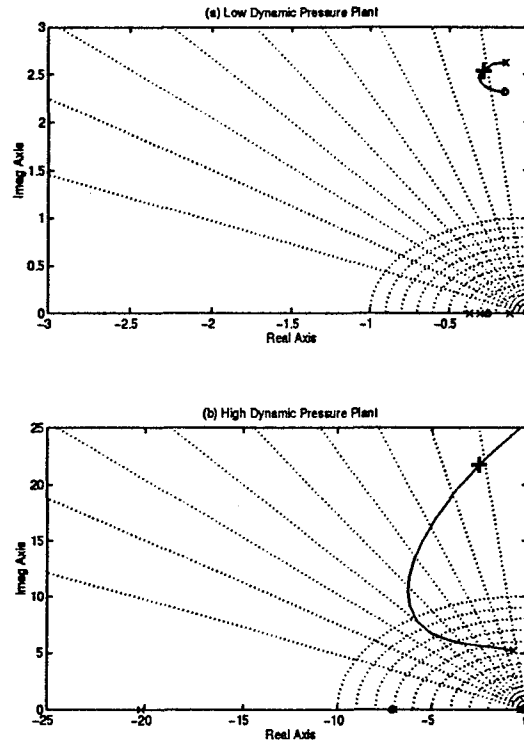
Figure 5.3   Root Locus Plots and Closed Loop Roots for $H_{wo} = \frac{2.6s}{s+0.3}$

dutch roll mode roots of the high and low $\bar{q}$ plants for the washout filter of Equation (5.2).

$$H_{wo} = \frac{2.6s}{s+0.3} \qquad (5.2)$$

The right is reserved to adjust K once the outer loops are in place, since the outer loops will no doubt interact to some extent with the dutch roll mode damping loop.

5.2   Lateral Channel Outer Loop Design

5.2.1   Lateral Outer Loop Control Parameters.
As in Reynold's thesis, the lateral outer loop control parameters in this design are roll rate p and sideslip angle β [8]. In this design, the emphasis is placed on the p feedback control loop since β commands are rarely used by pilots to accomplish inflight lateral tracking tasks.

5.2.2 Lateral QFT Specifications. As in the longitudinal channel, the Military Standard 1797A is used as the basis for the synthesis of frequency domain specifications to use in the QFT portion of the lateral design [2].

5.2.2.1 QFT Tracking Specifications. In the roll channel, the Mil Std specifies a minimum roll mode time constant of $\tau_{roll} = 1$ second. This is interpreted as a 4 second maximum limit on step response settling time. The Mil Std also requires that the aircraft be able to roll through 360 degrees of bank in 2.8 seconds or less in order to achieve Level 1 flying qualities. An additional Level 1 combat specification is the capability to roll through 90 degrees of bank in 1 second or less. These bank angle change specifications are interpreted as applicable only to reasonable aircraft energy levels, and not to flight conditions of low dynamic pressure.

The Mil Std also stipulates limits on the cross-coupling of roll rate commands into the yaw channel. It states that a roll rate command of 1 degree per second result in no more than 0.022 degrees of sideslip except at low airspeeds where it must be held to a maximum of 0.067 degrees. Also, the sideslip resulting from a maximum roll rate command must not exceed 6 degrees.

Roll Rate QFT Tracking Specification Models. The only one of the Mil Std specifications used in the synthesis of QFT upper and lower roll rate response tracking models is the roll mode time constant minimum of 1 second. Although time to roll performance requirements are set forth by the Mil Std, they are not used in the development of tracking specification models. Instead, these requirements are examined during time domain simulation.

The upper p tracking specification model is chosen as an underdamped response with a ζ of 0.5 whose settling time does not exceed 4 seconds. By applying the two percent settling time formula

$$T_s = \frac{4}{\zeta \omega_n},$$

(5.3)
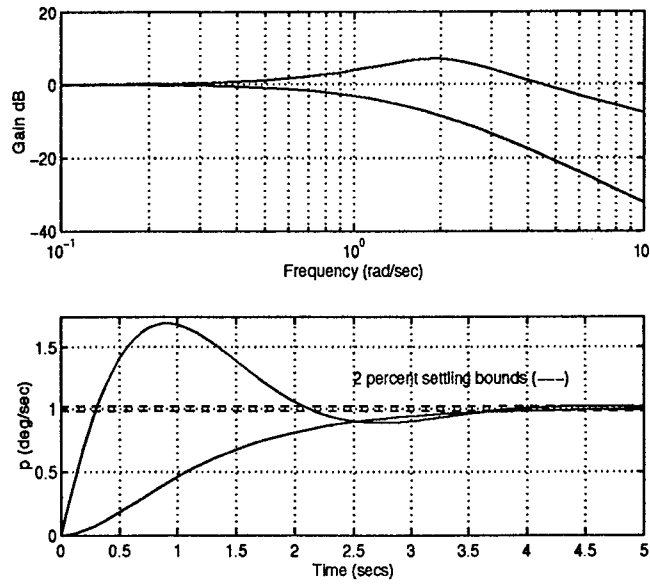
Figure 5.4   Roll Rate QFT Upper and Lower Tracking Specification Model Frequency and Step Time Responses

a settling time of 4 seconds dictates an undamped natural frequency of $\omega_n = 2$ rps [5]. The T_{RU} model includes a zero to achieve divergence with T_{RL} above T_{RU}'s 0 dB crossing frequency. This zero is also placed to set the model's bandwidth to 5 rps. The resulting model is

$$T_{RU} = \frac{4(s+1)}{s^2 + 2s + 4}.$$
(5.4)

The lower p tracking specification model is initially chosen as $\frac{2}{s+2}$ to set a bandwidth of 2 rps. Then, this initial model is augmented with a pole to promote divergence with T_{RU} as discussed in the last paragraph. This additional pole is placed such that the settling time of the model does not exceed 4 seconds. The resulting model is

$$T_{RL} = \frac{2.5}{(s+1.25)(s+2)}.$$
(5.5)

Figure 5.4 depicts both the frequency and step input time responses of T_{RU} and T_{RL} for the roll rate loop.

5-5

As mentioned before, β is not typically commanded by the pilot; hence, the cross-coupling effect of β_{cmd} to p is of little concern. In the rare case that the pilot does command sideslip, the rudder inputs from the pilot are filtered as necessary to reduce any undesired cross-coupling effects. The required filtering of sideslip commands is determined from the results of time domain simulation.

On the other hand, the cross-coupling effects of rudder deflection as a result of the dutch roll damping and β regulation loops definitely warrant attention. It is not evident what level of rejection is required to eliminate any undesirable cross-coupling in the roll rate response, so the roll rate loop compensator is designed assuming no cross-coupling. The roll rate command time response of the system is analyzed to determine if enough cross-coupling rejection is present. If the yaw damping and β loops adversely affect the roll rate response, the roll rate compensator and/or these two loops resposible for the cross-coupling are adjusted.

Sideslip QFT Tracking Specification Models. The limits imposed by the Mil Std on sideslip angle due to rolling maneuvers is modelled as an upper cross-coupling bound for the β feedback loop design. A constant cross-coupling upper bound of 0.067 is used. The Mil Std stipulates no explicit requirements for the sideslip angle response to pilot rudder inputs; therefore, no tracking models are required for the β response. However, the QFTCAD requires the input of tracking bounds for this MISO loop in order to generate the cross-coupling bounds and to use the 'Design Prefilter' feature, so arbitrary tracking models are selected and entered into the CAD. The p loop upper tracking bound model of Equation 5.4 is adopted for the β loop and the lower tracking bound model

$$T_{RL} = \frac{1}{(s+1)^2} \tag{5.6}$$

is utilized.
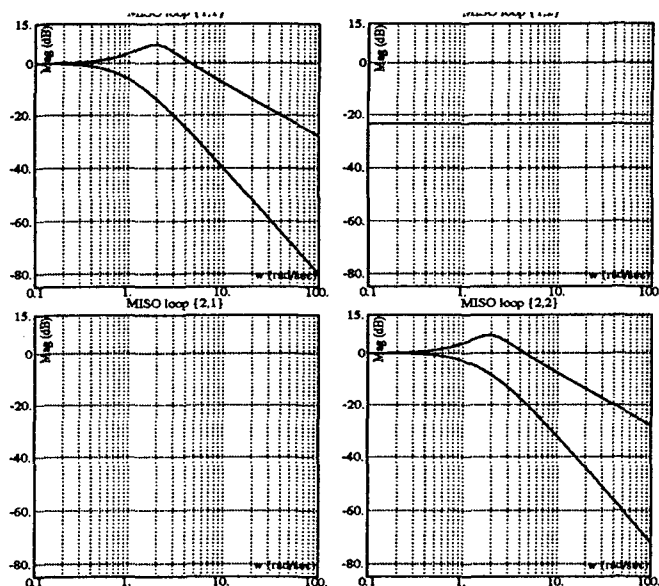
Figure 5.5   Lateral Channel QFT Tracking Boundaries

Lateral Tracking Bound Summary.   The tracking bounds for all four QFT MISO loops are illustrated in Figure 5.5

5.2.2.2   QFT Lateral Stability Specifications.   As in the longitudinal channel, the p and β OLTF's must have a phase margin angle of at least 30 degrees and a gain margin of at least 6 dB.

5.2.3   Lateral Performance Specifications.   The Level 1 flying quality roll performance requirements from the Mil Std are used as the lateral FCS performance benchmarks. These benchmarks must be met in order to achieve an FCS comparable to the current F-16 FCS. The only difference between the lateral and longitudinal channel benchmarks is that the lateral benchmarks are not physically attainable by aircraft of low dynamic pressure. Therefore, during the time domain analysis, the dynamic pressure at which a Level 1 roll requirement is met must be subjectively evaluated as to its acceptability. The roll performance benchmarks are

1. Level 1 - 360° of bank in $\leq$ 2.8 seconds
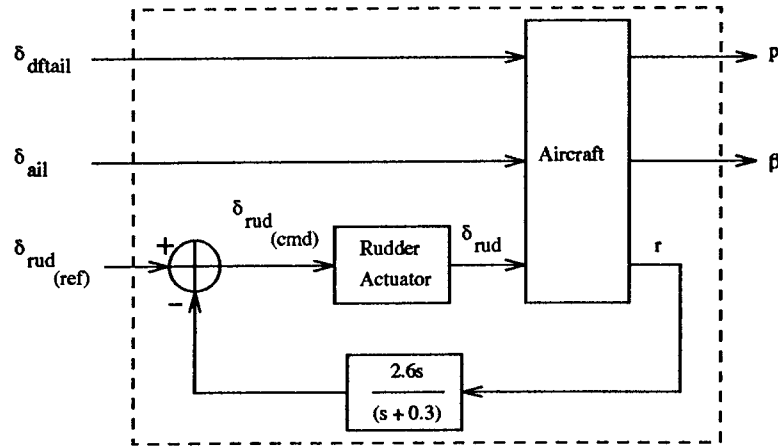
Figure 5.6   Lateral 3 X 2 MIMO Plant Structure including Dutch Roll Damping

2. Level 1 (combat) - 90° of bank in $\leq$ 1 second

5.2.4   QFT Lateral Channel Design.

5.2.4.1   QFTCAD Setup.   Lateral channel MIMO plants used in the lateral QFT design have 3 control inputs (δ_{dftail}, δ_{ail}, and $\delta_{rud_{(ref)}}$) and two outputs (p and β). *Matlab* is used to generate the appropriate transfer functions to represent the 3 X 2 MIMO system illustrated in Figure 5.6. Note that the previously designed dutch roll damping loop is incorporated into the MIMO system plant model.

Once generated, the 282 lateral plants are loaded into the QFTCAD. The lateral design structure entered into the QFTCAD is illustrated in Figure 5.7. The weighting matrix W allocates p_{cmd} into $\delta_{dftail_{(cmd)}}$ and $\delta_{ail_{(cmd)}}$ and transforms the 3 X 2 MIMO system into an effective 2 X 2 MIMO system. In Reynold's research, it was determined that the weighting matrix of Equation (5.7) yielded the best results and is therefore adopted for use in this research [8].

$$
\begin{bmatrix} \delta_{dftail_{(cmd)}} \\ \delta_{ail_{(cmd)}} \\ \delta_{rud_{(ref)}} \end{bmatrix} = W * \begin{bmatrix} p_{cmd} \\ \beta_{cmd} \end{bmatrix} = \begin{bmatrix} 0.294 & 0 \\ 1 & 0 \\ 0 & 1 \end{bmatrix} \begin{bmatrix} p_{cmd} \\ \beta_{cmd} \end{bmatrix}. \tag{5.7}
$$
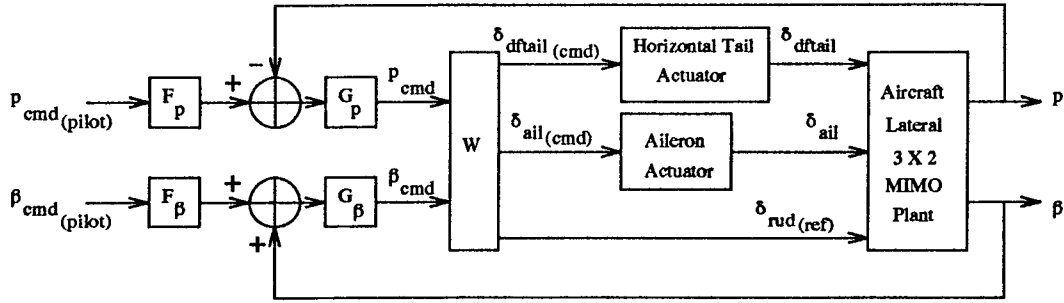
Figure 5.7   Lateral Design QFTCAD Structure

Next, the effective plant P_e (basic plant plus weighting matrix and actuators) and q transfer functions are generated by the QFTCAD. During the generation of these transfer functions, the QFTCAD cancels any poles and zeros within 0.001 of one another and eliminates all poles and zeros outside the dynamic frequency range of 10^{-5} to 10^4 rps. All 282 lateral plant, effective plant, and q transfer functions are listed in the supplement to this thesis. Finally, the specifications presented in Section 5.2.2 are entered into the QFTCAD.

Diagonal Dominance. The diagonal dominance of the Q matrices is evaluated by the QFTCAD and results in the plots of Figure 5.8. Diagonal dominance is a measure of the dominance of the system's response by the diagonal MISO loops over the off-diagonal MISO loops. The full explanation of this condition is found elsewhere [6]. At the frequencies where the QFTCAD diagonal dominance plots of Figure 5.8 are negative, diagonal dominance does not exist; therefore, diagonal dominance does not exist in the design frequency spectrum of 0.5 to 3.5 rps.

Three options are available when this condition of diagonal dominance is not met. The first option is to attempt a method 2 QFT design. In a method 2 design, the MISO loop expected to have the largest bandwidth is designed first. When the next MISO loop is designed, the cross-coupling input into the second loop reflects the compensator design of the first loop. In contrast, when using method 1, each loop is designed independently assuming the worst case cross-coupling effect possible for each loop. Therefore, method 2 decreases the overdesign inherent in the second
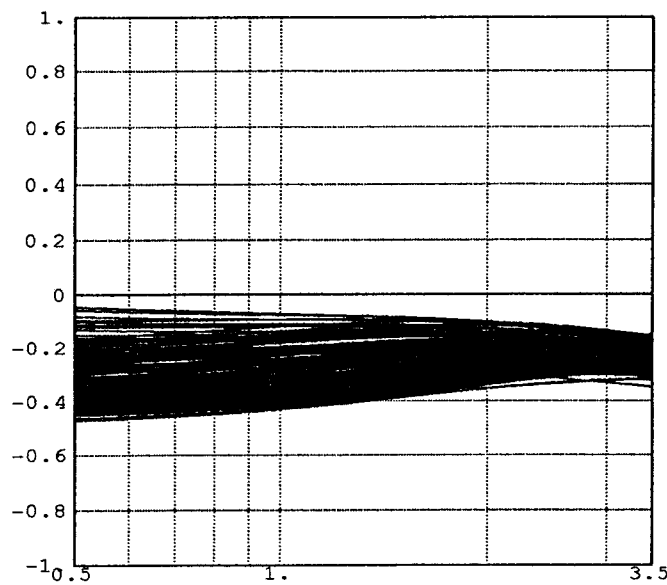
Figure 5.8   QFTCAD Diagonal Dominance Plot

and subsequent MISO loop designs that occurs when using method 1 [6]. The second option is to modify the weighting matrix until the diagonal dominance condition is met. Although techniques for arriving at such a weighting matrix exist, they are not useful when large parameter uncertainty is present; consequently, trial and error must be relied upon to properly modify W. The third option is to proceed with a method 1 design, but to design with only stability in mind. In this case, time domain simulation must be relied upon to verify that appropriate tracking and cross-coupling performance is achieved.

The third option is chosen for this design for several reasons. The lack of diagonal dominance drastically affects the generation of QFT tracking and cross-coupling rejection boundaries. In essence, it invalidates these boundaries. A method 2 design is attempted, but the boundaries generated by the QFTCAD are essentially the same as those for method 1. In other words, method 2 does not rectify the diagonal dominance problem and the first option is a dead end. Since Reynolds attempted to modify the W matrix during his research with poor results, the second option is not pursued [8]. A final consideration favoring the third option is that the detection of actuator rate
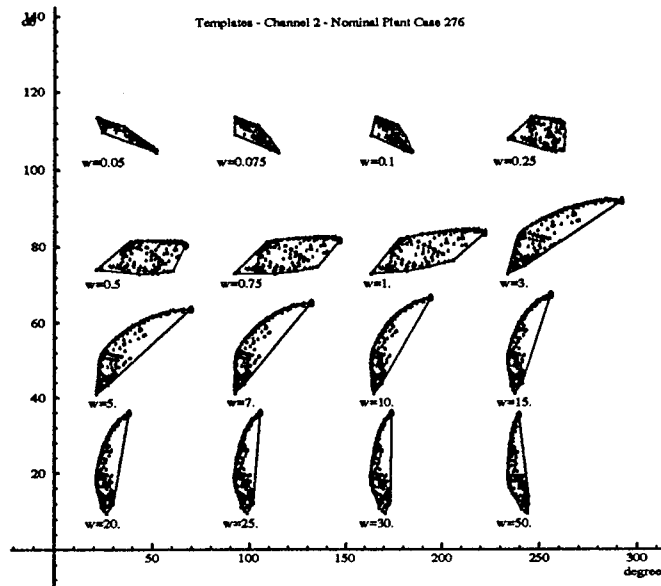
Figure 5.9   QFT Roll Rate Loop Frequency Templates

and control surface deflection saturations requires time simulation of the system; hence, the time simulations can easily be used to also examine the qualitative characteristics of the system response.

5.2.4.2   QFT Lateral Roll Rate Loop Design.   The QFTCAD frequency templates for the roll rate loop are shown in Figure 5.9. As indicated in the figure, plant number 276 has been chosen as the nominal plant due to its position at the top to the 30 rps template.

The roll rate nominal loop shape is depicted on the Nichols chart of Figure 5.10. The nominal loop satisfies all of the stability bounds on the chart. The compensator used to achieve this loop is

$$G_p = \frac{0.125(s+3)}{s} \tag{5.8}$$

The roll rate loop prefilter is chosen in the same manner as that for the longitudinal control loop. The prefilter

$$F_p = \frac{3.5}{s+3.5} \tag{5.9}$$
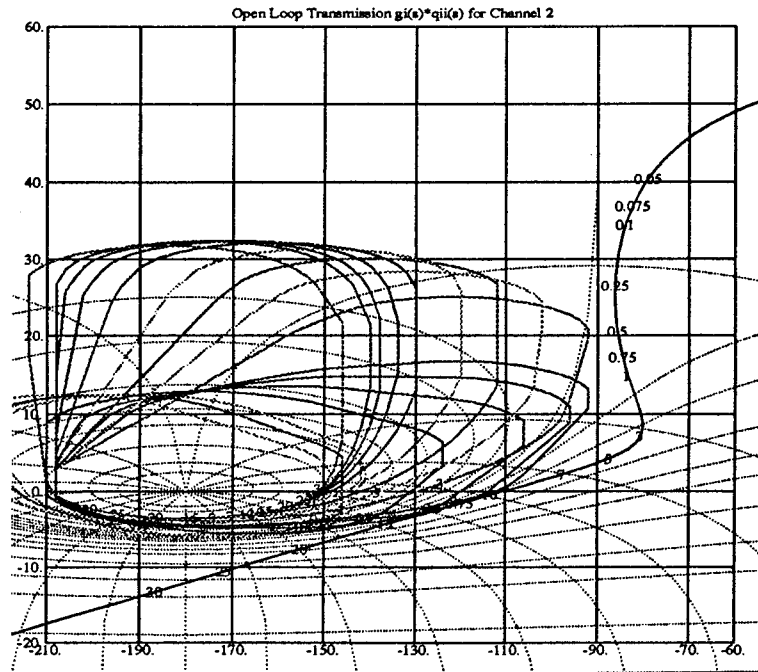
Figure 5.10   QFTCAD Roll Rate Nominal Loop Nichols Chart with $G_p = \frac{0.125(s+3)}{s}$

allows pilot roll commands of up to 3.5 rps to pass to the compensator; therefore, the pilot's control bandwidth is not restricted by the prefilter.

5.2.4.3   QFT Lateral β Loop Design.   The QFTCAD frequency templates for the β loop are shown in Figure 5.11. As indicated in the figure, plant number 276 has been chosen as the nominal plant due to its position at the top to the 30 rps template.

The β nominal loop shape is depicted on the Nichols chart of Figure 5.12. The nominal loop does satisfy all of the stability bounds on the chart. The compensator used to achieve this loop is

$$G_\beta = \frac{-20(s+1.7)(s+2)}{s(s+60)} \tag{5.10}$$

5-12
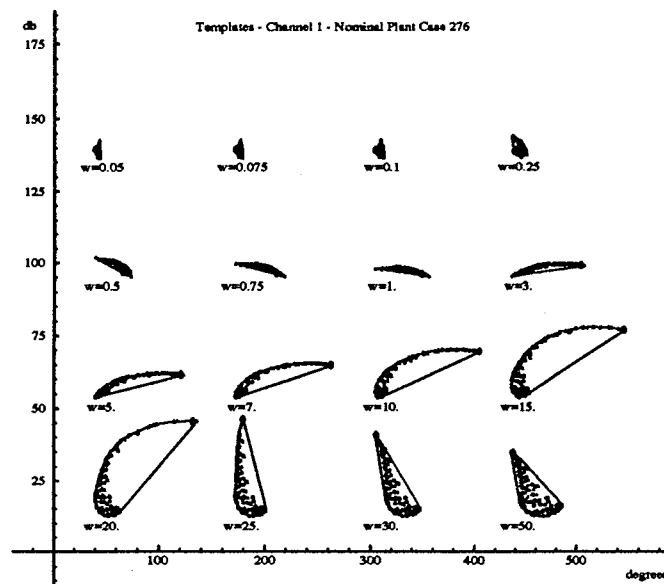
Figure 5.11   QFTCAD β Loop Frequency Templates
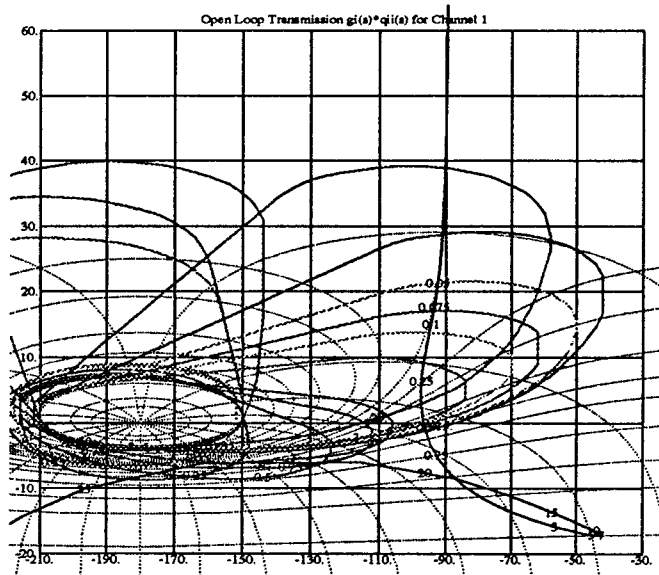
Figure 5.12   QFTCAD β Nominal Loop Nichols Chart
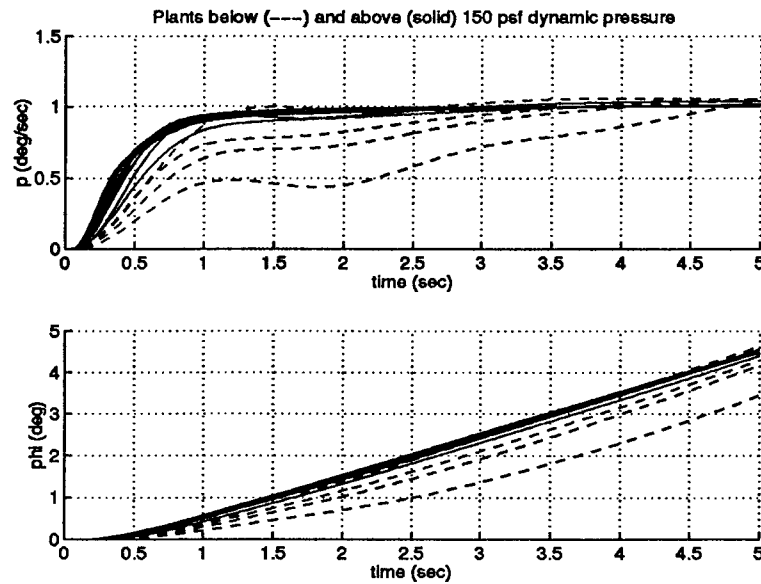
Figure 5.13   Initial Lateral Design Roll Rate Unit Step Input Time Response (1 of 4)

The selection of a β loop prefilter is discussed in the time analysis section since the filtering of pilot sideslip inputs is primarily dependent on the cross-coupling roll rate observed from a sideslip input.

5.2.5   Lateral Design Time Domain Analysis.   Time responses to a unit roll rate step input are made at this point as a progress check of the design. The *Matlab* plots resulting from this simulation for representative plants below (- - -) and above (solid) $\bar{q} = 150$ psf are shown in Figures 5.13 through 5.16. Two deficiencies of the design are revealed by inspecting these plots. First, the p responses of the low $\bar{q}$ plants in Figure 5.13 possess an undesirable droop prior to reaching the desired final value. Second, as seen in Figure 5.14, the low $\bar{q}$ plants also violate the 0.067 degree β restriction by a wide margin.

The first problem is rectified by decreasing the gain of the r feedback washout filter of Equation (5.1) from 2.6 to 1. The rudder deflection commanded by the washout filter with a gain of 2.6 slows the roll rate and results in the droop in the p response. By reducing the washout filter gain, thus reducing the magnitude of the rudder deflection, this droop is adequately reduced.
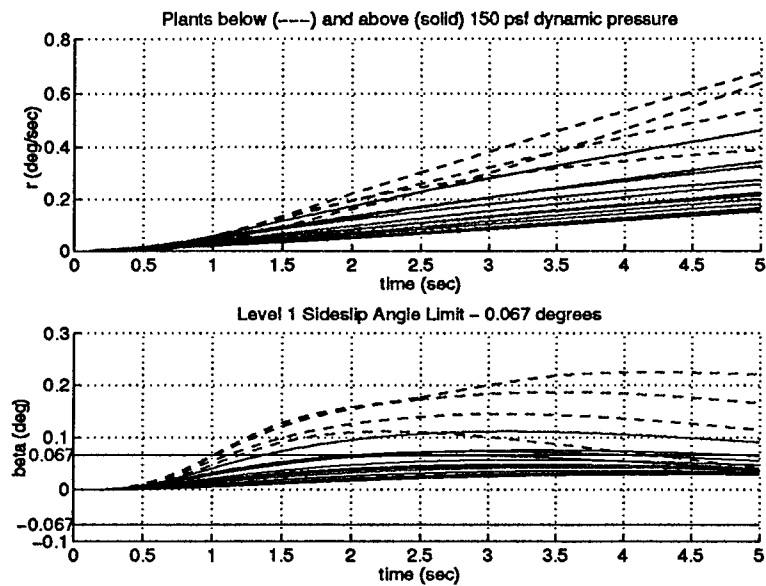
Figure 5.14   Initial Lateral Design Roll Rate Unit Step Input Time Response (2 of 4)
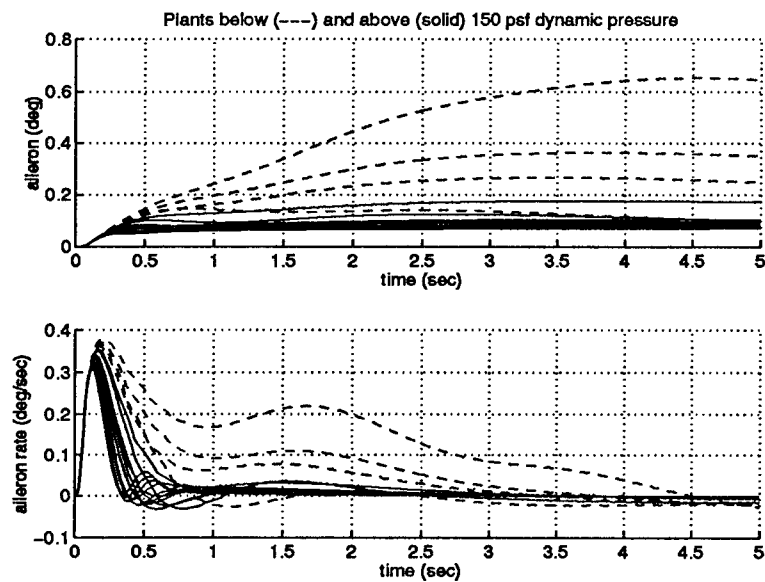
Figure 5.15   Initial Lateral Design Roll Rate Unit Step Input Time Response (3 of 4)
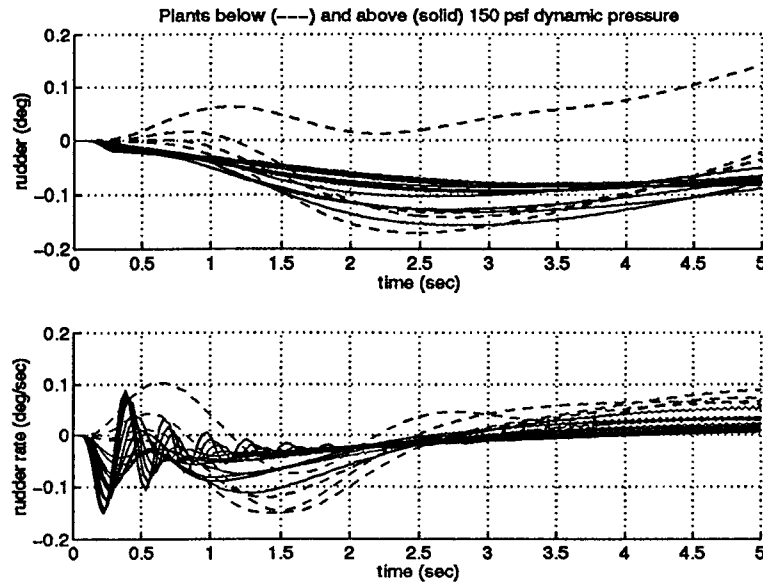
Figure 5.16   Initial Lateral Design Roll Rate Unit Step Input Time Response (4 of 4)

The second problem is solved by increasing the gain of the G_β of Equation (5.10). This action reduces the sideslip resulting from a roll rate command input and, because β is a slower variable than r, this change in gain has much less effect on the roll rate response than a change in the gain of the washout filter.

Modified MIMO plants are generated by *Matlab* using the lower washout filter gain and then input into the QFTCAD. The G_p of Equation (5.8) is unchanged, and the absolute gain of the G_β of Equation (5.10) can now be increased to 50 without violating stability specifications. The resulting QFTCAD nominal OLTF's for the p and β loops are illustrated in Figures 5.17 and 5.18.

Roll rate unit step input time responses reflecting the adjusted G_β and washout filter are depicted in Figures 5.19 through 5.22. Figure 5.19 clearly shows that the p response droop has been reduced; however, the maximum transient β of the low $\bar{q}$ plants still exceeds the 0.067 degree limit. Consequently, the β compensator design must be divided into two parts because the gain of G_β cannot be increased further without violating the gain margin restriction of 6 dB (see Figure 5.18).
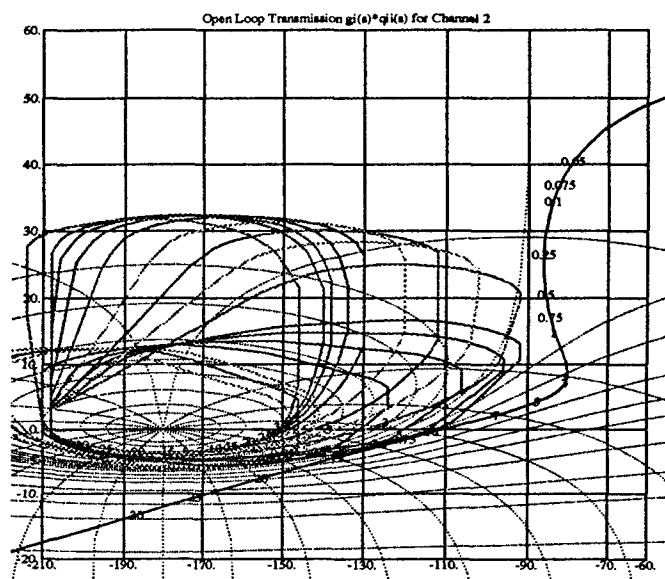
Figure 5.17   Adjusted Roll Rate Nominal Loop Nichols Chart with $G_p = \frac{0.125(s+3)}{s}$
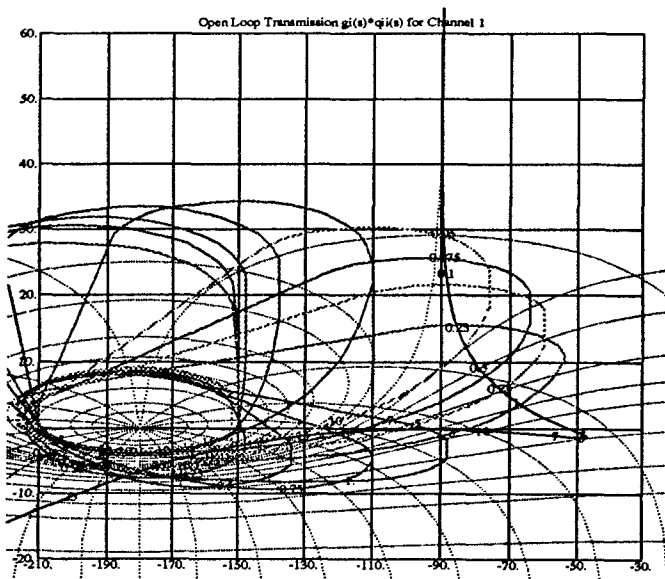
Figure 5.18   Adjusted Sideslip Nominal Loop Nichols Chart with $G_\beta = \frac{-50(s+1.7)(s+2)}{s(s+60)}$
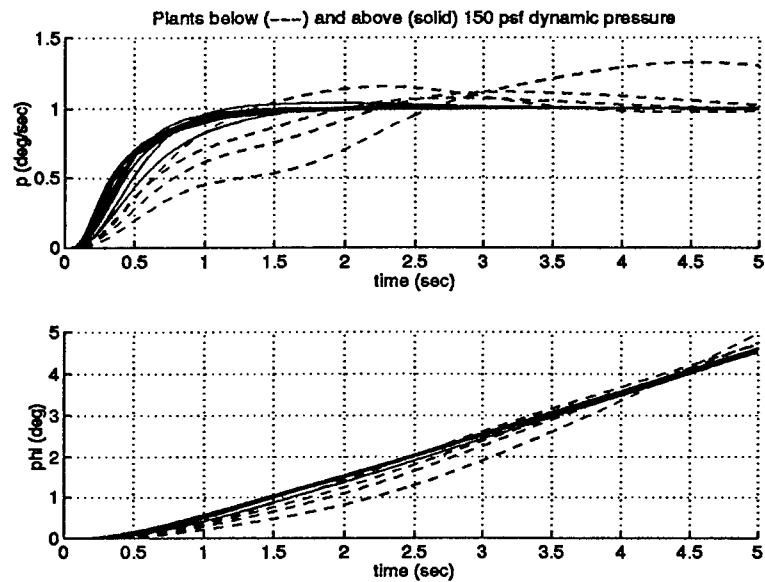
Figure 5.19   Adjusted Lateral Design Roll Rate Unit Step Input Time Response (1 of 4)
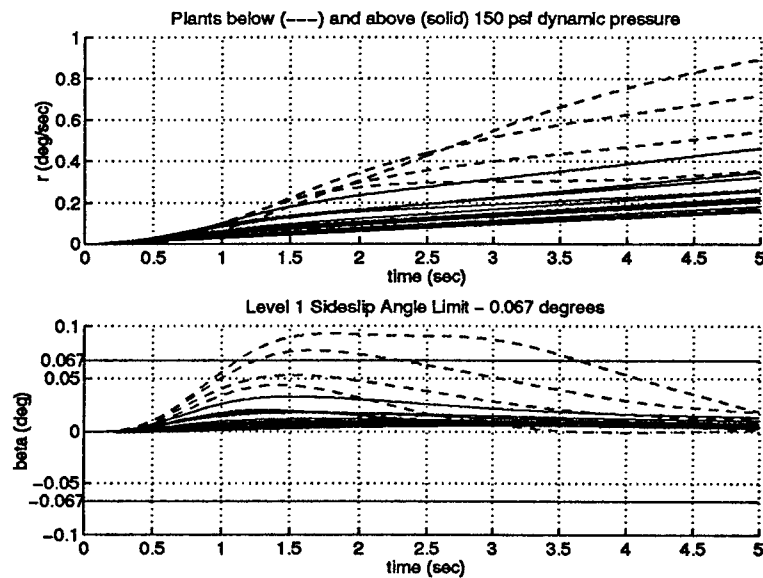
Figure 5.20   Adjusted Lateral Design Roll Rate Unit Step Input Time Response (2 of 4)
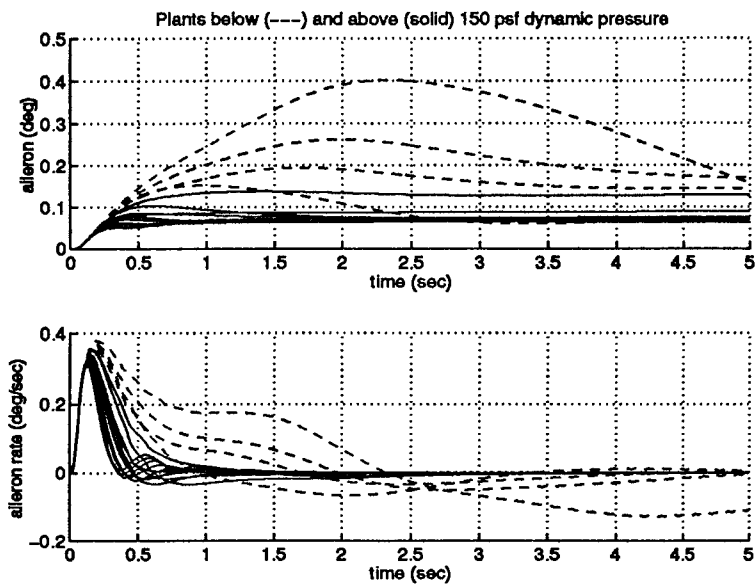
Figure 5.21 Adjusted Lateral Design Roll Rate Unit Step Input Time Response (3 of 4)
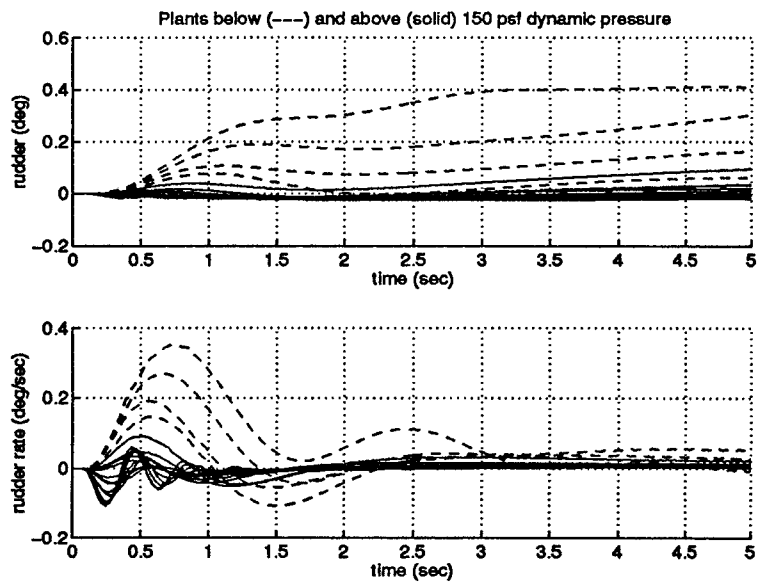
Figure 5.22 Adjusted Lateral Design Roll Rate Unit Step Input Time Response (4 of 4)
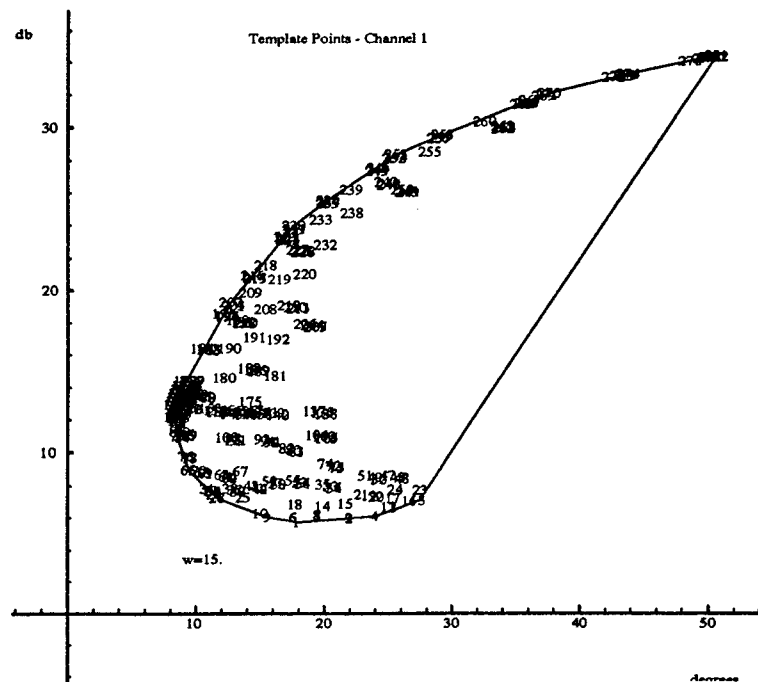
Figure 5.23   QFTCAD Expanded Frequency Template for β Loop

5.2.5.1   Modified β Loop Design.   The gain of G_β needs to be increased for the low $\bar{q}$ plants in order to comply with the 0.067 degree sideslip restriction. First, a determination is made at to where in the parameter space the compensator design will be divided. QFTCAD expanded frequency templates such as the one depicted in Figure 5.23 are examined to determine a prudent dynamic pressure at which to divide the design. Referencing Figure 5.23, the division is made beween plants 179 and 180 corresponding to $\bar{q} = 150$ psf.

The unit p step input time response of the low $\bar{q}$ plants with a G_β gain of -100 are shown in Figures 5.24 and 5.25. Figure 5.25 validates that this gain increase does reduce the transient sideslip to less than 0.067 degrees; consequently, the gain of G_β is switched between -100 and -50 at $\bar{q} = 150$ psf. Below a $\bar{q}$ of 150 psf, a gain of -100 is used, and when $\bar{q}$ increases above 150 psf, the gain of G_β is changed to -50. An added benefit of the gain switching is that the p response of the low $\bar{q}$ plants is improved over that shown in Figure 5.20. The p response ballooning exhibited by
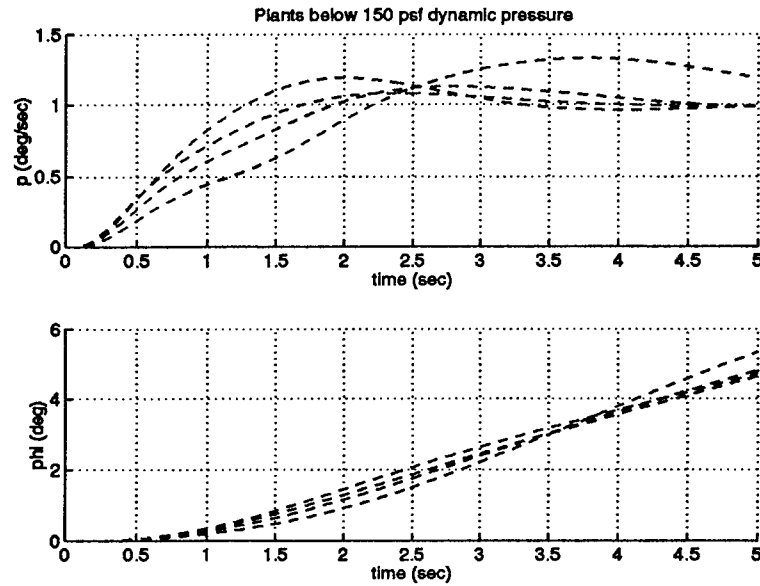
Figure 5.24 Unit Roll Rate Step Input Response of Low $\bar{q}$ Plants with $G_\beta = \frac{-100(s+1.7)(s+2)}{s(s+60)}$ (1 of 2)

the lowest $\bar{q}$ plant of Figure 5.24 is isolated to plants corresponding to dynamic pressures between 60 and 70 psf.

To facilitate the required gain switching, overlapping of the dynamic pressure regions accommodated by the two compensator gains is desired. Therefore, the two dynamic pressure regions of interest are selected as $\bar{q} \le 170$ psf and $\bar{q} \ge 130$ psf. The nominal loops for the low and high dynamic pressure regions are shown in Figures 5.26 and 5.27, respectively. As seen in the figures, both nominal loops meet the phase margin angle and gain margin specifications.

5.2.5.2 Synthesis of Lateral Maximum Command Input Profiles. The roll rate loop is evaluated first since it is the primary control loop in the lateral channel. The lateral system is subjected to a unit roll rate step input to determine if sideslip limitations are violated and to generate bounds on p_{cmd} to achieve desired performance while avoiding actuator rate and control surface deflection saturations. The results of this simulation for a representative set of plants spanning the entire range of $\bar{q}$ are displayed in Figures 5.28 through 5.31. A complete tabular listing of these results for all plants is found in Appendix E.1. Examination of the figures and the
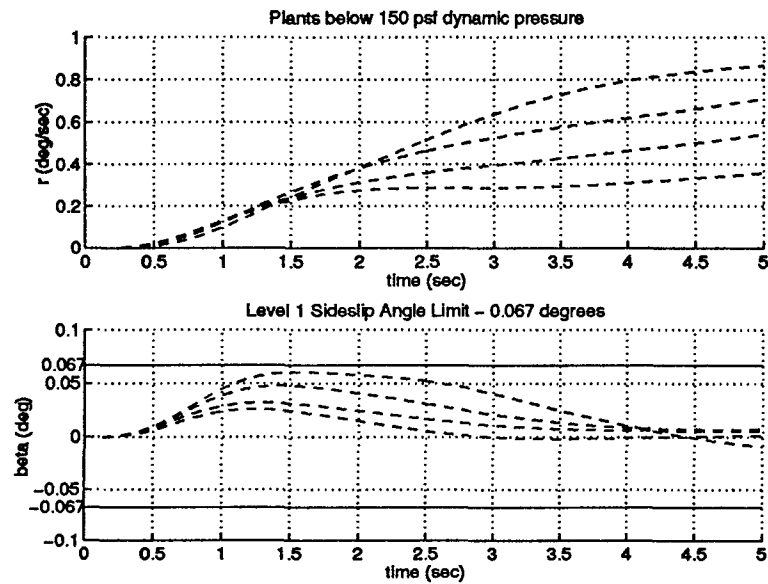
Figure 5.25   Unit Roll Rate Step Input Response of Low $\bar{q}$ Plants with $G_\beta = \frac{-100(s+1.7)(s+2)}{s(s+60)}$ (2 of 2)
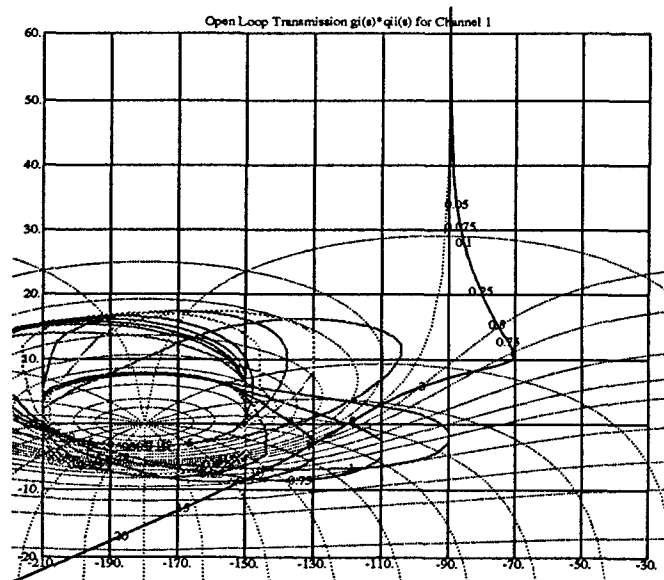
Figure 5.26   Nominal Open-Loop Nichols Chart for $\bar{q} \leq 170$ psf and $G_\beta = \frac{-100(s+1.7)(s+2)}{s(s+60)}$
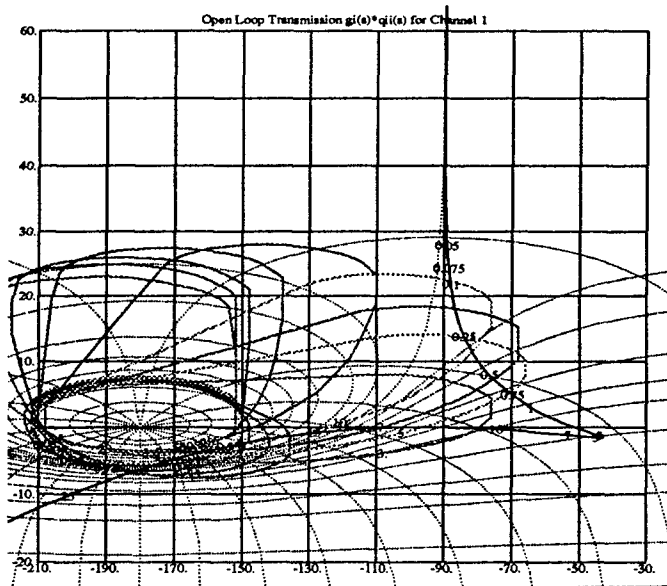
Figure 5.27   Nominal Open-Loop Nichols Chart for $\bar{q} \geq 130$ psf and $G_\beta = \frac{-50(s+1.7)(s+2)}{s(s+60)}$

appendix data reveals that the responses of all plants remain below the maximum β limit of ± 0.067 degrees.

Next, upper and lower bounds for the allowable maximum p_{cmd} at all dynamic pressures are generated from the unit step response data in Appendix E.1 by plotting the following versus $\bar{q}$.

$$\frac{60}{\dot{\delta}_{ail_{(max)}}} \tag{5.11}$$

$$\frac{60}{\dot{\delta}_{rud_{(max)}}} \tag{5.12}$$

$$\frac{20}{\delta_{ail_{(max)}}} \tag{5.13}$$

$$\frac{30}{\delta_{rud_{(max)}}} \tag{5.14}$$

$$\frac{360}{\phi_{(2.8\,sec)}} \tag{5.15}$$

$$\frac{90}{\phi_{(1\,sec)}} \tag{5.16}$$
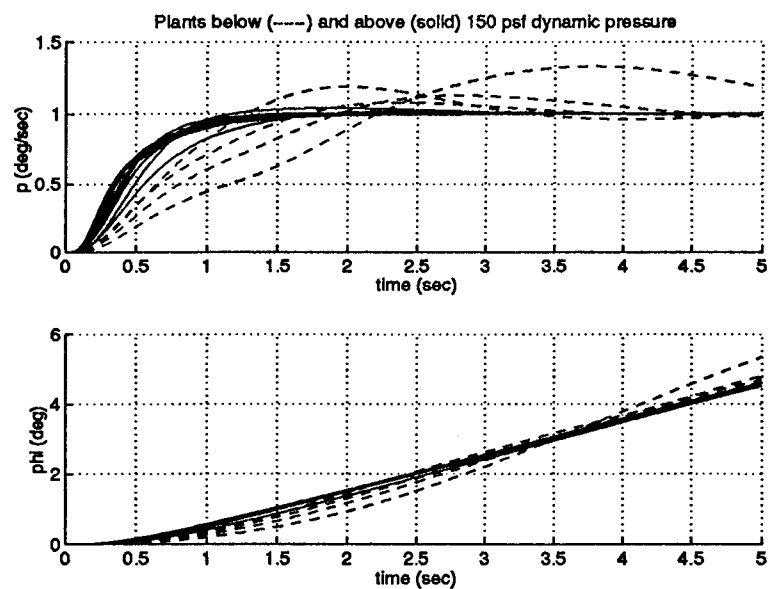
Figure 5.28   Lateral Design Unit p_{cmd} Step Responses (1 of 4)
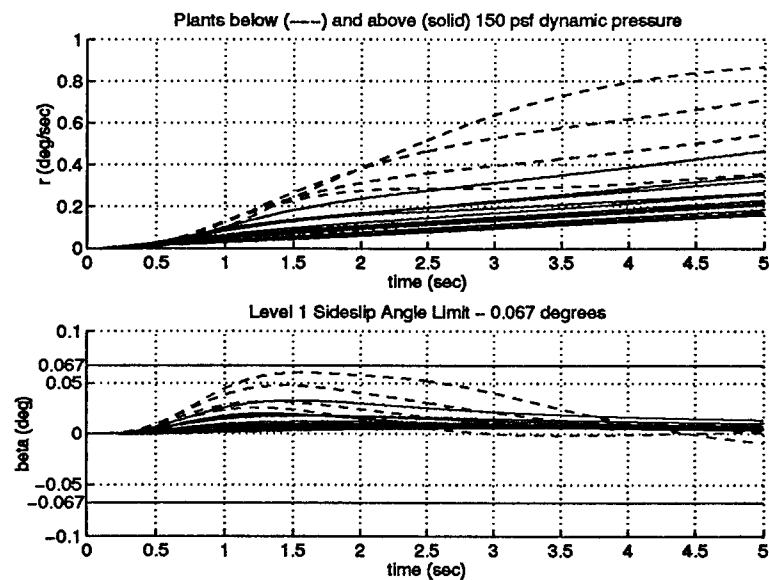
Figure 5.29   Lateral Design Unit p_{cmd} Step Responses (2 of 4)
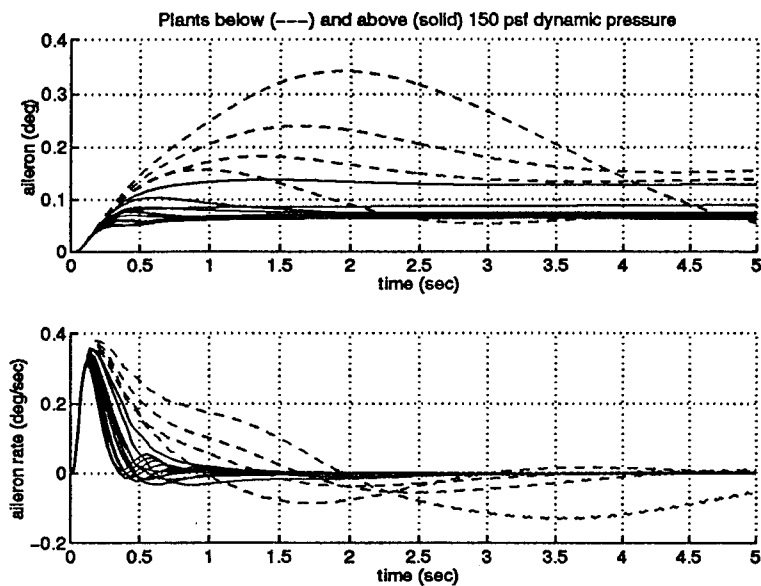
Figure 5.30 Lateral Design Unit p_{cmd} Step Responses (3 of 4)
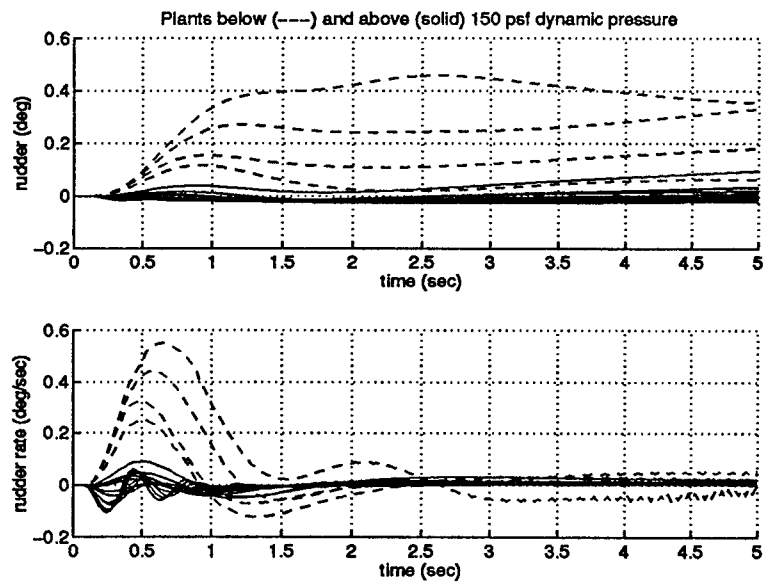
Figure 5.31 Lateral Design Unit p_{cmd} Step Responses (4 of 4)
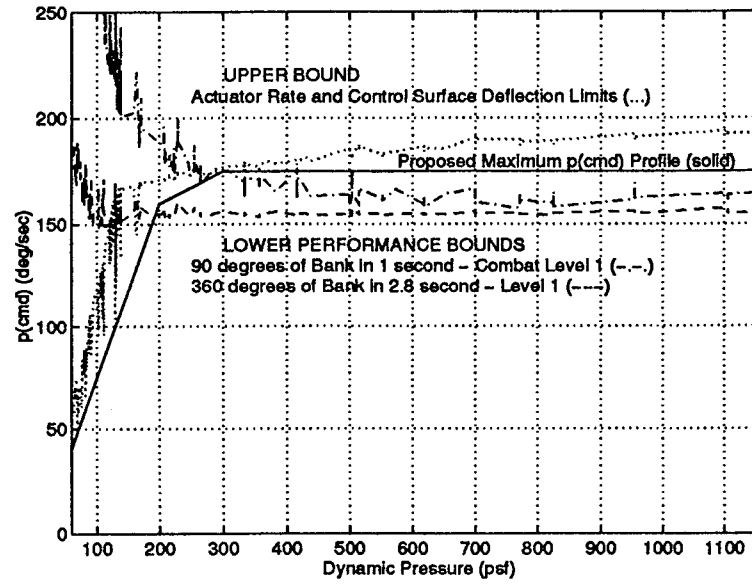
Figure 5.32   Proposed $p_{cmd_{(max)}}$ Profile to Avoid Saturations and Achieve Desired Performance

The plots of the data generated for all plants from Equations (5.11) through (5.16) are shown in Figure 5.32 along with a proposed $p_{cmd_{(max)}}$ profile. The $p_{cmd_{(max)}}$ profile must stay below the plots of Equations (5.11) through (5.14) to avoid actuator rate and control surface deflection saturations. In addition, the profile achieves the level 1 $\left(\frac{360\ deg}{2.8\ sec}\right)$ and combat level 1 $\left(\frac{90\ deg}{1\ sec}\right)$ roll performance requirements when it is above the bounds defined by Equations (5.15) and (5.16), respectively. The figure indicates that the proposed profile avoids all saturations, achieves level 1 roll performance above $\bar{q} \approx 200$ psf, and achieves level 1 combat roll performance above $\bar{q} \approx 300$ psf.

The sideslip channel prefilter is now synthesized by examining the cross-coupling effects reflected in p from a β_{cmd} step input. The time responses to a β_{cmd} unit step are displayed in Figures 5.33 through 5.36 for a represetative set of plants using a β prefilter of

$$F_\beta = \frac{0.5}{s + 0.5}. \tag{5.17}$$

This prefilter is chosen on the basis that fast responses to β commands from the pilot are not a necessity since β is rarely commanded by the pilot to accomplish lateral tracking tasks. Also, the
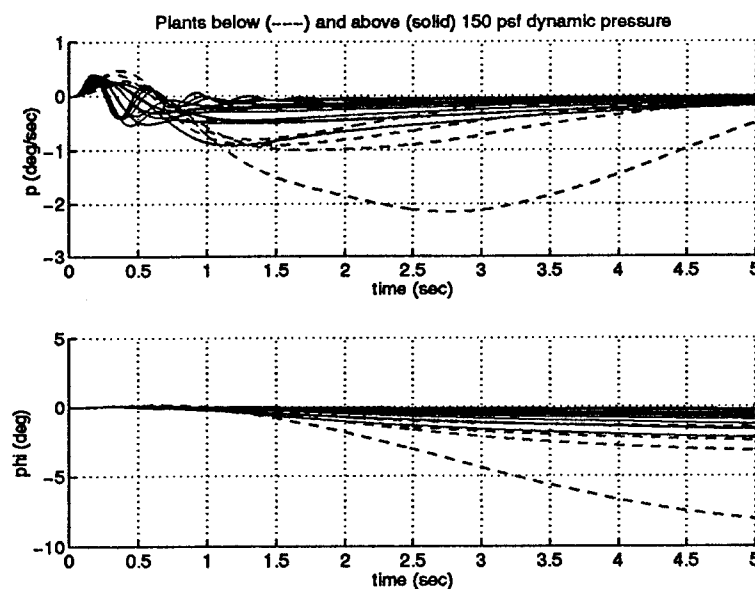
Figure 5.33 Lateral Design Unit β_{cmd} Step Responses (1 of 4)

frequency responses of MISO loop{2,1} in Figure 5.38 indicate that significant cross-coupling from a β input to roll rate are present; therefore, the β inputs of the pilot are heavily filtered to reduce the effects of this cross-coupling. A complete tabulation of the unit β_{cmd} step input responses for all plants is found in Appendix E.3.

In the same fashion as the roll rate loop, the unit β_{cmd} input step response data is used to synthesize a $\beta_{cmd_{(max)}}$ profile that avoids rate and deflection saturations. To facilitate this, the data generated for all plants by Equations (5.11) through (5.14) is plotted versus dynamic pressure to form an upper bound for the $\beta_{cmd_{(max)}}$ profile. As long as the profile remains below the composite bound formed by the minimum of Equations (5.11) through (5.14) for all $\bar{q}$, no rate or deflection saturations will occur. A plot of the composite upper bound and the proposed $\beta_{cmd_{(max)}}$ profile is shown in Figure 5.37. No performance lower bound is applicable since no performance requirements are dictated for β response.

5.2.6   Lateral Design Validation.

Plants below (---) and above (solid) 150 psf dynamic pressure
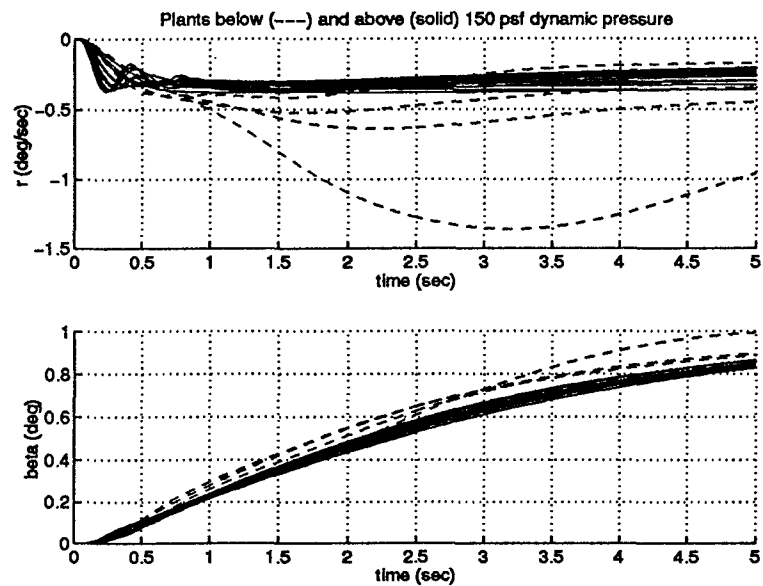
Figure 5.34   Lateral Design Unit β_{cmd} Step Responses (2 of 4)

Plants below (---) and above (solid) 150 psf dynamic pressure
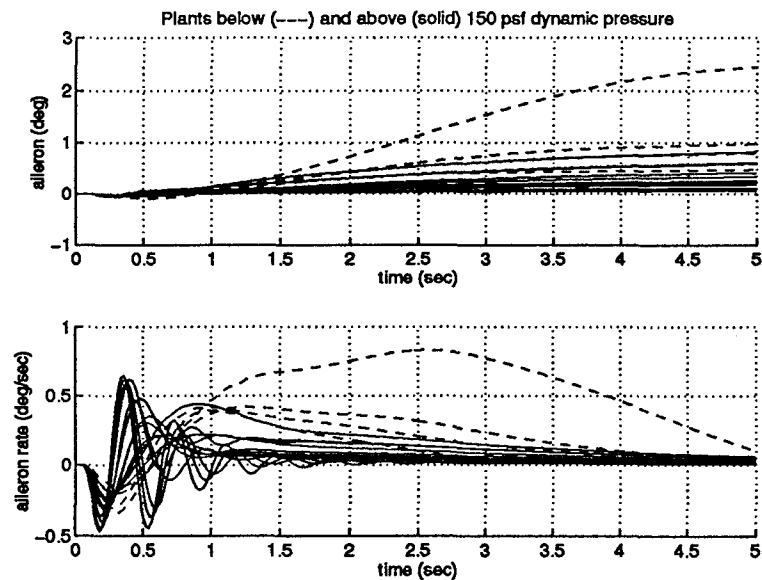
Figure 5.35   Lateral Design Unit β_{cmd} Step Responses (3 of 4)
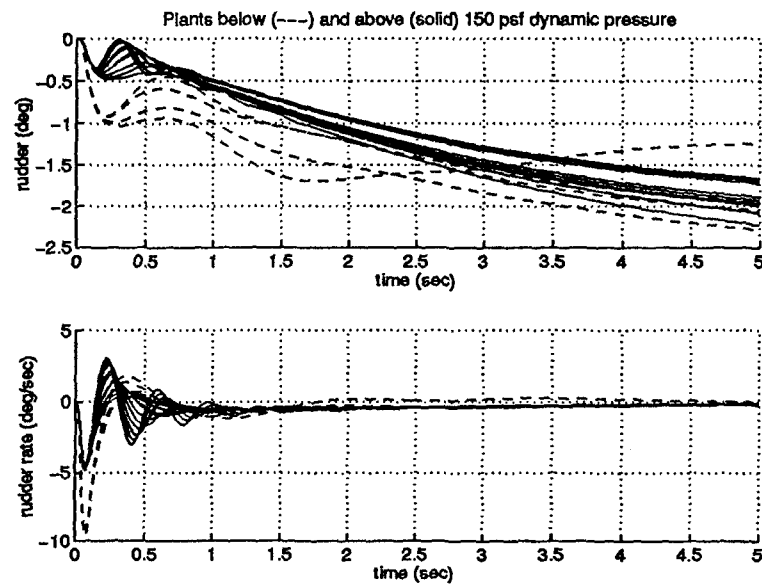
Figure 5.36   Lateral Design Unit β_{cmd} Step Responses (4 of 4)
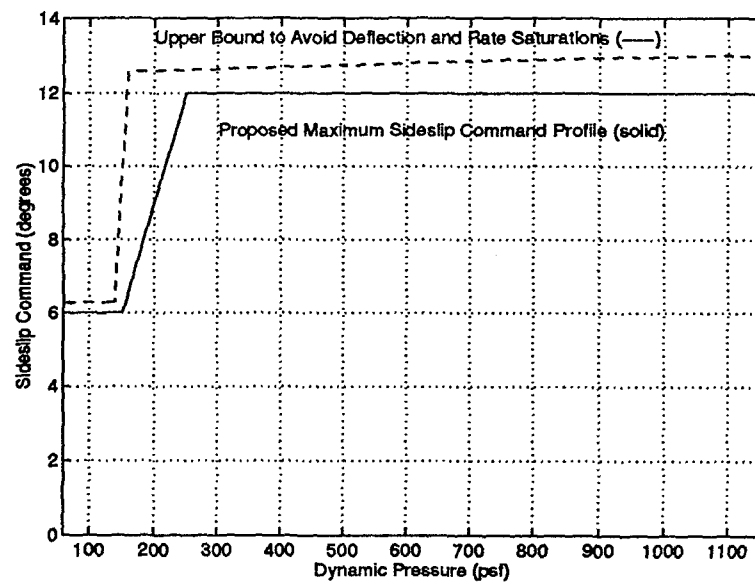
Figure 5.37   Proposed $\beta_{cmd_{(max)}}$ Profile to Avoid Saturations

5.2.6.1 QFTCAD Frequency Domain Lateral Design Validation. The QFTCAD tracking validation closed-loop Bode plots for the MIMO system are displayed in Figures 5.38 and 5.39. The four loops of the figures correspond to the following input output relationships.

- MISO loop{1,1} - β output from β input

- MISO loop{1,2} - β output from p input

- MISO loop{2,1} - p output from β input

- MISO loop{2,2} - p output from p input

Figure 5.38 depicts the tracking response for the low $\bar{q}$ plants. Recall that the tracking boundary models displayed for MISO loop{1,1} are arbitrarily chosen to enable the input of a β loop prefilter into the QFTCAD. The synthesis of the β loop prefilter is discussed in Section 5.2.5.2. The frequency responses of MISO loop{1,1} are robust, but do display some cross-coupling effects corresponding to the peak of the MISO loop{1,2} frequency response plots. The plots for MISO loop{1,2} indicate that some plants violate the 0.067 cross-coupling bound, so compliance with β cross-coupling limits must be confirmed through time domain analysis. MISO loop{2,1} of Figure 5.38 emerges as the reason for the lack of diagonal dominance in the lateral channel. Significant cross-coupling of sideslip to roll rate is present, especially below 1 rps. The MISO loop{2,2} frequency responses definitely reflect the effect of the cross-coupling, but are deemed acceptable. The physical explanation for the siginificant cross-coupling is that the dutch roll mode and β regulation loops impact the roll rate response at low dynamic pressures. As a pilot initiates a roll at low dynamic pressures, the rudder input commanded by the dutch roll mode damping and β regulation loops slows the roll rate. This results in the attenuation and delay of the roll rate response in the frequency domain. The closed loop bandwidth of all of the low $\bar{q}$ plants is less than 3.5 rps, but this fact makes physical sense since the aircraft is less responsive at these lower energy states.

In contrast to the responses of the low $\bar{q}$ plants, the high $\bar{q}$ plant responses illustrated in Figure 5.39 are very robust and MISO loops{1,1} and {2,2} show only slight evidence of cross-
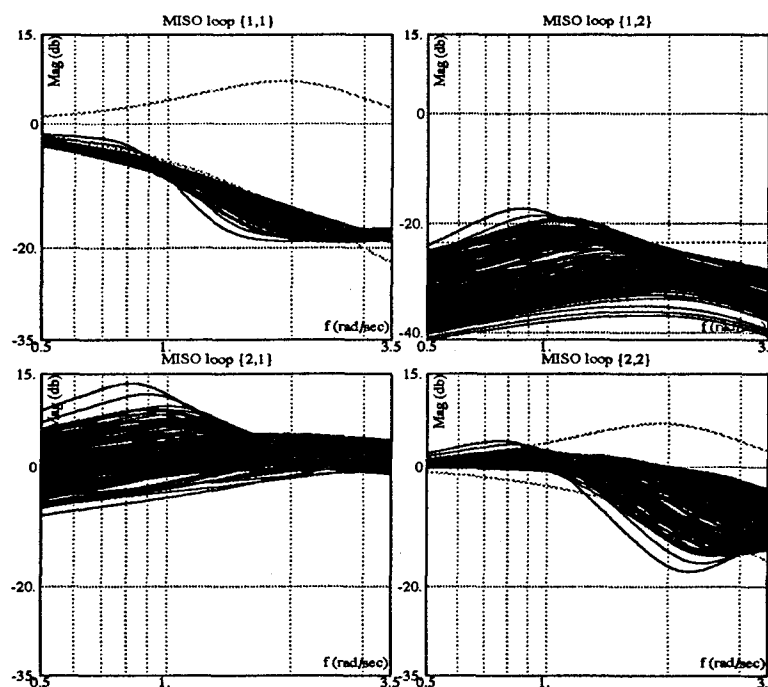
Figure 5.38   QFTCAD Tracking Validation for MIMO Lateral System for $\bar{q} \leq 170$ psf

coupling effects. All of the responses of MISO loop{1,2} remain below the desired cross-coupling bound, and the responses of MISO loop{2,1} show that the β cross-coupling effects on roll rate are much reduced at higher dynamic pressures.

The stability validations for the roll rate and the high and low $\bar{q}$ sideslip loops are depicted on the Nichols charts in Figures 5.40, 5.41, and 5.42, respectively. These figures indicate that the required stability has been achieved by both lateral loop designs.

5.2.6.2   Lateral Design Time Domain Validation.   The step input time responses of the lateral system to the $p_{cmd_{(max)}}$ profile are depicted in Figures 5.43 through 5.46 for a representative set of plants. A table containing the results of this simulation for all plants is contained in Appendix E.2. Figures 5.43 through 5.46 along with the appendix data clearly show that the sideslip limit of ± 6 degrees is not exceeded and that no actuator rate or control surface deflection saturations are present.
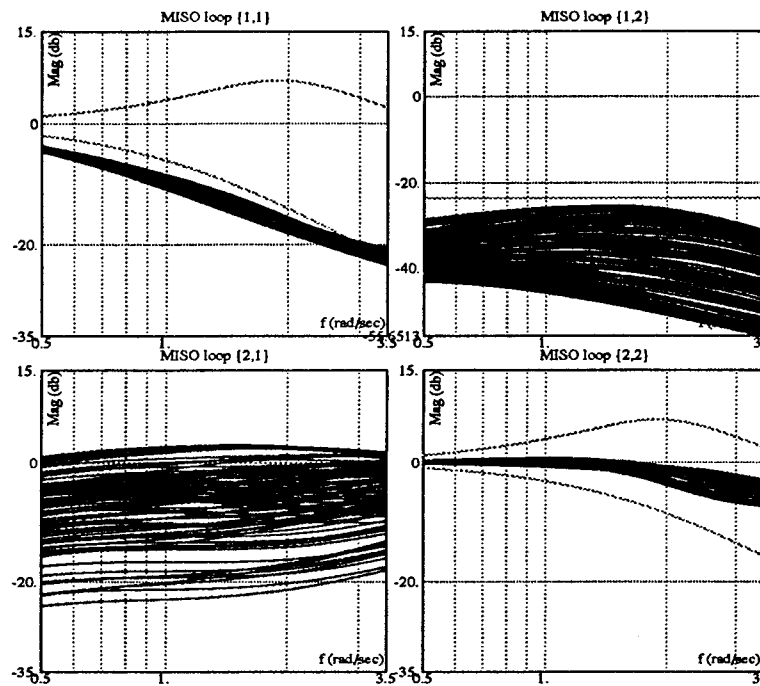
Figure 5.39 QFTCAD Tracking Validation for MIMO Lateral System for $\bar{q} \geq 130$ psf
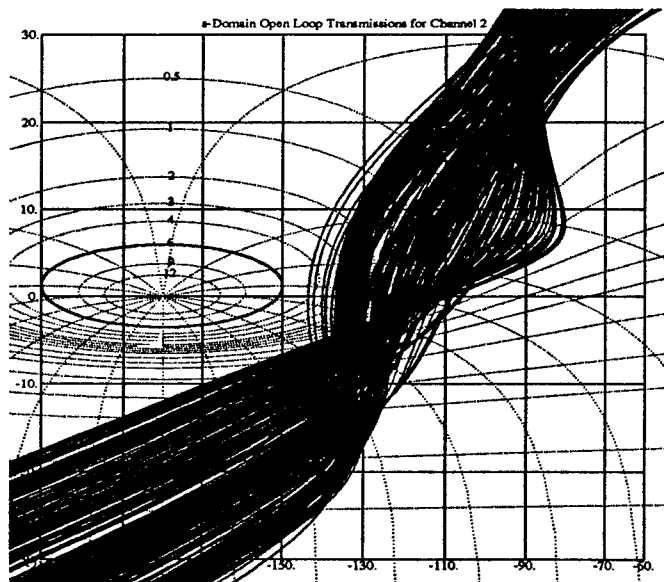
Figure 5.40 QFTCAD Stability Validation for Roll Rate Loop
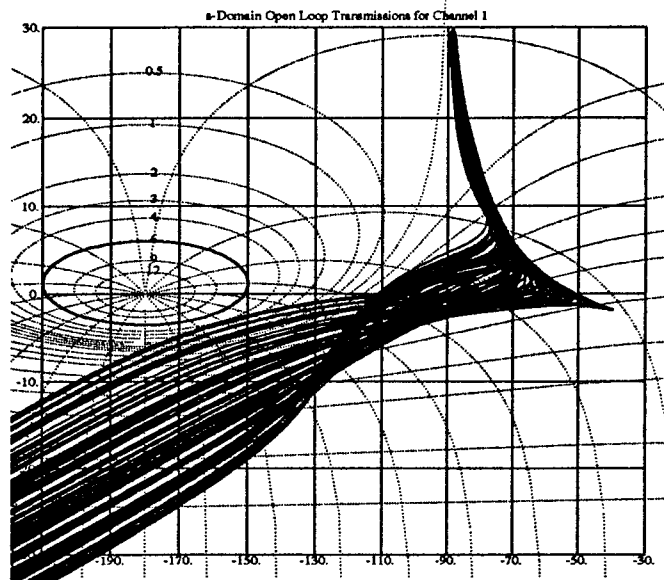
Figure 5.41   QFTCAD Stability Validation for High $\bar{q}$ Sideslip Loop
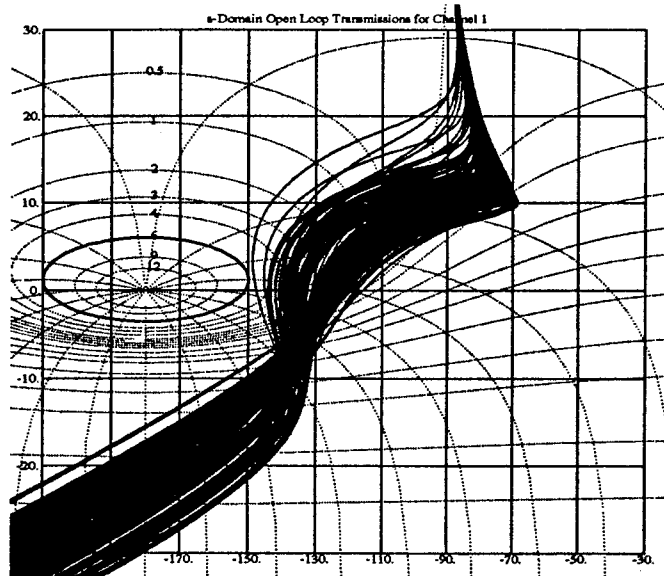
Figure 5.42   QFTCAD Stability Validation for Low $\bar{q}$ Sideslip Loop
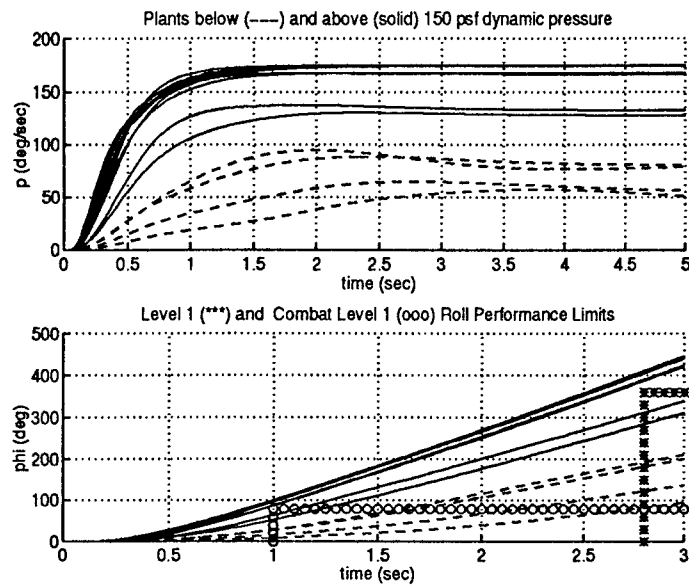
Figure 5.43   Lateral Design $p_{cmd_{(max)}}$ Step Responses (1 of 4)
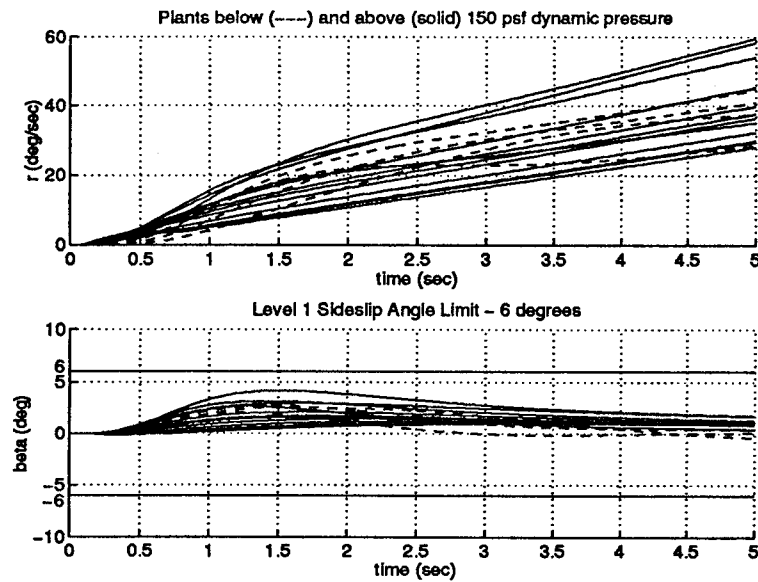
Figure 5.44   Lateral Design $p_{cmd_{(max)}}$ Step Responses (2 of 4)
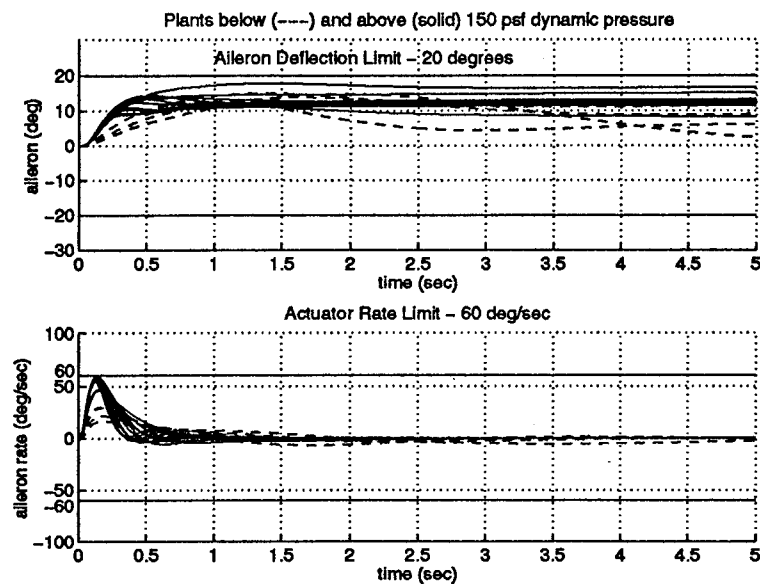
Figure 5.45   Lateral Design $p_{cmd_{(max)}}$ Step Responses (3 of 4)
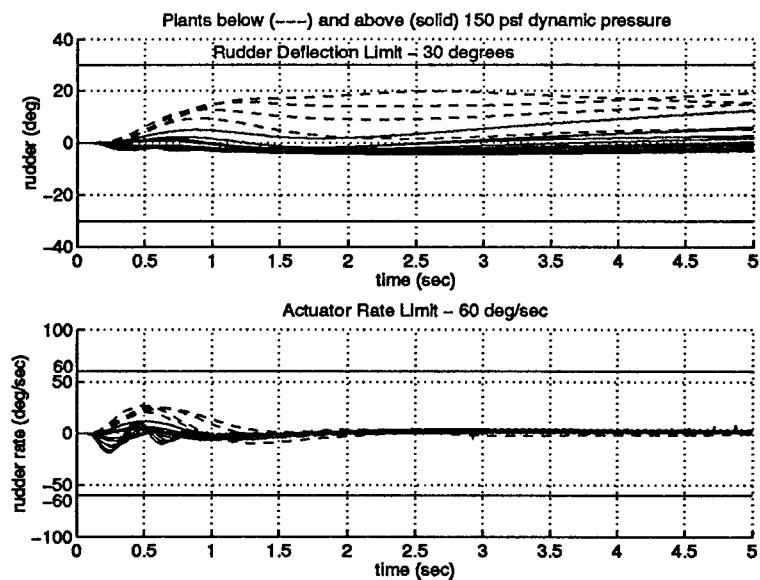
Figure 5.46   Lateral Design $p_{cmd_{(max)}}$ Step Responses (4 of 4)
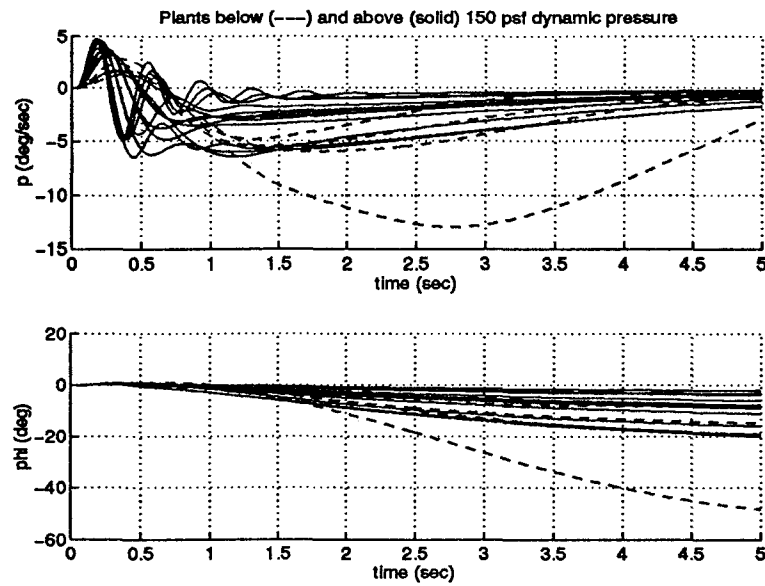
Figure 5.47   Lateral Design $\beta_{cmd_{(max)}}$ Step Responses (1 of 4)

The step input time responses of the lateral system to the $\beta_{cmd_{(max)}}$ profile are depicted in Figures 5.47 through 5.50 for a representative set of plants. A table containing the results of this simulation for all plants is contained in Appendix E.4. These figures and the appendix data confirm that no actuator rate or control surface deflection limits are exceeded.
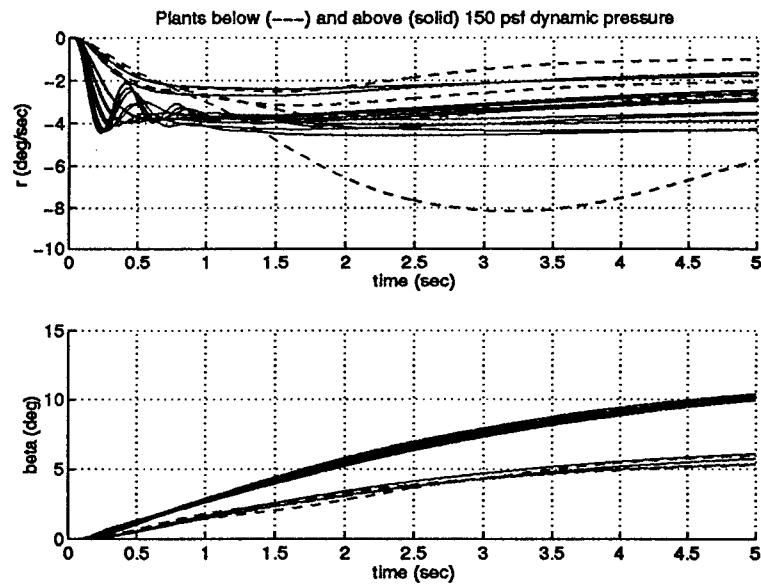
Figure 5.48   Lateral Design $\beta_{cmd_{(max)}}$ Step Responses (2 of 4)
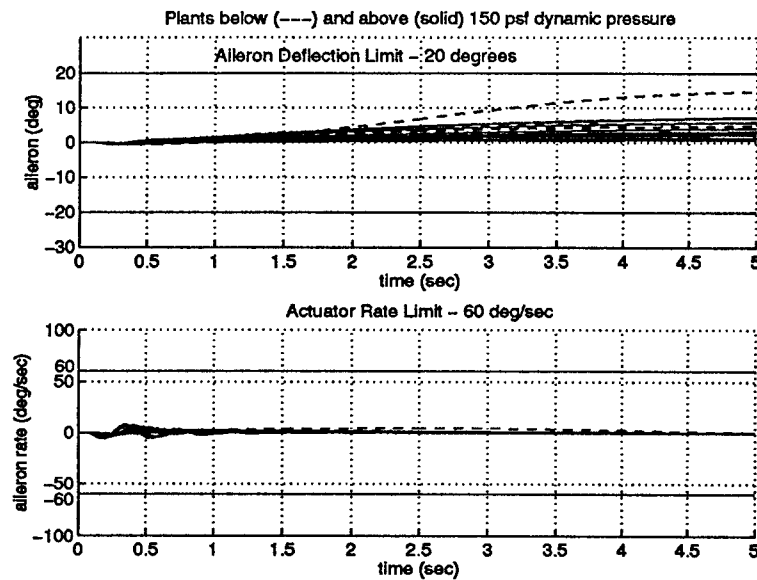
Figure 5.49   Lateral Design $\beta_{cmd_{(max)}}$ Step Responses (3 of 4)
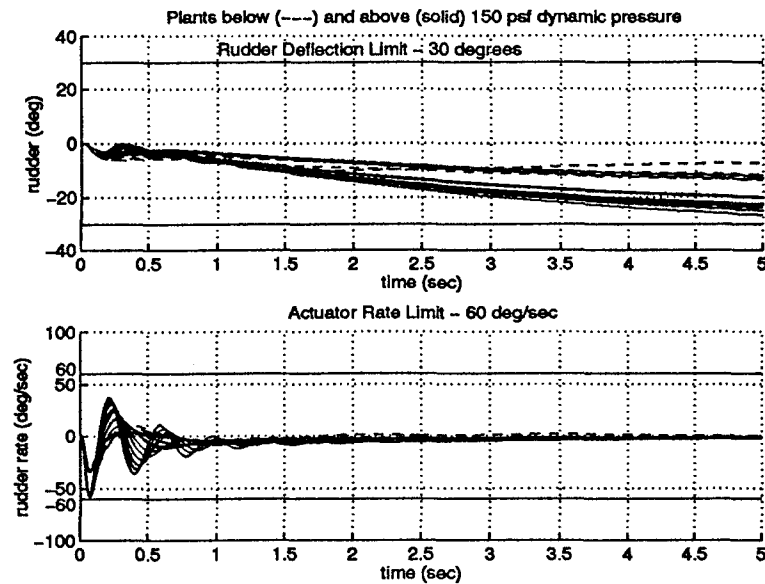
Figure 5.50   Lateral Design $\beta_{cmd_{(max)}}$ Step Responses (4 of 4)

5.3   Final Lateral Channel Design

The final design in the lateral channel is best described by the block diagram illustrated in Figure 5.51. To summarize, the roll stick force from the pilot is first scaled by the maximum p_{cmd} profile and then filtered. The filtered input is then passed to the roll rate compensator feedback loop where it is transformed into an appropriate aileron command. The horizontal tails receive a differential command equal to approximately one-third of the aileron command. A rudder force input from the pilot is first scaled by the maximum β_{cmd} profile and then filtered. The filtered input is then passed to the β compensator feedback loop to be transformed to a rudder reference signal. This rudder reference signal is then adjusted by the dutch roll mode damping feedback loop to generate an appropriate rudder command. The roll rate prefilter and both compensators meet the design guidelines set forth in Section 2.3. The β prefilter does not comply with the 3.5 rps minimum bandwidth requirement for the reasons discussed in Section 5.2.5.2. The necessary β channel compensator gain switching at $\bar{q} = 150$ psf is clearly indicated in Figure 5.51. This is the only direct gain scheduling present in either the longitudinal or lateral channel designs.

5-38
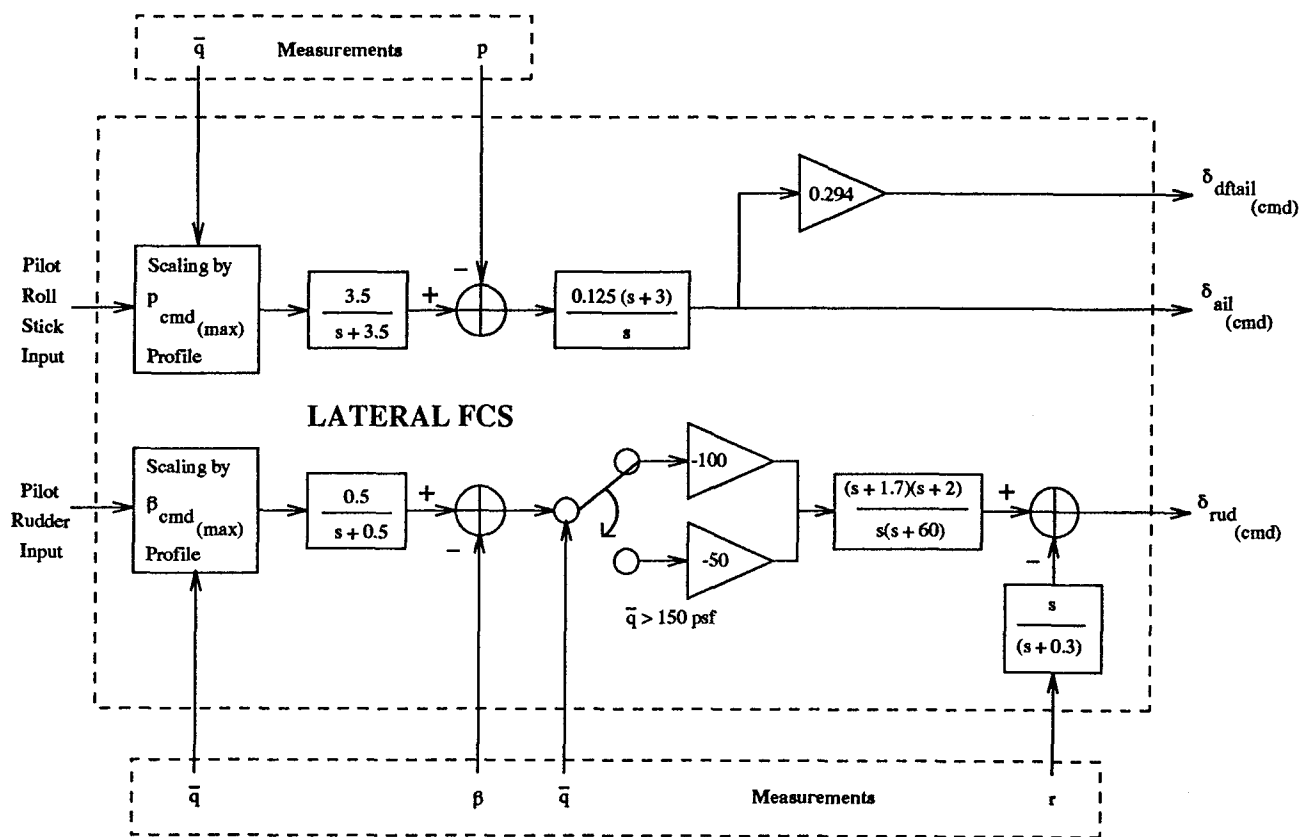
Figure 5.51 Final Lateral FCS Design Block Diagram

VI. Conclusions and Recommendations

6.1 Conclusions

In line with the research objectives proposed for this thesis, a full subsonic envelope FCS has been designed for the VISTA F-16. An integrated approach utilizing QFT along with time domain simulation has resulted in a design that is not only quite simple, but one that clearly reflects the physical limitations imposed by the "real world" (i.e., acutator rates and control surface deflections). QFT was an invaluable tool in the practical and efficient achievement of this task, allowing the designer to make insightful modifications to the design with full knowledge of the consequences of these modifications.

The importance of staying as close to the "real world" as possible when utilizing any robust control design technique cannot be overstated. In both the longitudinal and lateral channels, the first-cut QFT compensator designs produced very robust time responses to small command inputs; however, when inputs of the magnitude required to achieve the desired performance were considered, lengthy actuator rate and control surface deflection saturations occurred. Therefore, the robustness achieved by the high gain of these initial compensators had to be exchanged for the desired performance requirements by reducing the compensator gain. As an illustration, Reynold's final body axis roll rate compensator

$$G_p = \frac{1.6(s+7.6)(s+10)}{s(s+100)} \tag{6.1}$$

has a DC gain of 1.216 as compared to the roll rate compensator

$$G_p = \frac{0.125(s+3)}{s} \tag{6.2}$$

of this thesis which has a DC gain of 0.375 [8]. The responses of Reynold's system were very robust in response to small command inputs; however, with a compensator gain more than three

times that necessary to meet design tracking requirements while avoiding saturations, Reynold's suspicion about the possiblity of saturations when the system is acted upon by large inputs is clearly confirmed [8].

This FCS is void of any direct compensator gain scheduling except in the sideslip control loop. However, indirect scheduling of a sort is incorporated in all control loops through the scaling of the control stick force inputs of the pilot by a $\bar{q}$ dependent profile. These maximim allowable command input profiles are the means by which actuator rate and control deflection saturations are averted in this design, while at the same time achieving the desired performance. In this framework (and with a specified prefilter), the compensator gains themselves serve to establish the size of the allowable range of the maximum command input profiles. If the compensator gain is too high, then the actuator rate and control deflection upper bounds fall toward the performance bounds, thus closing the window for an acceptable maximum command input profile. An example of this effect of compensator gain is illustrated in Figure 6.1. Although higher gain increases robustness, it could result in lower than desired performance once saturations are taken into account. The location of the poles and zeros of the compensators affect the qualitative shape of the responses while also ensuring stability.

The application of the specifications set forth in Military Standard 1797A to an FCS design proves to be a difficult task. Many of the specifications are open-ended or incomplete. Some specifications are defined in both the time and frequency domains, but have no evident relationship to one another. Others are defined by only an upper or lower limit, rather than by both an upper and lower boundary of acceptable performance. Consequently, the engineer is given no clear-cut choice of what specifications to apply to a design. The validity of the particular specifications that are chosen to guide this design can only be tested by the evaluation of the resulting flying qualities by an actual pilot.
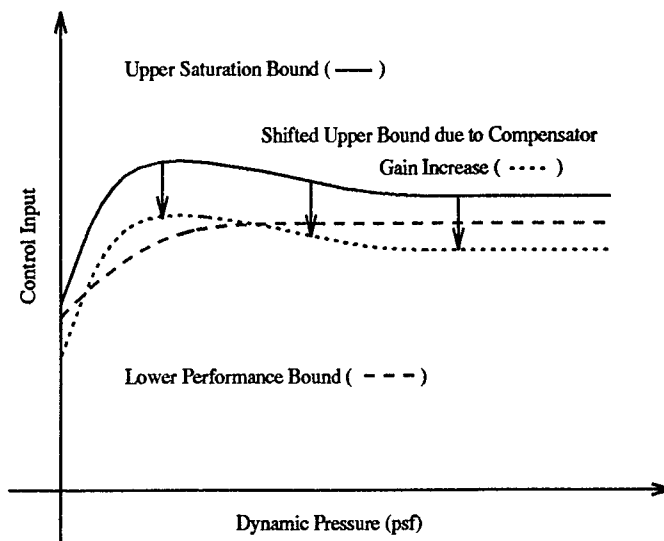
Figure 6.1   Effect of Compensator Gain Increase on Command Input Profile Bounds

The success of imbedding flying qualities into the longitudinal design by utilizing the dynamic C^* control parameter can only be measured by simulating the FCS with a pilot in the loop. Although the blend of plant parameters used in this thesis to create C^* may not be optimal, it provides an adequate starting point from which to continue the development of the concept.

The lack of diagonal dominance in the lateral channel resulted in applying QFT to only the stability specifications, leaving the tracking specifications up to time domain simulation analysis. This resulted in more trial and error than was necessary in the longitudinal design, but the QFT-CAD was still instrumental in allowing quick adjustments to the compensator to achieve the desired tracking performance while complying with stability constraints.

The FCS of this research effort has been validated thoroughly in both the time and frequency domains. In the lateral and longitudinal channels, some low $\bar{q}$ plants exhibit ballooning in response to roll rate and C^* command inputs. Whether or not this ballooning constitutes a nuisance to a pilot can only be determined by simulating the FCS with an actual pilot in the loop. However, if the ballooning is deemed a problem, it can be rectified by splitting the roll rate and C^* compensator designs as is done with the sideslip loop to achieve more robustness at low dynamic pressures. This

action will result in the degradation of large signal input performance due to the higher compensator gain needed to achieve the robustness.

The time domain validation of this design is based on step input responses. Other inputs that may be of interest in FCS design include pulses and doublets. Pulse or doublet control inputs may cause higher transient actuator rates and control surface deflections than those of a step. If this is the case, the gain of the compensator and/or the maximum command input profile can be adjusted to eliminate the saturations. The end result will be a slight degredation of aircraft performance in exchange for the elimination of any destabilizing saturations.

To summarize, this research effort

1. Introduces a new concept of imbedding flying qualities in an FCS through the use of a dynamic control parameter which attempts to accurately capture the true desires of a pilot as aircraft flight conditions vary.

2. Illuminates the benefits of applying QFT to a problem of large, but structured uncertainty (full subsonic envelope FCS design).

3. Demonstrates that robust control design techniques can be applied to practical problems and result in physically realizable solutions, but only when limitations imposed by the "real world" are kept close at hand during the design process.

6.2 Recommendations

To fully validate the concept of imbedding flying qualities in a longitudinal FCS design through the use of the C^* control parameter used in this thesis, it is recommended that a full nonlinear simulation of the FCS be conducted. If the nonlinear simulation does not reveal significant problems, the FCS should then be simulated with a pilot in the loop. The flying quality assessment resulting from the pilot-in-the-loop simulation will determine the overall effectiveness of the C^* parameter and will also allow qualitative assessment of the flight control system as a whole.

The integrated QFT and time domain simulation method utilized in this design required iteration to produce a viable design. If a way of generating Nichols chart boundaries to reflect actuator rate and control surface deflection limitations existed, then QFT could be applied without a requirement for time simulation. These physical restriction boundaries might appear as upper bounds on the Nichols chart. In this case, the job of the designer would be to synthesize a compensator to shape the nominal open-loop so that the nominal loop's magnitude-phase points are above the tracking bounds, but below these physical restriction bounds for all frequencies in the frequency spectrum of the design. If such a method could be incorporated into the QFTCAD, the iteration required to achieve a valid design could be greatly reduced. Therefore, it is recommended that future research efforts explore this possibility.

While on the subject of pilot-in-the-loop simulation, further research directed towards incorporating pilot compensation into the FCS design process is warranted. The imbedding of flying qualities in control parameters or placing pilot characteristics in system prefilters are but two examples of possible types of pilot compensation. Such research cannot hope to eliminate the need for pilot-in-the-loop simulation, but can reduce the number of design iterations required. In other words, if an FCS is designed with not only performance specifications but also pilot characteristics and desires in mind, the resulting design should require only slight modification following pilot-in-the-loop simulation. Therefore, if an effective means of emulating the characteristics and desires of a pilot can be employed from the outset of an FCS design, the design process will certainly be more efficient and less costly.

The Mil Std and other documents like it that are used to guide the design of flight control systems need to continue to evolve towards the definition of specifications that can be easily incorporated at the onset of a design process rather than those that must be be evaluated at the completion of the design. The task of developing one set of specifications for the full envelope of an aircraft is an impossible task due to the large variations in aircraft control response; however,

specifications in the form of upper and lower boundaries of acceptable performance could certainly be developed for specific regions of the flight envelope.

A couple of suggested improvements to the QFTCAD are

1. The QFTCAD currently has no feature to facilitate the input of a large number of plant models. This feature would have been a blessing in this design effort, and should be incorporated in future versions.

2. In some cases, the designer is interested in satisfying QFT tracking or disturbance boundaries for only some of the selected template frequencies. In fact, the frequencies of interest for tracking may be different than those for disturbance rejection. Currently, the QFTCAD composite boundaries are constructed using the tracking and disturbance boundaries for all template frequencies. It is suggested that the composite boundary feature be modified to allow the selection of which bounds are to be used for the composite at each template frequency.

Appendix A. Augmented Plant Generation and QFTCAD Plant Input

All of the augmented plants used in this thesis are generated in the following manner to avoid having to input them individually into the QFTCAD.

1. The augmented system's block diagram is constructed in the *Simulink* environment [10].

2. The *Matlab* 'linmod' command is used to generate state space matricies (**A**, **B**, **C**, and **D**) from the appropriate input(s) to the appropriate output(s) of the augmented system [11]. These matricies are generated for each of the basic SRF longitudinal or lateral aircraft models.

3. The state space matricies are then factored into gain-zero-pole form using the 'ss2zp' *Matlab* function [11]. This is the form that the QFTCAD requires.

4. The gain-zero-pole transfer functions are written to a file in the data format of the QFTCAD 'qftsave.m' file using the *Matlab* 'fprintf' command [11].

5. The formatted file is pasted into a 'qftsave.m' file which can then be loaded by the QFTCAD 'load' feature [1].

Concern was raised as to the validity of generating the augmented plants in this fashion using the *Matlab* 'linmod' function. The plant generation was validated by simulating both the original system block diagram and one containing only the augmented state space matricies. The time responses of both the original and augmented system representations were identical; hence, this plant generation technique is deemed valid.

An example *Matlab* m-file which automates this entire process for a 3 X 2 MIMO control system with no external disturbance follows [11].

% **Open transfer function data file**

```
fid = fopen('filename','a');
fprintf(fid,'plants = {');
```

% **Generate gain-zero-pole transfer functions from the SRF state space plants**

```
for u = 1:282;
    eval(['m' num2str(u)]);
    A=A_VISTA(5:8,5:8);
    B=[-B_VISTA(5:8,2),-B_VISTA(5:8,4),-B_VISTA(5:8,5)];
    [a,b,c,d]=linmod('Simulink model name');
    [z1,p1,k1]=ss2zp(a,b,c,d,1);
    [z2,p2,k2]=ss2zp(a,b,c,d,2);
    [z3,p3,k3]=ss2zp(a,b,c,d,3);
    z11=[z1(:,1)];
    z21=[z1(:,2)];
    z12=[z2(:,1)];
    z22=[z2(:,2)];
    z13=[z3(:,1)];
    z23=[z3(:,2)];
    p11=[p1];
    p21=[p1];
    p12=[p2];
    p22=[p2];
    p13=[p3];
    p23=[p3];
    k11=k1(1,1);
    k21=k1(2,1);
    k12=k2(1,1);
    k22=k2(2,1);
    k13=k3(1,1);
    k23=k3(2,1);
```

% **Write the gain, zeros, and poles to the data file**

```
fid = fopen('filename','a');
fprintf(fid,'{ "%i", {}, {{',u);
```

% **First output from first input**

```
fprintf(fid,'transferF[s, s, 0][%26.18E,\n {',k11);
w=size(z11,1);

if fix(w/2)<(w/2);
    for x=1:fix(w/2);
        fprintf(fid,'%26.18f+%26.18f*I,%26.18f-%26.18f*I,\n',real(z11(2*x-1)),
            abs(imag(z11(2*x-1))),real(z11(2*x)),abs(imag(z11(2*x))));
    end;
    fprintf(fid,'%26.18f+%26.18f*I}, {}, {',real(z11(w)),abs(imag(z11(w))));
else
```

```
          for x=1:(fix(w/2)-1);
                  fprintf(fid,'%26.18f+%26.18f*I,%26.18f-%26.18f*I,\n',real(z11(2*x-1)),
                        abs(imag(z11(2*x-1))),real(z11(2*x)),abs(imag(z11(2*x))));
          end;
          fprintf(fid,'%26.18f+%26.18f*I,%26.18f-%26.18f*I}, {}, {',real(z11(w-1)),
                  abs(imag(z11(w-1))),real(z11(w)),abs(imag(z11(w))));
end;

w=size(p11,1);

if fix(w/2)<(w/2);
          for x=1:fix(w/2);
                  fprintf(fid,'%26.18f+%26.18f*I,%26.18f-%26.18f*I,\n',real(p11(2*x-1)),
                        abs(imag(p11(2*x-1))),real(p11(2*x)),abs(imag(p11(2*x))));
          end;
          fprintf(fid,'%26.18f+%26.18f*I}, {}],\n',real(p11(w)),abs(imag(p11(w))));
else
          for x=1:(fix(w/2)-1);
                  fprintf(fid,'%26.18f+%26.18f*I,%26.18f-%26.18f*I,\n',real(p11(2*x-1)),
                        abs(imag(p11(2*x-1))),real(p11(2*x)),abs(imag(p11(2*x))));
          end;
          fprintf(fid,'%26.18f+%26.18f*I,%26.18f-%26.18f*I}, {}],\n',real(p11(w-1)),
                  abs(imag(p11(w-1))),real(p11(w)),abs(imag(p11(w))));
end;

          % First output from second input

Same as for 'First output from first input' with "z11", "p11", and "k11" replaced by "z12", "p12",
and "k12".

          % First output from third input

Same as for 'First output from first input' with "z11", "p11", and "k11" replaced by "z13", "p13",
and "k13". End with "...}, {}]}, {" instead of "...}, {}],".

          % Second output from first second and third input

Same as for first output with all "z1", "p1", and "k1" replaced by "z2", "p2", and "k2". End
with "...}, {}]}}, Null}," instead of "...}, {}]}, {".

end;
fclose(fid);

          % Final editing of 'filename' before pasting into 'qftsave.m'.
          % A UNIX editor source file is created which changes the last line of the file from "...Null},"
          % to "...Null}}" and replaces all exponential operators "E" with "*10^".

fid=fopen('edit','a');
fprintf(fid,'ed << !\ne filename\n,s/E/*10^/\n\\$s/Null},/Null}}/\nw filename\nq\n!\n');
fclose(fid);
!source edit
```

If the particular system of interest does have an external disturbance, then the transfer functions from the disturbance input to the system outputs are written in the **'filename'** file in place of "Null".

Appendix B. Parameter Space Data Points

This appendix contains a list of all of the data points for which LTI aircraft models are generated by the SRF.

#	U(ft/sec)	Mach	Alt(ft)	Tanks	$q(lb/ft^2)$
1	356.3108	0.38	30000	3	63.6460
2	306.8269	0.31	20000	1	65.4696
3	306.8179	0.31	20000	0	65.4696
4	282.6290	0.28	15000	1	65.5666
5	371.1044	0.39	30000	1	67.0399
6	371.0953	0.39	30000	0	67.0399
7	340.3061	0.35	25000	1	67.4267
8	340.2972	0.35	25000	0	67.4267
9	409.8783	0.44	35000	1	67.6717
10	407.3858	0.44	35000	3	67.6717
11	268.5053	0.26	10000	1	68.8746
12	268.4976	0.26	10000	0	68.8746
13	233.5497	0.22	1000	3	69.1382
14	316.8115	0.32	20000	3	69.7616
15	292.9719	0.29	15000	3	70.3335
16	252.9760	0.24	5000	1	70.9929
17	251.7848	0.24	5000	3	70.9929
18	349.9148	0.36	25000	3	71.3347
19	279.4878	0.27	10000	2	74.2746
20	280.3498	0.27	10000	1	74.2746
21	279.1366	0.27	10000	3	74.2746
22	280.3444	0.27	10000	0	74.2746
23	246.9440	0.23	1000	1	75.5664
24	264.9703	0.25	5000	0	77.0323
25	442.3595	0.47	35000	0	77.2143
26	496.4158	0.53	40000	1	77.2914
27	494.0463	0.53	40000	3	77.2914
28	496.4142	0.53	40000	0	77.2914
29	505.9001	0.54	40000	2	80.2356
30	507.2213	0.54	40000	1	80.2356
31	504.8485	0.54	40000	3	80.2356
32	507.2212	0.54	40000	0	80.2356
33	316.8614	0.31	15000	2	80.3692
34	317.7535	0.31	15000	1	80.3692
35	316.4457	0.31	15000	3	80.3692
36	317.7506	0.31	15000	0	80.3692
37	451.9645	0.48	35000	2	80.5349
38	453.1725	0.48	35000	1	80.5349
39	451.1247	0.48	35000	3	80.5349
40	453.1725	0.48	35000	0	80.5349
41	414.1389	0.43	30000	2	81.4969
42	415.2408	0.43	30000	1	81.4969
43	413.4491	0.43	30000	3	81.4969
44	415.2395	0.43	30000	0	81.4969
45	258.3013	0.24	1000	2	82.2802
46	258.9648	0.24	1000	1	82.2802
47	258.0598	0.24	1000	3	82.2802

#	U(ft/sec)	Mach	Alt(ft)	Tanks	$q(lb/ft^2)$
48	258.9626	0.24	1000	0	82.2802
49	276.1144	0.26	5000	2	83.3181
50	276.8024	0.26	5000	1	83.3181
51	275.8478	0.26	5000	3	83.3181
52	276.8001	0.26	5000	0	83.3181
53	351.7636	0.35	20000	2	83.4550
54	352.6862	0.35	20000	1	83.4550
55	351.2820	0.35	20000	3	83.4550
56	352.6857	0.35	20000	0	83.4550
57	384.2509	0.39	25000	2	83.7192
58	385.2349	0.39	25000	1	83.7192
59	383.6765	0.39	25000	3	83.7192
60	385.2340	0.39	25000	0	83.7192
61	473.5181	0.50	35000	2	87.3860
62	474.5858	0.50	35000	1	87.3860
63	472.6632	0.50	35000	3	87.3860
64	474.5876	0.50	35000	0	87.3860
65	605.7848	0.64	45000	1	88.7159
66	605.7899	0.64	45000	0	88.7159
67	435.3305	0.45	30000	3	89.2543
68	538.1724	0.57	40000	2	89.3983
69	539.2541	0.57	40000	1	89.3983
70	537.0843	0.57	40000	3	89.3983
71	539.2568	0.57	40000	0	89.3983
72	314.4668	0.30	10000	2	91.6970
73	315.2011	0.30	10000	1	91.6970
74	314.1575	0.30	10000	3	91.6970
75	315.2010	0.30	10000	0	91.6970
76	625.6518	0.66	45000	2	94.3473
77	626.6525	0.66	45000	1	94.3473
78	626.6591	0.66	45000	0	94.3473
79	734.2271	0.77	50000	0	101.0962
80	362.6436	0.35	15000	2	102.4478
81	363.2888	0.35	15000	1	102.4478
82	362.1963	0.35	15000	3	102.4478
83	363.2904	0.35	15000	0	102.4478
84	655.5445	0.69	45000	3	103.1193
85	744.5969	0.78	50000	0	103.7392
86	667.0249	0.70	45000	2	106.1299
87	667.9643	0.70	45000	1	106.1299
88	665.8376	0.70	45000	3	106.1299
89	667.9745	0.70	45000	0	106.1299
90	754.9666	0.79	50000	0	106.4162
91	407.6037	0.40	20000	2	109.0025
92	408.2125	0.40	20000	1	109.0025
93	407.0826	0.40	20000	3	109.0025
94	408.2147	0.40	20000	0	109.0025

#	U(ft/sec)	Mach	Alt(ft)	Tanks	$q(lb/ft^2)$
95	764.1132	0.80	50000	2	109.1273
96	765.2863	0.80	50000	1	109.1273
97	765.3006	0.80	50000	0	109.1273
98	489.3799	0.50	30000	2	110.1905
99	490.0036	0.50	30000	1	110.1905
100	488.6942	0.50	30000	3	110.1905
101	490.0065	0.50	30000	0	110.1905
102	323.1903	0.30	5000	2	110.9265
103	323.7697	0.30	5000	1	110.9265
104	322.7902	0.30	5000	3	110.9265
105	323.7712	0.30	5000	0	110.9265
106	774.5156	0.81	50000	2	111.8726
107	775.6357	0.81	50000	1	111.8726
108	775.6498	0.81	50000	0	111.8726
109	784.8859	0.82	50000	2	114.6519
110	785.9575	0.82	50000	1	114.6519
111	785.9714	0.82	50000	0	114.6519
112	795.2271	0.83	50000	2	117.4653
113	796.2540	0.83	50000	1	117.4653
114	796.2675	0.83	50000	0	117.4653
115	805.5421	0.84	50000	2	120.3129
116	806.5272	0.84	50000	1	120.3129
117	803.9543	0.84	50000	3	120.3129
118	806.5403	0.84	50000	0	120.3129
119	718.4875	0.75	45000	2	121.8328
120	719.3352	0.75	45000	1	121.8328
121	717.1732	0.75	45000	3	121.8328
122	719.3445	0.75	45000	0	121.8328
123	815.8332	0.85	50000	2	123.1945
124	816.6036	0.85	50000	1	123.1945
125	814.2523	0.85	50000	3	123.1945
126	816.6129	0.85	50000	0	123.1945
127	825.9927	0.86	50000	2	126.1103
128	826.6674	0.86	50000	1	126.1103
129	824.5324	0.86	50000	3	126.1103
130	826.6767	0.86	50000	0	126.1103
131	836.0692	0.87	50000	2	129.0601
132	836.7357	0.87	50000	1	129.0601
133	834.7814	0.87	50000	3	129.0601
134	836.7450	0.87	50000	0	129.0601
135	330.6034	0.30	1000	2	129.4213
136	331.0931	0.30	1000	1	129.4213
137	330.2076	0.30	1000	3	129.4213
138	331.0943	0.30	1000	0	129.4213
139	411.7170	0.39	15000	2	129.8252
140	412.2256	0.39	15000	1	129.8252
141	411.1960	0.39	15000	3	129.8252

#	U(ft/sec)	Mach	Alt(ft)	Tanks	$q(lb/ft^2)$
142	412.2274	0.39	15000	0	129.8252
143	534.4108	0.54	30000	2	129.9582
144	534.9595	0.54	30000	1	129.9582
145	533.6214	0.54	30000	3	129.9582
146	534.9625	0.54	30000	0	129.9582
147	488.3471	0.49	25000	2	130.0074
148	488.8853	0.49	25000	1	130.0074
149	487.6650	0.49	25000	3	130.0074
150	488.8876	0.49	25000	0	130.0074
151	587.5572	0.61	35000	2	130.0653
152	588.1083	0.61	35000	1	130.0653
153	586.6335	0.61	35000	3	130.0653
154	588.1118	0.61	35000	0	130.0653
155	447.9792	0.44	20000	2	130.1006
156	448.5037	0.44	20000	1	130.1006
157	447.3843	0.44	20000	3	130.1006
158	448.5057	0.44	20000	0	130.1006
159	749.0121	0.78	45000	2	131.7744
160	749.5445	0.78	45000	1	131.7744
161	747.7755	0.78	45000	3	131.7744
162	749.5507	0.78	45000	0	131.7744
163	846.1508	0.88	50000	2	132.0441
164	846.8071	0.88	50000	1	132.0441
165	844.9784	0.88	50000	3	132.0441
166	846.8163	0.88	50000	0	132.0441
167	671.9930	0.70	40000	2	134.8266
168	672.4916	0.70	40000	1	134.8266
169	670.9288	0.70	40000	3	134.8266
170	672.4959	0.70	40000	0	134.8266
171	856.2359	0.89	50000	2	135.0621
172	856.8798	0.89	50000	1	135.0621
173	855.0580	0.89	50000	3	135.0621
174	856.8889	0.89	50000	0	135.0621
175	461.4592	0.45	20000	3	137.9562
176	866.3225	0.90	50000	2	138.1142
177	866.9518	0.90	50000	1	138.1142
178	865.1412	0.90	50000	3	138.1142
179	866.9608	0.90	50000	0	138.1142
180	592.3990	0.60	30000	3	158.6743
181	427.6254	0.40	10000	3	163.0169
182	848.8048	0.88	45000	2	167.7286
183	849.1861	0.88	45000	1	167.7286
184	847.9139	0.88	45000	3	167.7286
185	849.1904	0.88	45000	0	167.7286
186	515.3699	0.50	20000	2	170.3164
187	515.6489	0.50	20000	1	170.3164
188	514.9072	0.50	20000	3	170.3164

#	U(ft/sec)	Mach	Alt(ft)	Tanks	$\dot{q}(lb/ft^2)$
189	515.6502	0.50	20000	0	170.3164
190	643.1663	0.65	30000	3	186.2219
191	567.6104	0.55	20000	3	206.0828
192	482.4902	0.45	10000	3	206.3182
193	840.2690	0.87	40000	2	208.2658
194	840.5090	0.87	40000	1	208.2658
195	839.7098	0.87	40000	3	208.2658
196	840.5116	0.87	40000	0	208.2658
197	694.1871	0.70	30000	2	215.9733
198	694.4091	0.70	30000	1	215.9733
199	693.6675	0.70	30000	3	215.9733
200	694.4109	0.70	30000	0	215.9733
201	869.9337	0.90	40000	1	222.8766
202	869.2272	0.90	40000	3	222.8766
203	869.9363	0.90	40000	0	222.8766
204	443.5660	0.40	1000	2	228.5562
205	443.7502	0.40	1000	1	228.5562
206	443.2620	0.40	1000	3	228.5562
207	443.7508	0.40	1000	0	228.5562
208	620.0384	0.60	20000	3	245.2556
209	743.9712	0.75	30000	3	247.9286
210	537.3339	0.50	10000	2	254.7139
211	537.4980	0.50	10000	1	254.7139
212	536.9779	0.50	10000	3	254.7139
213	537.4987	0.50	10000	0	254.7139
214	845.4997	0.87	35000	2	264.5698
215	845.6716	0.87	35000	1	264.5698
216	845.0479	0.87	35000	3	264.5698
217	845.6735	0.87	35000	0	264.5698
218	794.1589	0.80	30000	3	282.0876
219	672.3800	0.65	20000	3	287.8346
220	591.2659	0.55	10000	3	308.2038
221	864.8840	0.87	30000	2	333.6127
222	865.0098	0.87	30000	1	333.6127
223	864.5085	0.87	30000	3	333.6127
224	865.0110	0.87	30000	0	333.6127
225	724.9935	0.70	20000	2	333.8201
226	725.1219	0.70	20000	1	333.8201
227	724.5963	0.70	20000	3	333.8201
228	725.1229	0.70	20000	0	333.8201
229	894.9976	0.90	30000	1	357.0172
230	894.5495	0.90	30000	3	357.0172
231	894.9987	0.90	30000	0	357.0172
232	645.4193	0.60	10000	3	366.7880
233	776.7334	0.75	20000	3	383.2118
234	883.6877	0.87	25000	2	416.6143
235	883.7897	0.87	25000	1	416.6143

#	U(ft/sec)	Mach	Alt(ft)	Tanks	$\dot{q}(lb/ft^2)$
236	883.3687	0.87	25000	3	416.6143
237	883.7905	0.87	25000	0	416.6143
238	699.5460	0.65	10000	3	430.4664
239	828.8166	0.80	20000	3	436.0099
240	753.9324	0.70	10000	2	499.2391
241	754.0159	0.70	10000	1	499.2391
242	753.6174	0.70	10000	3	499.2391
243	754.0165	0.70	10000	0	499.2391
244	891.6245	0.86	20000	2	503.8640
245	891.7075	0.86	20000	1	503.8640
246	891.3319	0.86	20000	3	503.8640
247	891.7080	0.86	20000	0	503.8640
248	667.3123	0.60	1000	2	514.2514
249	667.3877	0.60	1000	1	514.2514
250	667.0334	0.60	1000	3	514.2514
251	667.3881	0.60	1000	0	514.2514
252	933.2764	0.90	20000	1	551.8250
253	932.9374	0.90	20000	3	551.8250
254	933.2769	0.90	20000	0	551.8250
255	807.6479	0.75	10000	3	573.1062
256	909.3434	0.86	15000	2	618.5337
257	909.4110	0.86	15000	1	618.5337
258	909.0850	0.86	15000	3	618.5337
259	909.4115	0.86	15000	0	618.5337
260	861.6325	0.80	10000	3	652.0676
261	778.8329	0.70	1000	2	699.9532
262	778.8885	0.70	1000	1	699.9532
263	778.5750	0.70	1000	3	699.9532
264	778.8887	0.70	1000	0	699.9532
265	937.4566	0.87	10000	2	771.1717
266	937.5140	0.87	10000	1	771.1717
267	937.2269	0.87	10000	3	771.1717
268	937.5142	0.87	10000	0	771.1717
269	969.8751	0.90	10000	1	825.2729
270	969.6061	0.90	10000	3	825.2729
271	969.8754	0.90	10000	0	825.2729
272	965.6384	0.88	5000	2	954.4603
273	965.6884	0.88	5000	1	954.4603
274	965.4279	0.88	5000	3	954.4603
275	965.6886	0.88	5000	0	954.4603
276	979.3263	0.88	1000	2	1106.2120
277	979.3723	0.88	1000	1	1106.2120
278	979.1241	0.88	1000	3	1106.2120
279	979.3725	0.88	1000	0	1106.2120
280	1001.6410	0.90	1000	1	1157.0650
281	1001.4010	0.90	1000	3	1157.0650
282	1001.6410	0.90	1000	0	1157.0650

Appendix C. Longitudinal Channel Time Domain Simulation Data

This appendix contains all longitudinal channel time domain simulation results.

C.1 Longitudinal Unit C^*_{cmd} Step Input Time Response Data

#	q	t_1	Δt_{min}	Δt	Δt_{max}	$\frac{\Delta q_2}{\Delta q_1}$	$\dot{\delta}_{elev(max)}$	$\delta_{elev(max)_{pert}}$	$g_{pil(ss)}$	$\alpha_{ss_{pert}}$
1	65.4696	0.110	0.029	0.590	1.630	0.00000	5.561	0.687	1.177	2.539
2	65.4696	0.120	0.029	0.750	1.630	0.00000	5.650	0.786	1.178	2.561
3	65.5666	0.110	0.032	0.595	1.769	0.00000	5.562	0.688	1.166	2.410
4	67.0399	0.120	0.024	0.735	1.347	0.00000	5.646	0.780	1.205	2.869
5	67.0399	0.120	0.024	0.730	1.347	0.00000	5.645	0.778	1.204	2.860
6	67.4267	0.120	0.026	0.740	1.469	0.00000	5.647	0.782	1.194	2.724
7	67.4267	0.120	0.026	0.735	1.469	0.00000	5.646	0.780	1.194	2.716
8	67.6717	0.120	0.022	0.725	1.220	0.00000	5.643	0.776	1.218	3.029
9	68.8746	0.120	0.034	0.755	1.862	0.00000	5.648	0.786	1.166	2.322
10	68.8746	0.120	0.034	0.750	1.862	0.00000	5.647	0.784	1.165	2.317
11	70.9929	0.120	0.036	0.755	1.976	0.00000	5.646	0.784	1.160	2.207
12	74.2746	0.115	0.032	0.720	1.789	0.00000	5.632	0.765	1.176	2.363
13	74.2746	0.120	0.032	0.735	1.783	0.00000	5.640	0.776	1.178	2.338
14	74.2746	0.120	0.032	0.730	1.784	0.00000	5.639	0.775	1.178	2.332
15	75.5664	0.120	0.036	0.745	2.025	0.00000	5.640	0.778	1.162	2.124
16	77.0323	0.120	0.034	0.730	1.887	0.00000	5.636	0.773	1.173	2.216
17	77.2143	0.120	0.020	0.700	1.130	0.00000	5.627	0.755	1.253	3.442
18	77.2914	0.120	0.018	0.695	1.007	0.00000	5.625	0.753	1.265	3.691
19	77.2914	0.120	0.018	0.690	1.007	0.00000	5.624	0.752	1.264	3.669
20	80.2356	0.120	0.018	0.675	0.988	0.00000	5.617	0.745	1.268	3.700
21	80.2356	0.120	0.018	0.680	0.986	0.00000	5.618	0.745	1.274	3.720
22	80.2356	0.120	0.018	0.675	0.986	0.00000	5.617	0.744	1.273	3.697
23	80.3692	0.115	0.028	0.705	1.578	0.00000	5.623	0.754	1.213	2.707
24	80.3692	0.120	0.028	0.710	1.574	0.00000	5.628	0.760	1.217	2.699
25	80.3692	0.120	0.028	0.705	1.574	0.00000	5.627	0.758	1.216	2.687
26	80.5349	0.120	0.020	0.680	1.106	0.00000	5.618	0.746	1.257	3.468
27	80.5349	0.120	0.020	0.685	1.103	0.00000	5.620	0.748	1.264	3.484
28	80.5349	0.120	0.020	0.685	1.103	0.00000	5.619	0.746	1.262	3.465
29	81.4969	0.115	0.022	0.685	1.207	0.00000	5.617	0.746	1.250	3.275
30	81.4969	0.120	0.022	0.690	1.204	0.00000	5.620	0.748	1.256	3.285
31	81.4969	0.120	0.022	0.685	1.204	0.00000	5.619	0.747	1.254	3.267
32	82.2802	0.115	0.035	0.705	1.936	0.00000	5.621	0.754	1.186	2.261
33	82.2802	0.115	0.035	0.715	1.931	0.00000	5.627	0.761	1.190	2.239
34	82.2802	0.115	0.035	0.710	1.931	0.00000	5.626	0.760	1.190	2.232
35	83.3181	0.115	0.033	0.700	1.811	0.00000	5.618	0.750	1.198	2.389
36	83.3181	0.115	0.033	0.705	1.806	0.00000	5.624	0.757	1.203	2.371
37	83.3181	0.115	0.033	0.705	1.806	0.00000	5.623	0.756	1.202	2.362
38	83.4550	0.115	0.026	0.685	1.421	0.00000	5.615	0.745	1.231	2.898
39	83.4550	0.115	0.026	0.695	1.418	0.00000	5.619	0.750	1.237	2.895
40	83.4550	0.115	0.026	0.690	1.418	0.00000	5.618	0.748	1.235	2.881
41	83.7192	0.115	0.023	0.680	1.301	0.00000	5.613	0.742	1.244	3.089
42	83.7192	0.115	0.023	0.690	1.298	0.00000	5.617	0.746	1.250	3.094
43	83.7192	0.115	0.023	0.685	1.298	0.00000	5.616	0.744	1.249	3.079
44	87.3860	0.115	0.019	0.650	1.056	0.00000	5.602	0.731	1.277	3.528
45	87.3860	0.115	0.019	0.655	1.054	0.00000	5.604	0.732	1.284	3.539
46	87.3860	0.115	0.019	0.655	1.054	0.00000	5.603	0.731	1.282	3.519

#	q	t_1	Δt_{min}	Δt	Δt_{max}	$\frac{\Delta q_2}{\Delta q_1}$	$\dot{\delta}_{elev(max)}$	$\delta_{elev(max)_{pert}}$	$g_{pil(ss)}$	$\alpha_{ss_{pert}}$
47	88.7159	0.115	0.013	0.655	0.825	0.00000	5.588	-1.777	1.382	4.383
48	88.7159	0.115	0.015	0.650	0.825	0.00000	5.586	-1.702	1.379	4.349
49	89.3983	0.115	0.017	0.635	0.929	0.00000	5.596	0.724	1.296	3.800
50	89.3983	0.115	0.017	0.670	0.927	0.00000	5.596	-1.876	1.365	4.206
51	89.3983	0.115	0.017	0.665	0.927	0.00000	5.595	-1.800	1.362	4.173
52	91.6970	0.115	0.029	0.660	1.590	0.00000	5.600	0.731	1.230	2.575
53	91.6970	0.115	0.029	0.665	1.586	0.00000	5.605	0.737	1.234	2.557
54	91.6970	0.115	0.029	0.665	1.586	0.00000	5.604	0.736	1.233	2.547
55	94.3473	0.115	0.014	0.615	0.799	0.00000	5.572	-1.643	1.397	4.383
56	94.3473	0.115	0.014	0.615	0.798	0.00000	5.572	-1.685	1.403	4.354
57	94.3473	0.115	0.014	0.610	0.798	0.00000	5.571	-1.613	1.400	4.321
58	101.0962	0.110	0.012	0.545	0.681	0.00000	5.535	-1.145	1.429	4.381
59	102.4478	0.115	0.025	0.615	1.379	0.00000	5.577	-0.876	1.277	2.955
60	102.4478	0.115	0.025	0.615	1.376	0.00000	5.582	-1.048	1.283	2.938
61	102.4478	0.115	0.025	0.615	1.376	0.00000	5.581	-0.997	1.282	2.923
62	103.7392	0.110	0.012	0.580	0.672	0.00000	5.527	-2.182	1.454	5.285
63	106.1299	0.110	0.013	0.555	0.750	0.00000	5.540	-1.523	1.441	4.354
64	106.1299	0.110	0.013	0.580	0.749	0.00000	5.541	-1.848	1.431	4.852
65	106.1299	0.110	0.013	0.575	0.749	0.00000	5.539	-1.775	1.428	4.815
66	106.4162	0.110	0.012	0.560	0.662	0.00000	5.519	-2.159	1.465	5.289
67	109.0025	0.110	0.022	0.590	1.227	0.00000	5.564	-1.034	1.316	3.157
68	109.0025	0.115	0.022	0.585	1.225	0.00000	5.568	-1.193	1.323	3.139
69	109.0025	0.115	0.022	0.585	1.225	0.00000	5.566	-1.137	1.321	3.122
70	109.1273	0.110	0.012	0.540	0.654	0.00000	5.511	-1.689	1.447	5.143
71	109.1273	0.110	0.012	0.550	0.653	0.00000	5.512	-2.210	1.479	5.333
72	109.1273	0.110	0.012	0.545	0.653	0.00000	5.511	-2.129	1.475	5.288
73	110.1905	0.115	0.018	0.570	1.022	0.00000	5.558	-1.402	1.374	3.644
74	110.1905	0.115	0.018	0.570	1.020	0.00000	5.560	-1.538	1.382	3.629
75	110.1905	0.115	0.018	0.565	1.020	0.00000	5.559	-1.473	1.379	3.605
76	110.9265	0.110	0.028	0.600	1.547	0.00000	5.564	0.701	1.258	2.611
77	110.9265	0.110	0.028	0.605	1.544	0.00000	5.571	-0.819	1.263	2.576
78	110.9265	0.110	0.028	0.605	1.544	0.00000	5.569	-0.774	1.262	2.565
79	111.8726	0.110	0.012	0.520	0.646	0.00000	5.503	-1.422	1.447	5.007
80	111.8726	0.110	0.012	0.525	0.645	0.00000	5.503	-1.911	1.478	5.182
81	111.8726	0.110	0.012	0.525	0.645	0.00000	5.501	-1.834	1.474	5.140
82	114.6519	0.110	0.011	0.500	0.637	0.00000	5.494	-1.180	1.448	4.885
83	114.6519	0.110	0.011	0.505	0.636	0.00000	5.493	-1.643	1.477	5.048
84	114.6519	0.110	0.011	0.500	0.636	0.00000	5.492	-1.571	1.474	5.009
85	117.4653	0.110	0.011	0.480	0.629	0.00000	5.485	-0.964	1.450	4.777
86	117.4653	0.110	0.011	0.485	0.628	0.00000	5.484	-1.406	1.478	4.931
87	117.4653	0.110	0.011	0.480	0.628	0.00000	5.482	-1.338	1.475	4.894
88	120.3129	0.105	0.011	0.470	0.621	0.00000	5.476	-0.770	1.452	4.682
89	120.3129	0.105	0.011	0.470	0.620	0.00000	5.473	-1.196	1.479	4.829
90	120.3129	0.105	0.011	0.470	0.620	0.00000	5.471	-1.131	1.476	4.793
91	121.8328	0.110	0.013	0.500	0.696	0.00000	5.497	-1.527	1.469	4.855
92	121.8328	0.110	0.013	0.505	0.695	0.00000	5.499	-1.911	1.494	4.967

#	q	t_1	Δt_{min}	Δt	Δt_{max}	$\frac{\Delta q_2}{\Delta q_1}$	$\dot{\delta}_{elev(max)}$	$\delta_{elev(max)_{pert}}$	$g_{pil(ss)}$	$\alpha_{ss_{pert}}$
93	121.8328	0.110	0.013	0.500	0.695	0.00000	5.497	-1.839	1.491	4.929
94	123.1945	0.105	0.011	0.455	0.613	0.00000	5.465	0.622	1.454	4.599
95	123.1945	0.105	0.011	0.430	0.612	0.00000	5.463	-2.247	1.602	4.590
96	123.1945	0.105	0.011	0.430	0.612	0.00000	5.462	-2.166	1.597	4.552
97	126.1103	0.105	0.011	0.430	0.605	0.00000	5.455	-1.814	1.581	4.517
98	126.1103	0.105	0.011	0.420	0.605	0.00000	5.454	-2.308	1.615	4.649
99	126.1103	0.105	0.011	0.420	0.605	0.00000	5.452	-2.228	1.611	4.611
100	129.0601	0.105	0.011	0.420	0.598	0.00000	5.446	-1.879	1.595	4.577
101	129.0601	0.105	0.011	0.410	0.598	0.00000	5.445	-2.370	1.629	4.706
102	129.0601	0.105	0.011	0.410	0.598	0.00000	5.444	-2.291	1.624	4.669
103	129.4213	0.110	0.027	0.560	1.512	0.00000	5.537	0.681	1.278	2.585
104	129.4213	0.110	0.027	0.565	1.510	0.00000	5.546	0.689	1.282	2.582
105	129.4213	0.110	0.027	0.565	1.510	0.00000	5.545	0.687	1.281	2.573
106	129.8252	0.110	0.022	0.540	1.214	0.00000	5.533	-0.790	1.336	3.160
107	129.8252	0.110	0.022	0.545	1.213	0.00000	5.540	-0.923	1.342	3.150
108	129.8252	0.110	0.022	0.545	1.213	0.00000	5.539	-0.878	1.340	3.135
109	129.9582	0.110	0.017	0.525	0.936	0.00000	5.528	-1.091	1.410	3.852
110	129.9582	0.110	0.017	0.525	0.935	0.00000	5.530	-1.210	1.417	3.847
111	129.9582	0.110	0.017	0.520	0.935	0.00000	5.529	-1.156	1.415	3.824
112	130.0074	0.110	0.018	0.530	1.024	0.00000	5.530	-0.982	1.384	3.604
113	130.0074	0.110	0.018	0.530	1.023	0.00000	5.534	-1.108	1.391	3.598
114	130.0074	0.110	0.018	0.530	1.023	0.00000	5.533	-1.057	1.389	3.578
115	130.0653	0.110	0.015	0.515	0.851	0.00000	5.523	-1.228	1.438	4.135
116	130.0653	0.110	0.015	0.515	0.850	0.00000	5.524	-1.348	1.446	4.132
117	130.0653	0.110	0.015	0.515	0.850	0.00000	5.522	-1.289	1.444	4.105
118	130.1006	0.110	0.020	0.535	1.116	0.00000	5.531	-0.883	1.359	3.374
119	130.1006	0.110	0.020	0.540	1.115	0.00000	5.537	-1.014	1.366	3.366
120	130.1006	0.110	0.020	0.535	1.115	0.00000	5.536	-0.966	1.364	3.349
121	131.7744	0.105	0.012	0.425	0.668	0.00000	5.469	-1.497	1.560	3.888
122	131.7744	0.105	0.012	0.410	0.667	0.00000	5.472	-1.941	1.585	3.954
123	131.7744	0.105	0.012	0.415	0.667	0.00000	5.470	-1.857	1.581	3.922
124	132.0441	0.105	0.011	0.410	0.591	0.00000	5.438	-1.942	1.608	4.635
125	132.0441	0.105	0.011	0.395	0.590	0.00000	5.436	-2.432	1.643	4.762
126	132.0441	0.105	0.011	0.395	0.590	0.00000	5.435	-2.353	1.638	4.724
127	134.8266	0.110	0.013	0.475	0.744	0.00000	5.489	-1.394	1.484	4.536
128	134.8266	0.110	0.013	0.420	0.744	0.00000	5.490	-1.834	1.545	3.672
129	134.8266	0.110	0.013	0.425	0.743	0.00000	5.489	-1.751	1.541	3.645
130	135.0621	0.105	0.011	0.395	0.584	0.00000	5.429	-2.003	1.622	4.691
131	135.0621	0.105	0.011	0.385	0.584	0.00000	5.428	-2.494	1.656	4.814
132	135.0621	0.105	0.011	0.385	0.584	0.00000	5.426	-2.416	1.652	4.776
133	138.1142	0.105	0.010	0.385	0.577	0.00000	5.421	-2.061	1.635	4.743
134	138.1142	0.105	0.010	0.375	0.577	0.00000	5.419	-2.557	1.670	4.864
135	138.1142	0.105	0.010	0.375	0.577	0.00000	5.417	-2.479	1.666	4.826
136	167.7286	0.100	0.011	0.315	0.589	0.00000	5.375	-1.906	1.680	4.135
137	167.7286	0.100	0.011	0.335	0.589	0.00000	5.376	0.577	1.614	2.829
138	167.7286	0.100	0.011	0.335	0.589	0.00000	5.375	0.576	1.612	2.818

#	q	t_1	Δt_{min}	Δt	Δt_{max}	$\frac{\Delta q_2}{\Delta q_1}$	$\dot{\delta}_{elev(max)}$	$\delta_{elev(max)_{pert}}$	$g_{pil(ss)}$	$\alpha_{ss_{pert}}$
139	170.3164	0.105	0.017	0.410	0.970	0.00000	5.475	-1.244	1.459	2.712
140	170.3164	0.105	0.017	0.400	0.970	0.00000	5.479	-1.382	1.460	2.654
141	170.3164	0.105	0.017	0.405	0.970	0.00000	5.477	-1.316	1.459	2.648
142	208.2658	0.100	0.011	0.295	0.595	0.00000	5.317	0.555	1.645	2.528
143	208.2658	0.100	0.011	0.295	0.595	0.00000	5.321	0.557	1.653	2.486
144	208.2658	0.100	0.011	0.295	0.595	0.00000	5.319	0.556	1.652	2.481
145	215.9733	0.100	0.013	0.335	0.720	0.00000	5.368	0.583	1.586	2.618
146	215.9733	0.100	0.013	0.330	0.720	0.00096	5.371	0.584	1.590	2.566
147	215.9733	0.100	0.013	0.330	0.720	0.00064	5.369	0.583	1.589	2.563
148	222.8766	0.100	0.010	0.280	0.575	0.00000	5.292	0.546	1.674	2.244
149	222.8766	0.100	0.010	0.275	0.575	0.00000	5.290	0.545	1.673	2.239
150	228.5562	0.100	0.020	0.415	1.127	0.00000	5.411	0.615	1.433	2.008
151	228.5562	0.105	0.020	0.415	1.127	0.00062	5.420	0.620	1.434	1.963
152	228.5562	0.105	0.020	0.415	1.127	0.00036	5.418	0.619	1.434	1.962
153	254.7139	0.100	0.017	0.360	0.931	0.00525	5.372	0.596	1.517	2.094
154	254.7139	0.100	0.017	0.360	0.930	0.00912	5.377	0.598	1.516	2.045
155	254.7139	0.100	0.017	0.360	0.930	0.00780	5.375	0.597	1.516	2.045
156	264.5698	0.095	0.011	0.260	0.591	0.00000	5.240	0.532	1.689	2.142
157	264.5698	0.095	0.011	0.260	0.591	0.00947	5.246	0.534	1.692	2.089
158	264.5698	0.095	0.011	0.260	0.591	0.00719	5.244	0.533	1.691	2.087
159	333.6127	0.095	0.010	0.225	0.578	0.00735	5.142	0.509	1.733	1.819
160	333.6127	0.095	0.010	0.225	0.578	0.02622	5.151	0.512	1.733	1.769
161	333.6127	0.095	0.010	0.225	0.578	0.02231	5.148	0.511	1.734	1.768
162	333.8201	0.095	0.012	0.260	0.690	0.04213	5.221	0.539	1.667	1.988
163	333.8201	0.095	0.012	0.260	0.690	0.06352	5.226	0.540	1.663	1.929
164	333.8201	0.095	0.012	0.260	0.690	0.05815	5.223	0.539	1.664	1.932
165	357.0172	0.095	0.010	0.210	0.559	0.01791	5.113	0.501	1.756	1.678
166	357.0172	0.095	0.010	0.210	0.559	0.01453	5.111	0.500	1.756	1.677
167	416.6143	0.090	0.010	0.195	0.566	0.01124	5.096	0.488	1.773	1.611
168	416.6143	0.095	0.010	0.195	0.566	0.03074	5.103	0.490	1.773	1.563
169	416.6143	0.095	0.010	0.190	0.566	0.02667	5.102	0.489	1.773	1.563
170	499.2391	0.095	0.012	0.205	0.663	0.04329	5.141	0.503	1.746	1.591
171	499.2391	0.095	0.012	0.205	0.663	0.06222	5.147	0.505	1.746	1.549
172	499.2391	0.095	0.012	0.205	0.663	0.05648	5.145	0.503	1.746	1.549
173	503.8640	0.090	0.010	0.175	0.561	0.01392	5.061	0.471	1.801	1.419
174	503.8640	0.090	0.010	0.175	0.561	0.03060	5.073	0.474	1.801	1.378
175	503.8640	0.090	0.010	0.175	0.561	0.02696	5.070	0.473	1.801	1.377
176	514.2514	0.095	0.013	0.225	0.749	0.03773	5.179	0.523	1.712	1.560
177	514.2514	0.095	0.013	0.225	0.749	0.04305	5.184	0.523	1.712	1.527
178	514.2514	0.095	0.013	0.225	0.749	0.03831	5.182	0.522	1.712	1.527
179	551.8250	0.090	0.010	0.160	0.536	0.01413	5.021	0.457	1.826	1.211
180	551.8250	0.090	0.010	0.160	0.536	0.01211	5.018	0.456	1.826	1.210
181	618.5337	0.090	0.010	0.150	0.550	0.00854	4.975	0.445	1.829	1.212
182	618.5337	0.090	0.010	0.150	0.550	0.01909	4.989	0.448	1.829	1.177
183	618.5337	0.090	0.010	0.150	0.550	0.01656	4.986	0.447	1.829	1.176
184	699.9532	0.090	0.012	0.165	0.642	0.02106	5.001	0.451	1.785	1.228

#	q	t_1	Δt_{min}	Δt	Δt_{max}	$\frac{\Delta q_2}{\Delta q_1}$	$\dot{\delta}_{elev(max)}$	$\delta_{elev(max)_{pert}}$	$g_{pil(ss)}$	$\alpha_{ss_{pert}}$
185	699.9532	0.090	0.012	0.165	0.642	0.03137	5.010	0.453	1.785	1.195
186	699.9532	0.090	0.012	0.165	0.642	0.02803	5.006	0.452	1.785	1.194
187	771.1717	0.085	0.010	0.135	0.533	0.00076	4.815	0.396	1.838	0.964
188	771.1717	0.085	0.010	0.135	0.533	0.00407	4.832	0.399	1.838	0.936
189	771.1717	0.085	0.010	0.135	0.533	0.00311	4.828	0.398	1.838	0.936
190	825.2729	0.080	0.009	0.130	0.516	0.00020	4.761	0.381	1.847	0.839
191	825.2729	0.080	0.009	0.130	0.516	0.00006	4.758	0.380	1.847	0.839
192	954.4603	0.080	0.009	0.120	0.518	0.00000	4.644	0.353	1.846	0.792
193	954.4603	0.080	0.009	0.120	0.518	0.00021	4.664	0.356	1.846	0.769
194	954.4603	0.080	0.009	0.120	0.518	0.00008	4.660	0.356	1.846	0.768
195	1106.2120	0.075	0.009	0.115	0.511	0.00000	4.525	0.327	1.850	0.700
196	1106.2120	0.075	0.009	0.115	0.511	0.00000	4.546	0.330	1.850	0.680
197	1106.2120	0.075	0.009	0.115	0.511	0.00000	4.542	0.329	1.850	0.679
198	1157.0650	0.075	0.009	0.110	0.499	0.00000	4.493	0.319	1.856	0.633
199	1157.0650	0.075	0.009	0.110	0.499	0.00000	4.489	0.319	1.856	0.633

C.2 Longitudinal Maximum C*cmd Step Input Time Response Data Without Limiters

#	q	$\dot{\delta}_{elev(max)}$	$\delta_{elev(max)}$	$g_{pil(ss)}$	$g_{pil(max)}$	α_{ss}	α_{max}
1	65.4696	26.107	3.209	1.926	1.926	30.712	30.712
2	65.4696	26.549	3.941	1.927	1.927	30.738	30.738
3	65.5666	26.133	3.189	1.860	1.860	29.836	29.836
4	67.0399	26.863	3.804	2.122	2.122	32.716	32.716
5	67.0399	26.858	4.059	2.121	2.121	32.709	32.709
6	67.4267	26.949	3.793	2.044	2.044	31.580	31.580
7	67.4267	26.943	4.047	2.043	2.043	31.579	31.579
8	67.6717	26.984	3.860	2.231	2.231	33.969	33.969
9	68.8746	27.260	3.839	1.855	1.855	28.606	28.606
10	68.8746	27.254	4.092	1.855	1.855	28.613	28.613
11	70.9929	27.695	3.944	1.829	1.829	27.582	27.582
12	74.2746	28.311	5.754	1.947	1.947	28.912	28.912
13	74.2746	28.352	4.165	1.951	1.951	28.010	28.010
14	74.2746	28.346	4.399	1.950	1.950	28.016	28.016
15	75.5664	28.589	4.193	1.856	1.856	26.493	26.493
16	77.0323	28.905	4.516	1.931	1.931	26.958	26.958
17	77.2143	28.894	4.275	2.489	2.489	35.017	35.017
18	77.2914	28.850	4.021	2.631	2.631	37.407	37.407
19	77.2914	28.844	4.238	2.628	2.628	37.367	37.367
20	80.2356	29.469	4.800	2.702	2.702	38.188	38.188
21	80.2356	29.472	4.043	2.718	2.718	37.370	37.370
22	80.2356	29.465	4.250	2.715	2.715	37.326	37.326
23	80.3692	29.525	5.561	2.147	2.147	29.505	29.505
24	80.3692	29.550	4.178	2.150	2.150	28.566	28.566
25	80.3692	29.544	4.393	2.150	2.150	28.576	28.576
26	80.5349	29.520	5.051	2.567	2.567	35.830	35.830
27	80.5349	29.529	4.128	2.579	2.579	34.957	34.957
28	80.5349	29.523	4.336	2.577	2.577	34.935	34.935
29	81.4969	29.728	5.244	2.475	2.475	33.924	33.924
30	81.4969	29.742	4.200	2.484	2.484	33.034	33.034
31	81.4969	29.735	4.406	2.483	2.483	33.023	33.023
32	82.2802	29.907	6.201	1.965	1.989	26.499	26.802
33	82.2802	29.941	4.763	1.967	2.018	25.578	26.198
34	82.2802	29.934	4.974	1.967	2.012	25.592	26.145
35	83.3181	30.106	6.229	2.040	2.059	27.170	27.408
36	83.3181	30.137	4.862	2.042	2.088	26.246	26.807
37	83.3181	30.131	5.070	2.042	2.082	26.261	26.750
38	83.4550	30.118	5.559	2.306	2.306	30.683	30.683
39	83.4550	30.140	4.312	2.311	2.311	29.756	29.756
40	83.4550	30.134	4.516	2.310	2.310	29.763	29.763
41	83.7192	30.153	5.435	2.417	2.417	32.187	32.187
42	83.7192	30.172	4.289	2.424	2.424	31.255	31.255
43	83.7192	30.165	4.490	2.423	2.423	31.253	31.253
44	87.3860	30.851	5.003	2.758	2.758	35.732	35.732
45	87.3860	30.859	4.209	2.770	2.770	34.887	34.887
46	87.3860	30.852	4.395	2.768	2.768	34.860	34.860

#	q	$\dot{\delta}_{elev(max)}$	$\delta_{elev(max)}$	$g_{pil(ss)}$	$g_{pil(max)}$	α_{ss}	α_{max}
47	88.7159	31.042	10.299	3.261	3.261	38.108	38.108
48	88.7159	31.035	9.762	3.259	3.259	38.085	38.085
49	89.3983	31.224	4.646	2.981	2.981	38.298	38.298
50	89.3983	31.224	10.524	3.057	3.084	35.994	36.313
51	89.3983	31.218	9.933	3.057	3.074	35.991	36.201
52	91.6970	31.711	6.703	2.284	2.300	27.850	28.033
53	91.6970	31.740	5.402	2.287	2.322	26.954	27.362
54	91.6970	31.733	5.586	2.287	2.316	26.964	27.298
55	94.3473	32.089	9.337	3.449	3.449	38.800	38.800
56	94.3473	32.089	9.879	3.455	3.455	37.868	37.868
57	94.3473	32.082	9.355	3.453	3.453	37.842	37.842
58	101.0962	33.198	7.334	3.940	3.940	40.071	40.071
59	102.4478	33.724	6.037	2.626	2.673	28.969	29.483
60	102.4478	33.755	5.624	2.627	2.717	27.966	28.927
61	102.4478	33.746	5.192	2.627	2.707	27.970	28.818
62	103.7392	33.716	14.118	4.075	4.075	45.475	45.475
63	106.1299	34.202	8.826	3.869	3.869	38.613	38.613
64	106.1299	34.209	11.682	3.871	3.871	42.142	42.142
65	106.1299	34.200	11.145	3.869	3.869	42.092	42.092
66	106.4162	34.183	14.045	4.181	4.181	45.505	45.505
67	109.0025	34.992	6.079	2.918	2.986	29.927	30.633
68	109.0025	35.020	6.637	2.917	3.035	28.948	30.121
69	109.0025	35.011	6.134	2.918	3.022	28.955	29.993
70	109.1273	34.580	11.133	4.246	4.246	46.836	46.836
71	109.1273	34.589	14.507	4.293	4.293	45.605	45.605
72	109.1273	34.579	13.930	4.289	4.289	45.526	45.526
73	110.1905	35.185	7.528	3.276	3.365	32.616	33.510
74	110.1905	35.200	8.919	3.275	3.414	31.657	33.011
75	110.1905	35.190	8.360	3.276	3.398	31.668	32.852
76	110.9265	35.286	7.150	2.584	2.643	27.049	27.669
77	110.9265	35.326	5.959	2.585	2.689	26.000	27.056
78	110.9265	35.317	6.105	2.585	2.680	26.001	26.956
79	111.8726	35.046	9.240	4.337	4.337	46.467	46.467
80	111.8726	35.047	12.633	4.389	4.389	45.332	45.332
81	111.8726	35.037	12.055	4.384	4.384	45.242	45.242
82	114.6519	35.508	7.461	4.430	4.430	46.131	46.131
83	114.6519	35.502	10.875	4.486	4.486	45.071	45.071
84	114.6519	35.491	10.303	4.481	4.481	44.979	44.979
85	117.4653	36.014	5.972	4.526	4.526	45.833	45.833
86	117.4653	36.002	9.244	4.585	4.585	44.840	44.840
87	117.4653	35.991	8.678	4.579	4.579	44.744	44.744
88	120.3129	36.567	6.161	4.623	4.623	45.574	45.574
89	120.3129	36.548	7.739	4.686	4.686	44.639	44.639
90	120.3129	36.537	7.185	4.680	4.680	44.538	44.538
91	121.8328	37.012	9.900	4.443	4.443	44.011	44.011
92	121.8328	37.024	12.483	4.462	4.474	42.716	42.839

#	q	$\bar{\delta}_{elev(max)}$	$\delta_{elev(max)}$	$g_{pil(ss)}$	$g_{pil(max)}$	α_{ss}	α_{max}
93	121.8328	37.013	11.927	4.461	4.466	42.678	42.735
94	123.1945	37.084	6.318	4.724	4.724	45.358	45.358
95	123.1945	37.071	13.638	4.844	5.094	36.537	38.485
96	123.1945	37.060	12.986	4.847	5.065	36.538	38.234
97	126.1103	37.627	10.370	4.975	5.051	38.240	38.846
98	126.1103	37.620	14.114	4.958	5.249	36.877	39.118
99	126.1103	37.609	13.463	4.962	5.218	36.879	38.857
100	129.0601	38.181	10.842	5.094	5.197	38.617	39.429
101	129.0601	38.173	14.610	5.073	5.409	37.196	39.761
102	129.0601	38.161	13.959	5.078	5.378	37.202	39.491
103	129.4213	38.900	7.495	2.896	2.955	26.987	27.556
104	129.4213	38.965	6.389	2.898	3.001	26.179	27.158
105	129.4213	38.955	6.512	2.898	2.992	26.169	27.057
106	129.8252	38.958	6.701	3.307	3.363	30.631	31.181
107	129.8252	39.006	5.938	3.307	3.408	29.741	30.698
108	129.8252	38.996	6.058	3.308	3.396	29.735	30.575
109	129.9582	38.945	6.350	3.884	3.910	35.649	35.908
110	129.9582	38.966	7.546	3.885	3.946	34.744	35.331
111	129.9582	38.955	7.042	3.885	3.934	34.734	35.197
112	130.0074	38.970	6.338	3.674	3.712	33.804	34.173
113	130.0074	39.001	6.757	3.675	3.753	32.900	33.644
114	130.0074	38.991	6.271	3.675	3.740	32.894	33.511
115	130.0653	38.867	7.598	4.122	4.138	37.793	37.955
116	130.0653	38.877	8.629	4.123	4.171	36.878	37.329
117	130.0653	38.867	8.102	4.124	4.158	36.866	37.197
118	130.1006	38.927	6.540	3.486	3.535	32.137	32.610
119	130.1006	38.967	6.047	3.486	3.579	31.236	32.110
120	130.1006	38.957	6.011	3.487	3.566	31.232	31.981
121	131.7744	38.816	9.309	4.828	4.978	34.055	35.125
122	131.7744	38.835	12.815	4.812	5.198	32.872	35.528
123	131.7744	38.823	12.116	4.816	5.160	32.874	35.244
124	132.0441	38.739	11.318	5.215	5.349	38.970	40.016
125	132.0441	38.729	15.121	5.189	5.576	37.495	40.412
126	132.0441	38.716	14.465	5.195	5.543	37.503	40.130
127	134.8266	39.684	8.991	4.600	4.605	41.273	41.324
128	134.8266	39.695	12.230	4.578	5.015	31.355	34.355
129	134.8266	39.683	11.520	4.581	4.976	31.359	34.072
130	135.0621	39.223	11.797	5.337	5.506	39.301	40.607
131	135.0621	39.212	15.647	5.307	5.749	37.763	41.063
132	135.0621	39.199	14.990	5.313	5.714	37.773	40.772
133	138.1142	39.876	12.269	5.460	5.668	39.608	41.198
134	138.1142	39.866	16.188	5.426	5.929	38.006	41.720
135	138.1142	39.854	15.528	5.432	5.893	38.017	41.418
136	167.7286	45.361	13.211	6.240	6.853	36.999	40.800
137	167.7286	45.375	7.455	6.268	6.268	29.161	29.161
138	167.7286	45.359	7.519	6.267	6.267	29.137	29.137

#	q	$\dot{\delta}_{elev(max)}$	$\delta_{elev(max)}$	$g_{pil(ss)}$	$g_{pil(max)}$	α_{ss}	α_{max}
139	170.3164	46.727	8.719	4.704	5.263	28.362	31.734
140	170.3164	46.760	10.272	4.714	5.378	27.633	31.539
141	170.3164	46.745	9.619	4.711	5.335	27.608	31.280
142	208.2658	52.795	8.063	7.455	7.455	29.567	29.567
143	208.2658	52.833	7.866	7.457	7.457	28.628	28.631
144	208.2658	52.815	7.914	7.457	7.457	28.608	28.608
145	215.9733	54.864	7.785	6.912	7.032	31.261	31.814
146	215.9733	54.896	7.625	6.914	7.214	30.395	31.735
147	215.9733	54.877	7.677	6.913	7.169	30.384	31.528
148	222.8766	55.461	8.257	8.056	8.056	27.099	27.099
149	222.8766	55.440	8.300	8.056	8.056	27.077	27.077
150	228.5562	57.299	9.037	5.532	5.635	25.975	26.467
151	228.5562	57.395	8.426	5.534	5.719	25.204	26.066
152	228.5562	57.374	8.484	5.534	5.691	25.198	25.931
153	254.7139	58.060	8.613	6.511	6.772	26.774	27.860
154	254.7139	58.118	8.268	6.513	6.875	26.038	27.510
155	254.7139	58.095	8.316	6.513	6.832	26.031	27.331
156	264.5698	57.044	8.128	8.461	8.461	26.602	26.602
157	264.5698	57.115	8.019	8.462	8.591	25.756	26.161
158	264.5698	57.089	8.053	8.462	8.550	25.737	26.015
159	333.6127	58.677	8.024	9.292	9.310	23.341	23.393
160	333.6127	58.762	8.027	9.292	9.589	22.596	23.337
161	333.6127	58.741	8.053	9.292	9.533	22.579	23.181
162	333.8201	59.496	7.883	8.562	9.160	25.806	27.639
163	333.8201	59.550	7.835	8.562	9.432	25.080	27.676
164	333.8201	59.519	7.865	8.562	9.363	25.070	27.458
165	357.0172	58.509	8.230	9.542	9.708	21.324	21.709
166	357.0172	58.484	8.253	9.542	9.655	21.309	21.574
167	416.6143	58.037	7.795	9.735	9.799	20.495	20.639
168	416.6143	58.155	7.839	9.735	10.132	19.798	20.631
169	416.6143	58.124	7.858	9.735	10.070	19.785	20.488
170	499.2391	58.362	7.437	9.445	10.081	20.249	21.647
171	499.2391	58.440	7.440	9.446	10.337	19.620	21.524
172	499.2391	58.407	7.455	9.446	10.267	19.611	21.367
173	503.8640	57.214	7.490	10.040	10.204	17.975	18.281
174	503.8640	57.353	7.572	10.040	10.558	17.352	18.277
175	503.8640	57.318	7.586	10.040	10.493	17.339	18.148
176	514.2514	58.521	7.753	9.006	9.591	19.848	21.167
177	514.2514	58.572	7.685	9.006	9.670	19.315	20.778
178	514.2514	58.538	7.700	9.006	9.610	19.309	20.640
179	551.8250	55.430	7.653	10.118	10.393	14.974	15.395
180	551.8250	55.393	7.664	10.118	10.337	14.962	15.298
181	618.5337	53.143	6.946	9.866	10.037	14.609	14.870
182	618.5337	53.304	7.056	9.866	10.351	14.082	14.795
183	618.5337	53.265	7.065	9.866	10.292	14.072	14.699
184	699.9532	51.384	6.452	9.064	9.591	14.285	15.133

#	q	$\dot{\delta}_{elev(max)}$	$\delta_{elev(max)}$	$g_{pil(ss)}$	$g_{pil(max)}$	α_{ss}	α_{max}
185	699.9532	51.472	6.523	9.064	9.789	13.801	14.937
186	699.9532	51.433	6.531	9.064	9.736	13.795	14.846
187	771.1717	47.645	6.583	9.299	9.385	10.983	11.086
188	771.1717	47.821	6.710	9.299	9.595	10.563	10.904
189	771.1717	47.782	6.717	9.299	9.554	10.556	10.850
190	825.2729	45.812	6.690	9.156	9.292	9.280	9.420
191	825.2729	45.773	6.697	9.156	9.263	9.273	9.382
192	954.4603	44.233	6.149	9.036	9.092	8.764	8.817
193	954.4603	44.426	6.292	9.037	9.236	8.404	8.590
194	954.4603	44.387	6.296	9.037	9.208	8.398	8.558
195	1106.2120	43.047	5.932	9.073	9.132	7.790	7.839
196	1106.2120	43.253	6.086	9.073	9.252	7.455	7.601
197	1106.2120	43.212	6.090	9.073	9.229	7.449	7.577
198	1157.0650	42.730	6.158	9.131	9.250	6.974	7.064
199	1157.0650	42.688	6.162	9.131	9.231	6.969	7.044

C.3 Longitudinal Maximum C^*_{cmd} Step Input Time Responses With Limiters

#	q	$\dot{\delta}_{elev(max)}$	$\delta_{elev(max)}$	$g_{pil(ss)}$	$g_{pil(max)}$	α_{ss}	α_{max}
1	65.4696	26.107	3.209	1.683	1.683	27.226	27.226
2	65.4696	26.549	3.941	1.683	1.683	27.231	27.231
3	65.5666	26.133	3.189	1.661	1.661	26.959	26.959
4	67.0399	26.863	3.804	1.765	1.765	27.722	27.722
5	67.0399	26.858	4.059	1.764	1.764	27.722	27.722
6	67.4267	26.949	3.793	1.747	1.747	27.420	27.420
7	67.4267	26.943	4.047	1.747	1.747	27.422	27.422
8	67.6717	26.984	3.860	1.801	1.801	28.006	28.006
9	68.8746	27.260	3.839	1.704	1.704	26.491	26.491
10	68.8746	27.254	4.092	1.703	1.703	26.495	26.495
11	70.9929	27.695	3.944	1.721	1.721	26.098	26.098
12	74.2746	28.311	5.754	1.772	1.772	26.560	26.560
13	74.2746	28.352	4.165	1.814	1.814	26.217	26.217
14	74.2746	28.346	4.399	1.813	1.813	26.219	26.219
15	75.5664	28.589	4.193	1.791	1.791	25.642	25.642
16	77.0323	28.905	4.516	1.841	1.841	25.813	25.813
17	77.2143	28.894	4.275	1.969	1.969	27.965	27.965
18	77.2914	28.850	4.021	1.984	1.984	28.413	28.413
19	77.2914	28.844	4.238	1.984	1.984	28.411	28.411
20	80.2356	29.469	4.800	2.004	2.004	28.544	28.544
21	80.2356	29.472	4.043	2.051	2.051	28.339	28.339
22	80.2356	29.465	4.250	2.051	2.051	28.337	28.337
23	80.3692	29.525	5.561	1.921	1.921	26.639	26.639
24	80.3692	29.550	4.178	1.969	1.969	26.315	26.315
25	80.3692	29.544	4.393	1.968	1.968	26.319	26.319
26	80.5349	29.520	5.051	1.994	1.994	28.114	28.114
27	80.5349	29.529	4.128	2.043	2.043	27.882	27.882
28	80.5349	29.523	4.336	2.043	2.043	27.882	27.882
29	81.4969	29.728	5.244	2.001	2.001	27.713	27.713
30	81.4969	29.742	4.200	2.050	2.050	27.463	27.463
31	81.4969	29.735	4.406	2.049	2.049	27.463	27.463
32	82.2802	29.907	6.201	1.893	1.896	25.625	25.668
33	82.2802	29.941	4.763	1.939	1.945	25.251	25.329
34	82.2802	29.934	4.974	1.939	1.943	25.256	25.321
35	83.3181	30.106	6.229	1.932	1.934	25.868	25.887
36	83.3181	30.137	4.862	1.979	1.986	25.513	25.600
37	83.3181	30.131	5.070	1.978	1.984	25.517	25.590
38	83.4550	30.118	5.559	2.005	2.005	26.923	26.923
39	83.4550	30.140	4.312	2.055	2.055	26.629	26.629
40	83.4550	30.134	4.516	2.054	2.054	26.632	26.632
41	83.7192	30.153	5.435	2.030	2.030	27.291	27.291
42	83.7192	30.172	4.289	2.081	2.081	27.015	27.015
43	83.7192	30.165	4.490	2.081	2.081	27.016	27.016
44	87.3860	30.851	5.003	2.146	2.146	27.962	27.962
45	87.3860	30.859	4.209	2.197	2.197	27.747	27.747
46	87.3860	30.852	4.395	2.197	2.197	27.746	27.746

#	q	$\dot{\delta}_{elev(max)}$	$\delta_{elev(max)}$	$g_{pil(ss)}$	$g_{pil(max)}$	α_{ss}	α_{max}
47	88.7159	31.042	7.187	2.394	2.394	28.186	28.186
48	88.7159	31.035	6.753	2.394	2.394	28.184	28.184
49	89.3983	31.224	4.646	2.208	2.208	28.368	28.368
50	89.3983	31.224	7.684	2.349	2.349	27.857	27.857
51	89.3983	31.218	7.232	2.349	2.349	27.856	27.856
52	91.6970	31.711	6.703	2.123	2.123	26.047	26.047
53	91.6970	31.740	5.402	2.175	2.178	25.731	25.772
54	91.6970	31.733	5.586	2.174	2.176	25.734	25.762
55	94.3473	32.089	6.234	2.491	2.491	28.251	28.251
56	94.3473	32.089	6.919	2.547	2.547	28.072	28.072
57	94.3473	32.082	6.496	2.547	2.547	28.069	28.069
58	101.0962	33.198	4.830	2.787	2.787	28.308	28.308
59	102.4478	33.724	6.037	2.375	2.375	26.292	26.292
60	102.4478	33.755	5.033	2.436	2.443	25.993	26.074
61	102.4478	33.746	5.192	2.436	2.442	25.992	26.057
62	103.7392	33.716	8.124	2.647	2.647	28.866	28.866
63	106.1299	34.202	5.898	2.802	2.802	28.087	28.087
64	106.1299	34.209	7.349	2.659	2.659	28.507	28.507
65	106.1299	34.200	6.957	2.660	2.660	28.503	28.503
66	106.4162	34.183	8.083	2.715	2.715	28.835	28.835
67	109.0025	34.992	6.079	2.574	2.574	26.501	26.501
68	109.0025	35.020	5.345	2.638	2.643	26.235	26.290
69	109.0025	35.011	5.415	2.638	2.642	26.234	26.273
70	109.1273	34.580	5.980	2.695	2.695	29.012	29.012
71	109.1273	34.589	8.406	2.783	2.783	28.809	28.809
72	109.1273	34.579	8.018	2.784	2.784	28.804	28.804
73	110.1905	35.185	5.723	2.708	2.708	27.088	27.088
74	110.1905	35.200	6.807	2.770	2.770	26.869	26.869
75	110.1905	35.190	6.380	2.771	2.771	26.868	26.868
76	110.9265	35.286	7.150	2.451	2.455	25.706	25.752
77	110.9265	35.326	5.959	2.519	2.528	25.359	25.455
78	110.9265	35.317	6.105	2.520	2.527	25.358	25.440
79	111.8726	35.046	5.499	2.772	2.772	28.957	28.957
80	111.8726	35.047	7.267	2.859	2.859	28.760	28.760
81	111.8726	35.037	6.884	2.861	2.861	28.754	28.754
82	114.6519	35.508	5.753	2.849	2.849	28.905	28.905
83	114.6519	35.502	6.206	2.938	2.938	28.714	28.714
84	114.6519	35.491	5.832	2.939	2.939	28.708	28.708
85	117.4653	36.014	5.972	2.927	2.927	28.857	28.857
86	117.4653	36.002	5.451	3.016	3.016	28.671	28.671
87	117.4653	35.991	5.557	3.018	3.018	28.665	28.665
88	120.3129	36.567	6.161	3.005	3.005	28.813	28.813
89	120.3129	36.548	5.650	3.096	3.096	28.631	28.631
90	120.3129	36.537	5.750	3.098	3.098	28.625	28.625
91	121.8328	37.012	5.776	2.951	2.951	28.604	28.604
92	121.8328	37.024	7.741	3.036	3.036	28.412	28.412

#	q	$\dot{\delta}_{elev(max)}$	$\delta_{elev(max)}$	$g_{pil(ss)}$	$g_{pil(max)}$	α_{ss}	α_{max}
93	121.8328	37.013	7.365	3.038	3.038	28.408	28.408
94	123.1945	37.084	6.318	3.085	3.085	28.773	28.773
95	123.1945	37.071	8.929	3.666	3.666	27.573	27.573
96	123.1945	37.060	8.518	3.668	3.668	27.568	27.568
97	126.1103	37.627	6.531	3.631	3.631	27.809	27.809
98	126.1103	37.620	9.040	3.729	3.729	27.612	27.612
99	126.1103	37.609	8.638	3.731	3.731	27.607	27.607
100	129.0601	38.181	6.680	3.693	3.693	27.845	27.845
101	129.0601	38.173	9.154	3.795	3.795	27.647	27.647
102	129.0601	38.161	8.761	3.797	3.797	27.643	27.643
103	129.4213	38.900	7.495	2.752	2.754	25.641	25.663
104	129.4213	38.965	6.389	2.811	2.817	25.389	25.448
105	129.4213	38.955	6.512	2.812	2.817	25.385	25.437
106	129.8252	38.958	6.701	2.874	2.874	26.565	26.565
107	129.8252	39.006	5.938	2.938	2.938	26.343	26.343
108	129.8252	38.996	6.058	2.939	2.939	26.339	26.339
109	129.9582	38.945	6.095	3.016	3.016	27.500	27.500
110	129.9582	38.966	5.728	3.079	3.079	27.325	27.325
111	129.9582	38.955	5.843	3.080	3.080	27.322	27.322
112	130.0074	38.970	6.338	2.970	2.970	27.192	27.192
113	130.0074	39.001	5.822	3.033	3.033	27.001	27.001
114	130.0074	38.991	5.939	3.034	3.034	26.998	26.998
115	130.0653	38.867	5.842	3.063	3.063	27.815	27.815
116	130.0653	38.877	6.143	3.126	3.126	27.654	27.654
117	130.0653	38.867	5.762	3.127	3.127	27.651	27.651
118	130.1006	38.927	6.540	2.926	2.926	26.880	26.880
119	130.1006	38.967	5.893	2.990	2.990	26.672	26.672
120	130.1006	38.957	6.011	2.991	2.991	26.669	26.669
121	131.7744	38.816	6.701	3.836	3.836	27.167	27.167
122	131.7744	38.835	9.141	3.935	3.938	26.957	26.975
123	131.7744	38.823	8.685	3.937	3.938	26.952	26.959
124	132.0441	38.739	6.832	3.758	3.758	27.878	27.878
125	132.0441	38.729	9.266	3.862	3.863	27.679	27.680
126	132.0441	38.716	8.882	3.865	3.865	27.674	27.674
127	134.8266	39.684	5.935	3.204	3.204	28.216	28.216
128	134.8266	39.695	8.894	3.881	3.890	26.665	26.728
129	134.8266	39.683	8.419	3.882	3.888	26.662	26.703
130	135.0621	39.275	7.024	3.825	3.825	27.906	27.906
131	135.0621	39.272	9.380	3.933	3.934	27.706	27.710
132	135.0621	39.250	9.005	3.936	3.936	27.701	27.701
133	138.1142	39.824	7.220	3.894	3.894	27.931	27.931
134	138.1142	39.831	9.497	4.007	4.008	27.728	27.739
135	138.1142	39.801	9.128	4.009	4.010	27.723	27.726
136	167.7286	45.231	7.678	4.678	4.678	27.515	27.515
137	167.7286	45.241	7.340	5.596	5.596	26.063	26.063
138	167.7286	45.221	7.401	5.599	5.599	26.058	26.058

#	q	$\dot{\delta}_{elev(max)}$	$\delta_{elev(max)}$	$g_{pil(ss)}$	$g_{pil(max)}$	α_{ss}	α_{max}
139	170.3164	46.727	7.310	4.290	4.311	25.917	26.041
140	170.3164	46.760	7.472	4.382	4.415	25.714	25.911
141	170.3164	46.745	7.027	4.383	4.412	25.712	25.888
142	208.2658	52.429	7.599	6.578	6.578	26.130	26.130
143	208.2658	52.524	7.409	6.745	6.745	25.918	25.918
144	208.2658	52.258	7.454	6.749	6.749	25.913	25.913
145	215.9733	54.648	7.458	5.846	5.846	26.502	26.502
146	215.9733	54.682	7.309	5.977	5.977	26.319	26.319
147	215.9733	54.665	7.353	5.979	5.979	26.316	26.316
148	222.8766	54.669	7.640	7.590	7.590	25.549	25.549
149	222.8766	54.679	7.681	7.595	7.595	25.544	25.544
150	228.5562	57.086	8.820	5.382	5.382	25.277	25.278
151	228.5562	57.259	8.240	5.502	5.502	25.059	25.061
152	228.5562	57.228	8.292	5.503	5.503	25.057	25.059
153	254.7139	57.772	8.191	6.193	6.193	25.481	25.483
154	254.7139	57.890	7.867	6.323	6.325	25.286	25.294
155	254.7139	57.858	7.912	6.324	6.326	25.284	25.290
156	264.5698	55.966	7.340	8.082	8.082	25.423	25.423
157	264.5698	56.100	7.245	8.279	8.279	25.204	25.204
158	264.5698	56.065	7.278	8.284	8.284	25.199	25.199
159	333.6127	57.217	6.967	9.075	9.080	22.803	22.820
160	333.6127	57.400	6.988	9.075	9.107	22.071	22.161
161	333.6127	57.360	7.013	9.075	9.103	22.055	22.136
162	333.8201	58.509	6.954	8.364	8.366	25.218	25.223
163	333.8201	58.408	6.923	8.542	8.543	25.022	25.024
164	333.8201	58.310	6.951	8.545	8.545	25.019	25.021
165	357.0172	56.694	7.117	9.136	9.232	20.423	20.679
166	357.0172	56.652	7.138	9.136	9.227	20.408	20.653
167	416.6143	55.792	6.556	9.181	9.283	19.342	19.604
168	416.6143	56.040	6.620	9.181	9.315	18.677	18.999
169	416.6143	55.996	6.637	9.181	9.310	18.665	18.975
170	499.2391	56.179	6.161	9.113	9.254	19.539	19.893
171	499.2391	56.342	6.185	9.113	9.278	18.928	19.324
172	499.2391	56.292	6.197	9.113	9.273	18.920	19.305
173	503.8640	54.476	6.111	9.250	9.356	16.576	16.812
174	503.8640	54.711	6.212	9.250	9.382	15.993	16.266
175	503.8640	54.661	6.224	9.250	9.377	15.981	16.246
176	514.2514	56.565	6.529	9.002	9.086	19.839	20.050
177	514.2514	56.658	6.480	9.002	9.101	19.305	19.548
178	514.2514	56.619	6.492	9.002	9.092	19.299	19.521
179	551.8250	52.478	6.265	9.267	9.373	13.726	13.921
180	551.8250	52.425	6.277	9.267	9.369	13.715	13.903
181	618.5337	50.206	5.603	9.211	9.308	13.652	13.832
182	618.5337	50.446	5.726	9.211	9.333	13.152	13.364
183	618.5337	50.397	5.736	9.211	9.328	13.143	13.348
184	699.9532	48.983	5.279	9.017	9.113	14.211	14.388

#	q	$\delta_{elev(max)}$	$\delta_{elev(max)}$	$g_{pil(ss)}$	$g_{pil(max)}$	α_{ss}	α_{max}
185	699.9532	49.127	5.366	9.017	9.140	13.729	13.948
186	699.9532	49.083	5.373	9.017	9.133	13.723	13.929
187	771.1717	44.735	5.481	9.077	9.143	10.728	10.826
188	771.1717	45.039	5.619	9.077	9.169	10.315	10.444
189	771.1717	44.963	5.627	9.077	9.165	10.307	10.430
190	825.2729	43.014	5.678	9.040	9.095	9.166	9.235
191	825.2729	42.968	5.684	9.040	9.090	9.159	9.222
192	954.4603	41.128	5.199	9.010	9.028	8.739	8.761
193	954.4603	41.430	5.349	9.010	9.053	8.380	8.428
194	954.4603	41.381	5.355	9.010	9.049	8.374	8.417
195	1106.2120	39.764	5.031	9.019	9.045	7.745	7.772
196	1106.2120	40.103	5.192	9.019	9.066	7.412	7.458
197	1106.2120	40.053	5.197	9.019	9.062	7.406	7.449
198	1157.0650	39.483	5.281	9.034	9.078	6.903	6.944
199	1157.0650	39.435	5.285	9.034	9.075	6.897	6.936

Appendix D. Rate Limiter Two-Dimensional Arrays

The two-dimensional array used to limit $\dot{\alpha}$ indexed on α and $\dot{\alpha}$ is,

$\dot{\alpha}$ (deg/sec) $\Downarrow$	α (deg) $\Rightarrow$					
	0	2	15	20	25	30
0	1	1	1	1	1	1
2	1	1	1	1	0.9	0.1
5	1	1	1	0.8	0.7	0
8	1	1	0.8	0.7	0.5	0
11	1	1	0.6	0.4	0.2	0
15	1	1	0.5	0.2	0.1	0

The two-dimensional array used to limit $\dot{g}_{pil}$ indexed on g_{pil} and $\dot{g}_{pil}$ is,

g_{pil} (g's) $\Downarrow$	$\dot{g}_{pil}$ (g's/sec) $\Rightarrow$					
	0	1	2	4	6	10
1	1	1	1	1	1	1
1.4	1	1	1	.4	.2	0
2	1	1	1	.6	.4	.2
3	1	1	1	1	.5	.3
4	1	1	1	1	.7	.5
6	1	1	1	1	.75	.65
8	1	1	1	.75	.6	.3
9	1	1	.8	.6	.5	.2
10	1	1	.7	.6	.4	.1

Appendix E. Lateral Channel Time Domain Simulation Data

This appendix contains all lateral channel time domain simulation results.

E.1 Lateral Unit p_{cmd} Step Input Time Response Data

#	q	p_{max}	β_{max}	$\dot{\delta}_{ail(max)}$	$\delta_{ail(max)}$	$\dot{\delta}_{rud(max)}$	$\delta_{rud(max)}$	$\phi_{(2.8\ sec)}$	$\phi_{(1\ sec)}$
1	63.6460	1.330	0.060	0.380	0.342	0.551	0.458	1.923	0.203
2	65.4696	1.212	0.062	0.376	0.285	0.557	0.409	2.057	0.243
3	65.4696	1.212	0.062	0.376	0.285	0.556	0.408	2.038	0.243
4	65.5666	1.191	0.063	0.376	0.289	0.558	0.464	2.026	0.243
5	67.0399	1.244	0.059	0.376	0.273	0.537	0.366	2.109	0.247
6	67.0399	1.244	0.059	0.376	0.273	0.537	0.365	2.127	0.247
7	67.4267	1.222	0.059	0.376	0.274	0.538	0.368	2.097	0.249
8	67.4267	1.221	0.059	0.376	0.274	0.537	0.367	2.107	0.249
9	67.6717	1.261	0.057	0.376	0.270	0.527	0.354	2.131	0.248
10	67.6717	1.301	0.055	0.378	0.307	0.509	0.351	2.033	0.211
11	68.8746	1.156	0.060	0.375	0.278	0.533	0.482	2.056	0.248
12	68.8746	1.156	0.060	0.375	0.278	0.532	0.481	2.037	0.249
13	69.1382	1.140	0.057	0.376	0.316	0.498	0.597	1.908	0.229
14	69.7616	1.216	0.054	0.377	0.299	0.497	0.382	2.027	0.231
15	70.3335	1.191	0.054	0.376	0.300	0.493	0.427	1.976	0.233
16	70.9929	1.130	0.059	0.374	0.274	0.517	0.511	2.031	0.248
17	70.9929	1.148	0.055	0.376	0.304	0.488	0.526	1.939	0.231
18	71.3347	1.229	0.052	0.376	0.291	0.485	0.324	2.059	0.235
19	74.2746	1.150	0.057	0.372	0.274	0.527	0.442	2.049	0.254
20	74.2746	1.135	0.055	0.373	0.257	0.495	0.425	2.096	0.268
21	74.2746	1.154	0.052	0.375	0.287	0.469	0.437	1.999	0.243
22	74.2746	1.135	0.055	0.373	0.257	0.494	0.425	2.093	0.268
23	75.5664	1.100	0.055	0.372	0.260	0.484	0.499	2.067	0.263
24	77.0323	1.109	0.053	0.372	0.252	0.475	0.444	2.096	0.259
25	77.2143	1.213	0.047	0.373	0.241	0.450	0.272	2.208	0.264
26	77.2914	1.235	0.046	0.374	0.240	0.443	0.265	2.219	0.267
27	77.2914	1.266	0.045	0.376	0.270	0.434	0.262	2.145	0.234
28	77.2914	1.235	0.046	0.374	0.240	0.443	0.264	2.231	0.259
29	80.2356	1.229	0.046	0.372	0.238	0.453	0.262	2.213	0.263
30	80.2356	1.222	0.044	0.372	0.226	0.430	0.249	2.260	0.274
31	80.2356	1.251	0.043	0.375	0.262	0.414	0.241	2.151	0.241
32	80.2356	1.222	0.044	0.372	0.226	0.430	0.248	2.253	0.280
33	80.3692	1.140	0.050	0.371	0.252	0.475	0.343	2.088	0.277
34	80.3692	1.128	0.048	0.371	0.240	0.442	0.332	2.115	0.278
35	80.3692	1.149	0.046	0.374	0.264	0.430	0.340	2.078	0.247
36	80.3692	1.128	0.048	0.371	0.240	0.442	0.331	2.115	0.278
37	80.5349	1.207	0.046	0.372	0.240	0.458	0.268	2.179	0.275
38	80.5349	1.199	0.045	0.372	0.228	0.433	0.253	2.242	0.278
39	80.5349	1.225	0.044	0.375	0.260	0.418	0.245	2.144	0.248
40	80.5349	1.199	0.045	0.372	0.228	0.432	0.252	2.237	0.275
41	81.4969	1.185	0.047	0.371	0.238	0.459	0.269	2.166	0.279
42	81.4969	1.177	0.045	0.372	0.227	0.431	0.252	2.197	0.283
43	81.4969	1.201	0.044	0.374	0.257	0.416	0.243	2.141	0.249
44	81.4969	1.177	0.045	0.372	0.227	0.431	0.251	2.198	0.283
45	82.2802	1.093	0.052	0.370	0.257	0.472	0.454	2.046	0.273
46	82.2802	1.080	0.049	0.371	0.245	0.439	0.434	2.068	0.281
47	82.2802	1.097	0.048	0.373	0.266	0.426	0.443	2.018	0.251

#	q	p_{max}	β_{max}	$\dot{\delta}_{ail(max)}$	$\delta_{ail(max)}$	$\dot{\delta}_{rud(max)}$	$\delta_{rud(max)}$	$\phi_{(2.8\ sec)}$	$\phi_{(1\ sec)}$
48	82.2802	1.080	0.049	0.371	0.245	0.438	0.433	2.068	0.281
49	83.3181	1.101	0.050	0.370	0.250	0.467	0.409	2.082	0.277
50	83.3181	1.089	0.048	0.370	0.238	0.434	0.392	2.095	0.284
51	83.3181	1.107	0.047	0.372	0.260	0.422	0.401	2.042	0.253
52	83.3181	1.089	0.048	0.370	0.238	0.434	-0.392	2.095	0.284
53	83.4550	1.144	0.047	0.370	0.239	0.453	0.287	2.131	0.284
54	83.4550	1.135	0.045	0.371	0.228	0.422	0.279	2.158	0.288
55	83.4550	1.156	0.044	0.373	0.253	0.412	0.285	2.095	0.259
56	83.4550	1.135	0.044	0.371	0.228	0.422	0.278	2.159	0.288
57	83.7192	1.160	0.046	0.370	0.234	0.450	0.261	2.160	0.286
58	83.7192	1.151	0.044	0.371	0.223	0.421	0.247	2.187	0.290
59	83.7192	1.173	0.043	0.373	0.250	0.409	0.252	2.111	0.250
60	83.7192	1.151	0.044	0.371	0.223	0.420	0.247	2.188	0.290
61	87.3860	1.178	0.042	0.369	0.212	0.426	0.232	2.261	0.294
62	87.3860	1.174	0.040	0.369	0.203	0.400	0.218	2.273	0.307
63	87.3860	1.196	0.040	0.372	0.231	0.390	0.215	2.195	0.275
64	87.3860	1.173	0.040	0.369	0.203	0.401	0.217	2.274	0.307
65	88.7159	1.209	0.037	0.369	0.189	0.375	0.197	2.353	0.318
66	88.7159	1.209	0.037	0.369	0.189	0.375	0.196	2.353	0.317
67	89.2543	1.172	0.040	0.371	0.227	0.385	0.210	2.184	0.281
68	89.3983	1.189	0.040	0.368	0.198	0.416	0.218	2.307	0.305
69	89.3983	1.187	0.038	0.368	0.191	0.390	0.204	2.296	0.315
70	89.3983	1.210	0.038	0.371	0.218	0.383	0.204	2.253	0.286
71	89.3983	1.186	0.038	0.368	0.191	0.390	0.204	2.335	0.314
72	91.6970	1.092	0.044	0.367	0.224	0.423	0.316	2.118	0.299
73	91.6970	1.084	0.042	0.368	0.216	0.390	0.302	2.153	0.293
74	91.6970	1.101	0.042	0.371	0.235	0.386	0.311	2.104	0.283
75	91.6970	1.084	0.041	0.368	0.216	0.389	0.301	2.145	0.290
76	94.3473	1.192	0.036	0.368	0.182	0.368	0.185	2.355	0.319
77	94.3473	1.193	0.034	0.369	0.177	0.341	0.172	2.371	0.315
78	94.3473	1.193	0.034	0.369	0.177	0.341	0.171	2.378	0.333
79	101.0962	1.201	0.028	0.369	0.168	0.274	0.132	2.394	0.339
80	102.4478	1.078	0.035	0.365	0.200	0.352	0.227	2.167	0.306
81	102.4478	1.074	0.033	0.366	0.195	0.322	0.216	2.180	0.312
82	102.4478	1.090	0.035	0.368	0.209	0.331	0.228	2.156	0.297
83	102.4478	1.074	0.033	0.366	0.195	0.322	0.216	2.159	0.299
84	103.1193	1.193	0.031	0.369	0.179	0.302	0.146	2.360	0.325
85	103.7392	1.195	0.027	0.368	0.163	0.262	0.124	2.400	0.349
86	106.1299	1.163	0.030	0.366	0.161	0.306	0.143	2.359	0.357
87	106.1299	1.167	0.028	0.367	0.158	0.279	0.130	2.381	0.357
88	106.1299	1.186	0.030	0.369	0.174	0.288	0.138	2.366	0.332
89	106.1299	1.167	0.028	0.366	0.158	0.280	0.130	2.369	0.352
90	106.4162	1.188	0.026	0.368	0.157	0.251	0.117	2.410	0.336
91	109.0025	1.079	0.032	0.364	0.183	0.324	0.180	2.218	0.327
92	109.0025	1.077	0.030	0.365	0.179	0.296	0.172	2.203	0.336
93	109.0025	1.093	0.032	0.367	0.192	0.306	0.182	2.210	0.319
94	109.0025	1.077	0.030	0.365	0.179	0.296	0.171	2.205	0.336

#	q	p_{max}	β_{max}	$\dot{\delta}_{ail(max)}$	$\delta_{ail(max)}$	$\dot{\delta}_{rud(max)}$	$\delta_{rud(max)}$	$\phi_{(2.8\ sec)}$	$\phi_{(1\ sec)}$
95	109.1273	1.178	0.027	0.366	0.153	0.265	0.122	2.391	0.357
96	109.1273	1.182	0.025	0.367	0.152	0.240	0.110	2.404	0.352
97	109.1273	1.182	0.025	0.367	0.152	0.241	0.109	2.406	0.353
98	110.1905	1.103	0.031	0.363	0.167	0.322	0.149	2.289	0.345
99	110.1905	1.104	0.029	0.364	0.164	0.295	0.136	2.283	0.359
100	110.1905	1.120	0.030	0.366	0.177	0.304	0.144	2.273	0.337
101	110.1905	1.104	0.029	0.364	0.164	0.295	0.136	2.297	0.361
102	110.9265	1.040	0.033	0.364	0.202	0.317	0.248	2.104	0.301
103	110.9265	1.036	0.031	0.365	0.198	0.287	0.234	2.116	0.307
104	110.9265	1.051	0.033	0.367	0.209	0.302	0.250	2.099	0.297
105	110.9265	1.036	0.031	0.365	0.198	0.288	0.234	2.099	0.306
106	111.8726	1.169	0.025	0.366	0.149	0.254	0.114	2.387	0.358
107	111.8726	1.172	0.024	0.366	0.147	0.230	0.103	2.411	0.365
108	111.8726	1.173	0.024	0.366	0.147	0.230	0.102	2.408	0.383
109	114.6519	1.160	0.024	0.365	0.144	0.243	0.107	2.409	0.359
110	114.6519	1.163	0.022	0.365	0.142	0.219	0.096	2.421	0.385
111	114.6519	1.164	0.022	0.365	0.142	0.220	0.096	2.419	0.384
112	117.4653	1.151	0.023	0.364	0.138	0.233	0.100	2.401	0.399
113	117.4653	1.155	0.021	0.364	0.137	0.209	0.089	2.395	0.401
114	117.4653	1.155	0.021	0.364	0.137	0.210	0.089	2.416	0.397
115	120.3129	1.142	0.022	0.363	0.133	0.222	0.093	2.404	0.393
116	120.3129	1.146	0.020	0.363	0.132	0.199	0.083	2.416	0.405
117	120.3129	1.173	0.022	0.367	0.153	0.210	0.091	2.383	0.362
118	120.3129	1.146	0.020	0.363	0.131	0.200	0.083	2.415	0.405
119	121.8328	1.132	0.023	0.362	0.135	0.243	0.102	2.398	0.382
120	121.8328	1.137	0.022	0.363	0.134	0.218	0.091	2.387	0.411
121	121.8328	1.158	0.024	0.366	0.152	0.230	0.100	2.353	0.334
122	121.8328	1.137	0.022	0.363	0.134	0.218	0.091	2.401	0.379
123	123.1945	1.133	0.021	0.361	0.128	0.213	0.086	2.398	0.402
124	123.1945	1.140	0.019	0.362	0.129	0.189	0.077	2.406	0.404
125	123.1945	1.165	0.021	0.366	0.148	0.202	0.085	2.390	0.379
126	123.1945	1.140	0.019	0.362	0.129	0.190	0.077	2.409	0.405
127	126.1103	1.126	0.019	0.361	0.125	0.203	0.080	2.388	0.393
128	126.1103	1.134	0.018	0.362	0.127	0.178	0.072	2.396	0.403
129	126.1103	1.156	0.020	0.365	0.142	0.193	0.080	2.400	0.389
130	126.1103	1.134	0.018	0.362	0.127	0.179	0.072	2.397	0.404
131	129.0601	1.120	0.019	0.360	0.123	0.191	0.075	2.396	0.415
132	129.0601	1.129	0.017	0.361	0.125	0.167	0.066	2.388	0.401
133	129.0601	1.148	0.019	0.364	0.137	0.186	0.075	2.397	0.371
134	129.0601	1.129	0.017	0.361	0.125	0.167	0.066	2.406	0.400
135	129.4213	1.014	0.026	0.360	0.183	0.250	0.203	2.124	0.335
136	129.4213	1.013	0.025	0.361	0.178	0.225	0.193	2.125	0.347
137	129.4213	1.023	0.027	0.364	0.192	0.241	0.207	2.112	0.274
138	129.4213	1.013	0.025	0.361	0.178	0.225	0.192	2.134	0.341
139	129.8252	1.041	0.025	0.360	0.158	0.252	0.146	2.216	0.361
140	129.8252	1.043	0.023	0.361	0.155	0.227	0.139	2.209	0.371
141	129.8252	1.053	0.025	0.363	0.167	0.243	0.150	2.204	0.334

#	q	p_{max}	β_{max}	$\dot{\delta}_{ail(max)}$	$\delta_{ail(max)}$	$\dot{\delta}_{rud(max)}$	$\delta_{rud(max)}$	$\phi_{(2.8\ sec)}$	$\phi_{(1\ sec)}$
142	129.8252	1.043	0.023	0.361	0.155	0.228	0.138	2.214	0.374
143	129.9582	1.075	0.024	0.359	0.137	0.257	0.105	2.298	0.406
144	129.9582	1.079	0.022	0.360	0.135	0.231	0.095	2.304	0.401
145	129.9582	1.092	0.024	0.362	0.147	0.248	0.104	2.296	0.364
146	129.9582	1.079	0.022	0.360	0.135	0.231	0.095	2.306	0.405
147	130.0074	1.063	0.024	0.359	0.144	0.255	0.114	2.289	0.385
148	130.0074	1.067	0.023	0.360	0.141	0.230	0.108	2.268	0.387
149	130.0074	1.078	0.025	0.363	0.153	0.246	0.117	2.272	0.326
150	130.0074	1.067	0.023	0.360	0.141	0.231	0.108	2.292	0.390
151	130.0653	1.086	0.023	0.358	0.131	0.254	0.103	2.329	0.418
152	130.0653	1.091	0.022	0.359	0.130	0.229	0.092	2.331	0.415
153	130.0653	1.105	0.024	0.362	0.142	0.246	0.102	2.350	0.396
154	130.0653	1.091	0.022	0.359	0.130	0.229	0.092	2.350	0.405
155	130.1006	1.052	0.024	0.359	0.150	0.253	0.129	2.246	0.377
156	130.1006	1.054	0.023	0.361	0.148	0.228	0.122	2.257	0.377
157	130.1006	1.065	0.025	0.363	0.160	0.244	0.132	2.247	0.346
158	130.1006	1.054	0.023	0.360	0.148	0.229	0.122	2.231	0.379
159	131.7744	1.116	0.020	0.359	0.122	0.209	0.082	2.388	0.403
160	131.7744	1.121	0.019	0.361	0.125	0.187	0.073	2.375	0.393
161	131.7744	1.142	0.021	0.364	0.138	0.201	0.081	2.397	0.389
162	131.7744	1.122	0.019	0.361	0.125	0.187	0.074	2.377	0.392
163	132.0441	1.115	0.018	0.360	0.121	0.179	0.069	2.383	0.441
164	132.0441	1.124	0.016	0.361	0.123	0.155	0.060	2.399	0.424
165	132.0441	1.140	0.018	0.363	0.132	0.179	0.070	2.394	0.411
166	132.0441	1.124	0.016	0.361	0.123	0.156	0.060	2.393	0.441
167	134.8266	1.095	0.021	0.358	0.122	0.219	0.086	2.356	0.436
168	134.8266	1.101	0.019	0.359	0.123	0.195	0.077	2.373	0.423
169	134.8266	1.119	0.021	0.362	0.135	0.212	0.085	2.352	0.395
170	134.8266	1.102	0.019	0.359	0.123	0.196	0.077	2.378	0.421
171	135.0621	1.109	0.017	0.359	0.119	0.166	0.063	2.374	0.434
172	135.0621	1.119	0.015	0.360	0.121	0.143	0.055	2.382	0.426
173	135.0621	1.135	0.018	0.363	0.130	0.168	0.065	2.408	0.406
174	135.0621	1.120	0.015	0.360	0.121	0.143	0.055	2.397	0.445
175	137.9562	1.058	0.023	0.361	0.149	0.225	0.119	2.264	0.370
176	138.1142	1.104	0.016	0.359	0.117	0.154	0.057	2.380	0.415
177	138.1142	1.115	0.015	0.360	0.119	0.130	0.049	2.377	0.446
178	138.1142	1.130	0.017	0.362	0.128	0.157	0.060	2.401	0.407
179	138.1142	1.116	0.015	0.360	0.119	0.131	0.049	2.380	0.448
180	158.6743	1.049	0.031	0.356	0.115	0.097	0.061	2.311	0.445
181	163.0169	1.017	0.033	0.357	0.138	0.090	0.096	2.205	0.407
182	167.7286	1.040	0.020	0.354	0.104	0.050	0.020	2.354	0.474
183	167.7286	1.048	0.019	0.356	0.106	0.049	0.017	2.346	0.476
184	167.7286	1.058	0.022	0.358	0.113	0.059	0.022	2.337	0.450
185	167.7286	1.049	0.019	0.356	0.106	0.049	0.018	2.343	0.481
186	170.3164	1.019	0.028	0.351	0.110	0.084	0.065	2.269	0.460
187	170.3164	1.021	0.026	0.352	0.109	0.071	0.058	2.277	0.461
188	170.3164	1.027	0.029	0.355	0.117	0.084	0.068	2.286	0.430

#	q	p_{max}	β_{max}	$\dot{\delta}_{ail(max)}$	$\delta_{ail(max)}$	$\dot{\delta}_{rud(max)}$	$\delta_{rud(max)}$	$\phi_{(2.8\ sec)}$	$\phi_{(1\ sec)}$
189	170.3164	1.021	0.026	0.352	0.109	0.071	0.058	2.277	0.460
190	186.2219	1.032	0.025	0.353	0.103	0.067	0.041	2.334	0.468
191	206.0828	1.014	0.023	0.349	0.098	0.055	0.047	2.319	0.480
192	206.3182	1.005	0.025	0.350	0.107	0.053	0.061	2.273	0.459
193	208.2658	1.017	0.016	0.349	0.093	0.034	0.014	2.343	0.501
194	208.2658	1.025	0.015	0.351	0.096	0.033	0.018	2.316	0.496
195	208.2658	1.028	0.017	0.353	0.101	0.040	0.017	2.321	0.484
196	208.2658	1.025	0.015	0.351	0.096	0.034	0.018	2.354	0.495
197	215.9733	1.011	0.019	0.345	0.087	0.042	0.026	2.326	0.506
198	215.9733	1.013	0.017	0.347	0.089	0.044	0.022	2.325	0.493
199	215.9733	1.019	0.020	0.349	0.094	0.048	0.028	2.349	0.498
200	215.9733	1.013	0.017	0.346	0.089	0.044	0.022	2.330	0.490
201	222.8766	1.022	0.013	0.350	0.094	0.027	0.018	2.335	0.517
202	222.8766	1.024	0.015	0.352	0.099	0.034	0.018	2.342	0.483
203	222.8766	1.023	0.013	0.350	0.094	0.028	0.019	2.335	0.517
204	228.5562	0.994	0.021	0.343	0.112	0.032	0.056	2.240	0.469
205	228.5562	0.994	0.020	0.345	0.112	0.032	0.050	2.247	0.475
206	228.5562	0.996	0.023	0.348	0.115	0.038	0.063	2.248	0.450
207	228.5562	0.994	0.020	0.345	0.112	0.032	0.050	2.251	0.475
208	245.2556	1.005	0.019	0.344	0.086	0.041	0.033	2.327	0.502
209	247.9286	1.010	0.017	0.346	0.089	0.037	0.018	2.339	0.520
210	254.7139	0.998	0.018	0.339	0.090	0.031	0.036	2.286	0.512
211	254.7139	0.997	0.016	0.341	0.090	0.033	0.030	2.298	0.513
212	254.7139	0.999	0.019	0.344	0.090	0.033	0.040	2.279	0.481
213	254.7139	0.997	0.016	0.341	0.090	0.034	0.030	2.296	0.498
214	264.5698	1.006	0.012	0.344	0.084	0.022	0.015	2.337	0.525
215	264.5698	1.005	0.011	0.345	0.086	0.024	0.018	2.322	0.531
216	264.5698	1.009	0.013	0.348	0.090	0.027	0.018	2.339	0.503
217	264.5698	1.005	0.011	0.345	0.086	0.023	0.018	2.320	0.532
218	282.0876	1.007	0.014	0.344	0.085	0.029	0.016	2.329	0.514
219	287.8346	1.001	0.016	0.341	0.080	0.032	0.021	2.317	0.515
220	308.2038	0.998	0.016	0.338	0.081	0.027	0.026	2.314	0.513
221	333.6127	1.002	0.010	0.338	0.075	0.036	0.016	2.327	0.530
222	333.6127	1.000	0.009	0.340	0.077	0.043	0.019	2.335	0.540
223	333.6127	1.004	0.011	0.342	0.081	0.030	0.018	2.316	0.529
224	333.6127	1.000	0.009	0.340	0.077	0.042	0.019	2.329	0.541
225	333.8201	0.999	0.012	0.334	0.071	0.025	0.016	2.339	0.553
226	333.8201	0.999	0.011	0.336	0.073	0.032	0.019	2.323	0.548
227	333.8201	1.001	0.013	0.338	0.076	0.025	0.017	2.325	0.522
228	333.8201	0.999	0.011	0.336	0.073	0.031	0.019	2.323	0.523
229	357.0172	1.000	0.008	0.339	0.075	0.050	0.019	2.346	0.526
230	357.0172	1.003	0.010	0.341	0.079	0.037	0.019	2.326	0.535
231	357.0172	1.000	0.006	0.339	0.075	0.048	0.019	2.349	0.523
232	366.7880	0.998	0.014	0.333	0.075	0.024	0.018	2.321	0.527
233	383.2118	1.001	0.011	0.336	0.073	0.031	0.017	2.296	0.544
234	416.6143	1.001	0.009	0.332	0.069	0.053	0.017	2.338	0.511
235	416.6143	0.999	0.008	0.334	0.070	0.059	0.020	2.339	0.557

#	q	p_{max}	β_{max}	$\dot{\delta}_{ail(max)}$	$\delta_{ail(max)}$	$\dot{\delta}_{rud(max)}$	$\delta_{rud(max)}$	$\phi_{(2.8\ sec)}$	$\phi_{(1\ sec)}$
236	416.6143	1.002	0.009	0.337	0.074	0.046	0.019	2.337	0.545
237	416.6143	0.999	0.008	0.334	0.070	0.058	0.020	2.322	0.522
238	430.4664	0.999	0.012	0.330	0.073	0.038	0.018	2.324	0.540
239	436.0099	1.002	0.010	0.334	0.071	0.043	0.018	2.334	0.551
240	499.2391	0.998	0.010	0.323	0.070	0.060	0.018	2.326	0.549
241	499.2391	0.998	0.009	0.325	0.070	0.067	0.021	2.318	0.567
242	499.2391	0.999	0.010	0.328	0.071	0.051	0.019	2.335	0.550
243	499.2391	0.998	0.009	0.325	0.070	0.065	0.021	2.320	0.567
244	503.8640	1.000	0.008	0.327	0.068	0.065	0.018	2.336	0.552
245	503.8640	0.999	0.007	0.329	0.066	0.070	0.020	2.321	0.550
246	503.8640	1.001	0.008	0.332	0.070	0.057	0.019	2.327	0.510
247	503.8640	0.999	0.007	0.329	0.066	0.069	0.020	2.336	0.548
248	514.2514	0.997	0.011	0.320	0.075	0.060	0.020	2.309	0.564
249	514.2514	0.997	0.010	0.322	0.075	0.067	0.023	2.313	0.542
250	514.2514	0.998	0.011	0.324	0.076	0.051	0.019	2.322	0.551
251	514.2514	0.997	0.010	0.322	0.075	0.065	0.023	2.330	0.540
252	551.8250	0.999	0.007	0.327	0.066	0.077	0.021	2.320	0.556
253	551.8250	1.001	0.008	0.330	0.069	0.063	0.020	2.314	0.548
254	551.8250	0.999	0.007	0.327	0.066	0.075	0.021	2.336	0.559
255	573.1062	1.000	0.009	0.325	0.071	0.061	0.019	2.324	0.540
256	618.5337	1.000	0.007	0.321	0.068	0.077	0.019	2.325	0.566
257	618.5337	0.999	0.007	0.323	0.067	0.083	0.021	2.321	0.569
258	618.5337	1.000	0.008	0.326	0.070	0.069	0.020	2.335	0.554
259	618.5337	0.999	0.007	0.323	0.067	0.081	0.021	2.330	0.570
260	652.0676	1.000	0.008	0.323	0.072	0.068	0.019	2.324	0.548
261	699.9532	0.998	0.008	0.314	0.071	0.082	0.020	2.313	0.540
262	699.9532	0.998	0.008	0.316	0.071	0.088	0.022	2.333	0.556
263	699.9532	0.999	0.009	0.319	0.074	0.072	0.020	2.311	0.564
264	699.9532	0.998	0.008	0.316	0.071	0.086	0.023	2.333	0.560
265	771.1717	1.000	0.007	0.316	0.069	0.089	0.020	2.326	0.571
266	771.1717	0.999	0.006	0.318	0.067	0.093	0.022	2.326	0.550
267	771.1717	1.000	0.007	0.321	0.070	0.079	0.020	2.317	0.551
268	771.1717	0.999	0.006	0.318	0.067	0.092	0.022	2.326	0.558
269	825.2729	0.999	0.006	0.317	0.067	0.097	0.023	2.334	0.562
270	825.2729	1.000	0.006	0.320	0.070	0.083	0.021	2.319	0.544
271	825.2729	0.999	0.006	0.317	0.067	0.096	0.023	2.318	0.569
272	954.4603	1.000	0.006	0.312	0.074	0.098	0.021	2.306	0.556
273	954.4603	0.999	0.006	0.314	0.071	0.102	0.023	2.325	0.554
274	954.4603	1.000	0.006	0.317	0.074	0.087	0.022	2.316	0.531
275	954.4603	0.999	0.006	0.314	0.071	0.100	0.024	2.324	0.553
276	1106.2120	1.000	0.006	0.310	0.077	0.103	0.022	2.283	0.547
277	1106.2120	0.998	0.006	0.311	0.074	0.106	0.025	2.319	0.549
278	1106.2120	1.000	0.006	0.314	0.078	0.092	0.022	2.296	0.558
279	1106.2120	0.998	0.006	0.311	0.074	0.105	0.025	2.319	0.549
280	1157.0650	0.998	0.006	0.311	0.075	0.108	0.025	2.317	0.547
281	1157.0650	1.000	0.006	0.314	0.079	0.094	0.023	2.294	0.558
282	1157.0650	0.998	0.005	0.311	0.075	0.107	0.025	2.293	0.547

E.2 Lateral Maximum p_{cmd} Step Input Time Response Data

#	q	p_{max}	β_{max}	$\dot{\delta}_{ail(max)}$	$\delta_{ail(max)}$	$\dot{\delta}_{rud(max)}$	$\delta_{rud(max)}$	$\phi(2.8\,sec)$	$\phi(1\,sec)$
1	63.6460	57.343	2.596	16.399	14.767	23.713	19.753	82.033	8.689
2	65.4696	54.166	2.770	16.835	12.745	24.921	18.268	92.460	10.360
3	65.4696	54.161	2.761	16.834	12.743	24.887	18.231	92.476	10.354
4	65.5666	53.344	2.799	16.856	12.932	24.992	20.791	91.537	10.395
5	67.0399	57.265	2.705	17.344	12.585	24.750	16.861	97.886	10.783
6	67.0399	57.258	2.698	17.343	12.584	24.720	16.790	97.901	10.777
7	67.4267	56.641	2.740	17.452	12.716	24.950	17.074	97.787	10.961
8	67.4267	56.634	2.732	17.452	12.715	24.918	17.000	97.828	10.960
9	67.6717	58.729	2.667	17.554	12.555	24.539	16.488	100.132	10.909
10	67.6717	60.597	2.569	17.650	14.297	23.736	16.337	94.369	9.868
11	68.8746	55.049	2.856	17.871	13.228	25.381	22.928	97.308	11.974
12	68.8746	55.041	2.847	17.870	13.227	25.350	22.884	98.054	11.705
13	69.1382	54.513	2.708	18.029	15.126	23.852	28.561	91.794	10.441
14	69.7616	58.793	2.619	18.255	14.469	24.038	18.479	97.150	10.586
15	70.3335	58.213	2.647	18.424	14.643	24.121	20.866	97.337	10.779
16	70.9929	55.824	2.900	18.513	13.519	25.552	25.252	101.702	12.014
17	70.9929	56.737	2.707	18.607	15.039	24.151	25.973	97.078	11.147
18	71.3347	61.077	2.602	18.756	14.461	24.110	16.115	101.403	11.014
19	74.2746	60.061	2.991	19.489	14.295	27.541	23.085	106.090	13.708
20	74.2746	59.296	2.880	19.536	13.419	25.839	22.223	109.521	13.428
21	74.2746	60.292	2.715	19.636	14.970	24.596	22.822	104.402	11.922
22	74.2746	59.286	2.872	19.535	13.418	25.802	22.176	110.022	13.539
23	75.5664	58.701	2.943	19.915	13.889	25.812	26.607	108.859	14.220
24	77.0323	60.537	2.910	20.369	13.757	25.924	24.260	113.088	14.746
25	77.2143	66.420	2.581	20.494	13.222	24.632	14.867	119.522	13.968
26	77.2914	67.732	2.532	20.531	13.163	24.323	14.549	122.214	14.261
27	77.2914	69.377	2.494	20.650	14.797	23.805	14.355	115.897	12.780
28	77.2914	67.724	2.525	20.530	13.163	24.307	14.495	120.668	13.971
29	80.2356	70.467	2.615	21.377	13.627	25.955	15.036	126.979	15.488
30	80.2356	70.089	2.533	21.401	12.967	24.678	14.277	128.513	15.946
31	80.2356	71.713	2.460	21.560	15.007	23.680	13.838	123.994	13.927
32	80.2356	70.081	2.527	21.400	12.968	24.666	14.227	128.485	15.919
33	80.3692	65.527	2.876	21.351	14.465	27.246	19.707	119.563	15.775
34	80.3692	64.825	2.739	21.401	13.779	25.315	19.049	118.602	16.038
35	80.3692	66.005	2.665	21.522	15.195	24.641	19.557	119.248	14.043
36	80.3692	64.817	2.731	21.399	13.777	25.288	19.024	121.720	16.011
37	80.5349	69.512	2.673	21.454	13.797	26.228	15.425	126.908	15.698
38	80.5349	69.072	2.581	21.485	13.125	24.925	14.553	127.415	15.988
39	80.5349	70.563	2.510	21.634	14.984	24.011	14.087	122.638	13.409
40	80.5349	69.063	2.574	21.483	13.125	24.911	14.498	127.432	15.968
41	81.4969	69.253	2.727	21.725	13.920	26.631	15.694	127.975	16.491
42	81.4969	68.774	2.619	21.762	13.255	25.160	14.707	128.227	16.396
43	81.4969	70.156	2.549	21.907	15.002	24.273	14.217	124.743	14.387
44	81.4969	68.765	2.612	21.761	13.255	25.145	14.651	128.257	16.379
45	82.2802	64.586	3.063	21.902	15.196	27.868	26.834	119.846	16.633
46	82.2802	63.823	2.913	21.961	14.464	25.862	25.629	123.290	16.281
47	82.2802	64.829	2.827	22.078	15.739	25.071	26.190	119.543	15.272

#	q	p_{max}	β_{max}	$\dot{\delta}_{ail(max)}$	$\delta_{ail(max)}$	$\dot{\delta}_{rud(max)}$	$\delta_{rud(max)}$	$\phi_{(2.8\ sec)}$	$\phi_{(1\ sec)}$
48	82.2802	63.813	2.904	21.960	14.461	25.833	25.570	122.002	16.727
49	83.3181	66.052	3.028	22.223	15.002	27.964	24.560	123.992	17.035
50	83.3181	65.355	2.884	22.282	14.289	25.980	23.546	125.830	16.037
51	83.3181	66.394	2.803	22.404	15.612	25.168	24.067	122.389	14.819
52	83.3181	65.345	2.875	22.281	14.286	25.953	23.492	126.663	16.348
53	83.4550	68.786	2.809	22.288	14.349	27.157	17.233	128.823	16.543
54	83.4550	68.213	2.681	22.336	13.690	25.267	16.744	130.060	16.751
55	83.4550	69.459	2.630	22.474	15.180	24.668	17.141	126.464	15.738
56	83.4550	68.205	2.673	22.335	13.687	25.245	16.708	130.537	16.485
57	83.7192	69.965	2.764	22.376	14.121	26.986	15.732	129.682	17.035
58	83.7192	69.468	2.647	22.420	13.454	25.204	14.920	133.245	16.803
59	83.7192	70.769	2.594	22.565	15.060	24.621	15.196	126.355	14.691
60	83.7192	69.458	2.640	22.419	13.456	25.183	14.885	132.481	16.616
61	87.3860	74.778	2.663	23.461	13.480	26.829	14.718	143.301	19.347
62	87.3860	74.494	2.556	23.498	12.874	25.193	13.814	145.119	19.374
63	87.3860	75.937	2.537	23.678	14.664	24.727	13.638	139.796	17.655
64	87.3860	74.485	2.549	23.496	12.873	25.204	13.768	143.340	18.082
65	88.7159	78.130	2.414	23.923	12.190	24.027	12.729	152.119	20.545
66	88.7159	78.126	2.408	23.921	12.194	24.050	12.692	151.801	20.324
67	89.2543	76.252	2.575	24.231	14.792	24.967	13.694	143.386	17.961
68	89.3983	77.513	2.604	24.027	12.939	26.916	14.188	150.003	20.130
69	89.3983	77.358	2.496	24.072	12.434	25.221	13.320	151.937	20.683
70	89.3983	78.860	2.506	24.268	14.222	24.875	13.310	148.143	18.017
71	89.3983	77.352	2.490	24.071	12.438	25.215	13.279	151.823	19.596
72	91.6970	73.316	2.956	24.739	15.071	28.252	21.195	143.798	19.374
73	91.6970	72.794	2.791	24.803	14.497	26.026	20.258	145.001	20.459
74	91.6970	73.957	2.793	24.952	15.790	25.771	20.918	141.048	19.117
75	91.6970	72.785	2.784	24.801	14.495	26.006	20.214	144.217	20.332
76	94.3473	82.796	2.473	25.569	12.614	25.326	12.880	163.192	22.930
77	94.3473	82.875	2.356	25.642	12.273	23.484	11.937	164.715	23.148
78	94.3473	82.871	2.350	25.640	12.277	23.511	11.903	164.717	23.076
79	101.0962	90.355	2.129	27.814	12.631	20.524	9.946	179.686	24.718
80	102.4478	82.305	2.704	27.925	15.271	26.740	17.347	164.851	23.324
81	102.4478	82.041	2.549	28.023	14.896	24.396	16.533	166.265	23.823
82	102.4478	83.241	2.653	28.174	15.983	25.124	17.384	162.572	22.948
83	102.4478	82.033	2.542	28.021	14.894	24.392	16.494	166.456	23.873
84	103.1193	91.780	2.371	28.482	13.783	23.168	11.268	182.159	24.893
85	103.7392	92.597	2.099	28.600	12.612	20.281	9.628	185.346	27.000
86	106.1299	92.488	2.360	29.122	12.798	24.204	11.404	188.379	27.174
87	106.1299	92.808	2.216	29.199	12.593	22.137	10.367	189.256	27.453
88	106.1299	94.360	2.350	29.399	13.876	22.915	10.940	188.641	25.598
89	106.1299	92.813	2.210	29.197	12.595	22.178	10.344	188.735	27.378
90	106.4162	94.808	2.066	29.381	12.548	20.018	9.304	191.055	28.453
91	109.0025	88.461	2.606	29.871	14.973	26.360	14.791	181.615	25.398
92	109.0025	88.344	2.455	29.974	14.671	24.115	14.087	181.519	27.988
93	109.0025	89.616	2.594	30.141	15.726	25.101	14.954	180.932	25.378
94	109.0025	88.339	2.449	29.972	14.672	24.152	14.053	182.097	26.304

#	q	p_{max}	β_{max}	$\dot{\delta}_{ail(max)}$	$\delta_{ail(max)}$	$\dot{\delta}_{rud(max)}$	$\delta_{rud(max)}$	$\phi_{(2.8\ sec)}$	$\phi_{(1\ sec)}$
95	109.1273	96.691	2.190	30.138	12.754	21.727	10.008	197.663	28.870
96	109.1273	97.014	2.038	30.174	12.492	19.705	8.992	197.448	29.611
97	109.1273	97.021	2.029	30.171	12.490	19.745	8.985	198.584	29.573
98	110.1905	91.584	2.535	30.175	13.873	26.642	12.358	190.099	28.947
99	110.1905	91.647	2.392	30.278	13.609	24.305	11.321	189.091	29.591
100	110.1905	93.000	2.530	30.460	14.707	25.234	11.980	188.419	28.156
101	110.1905	91.646	2.386	30.275	13.612	24.322	11.293	189.537	29.054
102	110.9265	87.039	2.743	30.446	16.867	26.362	20.758	176.027	26.946
103	110.9265	86.685	2.566	30.559	16.557	23.849	19.606	176.949	26.784
104	110.9265	87.924	2.735	30.723	17.494	25.177	20.901	176.166	24.820
105	110.9265	86.678	2.559	30.557	16.555	23.881	19.559	176.027	24.868
106	111.8726	98.715	2.145	30.915	12.622	21.381	9.641	202.526	30.087
107	111.8726	99.030	1.994	30.951	12.403	19.356	8.662	204.289	30.697
108	111.8726	99.040	1.989	30.948	12.402	19.406	8.648	204.076	30.654
109	114.6519	100.732	2.096	31.699	12.490	21.038	9.267	208.480	33.286
110	114.6519	101.041	1.947	31.734	12.303	18.998	8.314	209.067	32.589
111	114.6519	101.054	1.942	31.731	12.301	19.056	8.305	209.164	32.639
112	117.4653	102.742	2.045	32.483	12.354	20.673	8.880	214.280	32.617
113	117.4653	103.048	1.898	32.518	12.191	18.616	7.969	212.714	35.956
114	117.4653	103.056	1.893	32.515	12.188	18.681	7.962	214.081	35.368
115	120.3129	104.743	1.991	33.262	12.216	20.261	8.516	219.567	36.585
116	120.3129	105.053	1.846	33.301	12.068	18.200	7.612	212.708	37.628
117	120.3129	107.560	2.036	33.709	14.025	19.252	8.331	218.633	33.454
118	120.3129	105.069	1.837	33.297	12.066	18.272	7.600	220.528	36.587
119	121.8328	105.248	2.174	33.697	12.544	22.468	9.498	221.545	37.824
120	121.8328	105.696	2.014	33.766	12.497	20.178	8.491	220.736	35.377
121	121.8328	107.724	2.213	34.091	14.094	21.460	9.282	221.864	32.762
122	121.8328	105.726	2.009	33.763	12.499	20.249	8.483	222.552	34.902
123	123.1945	106.739	1.935	34.033	12.071	19.822	8.137	226.050	38.818
124	123.1945	107.308	1.806	34.132	12.146	17.679	7.279	226.213	36.753
125	123.1945	109.668	1.996	34.520	13.892	18.987	8.016	227.052	33.966
126	123.1945	107.331	1.801	34.129	12.148	17.756	7.278	226.661	36.676
127	126.1103	108.856	1.887	34.839	12.044	19.440	7.794	230.912	40.831
128	126.1103	109.619	1.762	34.977	12.249	17.071	6.926	232.086	41.451
129	126.1103	111.770	1.953	35.331	13.741	18.704	7.706	231.652	35.929
130	126.1103	109.638	1.759	34.974	12.250	17.153	6.926	232.592	40.891
131	129.0601	111.127	1.838	35.690	12.154	18.816	7.405	237.632	41.800
132	129.0601	111.967	1.716	35.834	12.359	16.374	6.548	238.306	39.584
133	129.0601	113.885	1.910	36.145	13.583	18.422	7.406	237.437	39.986
134	129.0601	111.993	1.713	35.831	12.362	16.460	6.549	238.006	39.081
135	129.4213	100.912	2.608	35.857	18.161	24.659	20.200	209.652	34.367
136	129.4213	100.832	2.458	35.954	17.677	22.246	19.167	210.166	32.270
137	129.4213	101.786	2.672	36.216	19.101	23.910	20.607	210.665	32.565
138	129.4213	100.828	2.452	35.952	17.673	22.270	19.119	210.337	33.877
139	129.8252	103.945	2.474	35.895	15.760	25.066	14.593	221.116	36.427
140	129.8252	104.114	2.327	35.995	15.431	22.603	13.853	221.616	36.065
141	129.8252	105.148	2.539	36.275	16.715	24.095	14.941	219.984	34.001

#	q	p_{max}	β_{max}	$\dot{\delta}_{ail(max)}$	$\delta_{ail(max)}$	$\dot{\delta}_{rud(max)}$	$\delta_{rud(max)}$	$\phi_{(2.8\ sec)}$	$\phi_{(1\ sec)}$
142	129.8252	104.113	2.321	35.993	15.433	22.645	13.819	220.315	36.234
143	129.9582	107.421	2.375	35.837	13.695	25.629	10.482	231.779	40.190
144	129.9582	107.865	2.221	35.966	13.523	23.036	9.504	231.386	38.511
145	129.9582	109.131	2.441	36.251	14.687	24.713	10.409	230.743	35.983
146	129.9582	107.873	2.216	35.963	13.528	23.091	9.480	230.638	40.113
147	130.0074	106.330	2.408	35.875	14.364	25.490	11.415	226.963	39.027
148	130.0074	106.679	2.257	35.981	14.135	22.959	10.822	228.525	38.262
149	130.0074	107.841	2.474	36.272	15.339	24.439	11.733	226.732	36.698
150	130.0074	106.683	2.250	35.978	14.138	23.015	10.795	228.714	38.856
151	130.0653	108.628	2.322	35.808	13.101	25.413	10.261	234.516	41.054
152	130.0653	109.188	2.167	35.922	12.997	22.874	9.228	235.126	40.720
153	130.0653	110.603	2.390	36.228	14.161	24.373	10.175	233.901	37.447
154	130.0653	109.198	2.162	35.919	13.002	22.943	9.220	232.002	40.605
155	130.1006	105.267	2.438	35.941	15.042	25.256	12.902	224.079	37.803
156	130.1006	105.517	2.288	36.044	14.768	22.747	12.236	224.667	37.483
157	130.1006	106.617	2.505	36.330	16.005	24.252	13.239	224.949	35.627
158	130.1006	105.527	2.283	36.041	14.767	22.796	12.207	224.151	37.187
159	131.7744	113.258	2.038	36.456	12.433	21.126	8.344	241.808	42.865
160	131.7744	113.841	1.901	36.591	12.684	18.756	7.467	239.312	43.523
161	131.7744	115.926	2.111	36.957	14.045	20.435	8.277	241.735	37.091
162	131.7744	113.867	1.897	36.588	12.685	18.826	7.463	242.730	42.648
163	132.0441	113.416	1.785	36.602	12.273	18.083	7.001	242.446	43.585
164	132.0441	114.355	1.666	36.748	12.485	15.692	6.143	243.950	42.065
165	132.0441	116.027	1.872	36.977	13.430	18.181	7.140	243.128	41.979
166	132.0441	114.385	1.662	36.745	12.486	15.777	6.146	243.720	42.690
167	134.8266	114.036	2.138	37.252	12.706	22.773	8.908	247.271	44.337
168	134.8266	114.703	1.996	37.370	12.844	20.358	7.979	246.572	44.557
169	134.8266	116.551	2.221	37.724	14.106	22.013	8.884	246.199	40.296
170	134.8266	114.725	1.992	37.367	12.848	20.432	7.980	244.912	42.827
171	135.0621	115.741	1.730	37.470	12.399	17.220	6.573	249.130	44.716
172	135.0621	116.797	1.613	37.624	12.616	14.790	5.714	249.616	44.714
173	135.0621	118.422	1.829	37.863	13.546	17.554	6.775	251.106	41.512
174	135.0621	116.825	1.609	37.621	12.617	14.880	5.720	248.449	46.217
175	137.9562	113.060	2.469	38.619	15.962	23.912	12.689	240.499	38.927
176	138.1142	118.093	1.671	38.309	12.533	16.344	6.122	252.795	46.890
177	138.1142	119.288	1.554	38.470	12.756	13.784	5.265	253.868	47.604
178	138.1142	120.867	1.781	38.722	13.673	16.810	6.389	255.626	41.475
179	138.1142	119.319	1.552	38.467	12.756	13.852	5.275	253.184	44.379
180	158.6743	130.637	3.839	44.381	14.338	11.994	7.562	289.124	55.999
181	163.0169	130.485	4.193	45.856	17.722	11.527	12.260	283.113	52.837
182	167.7286	137.675	2.675	46.849	13.725	6.642	2.625	311.196	63.207
183	167.7286	138.727	2.495	47.055	14.050	6.438	2.309	312.312	62.225
184	167.7286	140.029	2.869	47.361	15.011	7.812	2.879	310.573	59.513
185	167.7286	138.791	2.488	47.052	14.047	6.518	2.329	312.129	61.785
186	170.3164	137.099	3.739	47.229	14.849	11.277	8.813	306.270	61.131
187	170.3164	137.336	3.453	47.389	14.646	9.491	7.836	308.327	60.402
188	170.3164	138.219	3.960	47.816	15.732	11.217	9.199	306.053	59.502

E-11

#	q	p_{max}	β_{max}	$\dot{\delta}_{ail(max)}$	$\delta_{ail(max)}$	$\dot{\delta}_{rud(max)}$	$\delta_{rud(max)}$	$\phi_{(2.8\ sec)}$	$\phi_{(1\ sec)}$
189	170.3164	137.345	3.444	47.385	14.653	9.570	7.804	308.518	61.565
190	186.2219	152.972	3.648	52.229	15.265	9.848	6.138	344.312	70.565
191	206.0828	163.117	3.736	56.247	15.821	8.887	7.575	372.526	78.128
192	206.3182	161.674	3.961	56.376	17.194	8.556	9.839	365.329	74.937
193	208.2658	163.990	2.530	56.342	15.038	5.414	2.238	378.043	80.849
194	208.2658	165.287	2.362	56.581	15.472	5.378	2.825	375.293	80.139
195	208.2658	165.833	2.703	56.908	16.278	6.479	2.822	374.912	77.260
196	208.2658	165.340	2.355	56.577	15.470	5.426	2.844	377.725	81.171
197	215.9733	164.147	3.038	56.072	14.066	6.792	4.269	381.705	82.721
198	215.9733	164.451	2.788	56.345	14.508	7.126	3.605	377.980	82.592
199	215.9733	165.525	3.247	56.732	15.344	7.742	4.539	378.457	81.897
200	215.9733	164.468	2.780	56.341	14.507	7.237	3.582	381.166	83.098
201	222.8766	167.081	2.087	57.140	15.312	4.448	3.007	383.816	82.569
202	222.8766	167.335	2.403	57.510	16.147	5.486	3.023	380.866	78.567
203	222.8766	167.133	2.080	57.136	15.310	4.510	3.024	384.287	82.562
204	228.5562	163.373	3.505	56.397	18.442	5.305	9.183	370.590	75.412
205	228.5562	163.366	3.311	56.602	18.456	5.267	8.241	367.339	78.701
206	228.5562	163.690	3.850	57.062	18.908	7.410	10.382	367.731	76.850
207	228.5562	163.364	3.303	56.598	18.456	5.320	8.201	367.506	74.325
208	245.2556	167.628	3.154	57.402	14.304	6.881	5.522	386.999	87.251
209	247.9286	168.819	2.788	57.995	14.854	6.218	3.072	390.331	86.003
210	254.7139	167.789	2.976	57.145	15.147	5.229	6.013	386.525	86.118
211	254.7139	167.709	2.755	57.428	15.129	5.578	5.046	385.081	86.015
212	254.7139	168.050	3.262	57.866	15.166	5.510	6.773	388.322	83.437
213	254.7139	167.706	2.749	57.423	15.129	5.682	5.015	384.276	85.303
214	264.5698	170.622	2.053	58.418	14.180	3.695	2.578	394.853	88.331
215	264.5698	170.526	1.912	58.706	14.575	4.092	3.082	394.770	89.077
216	264.5698	171.135	2.230	59.082	15.322	4.648	3.028	394.151	84.226
217	264.5698	170.544	1.906	58.701	14.573	3.918	3.097	394.978	89.095
218	282.0876	173.463	2.441	59.404	14.654	4.961	2.755	402.513	89.453
219	287.8346	173.423	2.697	59.095	13.914	5.538	3.628	403.360	89.231
220	308.2038	174.666	2.777	59.275	14.256	4.801	4.620	404.568	90.907
221	333.6127	175.382	1.727	59.259	13.129	6.365	2.858	407.969	94.340
222	333.6127	175.032	1.611	59.559	13.505	7.495	3.292	408.293	95.511
223	333.6127	175.645	1.876	59.981	14.162	5.289	3.214	406.486	93.974
224	333.6127	175.029	1.607	59.554	13.503	7.299	3.301	410.349	92.459
225	333.8201	174.911	2.121	58.545	12.367	4.370	2.732	406.435	93.262
226	333.8201	174.848	1.971	58.862	12.735	5.651	3.292	407.474	94.418
227	333.8201	175.194	2.314	59.267	13.328	4.677	2.907	409.819	94.267
228	333.8201	174.846	1.966	58.857	12.734	5.443	3.306	405.890	95.127
229	357.0172	174.961	1.468	59.358	13.188	8.641	3.392	409.674	95.808
230	357.0172	175.484	1.702	59.812	13.874	6.572	3.322	406.483	93.148
231	357.0172	174.959	1.464	59.353	13.185	8.440	3.401	409.545	95.183
232	366.7880	174.685	2.379	58.439	13.084	4.190	3.081	405.948	95.980
233	383.2118	175.243	2.001	58.889	12.743	5.493	3.049	408.868	89.650
234	416.6143	175.154	1.492	58.295	11.989	9.194	3.020	404.621	95.437
235	416.6143	174.888	1.397	58.595	12.212	10.218	3.413	409.898	97.555

#	q	p_{max}	β_{max}	$\dot{\delta}_{ail(max)}$	$\delta_{ail(max)}$	$\dot{\delta}_{rud(max)}$	$\delta_{rud(max)}$	$\phi_{(2.8\,sec)}$	$\phi_{(1\,sec)}$
236	416.6143	175.296	1.603	59.066	12.863	7.997	3.319	407.838	94.502
237	416.6143	174.887	1.394	58.590	12.210	10.015	3.421	408.561	95.582
238	430.4664	174.798	2.047	57.923	12.701	6.749	3.154	405.991	96.026
239	436.0099	175.297	1.751	58.569	12.438	7.520	3.150	405.668	96.811
240	499.2391	174.719	1.668	56.557	12.262	10.584	3.221	407.657	97.536
241	499.2391	174.698	1.585	56.858	12.232	11.704	3.628	408.265	94.115
242	499.2391	174.908	1.791	57.427	12.512	8.944	3.282	402.610	97.542
243	499.2391	174.697	1.582	56.851	12.231	11.480	3.638	407.798	97.079
244	503.8640	175.031	1.373	57.335	11.934	11.392	3.118	406.967	98.217
245	503.8640	174.831	1.297	57.681	11.603	12.322	3.498	410.222	98.342
246	503.8640	175.152	1.459	58.214	12.191	9.970	3.381	405.188	93.078
247	503.8640	174.831	1.294	57.674	11.603	12.112	3.506	406.305	98.517
248	514.2514	174.454	1.878	56.075	13.038	10.668	3.414	407.486	97.852
249	514.2514	174.460	1.779	56.371	13.070	11.748	3.982	405.135	95.307
250	514.2514	174.566	1.995	56.801	13.245	8.998	3.327	407.264	89.363
251	514.2514	174.460	1.776	56.366	13.070	11.523	3.993	406.245	96.173
252	551.8250	174.815	1.181	57.397	11.480	13.450	3.644	408.860	97.215
253	551.8250	175.092	1.324	57.977	12.027	11.053	3.469	405.523	94.657
254	551.8250	174.815	1.179	57.390	11.479	13.239	3.650	409.680	99.569
255	573.1062	175.008	1.588	57.002	12.479	10.729	3.347	403.296	96.264
256	618.5337	174.974	1.270	56.333	11.974	13.548	3.252	408.120	99.976
257	618.5337	174.795	1.205	56.600	11.641	14.462	3.643	408.036	95.729
258	618.5337	175.063	1.330	57.199	12.182	11.988	3.454	406.132	98.023
259	618.5337	174.795	1.203	56.596	11.641	14.245	3.649	408.278	100.029
260	652.0676	175.077	1.432	56.638	12.517	11.898	3.367	404.776	97.260
261	699.9532	174.601	1.487	55.003	12.486	14.479	3.544	406.562	96.729
262	699.9532	174.609	1.430	55.406	12.499	15.370	3.929	408.287	96.013
263	699.9532	174.818	1.558	55.962	12.941	12.664	3.523	402.992	91.840
264	699.9532	174.608	1.428	55.399	12.499	15.149	3.938	405.022	95.581
265	771.1717	174.967	1.177	55.318	12.136	15.470	3.422	404.918	96.268
266	771.1717	174.773	1.118	55.679	11.737	16.250	3.841	409.590	96.219
267	771.1717	175.013	1.215	56.220	12.261	13.833	3.576	406.633	95.354
268	771.1717	174.772	1.117	55.673	11.738	16.030	3.848	409.095	96.336
269	825.2729	174.768	1.049	55.521	11.734	16.909	3.986	408.642	99.469
270	825.2729	174.994	1.137	56.071	12.237	14.521	3.677	404.875	96.888
271	825.2729	174.767	1.048	55.514	11.734	16.689	3.993	409.523	97.284
272	954.4603	174.954	1.099	54.648	12.884	17.071	3.643	406.550	98.649
273	954.4603	174.740	1.043	54.938	12.387	17.797	4.109	405.636	98.978
274	954.4603	174.971	1.118	55.578	12.934	15.309	3.768	404.527	98.395
275	954.4603	174.740	1.042	54.933	12.387	17.581	4.119	403.634	97.549
276	1106.2120	174.922	1.060	54.340	13.560	18.060	3.821	405.075	95.180
277	1106.2120	174.716	1.006	54.581	13.026	18.600	4.303	403.777	93.811
278	1106.2120	174.942	1.070	55.122	13.602	16.158	3.905	402.005	98.066
279	1106.2120	174.716	1.005	54.576	13.026	18.389	4.310	406.280	93.688
280	1157.0650	174.712	0.963	54.581	13.209	18.866	4.449	405.608	92.764
281	1157.0650	174.929	1.024	55.119	13.781	16.474	4.015	400.552	91.477
282	1157.0650	174.712	0.962	54.576	13.209	18.656	4.455	401.121	92.768

E.3 Lateral Unit β_{cmd} Step Input Time Response Data

#	q	p_{max}	β_{max}	$\dot{\delta}_{ail(max)}$	$\delta_{ail(max)}$	$\dot{\delta}_{rud(max)}$	$\delta_{rud(max)}$	$\phi_{(2.8\,sec)}$	$\phi_{(1\,sec)}$
1	63.6460	0.214	0.995	0.834	2.437	9.570	1.693	-3.822	-0.120
2	65.4696	0.247	0.925	0.479	1.290	9.566	2.003	-2.391	-0.035
3	65.4696	0.248	0.925	0.478	1.291	9.566	2.008	-2.367	-0.035
4	65.5666	0.237	0.923	0.472	1.294	9.564	2.062	-2.412	-0.045
5	67.0399	0.280	0.923	0.481	1.220	9.569	1.950	-2.370	-0.009
6	67.0399	0.281	0.923	0.480	1.220	9.569	1.955	-2.361	-0.009
7	67.4267	0.267	0.921	0.475	1.221	9.567	2.008	-2.360	-0.021
8	67.4267	0.268	0.920	0.474	1.221	9.567	2.013	-2.331	-0.021
9	67.6717	0.305	0.922	0.479	1.184	9.571	1.913	-2.306	0.008
10	67.6717	0.254	0.964	0.726	2.013	9.570	1.553	-3.442	-0.092
11	68.8746	0.231	0.913	0.447	1.179	9.560	2.158	-2.240	-0.061
12	68.8746	0.232	0.913	0.446	1.180	9.560	2.162	-2.261	-0.046
13	69.1382	0.202	0.914	0.563	1.711	9.556	2.561	-2.934	-0.134
14	69.7616	0.232	0.933	0.623	1.781	9.564	2.102	-3.086	-0.112
15	70.3335	0.224	0.927	0.600	1.738	9.562	2.231	-3.009	-0.123
16	70.9929	0.221	0.908	0.429	1.123	9.557	2.215	-2.155	-0.058
17	70.9929	0.208	0.916	0.559	1.672	9.557	2.448	-2.877	-0.139
18	71.3347	0.249	0.934	0.627	1.754	9.565	2.004	-3.131	-0.112
19	74.2746	0.245	0.932	0.516	1.384	9.557	1.466	-2.684	-0.097
20	74.2746	0.241	0.904	0.417	1.021	9.558	2.200	-2.027	-0.049
21	74.2746	0.222	0.915	0.544	1.582	9.558	2.326	-2.824	-0.109
22	74.2746	0.241	0.904	0.416	1.021	9.558	2.205	-2.034	-0.053
23	75.5664	0.212	0.901	0.402	1.014	9.553	2.253	-1.996	-0.075
24	77.0323	0.228	0.900	0.399	0.972	9.554	2.241	-1.939	-0.064
25	77.2143	0.382	0.900	0.428	0.920	9.567	2.163	-1.925	0.024
26	77.2914	0.424	0.900	0.424	0.874	9.569	2.127	-1.854	0.071
27	77.2914	0.354	0.930	0.626	1.599	9.568	1.781	-2.996	-0.035
28	77.2914	0.425	0.900	0.423	0.874	9.569	2.132	-1.873	0.054
29	80.2356	0.445	0.913	0.478	1.043	9.567	1.672	-2.216	0.017
30	80.2356	0.437	0.895	0.412	0.781	9.568	2.172	-1.736	0.063
31	80.2356	0.384	0.921	0.593	1.489	9.567	1.916	-2.857	-0.048
32	80.2356	0.438	0.895	0.410	0.781	9.567	2.178	-1.725	0.055
33	80.3692	0.274	0.921	0.512	1.296	9.557	1.608	-2.576	-0.112
34	80.3692	0.281	0.897	0.419	0.970	9.558	2.281	-1.948	-0.056
35	80.3692	0.246	0.910	0.535	1.494	9.558	2.282	-2.769	-0.142
36	80.3692	0.281	0.897	0.418	0.970	9.558	2.286	-1.959	-0.037
37	80.5349	0.399	0.915	0.492	1.113	9.565	1.658	-2.334	0.000
38	80.5349	0.397	0.895	0.416	0.830	9.566	2.203	-1.794	0.035
39	80.5349	0.349	0.917	0.573	1.478	9.566	2.018	-2.823	-0.042
40	80.5349	0.398	0.895	0.415	0.830	9.566	2.209	-1.785	0.036
41	81.4969	0.367	0.915	0.498	1.147	9.563	1.657	-2.401	-0.051
42	81.4969	0.366	0.895	0.417	0.855	9.564	2.234	-1.824	0.002
43	81.4969	0.323	0.913	0.552	1.454	9.564	2.113	-2.773	-0.056
44	81.4969	0.366	0.895	0.415	0.855	9.564	2.240	-1.823	0.001
45	82.2802	0.233	0.919	0.470	1.217	9.549	1.604	-2.405	-0.128
46	82.2802	0.240	0.895	0.369	0.880	9.550	2.293	-1.769	-0.054
47	82.2802	0.209	0.903	0.485	1.367	9.550	2.373	-2.538	-0.139

#	q	p_{max}	β_{max}	$\dot{\delta}_{ail(max)}$	$\delta_{ail(max)}$	$\dot{\delta}_{rud(max)}$	$\delta_{rud(max)}$	$\phi_{(2.8\ sec)}$	$\phi_{(1\ sec)}$
48	82.2802	0.241	0.895	0.369	0.881	9.550	2.298	-1.766	-0.062
49	83.3181	0.252	0.917	0.466	1.174	9.551	1.613	-2.289	-0.122
50	83.3181	0.259	0.895	0.367	0.845	9.552	2.288	-1.722	-0.061
51	83.3181	0.225	0.903	0.486	1.337	9.552	2.332	-2.510	-0.126
52	83.3181	0.260	0.894	0.367	0.845	9.551	2.292	-1.711	-0.060
53	83.4550	0.316	0.915	0.497	1.191	9.558	1.668	-2.418	-0.079
54	83.4550	0.320	0.894	0.410	0.886	9.559	2.283	-1.826	-0.019
55	83.4550	0.279	0.907	0.530	1.410	9.559	2.229	-2.671	-0.092
56	83.4550	0.320	0.894	0.408	0.886	9.559	2.288	-1.823	-0.020
57	83.7192	0.346	0.913	0.494	1.143	9.560	1.681	-2.364	-0.072
58	83.7192	0.347	0.893	0.408	0.844	9.561	2.269	-1.785	-0.008
59	83.7192	0.305	0.908	0.534	1.390	9.561	2.181	-2.679	-0.082
60	83.7192	0.347	0.893	0.407	0.844	9.561	2.274	-1.791	-0.006
61	87.3860	0.430	0.904	0.462	0.919	9.562	1.756	-2.041	-0.009
62	87.3860	0.425	0.888	0.390	0.674	9.563	2.268	-1.524	0.030
63	87.3860	0.383	0.903	0.515	1.194	9.563	2.097	-2.437	-0.054
64	87.3860	0.426	0.888	0.389	0.674	9.563	2.274	-1.525	0.029
65	88.7159	0.473	0.886	0.393	0.575	9.565	2.191	-1.399	0.059
66	88.7159	0.474	0.886	0.391	0.575	9.565	2.197	-1.388	0.063
67	89.2543	0.360	0.901	0.506	1.174	9.560	2.148	-2.379	-0.077
68	89.3983	0.476	0.899	0.452	0.806	9.563	1.787	-1.855	0.008
69	89.3983	0.463	0.886	0.389	0.605	9.564	2.275	-1.425	0.043
70	89.3983	0.426	0.900	0.502	1.064	9.563	2.069	-2.275	-0.036
71	89.3983	0.464	0.886	0.388	0.605	9.564	2.281	-1.412	0.057
72	91.6970	0.311	0.907	0.419	0.953	9.550	1.733	-1.973	-0.089
73	91.6970	0.316	0.889	0.339	0.690	9.551	2.334	-1.454	-0.022
74	91.6970	0.280	0.898	0.448	1.113	9.551	2.263	-2.187	-0.101
75	91.6970	0.317	0.889	0.338	0.690	9.551	2.339	-1.445	-0.022
76	94.3473	0.477	0.898	0.474	0.768	9.561	1.671	-1.835	-0.007
77	94.3473	0.461	0.885	0.388	0.537	9.562	2.208	-1.311	0.042
78	94.3473	0.462	0.885	0.387	0.537	9.562	2.214	-1.303	0.036
79	101.0962	0.468	0.887	0.390	0.495	9.557	2.086	-1.212	0.032
80	102.4478	0.365	0.899	0.420	0.873	9.548	1.888	-1.813	-0.094
81	102.4478	0.357	0.885	0.356	0.672	9.549	2.403	-1.390	-0.039
82	102.4478	0.335	0.895	0.447	0.995	9.549	2.194	-1.991	-0.104
83	102.4478	0.358	0.885	0.356	0.672	9.549	2.408	-1.394	-0.041
84	103.1193	0.437	0.893	0.464	0.774	9.556	1.975	-1.776	-0.036
85	103.7392	0.468	0.887	0.391	0.484	9.556	2.071	-1.180	0.027
86	106.1299	0.470	0.897	0.467	0.691	9.555	1.695	-1.621	-0.035
87	106.1299	0.452	0.885	0.389	0.503	9.556	2.228	-1.180	0.010
88	106.1299	0.436	0.892	0.461	0.751	9.555	1.974	-1.727	-0.042
89	106.1299	0.452	0.884	0.388	0.502	9.556	2.234	-1.184	0.010
90	106.4162	0.467	0.888	0.393	0.477	9.554	2.050	-1.152	0.018
91	109.0025	0.392	0.896	0.416	0.792	9.548	1.941	-1.659	-0.090
92	109.0025	0.380	0.883	0.357	0.615	9.549	2.432	-1.295	-0.047
93	109.0025	0.363	0.892	0.437	0.889	9.548	2.178	-1.829	-0.092
94	109.0025	0.381	0.883	0.357	0.615	9.548	2.437	-1.290	-0.047

#	q	p_{max}	β_{max}	$\dot{\delta}_{ail(max)}$	$\delta_{ail(max)}$	$\dot{\delta}_{rud(max)}$	$\delta_{rud(max)}$	$\phi_{(2.8\ sec)}$	$\phi_{(1\ sec)}$
95	109.1273	0.491	0.898	0.456	0.606	9.552	1.571	-1.463	-0.027
96	109.1273	0.464	0.888	0.398	0.475	9.553	2.024	-1.134	0.009
97	109.1273	0.465	0.888	0.397	0.475	9.553	2.029	-1.133	0.014
98	110.1905	0.426	0.895	0.431	0.730	9.551	1.930	-1.592	-0.069
99	110.1905	0.408	0.882	0.367	0.557	9.552	2.444	-1.209	-0.036
100	110.1905	0.398	0.890	0.440	0.798	9.552	2.182	-1.696	-0.072
101	110.1905	0.409	0.882	0.366	0.557	9.552	2.450	-1.211	-0.037
102	110.9265	0.350	0.897	0.377	0.810	9.540	1.990	-1.642	-0.108
103	110.9265	0.342	0.884	0.324	0.633	9.541	2.465	-1.271	-0.052
104	110.9265	0.322	0.893	0.403	0.915	9.541	2.224	-1.798	-0.111
105	110.9265	0.343	0.883	0.323	0.633	9.541	2.470	-1.269	-0.051
106	111.8726	0.469	0.897	0.469	0.632	9.551	1.625	-1.490	-0.055
107	111.8726	0.441	0.888	0.422	0.530	9.552	2.048	-1.223	-0.036
108	111.8726	0.442	0.888	0.422	0.530	9.552	2.054	-1.225	-0.042
109	114.6519	0.446	0.896	0.485	0.666	9.550	1.675	-1.528	-0.085
110	114.6519	0.417	0.888	0.446	0.583	9.551	2.073	-1.312	-0.072
111	114.6519	0.418	0.888	0.445	0.583	9.550	2.079	-1.310	-0.063
112	117.4653	0.425	0.896	0.504	0.705	9.549	1.723	-1.587	-0.117
113	117.4653	0.397	0.888	0.469	0.634	9.549	2.097	-1.394	-0.104
114	117.4653	0.398	0.888	0.468	0.634	9.549	2.103	-1.394	-0.104
115	120.3129	0.404	0.895	0.524	0.748	9.547	1.766	-1.643	-0.152
116	120.3129	0.376	0.887	0.491	0.680	9.548	2.120	-1.465	-0.138
117	120.3129	0.370	0.892	0.566	0.958	9.548	1.978	-2.076	-0.175
118	120.3129	0.377	0.887	0.490	0.680	9.547	2.126	-1.462	-0.141
119	121.8328	0.478	0.896	0.425	0.508	9.546	1.714	-1.171	-0.049
120	121.8328	0.450	0.887	0.399	0.456	9.548	2.134	-1.028	-0.048
121	121.8328	0.439	0.892	0.449	0.657	9.547	1.935	-1.482	-0.090
122	121.8328	0.450	0.887	0.398	0.456	9.547	2.140	-1.027	-0.053
123	123.1945	0.382	0.895	0.546	0.794	9.546	1.806	-1.720	-0.189
124	123.1945	0.363	0.887	0.507	0.715	9.546	2.126	-1.521	-0.172
125	123.1945	0.351	0.891	0.585	0.996	9.546	2.014	-2.140	-0.227
126	123.1945	0.364	0.887	0.506	0.716	9.546	2.131	-1.523	-0.168
127	126.1103	0.365	0.894	0.569	0.842	9.544	1.823	-1.797	-0.226
128	126.1103	0.352	0.887	0.521	0.746	9.545	2.129	-1.564	-0.185
129	126.1103	0.334	0.891	0.603	1.031	9.545	2.050	-2.181	-0.239
130	126.1103	0.353	0.887	0.520	0.746	9.544	2.135	-1.564	-0.200
131	129.0601	0.355	0.894	0.594	0.897	9.543	1.833	-1.894	-0.263
132	129.0601	0.345	0.887	0.533	0.772	9.543	2.131	-1.606	-0.220
133	129.0601	0.318	0.890	0.619	1.060	9.543	2.079	-2.220	-0.275
134	129.0601	0.346	0.887	0.532	0.772	9.542	2.136	-1.608	-0.218
135	129.4213	0.377	0.891	0.334	0.642	9.531	2.137	-1.289	-0.105
136	129.4213	0.369	0.882	0.299	0.513	9.532	2.483	-1.023	-0.059
137	129.4213	0.347	0.891	0.367	0.773	9.531	2.176	-1.515	-0.127
138	129.4213	0.370	0.881	0.300	0.513	9.532	2.487	-1.024	-0.060
139	129.8252	0.414	0.891	0.368	0.603	9.537	2.074	-1.253	-0.081
140	129.8252	0.403	0.881	0.327	0.474	9.539	2.467	-0.983	-0.051
141	129.8252	0.382	0.890	0.385	0.689	9.538	2.158	-1.412	-0.103

#	$\bar{q}$	p_{max}	β_{max}	$\dot{\delta}_{ail(max)}$	$\delta_{ail(max)}$	$\dot{\delta}_{rud(max)}$	$\delta_{rud(max)}$	$\phi_{(2.8\,sec)}$	$\phi_{(1\,sec)}$
142	129.8252	0.404	0.881	0.327	0.474	9.538	2.471	-0.984	-0.053
143	129.9582	0.453	0.892	0.416	0.582	9.543	1.974	-1.250	-0.091
144	129.9582	0.438	0.880	0.363	0.443	9.544	2.456	-0.953	-0.051
145	129.9582	0.421	0.887	0.391	0.573	9.543	2.189	-1.234	-0.077
146	129.9582	0.439	0.880	0.363	0.443	9.544	2.461	-0.953	-0.053
147	130.0074	0.440	0.892	0.398	0.586	9.541	2.012	-1.251	-0.077
148	130.0074	0.427	0.881	0.350	0.452	9.542	2.457	-0.961	-0.050
149	130.0074	0.408	0.888	0.390	0.615	9.542	2.173	-1.308	-0.086
150	130.0074	0.428	0.881	0.350	0.452	9.542	2.463	-0.962	-0.051
151	130.0653	0.464	0.893	0.435	0.579	9.544	1.918	-1.262	-0.095
152	130.0653	0.448	0.881	0.376	0.434	9.545	2.432	-0.940	-0.052
153	130.0653	0.433	0.887	0.395	0.540	9.544	2.186	-1.188	-0.071
154	130.0653	0.449	0.881	0.375	0.434	9.545	2.438	-0.940	-0.054
155	130.1006	0.428	0.891	0.383	0.592	9.539	2.043	-1.250	-0.085
156	130.1006	0.416	0.881	0.339	0.463	9.540	2.459	-0.972	-0.051
157	130.1006	0.396	0.889	0.388	0.653	9.540	2.160	-1.361	-0.096
158	130.1006	0.416	0.881	0.338	0.462	9.540	2.463	-0.973	-0.053
159	131.7744	0.477	0.895	0.404	0.420	9.541	1.730	-0.956	-0.077
160	131.7744	0.443	0.888	0.415	0.467	9.542	2.071	-1.022	-0.084
161	131.7744	0.437	0.893	0.453	0.626	9.541	1.898	-1.379	-0.106
162	131.7744	0.444	0.888	0.415	0.467	9.541	2.077	-1.020	-0.080
163	132.0441	0.346	0.894	0.619	0.950	9.541	1.842	-1.979	-0.283
164	132.0441	0.340	0.887	0.544	0.792	9.541	2.130	-1.622	-0.237
165	132.0441	0.302	0.890	0.632	1.080	9.541	2.094	-2.236	-0.298
166	132.0441	0.341	0.887	0.544	0.792	9.541	2.135	-1.626	-0.235
167	134.8266	0.476	0.894	0.416	0.465	9.541	1.821	-1.035	-0.085
168	134.8266	0.449	0.885	0.393	0.426	9.542	2.240	-0.928	-0.080
169	134.8266	0.441	0.890	0.414	0.541	9.541	2.027	-1.194	-0.084
170	134.8266	0.450	0.884	0.392	0.426	9.542	2.246	-0.925	-0.061
171	135.0621	0.340	0.894	0.643	0.999	9.539	1.847	-2.060	-0.335
172	135.0621	0.338	0.887	0.554	0.807	9.539	2.127	-1.655	-0.253
173	135.0621	0.294	0.889	0.647	1.113	9.540	2.107	-2.282	-0.318
174	135.0621	0.339	0.887	0.553	0.807	9.539	2.132	-1.659	-0.254
175	137.9562	0.410	0.889	0.373	0.572	9.536	2.144	-1.196	-0.077
176	138.1142	0.336	0.894	0.667	1.046	9.537	1.851	-2.145	-0.309
177	138.1142	0.338	0.888	0.561	0.815	9.537	2.120	-1.667	-0.256
178	138.1142	0.288	0.889	0.660	1.140	9.538	2.119	-2.324	-0.359
179	138.1142	0.339	0.887	0.560	0.815	9.537	2.126	-1.657	-0.266
180	158.6743	0.269	0.846	0.234	0.349	4.772	2.054	-0.692	-0.018
181	163.0169	0.248	0.851	0.218	0.412	4.769	1.989	-0.772	-0.033
182	167.7286	0.231	0.865	0.440	0.813	4.767	1.720	-1.513	-0.173
183	167.7286	0.228	0.851	0.372	0.639	4.767	1.942	-1.174	-0.148
184	167.7286	0.205	0.854	0.456	0.906	4.766	1.930	-1.658	-0.204
185	167.7286	0.229	0.851	0.372	0.639	4.767	1.946	-1.179	-0.138
186	170.3164	0.273	0.852	0.231	0.374	4.769	1.954	-0.715	-0.048
187	170.3164	0.261	0.831	0.210	0.308	4.770	2.284	-0.584	-0.025
188	170.3164	0.262	0.849	0.221	0.352	4.769	1.999	-0.684	-0.032

#	$\bar{q}$	p_{max}	β_{max}	$\dot{\delta}_{ail(max)}$	$\delta_{ail(max)}$	$\dot{\delta}_{rud(max)}$	$\delta_{rud(max)}$	$\phi_{(2.8\ sec)}$	$\phi_{(1\ sec)}$
189	170.3164	0.261	0.830	0.210	0.307	4.770	2.289	-0.581	-0.028
190	186.2219	0.266	0.851	0.241	0.347	4.766	1.948	-0.681	-0.058
191	206.0828	0.271	0.850	0.226	0.268	4.764	1.958	-0.526	-0.049
192	206.3182	0.267	0.852	0.222	0.263	4.763	1.934	-0.514	-0.039
193	208.2658	0.265	0.867	0.408	0.705	4.760	1.666	-1.302	-0.202
194	208.2658	0.263	0.852	0.336	0.521	4.760	1.906	-0.952	-0.141
195	208.2658	0.233	0.857	0.420	0.795	4.759	1.855	-1.437	-0.239
196	208.2658	0.264	0.852	0.336	0.521	4.760	1.911	-0.954	-0.141
197	215.9733	0.278	0.862	0.246	0.306	4.761	1.738	-0.599	-0.076
198	215.9733	0.262	0.844	0.253	0.331	4.761	2.044	-0.623	-0.093
199	215.9733	0.260	0.856	0.262	0.382	4.760	1.861	-0.730	-0.102
200	215.9733	0.262	0.844	0.253	0.331	4.761	2.048	-0.623	-0.086
201	222.8766	0.280	0.849	0.338	0.489	4.758	1.945	-0.889	-0.144
202	222.8766	0.243	0.854	0.435	0.813	4.757	1.883	-1.457	-0.257
203	222.8766	0.281	0.849	0.338	0.488	4.758	1.949	-0.890	-0.142
204	228.5562	0.281	0.843	0.248	0.152	4.758	2.068	-0.304	-0.013
205	228.5562	0.266	0.832	0.233	0.182	4.759	2.248	-0.346	-0.028
206	228.5562	0.268	0.854	0.231	0.213	4.759	1.893	-0.419	-0.024
207	228.5562	0.266	0.832	0.234	0.182	4.759	2.252	-0.344	-0.028
208	245.2556	0.275	0.851	0.242	0.233	4.757	1.928	-0.455	-0.066
209	247.9286	0.260	0.861	0.306	0.465	4.754	1.767	-0.873	-0.135
210	254.7139	0.290	0.849	0.263	0.209	4.755	1.968	-0.405	-0.046
211	254.7139	0.275	0.831	0.247	0.206	4.756	2.252	-0.386	-0.053
212	254.7139	0.278	0.853	0.246	0.201	4.755	1.902	-0.397	-0.043
213	254.7139	0.275	0.831	0.248	0.206	4.756	2.257	-0.385	-0.051
214	264.5698	0.295	0.867	0.417	0.648	4.750	1.642	-1.180	-0.232
215	264.5698	0.295	0.852	0.327	0.416	4.751	1.892	-0.760	-0.128
216	264.5698	0.262	0.858	0.415	0.723	4.750	1.808	-1.302	-0.236
217	264.5698	0.296	0.852	0.327	0.416	4.750	1.897	-0.759	-0.145
218	282.0876	0.266	0.865	0.370	0.593	4.746	1.691	-1.083	-0.217
219	287.8346	0.278	0.856	0.261	0.290	4.749	1.845	-0.552	-0.099
220	308.2038	0.287	0.853	0.268	0.206	4.747	1.898	-0.398	-0.062
221	333.6127	0.323	0.867	0.456	0.606	4.737	1.626	-1.097	-0.237
222	333.6127	0.323	0.852	0.350	0.334	4.739	1.884	-0.606	-0.123
223	333.6127	0.290	0.859	0.437	0.664	4.739	1.783	-1.190	-0.234
224	333.6127	0.324	0.852	0.351	0.334	4.739	1.888	-0.607	-0.122
225	333.8201	0.308	0.864	0.303	0.256	4.740	1.687	-0.486	-0.089
226	333.8201	0.292	0.848	0.291	0.254	4.742	1.961	-0.467	-0.085
227	333.8201	0.284	0.860	0.319	0.373	4.741	1.765	-0.689	-0.127
228	333.8201	0.293	0.848	0.292	0.254	4.741	1.965	-0.465	-0.086
229	357.0172	0.342	0.849	0.365	0.302	4.735	1.940	-0.543	-0.115
230	357.0172	0.304	0.856	0.456	0.654	4.735	1.823	-1.162	-0.253
231	357.0172	0.343	0.848	0.366	0.302	4.735	1.945	-0.545	-0.114
232	366.7880	0.297	0.855	0.291	0.208	4.738	1.851	-0.394	-0.070
233	383.2118	0.290	0.863	0.394	0.482	4.731	1.703	-0.872	-0.189
234	416.6143	0.345	0.867	0.513	0.569	4.721	1.616	-1.022	-0.222
235	416.6143	0.346	0.851	0.390	0.264	4.724	1.894	-0.474	-0.095

E-18

#	q	p_{max}	β_{max}	$\dot{\delta}_{ail(max)}$	$\delta_{ail(max)}$	$\dot{\delta}_{rud(max)}$	$\delta_{rud(max)}$	$\phi_{(2.8\ sec)}$	$\phi_{(1\ sec)}$
236	416.6143	0.311	0.859	0.484	0.622	4.725	1.775	-1.099	-0.246
237	416.6143	0.347	0.851	0.392	0.264	4.724	1.898	-0.476	-0.094
238	430.4664	0.301	0.859	0.342	0.283	4.727	1.779	-0.523	-0.104
239	436.0099	0.298	0.865	0.481	0.604	4.720	1.664	-1.082	-0.239
240	499.2391	0.339	0.864	0.400	0.188	4.709	1.669	-0.349	-0.058
241	499.2391	0.326	0.849	0.380	0.176	4.713	1.934	-0.319	-0.058
242	499.2391	0.306	0.862	0.427	0.380	4.714	1.723	-0.685	-0.136
243	499.2391	0.327	0.849	0.382	0.176	4.712	1.938	-0.317	-0.058
244	503.8640	0.364	0.868	0.558	0.495	4.704	1.598	-0.884	-0.198
245	503.8640	0.362	0.852	0.436	0.215	4.709	1.886	-0.386	-0.077
246	503.8640	0.324	0.859	0.536	0.597	4.710	1.760	-1.056	-0.223
247	503.8640	0.363	0.851	0.438	0.215	4.708	1.891	-0.386	-0.076
248	514.2514	0.349	0.856	0.370	0.070	4.707	1.820	-0.143	-0.011
249	514.2514	0.334	0.835	0.353	0.092	4.712	2.164	-0.172	-0.019
250	514.2514	0.322	0.857	0.359	0.192	4.713	1.807	-0.359	-0.056
251	514.2514	0.334	0.835	0.355	0.092	4.711	2.169	-0.171	-0.019
252	551.8250	0.383	0.846	0.468	0.181	4.700	1.984	-0.321	-0.058
253	551.8250	0.345	0.856	0.573	0.575	4.703	1.814	-1.000	-0.228
254	551.8250	0.384	0.845	0.470	0.181	4.699	1.989	-0.321	-0.057
255	573.1062	0.312	0.863	0.523	0.496	4.700	1.684	-0.880	-0.199
256	618.5337	0.376	0.868	0.630	0.462	4.680	1.593	-0.817	-0.184
257	618.5337	0.375	0.850	0.495	0.170	4.687	1.909	-0.302	-0.059
258	618.5337	0.337	0.859	0.603	0.571	4.690	1.753	-0.995	-0.233
259	618.5337	0.376	0.850	0.497	0.170	4.686	1.914	-0.302	-0.059
260	652.0676	0.321	0.864	0.619	0.591	4.682	1.659	-1.038	-0.244
261	699.9532	0.382	0.863	0.495	0.073	4.664	1.694	-0.141	-0.018
262	699.9532	0.363	0.847	0.483	0.094	4.672	1.969	-0.171	-0.027
263	699.9532	0.332	0.861	0.549	0.382	4.678	1.717	-0.677	-0.147
264	699.9532	0.364	0.846	0.485	0.094	4.671	1.974	-0.172	-0.027
265	771.1717	0.382	0.866	0.738	0.493	4.651	1.616	-0.860	-0.202
266	771.1717	0.385	0.845	0.568	0.136	4.660	1.978	-0.239	-0.049
267	771.1717	0.348	0.857	0.691	0.557	4.665	1.785	-0.964	-0.232
268	771.1717	0.386	0.845	0.571	0.136	4.659	1.983	-0.241	-0.048
269	825.2729	0.395	0.839	0.592	0.112	4.654	2.080	-0.198	-0.038
270	825.2729	0.358	0.853	0.720	0.546	4.658	1.849	-0.940	-0.225
271	825.2729	0.396	0.839	0.595	0.112	4.653	2.085	-0.197	-0.038
272	954.4603	0.384	0.864	0.825	0.552	4.627	1.652	-0.949	-0.220
273	954.4603	0.389	0.840	0.617	0.099	4.637	2.069	-0.173	-0.028
274	954.4603	0.352	0.853	0.756	0.563	4.642	1.839	-0.952	-0.228
275	954.4603	0.390	0.839	0.620	0.099	4.636	2.075	-0.173	-0.028
276	1106.2120	0.381	0.862	0.863	0.565	4.611	1.677	-0.966	-0.224
277	1106.2120	0.387	0.836	0.640	0.077	4.621	2.124	-0.134	-0.015
278	1106.2120	0.350	0.850	0.793	0.576	4.627	1.874	-0.977	-0.224
279	1106.2120	0.388	0.835	0.644	0.077	4.620	2.130	-0.133	-0.014
280	1157.0650	0.390	0.830	0.641	0.060	4.620	2.218	-0.105	-0.007
281	1157.0650	0.352	0.846	0.800	0.576	4.625	1.938	-0.960	-0.219
282	1157.0650	0.391	0.829	0.644	0.061	4.619	2.224	-0.105	-0.007

E.4   Lateral Maximum β_{cmd} Step Input Time Response Data

#	q	p_{max}	β_{max}	$\dot{\delta}_{ail(max)}$	$\delta_{ail(max)}$	$\dot{\delta}_{rud(max)}$	$\delta_{rud(max)}$	$\phi_{(5\ sec)}$
1	63.6460	1.293	5.968	5.005	14.625	57.265	10.161	-48.251
2	65.4696	1.486	5.550	2.875	7.740	57.237	12.020	-26.169
3	65.4696	1.491	5.549	2.869	7.744	57.235	12.049	-26.184
4	65.5666	1.422	5.539	2.834	7.765	57.221	12.374	-26.345
5	67.0399	1.685	5.536	2.884	7.320	57.262	11.698	-24.499
6	67.0399	1.690	5.535	2.878	7.322	57.260	11.729	-24.508
7	67.4267	1.604	5.523	2.852	7.325	57.247	12.046	-24.569
8	67.4267	1.608	5.522	2.847	7.328	57.245	12.076	-24.578
9	67.6717	1.829	5.532	2.876	7.106	57.272	11.481	-23.679
10	67.6717	1.520	5.782	4.359	12.080	57.267	9.319	-39.287
11	68.8746	1.388	5.479	2.679	7.076	57.193	12.946	-23.961
12	68.8746	1.393	5.478	2.675	7.080	57.191	12.974	-23.976
13	69.1382	1.211	5.486	3.377	10.267	57.158	15.364	-34.392
14	69.7616	1.398	5.599	3.736	10.686	57.222	12.614	-35.049
15	70.3335	1.350	5.561	3.593	10.427	57.204	13.384	-34.315
16	70.9929	1.324	5.448	2.575	6.736	57.167	13.290	-22.807
17	70.9929	1.249	5.497	3.356	10.034	57.167	14.686	-33.306
18	71.3347	1.494	5.603	3.762	10.524	57.232	12.023	-34.228
19	74.2746	1.476	5.593	3.095	8.302	57.167	8.798	-27.728
20	74.2746	1.443	5.423	2.504	6.123	57.175	13.201	-20.558
21	74.2746	1.332	5.492	3.260	9.492	57.174	13.955	-31.139
22	74.2746	1.448	5.423	2.498	6.127	57.173	13.230	-20.569
23	75.5664	1.280	5.409	2.412	6.087	57.134	13.521	-20.497
24	77.0323	1.368	5.401	2.391	5.831	57.144	13.447	-19.543
25	77.2143	2.293	5.402	2.570	5.522	57.244	12.978	-18.105
26	77.2914	2.547	5.400	2.543	5.242	57.257	12.759	-17.189
27	77.2914	2.127	5.579	3.757	9.595	57.252	10.687	-30.458
28	77.2914	2.550	5.400	2.535	5.241	57.256	12.795	-17.185
29	80.2356	2.665	5.475	2.867	6.260	57.239	10.030	-20.253
30	80.2356	2.623	5.368	2.469	4.689	57.248	13.032	-15.378
31	80.2356	2.306	5.524	3.559	8.934	57.244	11.498	-28.206
32	80.2356	2.626	5.368	2.461	4.688	57.246	13.067	-15.373
33	80.3692	1.649	5.524	3.071	7.777	57.168	9.646	-25.326
34	80.3692	1.684	5.383	2.512	5.822	57.176	13.686	-19.019
35	80.3692	1.479	5.457	3.208	8.967	57.174	13.694	-28.764
36	80.3692	1.688	5.382	2.506	5.823	57.174	13.715	-19.022
37	80.5349	2.401	5.487	2.949	6.680	57.226	9.949	-21.628
38	80.5349	2.383	5.371	2.496	4.980	57.235	13.218	-16.272
39	80.5349	2.095	5.503	3.438	8.867	57.231	12.107	-28.079
40	80.5349	2.386	5.371	2.489	4.980	57.233	13.251	-16.268
41	81.4969	2.205	5.488	2.986	6.883	57.211	9.943	-22.246
42	81.4969	2.195	5.369	2.501	5.131	57.219	13.406	-16.707
43	81.4969	1.939	5.478	3.311	8.724	57.216	12.678	-27.653
44	81.4969	2.198	5.368	2.494	5.131	57.218	13.438	-16.706
45	82.2802	1.399	5.511	2.815	7.299	57.104	9.625	-24.148
46	82.2802	1.441	5.372	2.215	5.282	57.112	13.759	-17.591
47	82.2802	1.249	5.417	2.909	8.202	57.112	14.236	-26.693

#	q	p_{max}	β_{max}	$\dot{\delta}_{ail(max)}$	$\delta_{ail(max)}$	$\dot{\delta}_{rud(max)}$	$\delta_{rud(max)}$	$\phi_{(5\,sec)}$
48	82.2802	1.446	5.372	2.210	5.284	57.110	13.786	-17.597
49	83.3181	1.513	5.502	2.796	7.045	57.118	9.677	-23.211
50	83.3181	1.553	5.368	2.204	5.069	57.126	13.725	-16.836
51	83.3181	1.351	5.419	2.919	8.021	57.126	13.992	-25.986
52	83.3181	1.558	5.367	2.200	5.070	57.124	13.753	-16.842
53	83.4550	1.898	5.488	2.984	7.143	57.174	10.006	-23.055
54	83.4550	1.918	5.365	2.457	5.315	57.183	13.697	-17.247
55	83.4550	1.681	5.443	3.180	8.458	57.180	13.377	-26.880
56	83.4550	1.923	5.364	2.451	5.315	57.181	13.727	-17.247
57	83.7192	2.076	5.477	2.965	6.861	57.190	10.084	-22.097
58	83.7192	2.082	5.359	2.451	5.064	57.198	13.612	-16.431
59	83.7192	1.832	5.448	3.204	8.341	57.195	13.083	-26.423
60	83.7192	2.086	5.359	2.445	5.064	57.196	13.643	-16.431
61	87.3860	2.588	5.422	2.773	5.511	57.204	10.533	-17.683
62	87.3860	2.550	5.329	2.341	4.043	57.214	13.610	-13.133
63	87.3860	2.300	5.420	3.091	7.163	57.210	12.582	-22.541
64	87.3860	2.553	5.329	2.334	4.042	57.212	13.644	-13.129
65	88.7159	2.835	5.318	2.356	3.448	57.225	13.144	-11.195
66	88.7159	2.837	5.318	2.348	3.447	57.223	13.180	-11.191
67	89.2543	2.159	5.406	3.038	7.045	57.191	12.888	-22.145
68	89.3983	2.862	5.394	2.710	4.838	57.210	10.724	-15.494
69	89.3983	2.775	5.315	2.335	3.631	57.219	13.648	-11.772
70	89.3983	2.564	5.398	3.011	6.383	57.214	12.413	-20.054
71	89.3983	2.777	5.314	2.329	3.630	57.217	13.683	-11.768
72	91.6970	1.869	5.442	2.515	5.721	57.111	10.400	-18.631
73	91.6970	1.896	5.335	2.031	4.142	57.119	14.007	-13.626
74	91.6970	1.682	5.389	2.691	6.677	57.118	13.578	-21.371
75	91.6970	1.900	5.335	2.026	4.142	57.117	14.034	-13.626
76	94.3473	2.873	5.389	2.846	4.605	57.197	10.026	-14.458
77	94.3473	2.765	5.311	2.331	3.222	57.202	13.248	-10.328
78	94.3473	2.769	5.311	2.323	3.222	57.200	13.283	-10.325
79	101.0962	2.815	5.321	2.339	2.968	57.165	12.514	-9.316
80	102.4478	2.195	5.397	2.521	5.239	57.098	11.327	-16.468
81	102.4478	2.140	5.312	2.139	4.031	57.107	14.420	-12.736
82	102.4478	2.015	5.367	2.682	5.971	57.103	13.162	-18.583
83	102.4478	2.144	5.312	2.134	4.030	57.104	14.449	-12.734
84	103.1193	2.616	5.355	2.787	4.641	57.159	11.852	-14.316
85	103.7392	2.817	5.323	2.342	2.907	57.153	12.425	-9.070
86	106.1299	2.812	5.380	2.799	4.148	57.162	10.168	-12.731
87	106.1299	2.711	5.308	2.334	3.015	57.154	13.371	-9.404
88	106.1299	2.609	5.353	2.763	4.508	57.147	11.842	-13.842
89	106.1299	2.715	5.307	2.329	3.015	57.152	13.404	-9.402
90	106.4162	2.805	5.326	2.358	2.860	57.142	12.299	-8.866
91	109.0025	2.360	5.377	2.500	4.749	57.099	11.645	-14.754
92	109.0025	2.277	5.300	2.145	3.690	57.101	14.590	-11.535
93	109.0025	2.185	5.354	2.624	5.335	57.097	13.068	-16.453
94	109.0025	2.281	5.299	2.142	3.689	57.099	14.620	-11.532

#	q	p_{max}	β_{max}	$\dot{\delta}_{ail(max)}$	$\delta_{ail(max)}$	$\dot{\delta}_{rud(max)}$	$\delta_{rud(max)}$	$\phi_{(5\ sec)}$
95	109.1273	2.940	5.387	2.729	3.634	57.145	9.428	-11.103
96	109.1273	2.781	5.330	2.386	2.847	57.134	12.141	-8.767
97	109.1273	2.785	5.329	2.382	2.848	57.133	12.175	-8.769
98	110.1905	2.558	5.367	2.586	4.379	57.134	11.578	-13.521
99	110.1905	2.442	5.290	2.201	3.340	57.125	14.665	-10.423
100	110.1905	2.395	5.341	2.637	4.788	57.121	13.095	-14.730
101	110.1905	2.446	5.290	2.198	3.339	57.123	14.697	-10.420
102	110.9265	2.100	5.380	2.261	4.859	57.032	11.939	-15.286
103	110.9265	2.058	5.302	1.941	3.800	57.042	14.790	-11.987
104	110.9265	1.934	5.356	2.415	5.488	57.038	13.342	-17.103
105	110.9265	2.063	5.301	1.936	3.800	57.039	14.817	-11.985
106	111.8726	2.812	5.382	2.812	3.791	57.134	9.749	-11.446
107	111.8726	2.640	5.329	2.534	3.179	57.122	12.290	-9.604
108	111.8726	2.645	5.328	2.528	3.181	57.121	12.325	-9.606
109	114.6519	2.683	5.378	2.910	3.994	57.121	10.052	-11.917
110	114.6519	2.512	5.328	2.679	3.500	57.112	12.439	-10.407
111	114.6519	2.517	5.327	2.674	3.501	57.110	12.473	-10.409
112	117.4653	2.548	5.374	3.024	4.230	57.108	10.335	-12.482
113	117.4653	2.381	5.326	2.816	3.802	57.102	12.583	-11.160
114	117.4653	2.386	5.325	2.813	3.803	57.100	12.617	-11.162
115	120.3129	2.416	5.371	3.146	4.489	57.094	10.598	-13.108
116	120.3129	2.252	5.324	2.949	4.081	57.091	12.720	-11.848
117	120.3129	2.220	5.352	3.398	5.750	57.090	11.866	-16.696
118	120.3129	2.259	5.324	2.944	4.082	57.088	12.754	-11.850
119	121.8328	2.877	5.374	2.550	3.045	57.120	10.286	-9.291
120	121.8328	2.705	5.320	2.389	2.735	57.110	12.804	-8.307
121	121.8328	2.643	5.351	2.695	3.941	57.096	11.613	-11.852
122	121.8328	2.710	5.319	2.388	2.736	57.109	12.838	-8.308
123	123.1945	2.296	5.367	3.278	4.761	57.078	10.838	-13.771
124	123.1945	2.179	5.324	3.039	4.293	57.079	12.757	-12.371
125	123.1945	2.113	5.348	3.512	5.979	57.079	12.087	-17.230
126	123.1945	2.187	5.324	3.037	4.293	57.076	12.789	-12.371
127	126.1103	2.194	5.366	3.410	5.053	57.063	10.941	-14.499
128	126.1103	2.120	5.324	3.122	4.475	57.066	12.776	-12.815
129	126.1103	2.004	5.344	3.621	6.187	57.067	12.299	-17.708
130	126.1103	2.128	5.324	3.118	4.475	57.063	12.808	-12.814
131	129.0601	2.122	5.366	3.562	5.382	57.050	11.001	-15.333
132	129.0601	2.072	5.324	3.199	4.630	57.052	12.785	-13.181
133	129.0601	1.902	5.340	3.717	6.360	57.055	12.473	-18.096
134	129.0601	2.080	5.324	3.195	4.630	57.050	12.816	-13.181
135	129.4213	2.255	5.344	2.004	3.855	56.997	12.819	-11.994
136	129.4213	2.216	5.289	1.794	3.078	56.990	14.896	-9.601
137	129.4213	2.078	5.345	2.201	4.638	56.973	13.055	-14.230
138	129.4213	2.220	5.288	1.800	3.077	56.989	14.923	-9.599
139	129.8252	2.483	5.346	2.213	3.616	57.056	12.447	-11.134
140	129.8252	2.425	5.286	1.964	2.845	57.049	14.799	-8.819
141	129.8252	2.291	5.339	2.310	4.136	57.031	12.948	-12.633

#	q	p_{max}	β_{max}	$\dot{\delta}_{ail(max)}$	$\delta_{ail(max)}$	$\dot{\delta}_{rud(max)}$	$\delta_{rud(max)}$	$\phi_{(5\,sec)}$
142	129.8252	2.429	5.286	1.962	2.844	57.047	14.828	-8.817
143	129.9582	2.714	5.352	2.498	3.491	57.108	11.841	-10.614
144	129.9582	2.635	5.282	2.179	2.661	57.099	14.736	-8.188
145	129.9582	2.529	5.325	2.344	3.437	57.080	13.137	-10.537
146	129.9582	2.640	5.282	2.176	2.660	57.097	14.768	-8.186
147	130.0074	2.640	5.350	2.391	3.513	57.090	12.069	-10.734
148	130.0074	2.568	5.284	2.101	2.713	57.083	14.745	-8.375
149	130.0074	2.449	5.330	2.340	3.690	57.065	13.041	-11.290
150	130.0074	2.573	5.283	2.098	2.713	57.082	14.775	-8.373
151	130.0653	2.782	5.357	2.611	3.473	57.121	11.511	-10.498
152	130.0653	2.696	5.284	2.254	2.602	57.110	14.594	-7.980
153	130.0653	2.603	5.322	2.365	3.239	57.091	13.117	-9.935
154	130.0653	2.700	5.283	2.251	2.602	57.108	14.627	-7.977
155	130.1006	2.564	5.348	2.298	3.554	57.073	12.258	-10.901
156	130.1006	2.499	5.286	2.032	2.776	57.066	14.751	-8.585
157	130.1006	2.371	5.336	2.326	3.917	57.048	12.963	-11.968
158	130.1006	2.503	5.285	2.030	2.775	57.065	14.781	-8.583
159	131.7744	2.859	5.371	2.424	2.520	57.089	10.382	-7.698
160	131.7744	2.654	5.328	2.489	2.801	57.077	12.428	-8.356
161	131.7744	2.619	5.355	2.713	3.753	57.065	11.388	-11.146
162	131.7744	2.659	5.328	2.486	2.802	57.076	12.461	-8.358
163	132.0441	2.076	5.366	3.712	5.698	57.038	11.050	-16.127
164	132.0441	2.037	5.325	3.265	4.753	57.038	12.781	-13.463
165	132.0441	1.815	5.338	3.788	6.480	57.041	12.561	-18.347
166	132.0441	2.045	5.324	3.261	4.753	57.035	12.812	-13.461
167	134.8266	2.852	5.363	2.494	2.789	57.104	10.929	-8.471
168	134.8266	2.691	5.307	2.351	2.556	57.086	13.441	-7.727
169	134.8266	2.642	5.339	2.484	3.243	57.071	12.160	-9.796
170	134.8266	2.695	5.306	2.348	2.556	57.085	13.474	-7.727
171	135.0621	2.042	5.366	3.859	5.997	57.025	11.084	-16.873
172	135.0621	2.020	5.325	3.319	4.842	57.023	12.762	-13.650
173	135.0621	1.771	5.337	3.879	6.675	57.027	12.641	-18.813
174	135.0621	2.029	5.324	3.315	4.841	57.020	12.792	-13.647
175	137.9562	2.456	5.333	2.240	3.433	57.037	12.866	-10.501
176	138.1142	2.022	5.366	4.003	6.277	57.014	11.103	-17.565
177	138.1142	2.024	5.325	3.361	4.892	57.006	12.723	-13.732
178	138.1142	1.741	5.335	3.962	6.842	57.013	12.712	-19.203
179	138.1142	2.033	5.325	3.357	4.891	57.004	12.753	-13.729
180	158.6743	1.757	5.513	1.528	2.277	31.141	13.396	-7.014
181	163.0169	1.686	5.768	1.479	2.795	32.328	13.487	-8.534
182	167.7286	1.632	6.109	3.105	5.746	33.604	12.147	-15.932
183	167.7286	1.616	6.011	2.627	4.512	33.616	13.716	-12.545
184	167.7286	1.442	6.032	3.217	6.399	33.626	13.630	-17.754
185	167.7286	1.622	6.009	2.624	4.511	33.614	13.748	-12.540
186	170.3164	1.974	6.147	1.665	2.696	34.296	14.103	-8.166
187	170.3164	1.882	5.997	1.516	2.221	34.288	16.491	-6.753
188	170.3164	1.895	6.129	1.593	2.538	34.298	14.429	-7.796

E-23

#	q	p_{max}	β_{max}	$\dot{\delta}_{ail(max)}$	$\delta_{ail(max)}$	$\dot{\delta}_{rud(max)}$	$\delta_{rud(max)}$	$\phi(5\ sec)$
189	170.3164	1.886	5.995	1.516	2.220	34.286	16.523	-6.751
190	186.2219	2.172	6.955	1.969	2.837	38.907	15.924	-8.557
191	206.0828	2.537	7.962	2.116	2.508	44.735	18.338	-7.784
192	206.3182	2.496	7.991	2.090	2.469	44.778	18.139	-7.724
193	208.2658	2.512	8.229	3.878	6.691	45.316	15.819	-18.470
194	208.2658	2.497	8.091	3.196	4.945	45.329	18.103	-13.731
195	208.2658	2.213	8.134	3.989	7.546	45.328	17.613	-20.811
196 ·	208.2658	2.506	8.089	3.195	4.943	45.327	18.148	-13.725
197	215.9733	2.772	8.584	2.454	3.048	47.469	17.308	-9.077
198	215.9733	2.609	8.407	2.516	3.296	47.495	20.351	-9.585
199	215.9733	2.595	8.519	2.613	3.801	47.500	18.537	-11.161
200	215.9733	2.616	8.404	2.519	3.297	47.492	20.397	-9.586
201	222.8766	2.905	8.811	3.499	5.069	49.360	20.171	-14.009
202	222.8766	2.526	8.863	4.515	8.432	49.387	19.529	-23.079
203	222.8766	2.915	8.808	3.500	5.067	49.355	20.219	-14.002
204	228.5562	3.019	9.034	2.656	1.627	50.830	22.158	-5.476
205	228.5562	2.858	8.915	2.497	1.954	50.881	24.085	-6.183
206	228.5562	2.880	9.151	2.479	2.286	50.901	20.279	-7.319
207	228.5562	2.864	8.912	2.505	1.953	50.877	24.132	-6.181
208	245.2556	3.217	9.973	2.835	2.733	55.736	22.585	-8.474
209	247.9286	3.090	10.221	3.622	5.520	56.465	20.986	-15.751
210	254.7139	3.468	10.186	3.159	2.509	57.173	23.612	-7.788
211	254.7139	3.285	9.977	2.969	2.473	57.155	27.025	-7.515
212	254.7139	3.332	10.236	2.961	2.413	57.133	22.819	-7.650
213	254.7139	3.292	9.973	2.979	2.473	57.154	27.078	-7.513
214	264.5698	3.562	10.404	5.012	7.778	57.108	19.704	-21.312
215	264.5698	3.547	10.226	3.914	4.997	57.095	22.708	-13.858
216	264.5698	3.142	10.298	4.980	8.681	57.052	21.697	-23.800
217	264.5698	3.559	10.222	3.920	4.996	57.094	22.764	-13.853
218	282.0876	3.186	10.377	4.457	7.115	57.027	20.297	-19.821
219	287.8346	3.352	10.269	3.124	3.476	57.081	22.136	-10.298
220	308.2038	3.453	10.232	3.225	2.470	57.078	22.774	-7.628
221	333.6127	3.895	10.407	5.482	7.275	57.034	19.508	-19.814
222	333.6127	3.895	10.226	4.203	4.010	57.022	22.603	-11.125
223	333.6127	3.485	10.305	5.266	7.966	56.979	21.392	-21.741
224	333.6127	3.907	10.223	4.215	4.010	57.021	22.660	-11.123
225	333.8201	3.719	10.369	3.623	3.066	57.046	20.240	-8.955
226	333.8201	3.515	10.178	3.489	3.047	57.026	23.529	-8.751
227	333.8201	3.410	10.320	3.824	4.471	57.005	21.185	-12.783
228	333.8201	3.524	10.174	3.501	3.048	57.024	23.585	-8.753
229	357.0172	4.125	10.184	4.394	3.622	57.013	23.282	-10.041
230	357.0172	3.662	10.273	5.495	7.848	56.971	21.880	-21.335
231	357.0172	4.137	10.181	4.408	3.621	57.011	23.339	-10.037
232	366.7880	3.570	10.261	3.494	2.498	57.011	22.207	-7.590
233	383.2118	3.494	10.359	4.726	5.782	56.930	20.432	-16.109
234	416.6143	4.171	10.408	6.166	6.824	56.896	19.388	-18.506
235	416.6143	4.172	10.215	4.691	3.166	56.914	22.723	-8.811

#	q	p_{max}	β_{max}	$\dot{\delta}_{ail(max)}$	$\delta_{ail(max)}$	$\dot{\delta}_{rud(max)}$	$\delta_{rud(max)}$	$\phi_{(5\ sec)}$
236	416.6143	3.735	10.303	5.825	7.465	56.893	21.303	-20.304
237	416.6143	4.184	10.212	4.709	3.166	56.910	22.780	-8.809
238	430.4664	3.628	10.305	4.121	3.394	56.917	21.354	-9.832
239	436.0099	3.577	10.382	5.778	7.253	56.834	19.970	-19.860
240	499.2391	4.096	10.373	4.794	2.255	56.763	20.033	-6.596
241	499.2391	3.916	10.190	4.550	2.109	56.792	23.204	-6.074
242	499.2391	3.674	10.340	5.120	4.564	56.787	20.675	-12.806
243	499.2391	3.928	10.186	4.574	2.109	56.786	23.261	-6.074
244	503.8640	4.370	10.416	6.698	5.944	56.708	19.171	-16.126
245	503.8640	4.341	10.218	5.262	2.581	56.747	22.631	-7.217
246	503.8640	3.898	10.309	6.473	7.163	56.745	21.117	-19.444
247	503.8640	4.355	10.215	5.285	2.582	56.741	22.688	-7.217
248	514.2514	4.210	10.274	4.472	0.837	56.760	21.842	-2.921
249	514.2514	4.014	10.026	4.264	1.103	56.794	25.969	-3.462
250	514.2514	3.868	10.284	4.319	2.307	56.799	21.684	-6.937
251	514.2514	4.023	10.022	4.277	1.102	56.788	26.024	-3.460
252	551.8250	4.599	10.146	5.661	2.168	56.666	23.809	-6.082
253	551.8250	4.160	10.268	6.905	6.905	56.672	21.763	-18.691
254	551.8250	4.611	10.143	5.686	2.168	56.659	23.868	-6.081
255	573.1062	3.740	10.362	6.285	5.950	56.630	20.204	-16.353
256	618.5337	4.514	10.415	7.542	5.543	56.458	19.117	-15.001
257	618.5337	4.497	10.199	5.976	2.038	56.528	22.913	-5.735
258	618.5337	4.043	10.308	7.277	6.855	56.545	21.035	-18.569
259	618.5337	4.510	10.195	6.004	2.039	56.519	22.973	-5.736
260	652.0676	3.855	10.374	7.455	7.088	56.448	19.912	-19.263
261	699.9532	4.585	10.352	5.964	0.876	56.289	20.327	-2.865
262	699.9532	4.359	10.159	5.800	1.132	56.368	23.633	-3.405
263	699.9532	3.983	10.335	6.590	4.579	56.418	20.601	-12.730
264	699.9532	4.371	10.155	5.830	1.132	56.358	23.690	-3.405
265	771.1717	4.607	10.395	8.811	5.918	56.130	19.396	-15.929
266	771.1717	4.618	10.146	6.855	1.629	56.233	23.734	-4.627
267	771.1717	4.184	10.280	8.275	6.688	56.273	21.421	-18.085
268	771.1717	4.630	10.142	6.887	1.631	56.223	23.796	-4.630
269	825.2729	4.739	10.069	7.108	1.348	56.157	24.956	-3.867
270	825.2729	4.309	10.232	8.593	6.557	56.200	22.192	-17.698
271	825.2729	4.751	10.065	7.140	1.349	56.145	25.020	-3.870
272	954.4603	4.615	10.364	9.886	6.626	56.035	19.824	-17.720
273	954.4603	4.673	10.074	7.409	1.184	55.945	24.831	-3.429
274	954.4603	4.232	10.234	9.043	6.754	56.008	22.072	-18.216
275	954.4603	4.685	10.070	7.444	1.186	55.935	24.897	-3.434
276	1106.2120	4.571	10.342	10.316	6.780	55.994	20.127	-18.094
277	1106.2120	4.660	10.029	7.686	0.921	55.918	25.485	-2.726
278	1106.2120	4.194	10.203	9.494	6.909	55.809	22.489	-18.604
279	1106.2120	4.672	10.025	7.723	0.923	55.918	25.555	-2.731
280	1157.0650	4.689	9.956	7.692	0.726	55.944	26.613	-2.207
281	1157.0650	4.226	10.153	9.571	6.909	55.800	23.260	-18.578
282	1157.0650	4.701	9.951	7.729	0.728	55.944	26.685	-2.213

Bibliography

1. Air Force Institute of Technology, Department of Electrical and Computer Engineering, Wright-Patterson AFB,OH 45433-6503. *MIMO/QFT CAD program*, May 1993. Version 2.

2. ASA/ENES, Wright-Patterson AFB,OH 45433-6503. *Flying Qualities of Piloted Aircraft (Mil-Std 1797A)*, January 1990.

3. John H. Blakelock. *Automatic Control of Aircraft and Missiles*. John Wiley & Sons, Inc., New York, second edition, 1991.

4. Century Computing, Inc., 4141 Colonel Glen Hwy., Dayton, OH 45431-1662. *Simulation/Rapid-Prototyping Facility*, October 1992. Draft Sun/Unix Version.

5. John J. D'Azzo and Constantine H. Houpis. *Linear Control System Analysis and Design, Conventional and Modern*. McGraw-Hill, New York, third edition, 1988.

6. Constantine H. Houpis. Quantitative Feedback Theory (QFT) - Technique for Designing Multivariable Control Systems. Technical Report AFWAL-TR-68-3107, Flight Dynamics Laboratory AFWAL/FIGL, Wright-Patterson AFB,OH 45433-6553, January 1987.

7. Mier Pachter. Class Notes for EE641. Winter Quarter, 1994.

8. Odell R. Reynolds. Design of a Subsonic Envelope Flight Control System for the VISTA F-16 using Quantitative Feedback Theory. Master's thesis, Air Force Institute of Technology, 1993.

9. Richard R. Sating. Development of an Analog MIMO Quantitative Feedback Theory (QFT) CAD Package. Master's thesis, Air Force Institute of Technology, 1992.

10. The MathWorks, Inc., 24 Prime Park Way, Natick, MA 01760. *Simulink*, March 1992. Copyright 1990-92.

11. The MathWorks, Inc., 24 Prime Park Way, Natick, MA 01760. *Matlab*, May 1994. Version 4.2a, Copyright 1984-94.

Vita

Scott N. Phillips was born 22 September 1960 in Princeton, New Jersey. He was raised in an Air Force family and considers the Florida panhandle home. He graduated from Niceville Senior High School, Florida in 1978. He then attended the Air Force Academy culminating in a BS in Electrical Engineering in 1982. He was an F-4E and F-16A pilot at Moody AFB, Georgia from 1984 to 1988, and was then reassigned to MacDill AFB, Florida where he served as an F-16 Instructor pilot. In 1993, he was given the opportunity to pursue a Masters of Science degree in Electrical Engineering at AFIT. Following the 13 December 1994 AFIT graduation, he will proceed to Phillips Lab at Kirtland AFB, New Mexico.

Permanent address: 107 Antiqua Cove
Niceville, Florida 32578

REPORT DOCUMENTATION PAGE

Form Approved
OMB No. 0704-0188

1. AGENCY USE ONLY (Leave blank)	2. REPORT DATE	3. REPORT TYPE AND DATES COVERED
	December 1994	Master's Thesis

4. TITLE AND SUBTITLE
A QUANTITATIVE FEEDBACK THEORY FCS DESIGN FOR THE SUBSONIC ENVELOPE OF THE VISTA F-16 INCLUDING CONFIGURATION VARIATION

5. FUNDING NUMBERS

6. AUTHOR(S)
Scott N. Phillips
Major, USAF

7. PERFORMING ORGANIZATION NAME(S) AND ADDRESS(ES)
Air Force Institute of Technology, WPAFB OH 45433-6583

8. PERFORMING ORGANIZATION REPORT NUMBER
AFIT/GE/ENG/94D-24

9. SPONSORING / MONITORING AGENCY NAME(S) AND ADDRESS(ES)
Captain Steve Rasmussen
WL/FIGS
2210 Eighth St STE 11
Wright-Patterson AFB, OH 45433-7521

10. SPONSORING / MONITORING AGENCY REPORT NUMBER

11. SUPPLEMENTARY NOTES

12a. DISTRIBUTION / AVAILABILITY STATEMENT

Approved for public release; Distribution Unlimited

12b. DISTRIBUTION CODE

13. ABSTRACT (Maximum 200 words)

An aircraft's response to control inputs varies widely throughout its flight envelope. The aircraft configuration also impacts control response through variations in center of gravity and moments of inertia. Designing a flight control system (FCS) to accomodate the full flight envelope and configuration set of an aircraft is clearly a complex undertaking. Quantitative feedback theory (QFT) is a design tool which enables the engineer to attack this task in an efficient way. Although QFT is a robust control design technique, it is an interactive algorithm allowing the engineer full control over compensator order and gain. In this research effort, a full subsonic flight envelope FCS is designed for the VISTA F-16 aircraft using QFT. Four aircraft configurations are considered. The strict control of the compensator order and gain allowed by QFT facilitates the attainment of desired performance while avoiding physical saturations. In addition, flying qualities are imbedded in the longitudinal design through the use of a control parameter which varies with the aircraft's energy state. This parameter is synthesized to closely reflect the actual control desires of the pilot throughout the aircraft flight envelope. Linear simulations with realistically large control inputs are used to validate the design.

14. SUBJECT TERMS
Quantitative Feedback Theory, QFT, FCS, VISTA, F-16, Subsonic Envelope, Configuration Variation

15. NUMBER OF PAGES
169

16. PRICE CODE

17. SECURITY CLASSIFICATION OF REPORT	18. SECURITY CLASSIFICATION OF THIS PAGE	19. SECURITY CLASSIFICATION OF ABSTRACT	20. LIMITATION OF ABSTRACT
UNCLASSIFIED	UNCLASSIFIED	UNCLASSIFIED	UL